

Department of Civil and Environmental Engineering
University of Strathclyde

HOW CAN OPTIMAL SITES FOR MINE
WATER GEOTHERMAL ENERGY
SYSTEMS BE IDENTIFIED AND WHERE
ARE THEY IN SCOTLAND?

By

David Walls

BSc (Hons) (University of Glasgow)

2023

Thesis submitted in fulfilment of the requirement of the degree of
'DOCTOR OF PHILOSOPHY'

Declaration

This thesis is the result of the author's original research. It has been composed by the author and has not been previously submitted for examination which has led to the award of a degree.

The copyright of the unpublished portions of this thesis belongs to the author under the terms of the United Kingdom Copyright Acts as qualified by University of Strathclyde Regulation 3.50. Due acknowledgement must always be made of the use of any material contained in, or derived from, this thesis. Copyright of published papers included in this thesis is specified on the publisher's website or the published version of the paper.

Chapter 4 uses data which is primarily sourced from The Coal Authority (TCA). TCA is the owner of all copyright and/or Database rights and/or any other Intellectual Property Rights in the Data. The Intellectual Property Rights and other proprietary rights in the Data belonging to TCA shall remain the property of TCA. Relevant data has been attributed with the following statement: *Reproduced with the permission of © The Coal Authority. All rights reserved.*

Signed: 

Date: 18/04/2023

Abstract

Use of abandoned and flooded mines from across the Midland Valley of Scotland for low-carbon thermal energy provision and storage can assist decarbonisation of Scotland's heating and cooling demands. This thesis details configurations by which mine water can be harnessed for heating and/or cooling, plus it explores challenges and mitigations associated with conception, funding, project development, construction, lifecycle operation and maintenance of such systems. Mine water geothermal opportunities are present at surface via pumping and treatment schemes, or via contaminated mine drainages, many of which remain untreated. Combining mine water treatment with a thermal energy system provides low-carbon thermal energy whilst resolving local pollution. It is calculated that 48 MW of heat availability is present across Scotland from mine waters at surface.

Governing criteria for successful open loop mine water geothermal systems are defined and applied to archival mining data and have created a screening tool for mined workings in Scotland. The resultant Mine Water Geothermal Resource Atlas for Scotland (MiRAS) indicates a total coverage of 370 km² of suitable locations for mine water geothermal project development across 19 Scottish local authority areas, with the greatest area in North Lanarkshire.

Developments in areas affected by shallow mining can incorporate mine water geothermal investigatory boreholes into mandatory ground investigation works to generate a reduced cost geothermal screening technique. A principal finding of this technique is the importance of baseline- and continued hydrogeological and geochemical- monitoring to assess changes to mine water system dynamics, facilitating project longevity. Oxygen and hydrogen isotopic signatures infer meteoric recharge for mine drainages and subsurface mine water. Sulphur isotopes from sulphate in mine waters corresponds with standard sulphide oxidation in some instances, but also showed influence from heavier sources reflecting possible evaporite dissolution, ancient evaporitic brines, bacterial reduction or inclusion of carbonate associated sulphur.

Table of Contents

Declaration.....	ii
Abstract.....	iii
Table of Contents.....	iv
List of Figures.....	vii
List of Tables.....	xiv
List of Supplementary Material.....	xvi
Acknowledgements.....	xvii
Chapter 1 - Introduction and Setting.....	1
1.1 Introduction and study area.....	1
1.2 Aims and Research Questions.....	2
1.3 Thesis Outline and Style.....	4
Chapter 2 - A Review of the Performance of Minewater Heating and Cooling Systems ..	8
<i>Abstract</i>	8
2.1 Introduction.....	8
2.2 Low-Carbon Energy from Coal Mines.....	10
2.3 Types of Minewater Geothermal Energy Systems.....	12
2.4 Data Collection Methods.....	17
2.5 MWG Systems Status Results.....	18
2.6 Challenges.....	30
2.7 Conclusion.....	46
Author Contributions.....	47
Funding.....	47
Acknowledgments.....	47
Chapter 3 – Heat recovery potential and hydrochemistry of mine water discharges from Scotland’s coalfields.....	48
<i>Abstract</i>	48

3.1	Introduction.....	48
3.2	Materials and Methods.....	57
3.3	Results and Discussion – Thermal Resources	64
	Results and Discussion – Hydrochemical Data	68
3.4	Conclusion	82
	Author Contributions	83
	Acknowledgements	83
	Funding	83
Chapter 4 - GIS analysis for the selection of optimal sites for mine water geothermal energy application: a case study of Scotland’s mining regions		
	4.1 Introduction.....	84
	4.2 Data.....	87
	4.3 Methodology	91
	4.4 Results.....	100
	4.5 Discussion.....	102
	4.6 Integration of resource maps.....	104
	4.7 Conclusions.....	113
	Author Contributions	114
Chapter 5 - Combining ground stability investigation with exploratory drilling for mine water geothermal energy development. Lessons from exploration and monitoring.....		
	<i>Abstract</i>	115
	5.1 Introduction.....	115
	5.2 Methods.....	124
	5.3 Results and Discussion	132
	5.4 Reflections	145
	5.5 Limitations	147
	5.6 Conclusion	147
	Acknowledgements	148

Author Contributions	149
Funding Information	149
Chapter 6 The occurrence of elevated $\delta^{34}\text{S}$ in dissolved sulfate in a multi-level coal mine water system, Glasgow, UK.....	150
<i>Highlights</i>	150
<i>Abstract</i>	150
6.1 Introduction.....	150
6.3 Methods.....	155
6.4 Results.....	165
6.5 Discussion.....	173
6.6 Conclusion	182
Declaration of interests	184
Author contributions	184
Funding	184
Acknowledgements	184
Chapter 7 Conclusions, Recommendations and Further Work.....	185
7.1 Conclusions.....	185
7.2 Recommendations.....	191
7.3 Further Work.....	199
References.....	202

List of Figures

Figure 2.1 Schematic representation of the history of a mine, from (a) active mining with pumped dewatering; through (b) post-abandonment flooding; to (c) repurposed as a MWG system. 11

Figure 2.2 Temperatures of minewater in South Wales, presented as daily averages of half-hourly data recorded in surface outflow point, compared with monthly average high/low air temperatures for Neath in the period 1961-1990 (from <https://en.wikipedia.org/wiki/Neath>, based on Meteorological Office data). Note that the Tan-y-Garn minewater (3.9849°W 51.7696°N; (Taylor *et al.*, 2016a, 2016b)) temperature is a little higher than annual average air temperature, while the increasing temperatures at Glyncastle (3.6889°W, 51.7119°N) and Morlais (4.0680°W, 51.7004°N) and are believed to be due to increasing depth of minewater derivation. Minewater data provided by Gareth Farr of the British Geological Survey, with thanks, as reported in Farr *et al.* (2016). 12

Figure 2.3 Configurations of Minewater Geothermal Energy Systems: (a) Open system with discharge; (b) Open system with reinjection; (c) Borehole closed loop; (d) Surface closed loop; (e) Standing column. Edited from (Banks *et al.*, 2019) with permission from © David Banks..... 15

Figure 2.4 Periodic recirculation of citric acid solution through the plate heat exchanger at Abbotsford Road, Gateshead, UK (left), to remove accumulated ochre (which can be seen in the recirculation tank, right). Photos reproduced with permission of © David Banks, after (Banks, 2021)..... 22

Figure 2.5 (left) Shell-and-tube heat exchangers between minewater and secondary circuit to hospital, Barredo shaft-top building; (right) minewater to secondary circuit plate heat exchangers. University plant room. Photos by © David Banks..... 25

Figure 2.6 The pumped mine water discharge from Ewa shaft in Bytom, Poland (left), and its outfall into a lake within the ARMADA housing development complex (right). Photos reproduced with permission of © David Banks..... 27

Figure 2.7 Identified issues which minewater geothermal energy systems may face throughout their project lifetime. 30

Figure 2.8 Hydraulic pumping costs, as a % of total electricity cost, and system COP, as a function of elevation head (elevation up which water is pumped). A constant frictional head loss of 6 m is added to the elevation head loss. Only water pumping and heat pump power and costs are considered. The heat pump COP is set at values of 3, 4 and 5. System COP is defined

as Total heat output (kW) / Total electricity use (kW). Other assumptions: water density of 1 kg/L, temperature change across heat pump = 4 °C, volumetric heat capacity of water = 4.19 kJ/L/°C.	43
Figure 3.1 Map of Scotland’s central belt coal-bearing strata with heat available from discharges and treatment sites. Contains British Geological Survey materials © UKRI 2022.	51
Figure 3.2 Thermal outputs of treatment sites and gravity drainages. Heat available (top) and total heat pump delivery (bottom).	65
Figure 3.3 Box and whisker plots for total iron and physicochemical properties for all gravity drainages in Scotland including those treated by TCA (Bailey <i>et al.</i> , 2016) or the council (James Hutton Institute, 2016), and the untreated discharges sampled in this study.	68
Figure 3.4 Box and whisker plots following water chemistry analysis of the untreated gravity discharges sampled in this study (not including treated discharges by TCA or council). All values in mg/L except alkalinity in meq/L.	71
Figure 3.5 Durov plot for untreated gravity discharges sampled in this study, with total dissolved solids (TDS) shown on right hand extension plot.	72
Figure 3.6 Younger diagram with untreated discharges from this study, where bubble sizes reflect the EC value. The Cl ⁻ and SO ₄ ²⁻ on the x-axis are both meq/L. The typical plotting fields are: A – Acidic spoil leachates, tailings/bing drainage, and shallow oxygenated workings in pyrite rich strata; B – Majority of fresh, shallow, ferruginous coal mine waters; C – Previously acidic waters, since neutralised; D – Deep-sourced pumped, saline mine waters; E – Field in which few mine waters plot.	73
Figure 3.7 Images of Old Fordell (“Junkie’s Adit”) mine water discharge (top), which hosts the highest iron loading of the untreated discharges (1L bottle for scale), and the resulting downstream ochre precipitation on the River South Esk (bottom).	75
Figure 3.8 Oxygen and hydrogen isotope plot for the untreated MVS mine water discharges against the global meteoric water line (solid) and a local meteoric water line (dashed) derived from rainwater samples at the University of Glasgow.	76
Figure 3.9 Histogram of δ ³⁴ S values collected from the untreated mine water discharges in this study.	77
Figure 3.10 δ ³⁴ S plots against alkalinity to sulphate ratio, and calcium and magnesium (combined) to sulphate ratio (both as meq/L ratios).	79

Figure 3.11 Plot of the chloride : bromide ratio against chloride concentration, with circle sizes proportionate to $\delta^{34}\text{S}$ value. Seawater in black.	80
Figure 4.1 Necessary parties for conception of a mine water geothermal project before and after development of the Mine Water Geothermal Resource Atlas for Scotland.	85
Figure 4.2 Map of the study area, broken down into its comprising shapefiles. Coloured sections denote the Carboniferous bedrock outcrop, whilst the hatched area represents areas of coal workings from Jones <i>et al.</i> (2004). Coal workings exist outside the outcrop areas since the coal-bearing strata are concealed in these areas by younger strata. Contains British Geological Survey materials © UKRI 2022.....	87
Figure 4.3 Flow diagram showing the overall processing from input datasets to reach the suitability map. Each of the 4 criteria are indicated, or abbreviated to C.....	88
Figure 4.4 Flow diagram showing GIS processing of “underground workings” to reach “overlapping mined seams without mines shallower than 30 m”.....	92
Figure 4.5 Schematic representation of conversion from “underground workings” and “shallow workings” (left), to “overlapping mined seams without mines shallower than 30 m” (right).	93
Figure 4.6 Map of central Scotland showing areas of overlapping coal seams, without shallow seams (<30 m BGL). Reproduced with the permission of © The Coal Authority. All rights reserved.....	94
Figure 4.7 Map of predicted mine water table (m OD). GGERFS: Glasgow geothermal energy research field site. Contains data from © The Coal Authority. All rights reserved.....	95
Figure 4.8 Map of predicted depth to mine water level (head) (m BGL). Contains data from © The Coal Authority. All rights reserved. Crown copyright and database rights 2022 Ordnance Survey.	96
Figure 4.9 Map of coal mine elevation points, coloured to reflect depth relative to the 250 m BGL cut-off. Reproduced with the permission of © The Coal Authority. All rights reserved. Crown copyright and database rights 2022 Ordnance Survey.....	98
Figure 4.10 Mine Water Geothermal Resource Atlas for Scotland with optimal areas coloured corresponding to the depth to mine water (m BGL). Reproduced with the permission of © The Coal Authority. All rights reserved. Crown copyright and database rights 2022 Ordnance Survey.....	101
Figure 4.11 Enlarged Mine Water Geothermal Resource Atlas for Scotland, with optimal areas coloured corresponding to the mine water head (m BGL). Reproduced with the	

permission of © The Coal Authority. All rights reserved. Crown copyright and database rights 2022 Ordnance Survey..... 102

Figure 4.12 Schematic representation of difference between A) smaller total mined area but larger overlapping area; and B) larger total mined area but smaller overlapping area.... 103

Figure 4.13 The western portion of East Lothian which hosts the Mine Water Geothermal Resource Atlas for Scotland with surface thermal resources included. Reproduced with the permission of © The Coal Authority. All rights reserved. Crown copyright and database rights 2022 Ordnance Survey..... 105

Figure 4.14 The Mine Water Geothermal Resource Atlas for Scotland applied to Shettleston Housing Association abstraction and reinjection boreholes, Glasgow. Reproduced with the permission of © The Coal Authority. All rights reserved. Crown copyright and database rights..... 108

Figure 4.15 Single and overlapping coal seam locations near Shettleston Housing Association abstraction and reinjection boreholes, Glasgow. Reproduced with the permission of © The Coal Authority. All rights reserved. Crown copyright and database rights 109

Figure 4.16 The Mine Water Geothermal Resource Atlas for Scotland applied to the UKGEOS Cuningar Site, Glasgow. The 5 boreholes which are completed into coal mines are shown in black. Reproduced with the permission of © The Coal Authority. All rights reserved. Crown copyright and database rights. Contains NERC materials ©NERC 2020. 110

Figure 4.17 Areas of shallow (<30 m), overlapping and single coal seams beneath the Dollar Site, Clackmannanshire. The study area for Chapter 5 is shown by the black polygon. Shallow workings are shown as seen on TCA’s interactive map viewer (The Coal Authority, 2022). Reproduced with the permission of © The Coal Authority. All rights reserved. Crown copyright and database rights..... 111

Figure 4.18 The Mine Water Geothermal Resource Atlas for Scotland applied to the Dollar Site, Clackmannanshire. The study area for Chapter 5 is shown by the black polygon. Reproduced with the permission of © The Coal Authority. All rights reserved. Crown copyright and database rights..... 112

Figure 5.1 Simplified geological map of the eastern extent of Dollar, Clackmannanshire. Geological information derived from British Geological Survey (Armstrong et al., 1974a). Contains OS data © Crown copyright and database rights 2022..... 119

Figure 5.2 Topographic and hydrological map of the study area and surroundings with notable locations pertaining to the coal seams shown. Numbers correlate with discharge sample

names. Arrows indicate orientation of drift mines from Dollar Colliery. Pit names can be seen in Fig. 5.4. Contains OS data © Crown copyright and database rights 2022. 121

Figure 5.3 Schematic cross section through the coal seams with pit locations, along the line of the Day Level (shown in Figure 5.2) in the western part of the study area. The five completed boreholes have been projected onto the cross section from their locations 100 m to 150 m along strike, to the east. Pink reflects plain screen liner and red reflects slotted screen liner. Vertical brown sections at the base of GI01 and BH04 depict where each borehole was backfilled before completion with liner. 122

Figure 5.4 Borehole and sampling locations overlain on the mine abandonment plan for the Coalsnaughton Main Seam (National Coal Board, 1955), where red outlines extent and details of workings. Numbers correlate with discharge sample names. KBAS, Kelly Burn above site; KBBS, Kelly Burn below site. Arrows indicate orientation of drift mines from Dollar Colliery. Mine Plan as base map: Copyright Coal Authority. All rights reserved 2022. 123

Figure 5.5 Cross sectional interpretation of borehole logs between the southernmost (GI20) and northernmost (BH04) boreholes along line of section shown on Fig. 5.4. No vertical exaggeration. AOD; above Ordnance Datum. 133

Figure 5.6 (a) Discharge 1 before (13/11/2020) and (b) after (05/12/2020) it ceased to flow. 135

Figure 5.7(a) Day Level site prior to drilling period, digging to access fresh water (13/11/2020); (b) Day Level location following flooding and flow of mine water (Discharge 2A, 05/12/2020); and (c) the area north of the Discharge 2A upon first flooding, which since lowered to marshy ground and Discharges 2B and 2C (05/12/2020). 136

Figure 5.8 Meeting of two discharges from 5 m apart. Discharge 2C (from the left) has a channel base with mostly organic matter, whilst discharge 2B (from top of image) coats the channel base in orange ochre. 30 cm ruler for scale. 137

Figure 5.9 Total and component mine water discharge flow rates plotted against projected extrapolated flow rate from the ceased discharge (Discharge 1), and weekly rainfall data for Tillicoultry (Scottish Environment Protection Agency, 2022). Contains public sector information licensed under the Open Government Licence v3.0. 138

Figure 5.10 Manual dip and diver data for mine water levels, plotted against weekly rainfall data for Tillicoultry (Scottish Environment Protection Agency, 2022). Note that monthly sampling displaces the probes. Best efforts were made to ensure they were inserted at the same level as they were removed from, but discrepancies were due to adhesion between the probe string and the borehole liner. Contains public sector information licensed under the Open

Government Licence v.0. Note that absolute elevation values are only accurate to c. 1 m OD as each wellhead elevation is derived from a digital elevation model..... 139

Figure 5.11 Seasonal temperature data for mine water in 2021, plotted against monthly measured Kelly Burn stream temperature data and average maximum and minimum air temperature between 1991-2020 (Met Office, 2022) calculated using the methods outlined in Hollis and Perry (2004). Mine water probes are at depths (below ground level) of 10 m in GI01, 16 m in GI02, 15 m in GI11, 16 m in BH04 and 42 m in BH02; which equate to depths below water level of c. 1-2 m in GI01, 6 m in GI02, 9-10 m in GI11, 6 m in BH04 and 31 m in BH02. Contains public sector information licensed under the Open Government Licence v3.0. 140

Figure 5.12 Water chemistry data from sample locations presented using Piper diagrams; (a) borehole and (b) discharge water chemistry data from the entire year; (c) data from all points for October 2021 (including the Discharge 1 from Nov 2020 for comparison). 142

Figure 5.13(a) Dissolved sulphate $\delta^{34}\text{S}$ data for sampling points plotted across the sampling year (2021). (b) $\delta^{18}\text{O}$ and $\delta^2\text{H}$ stable isotope data plotted against global and local (Glasgow) meteoric water lines (GMWL (Craig, 1961); LMWL (Walls et al., 2022)). 144

Figure 6.1 Maps showing a) UKGEOS location within Scotland; b) GGC01 borehole and the Cuningar Loop location (red box) in Glasgow's east end; c) The borehole array at Cuningar Loop on the River Clyde. Contains NERC materials ©NERC 2020. Contains OS data © Crown Copyright and database right 2020 (Monaghan et al., 2019)..... 153

Figure 6.2 Block diagram showing the Cuningar Loop borehole array with coal seams labelled. No vertical exaggeration. Note depths are in metres relative to Ordnance Datum (m OD; sea level). Figure originally published by Monaghan et al. (2021c) ©BGS, UKRI 2021. 154

Figure 6.3 Lithostratigraphical correlation panel of the Glasgow Observatory boreholes modified from Monaghan et al. (2021c) (©BGS, UKRI 2021) by addition of coloured symbols representing groupings of sulfur isotopic values. 160

Figure 6.4 Plot of $\delta^{34}\text{S}$ isotope values versus depth for dissolved sulfate in water samples from both Dalmarnock and Cuningar Loop locations. Arithmetic means of the sulfide sulfur from this study and Bullock *et al.* (2018) are indicated by vertical dashed lines. Depths of coal seams are shown in blue bands (left) for the Dalmarnock location, and red bands (right) for Cuningar Loop. Note that the y-axis is in metres relative to Ordnance Datum (m OD), ground level is c. 10-12 m OD. Depth of the pumping test samples correlate with the depth of the screened section of the completed borehole. 166

Figure 6.5 Histograms of $\delta^{34}\text{S}$ isotope values from the Cuningar Loop boreholes. (a) Active samples (Sample types B and C): all water samples except for borehole fluids as these were not sampled during active drilling or pumping (this histogram is repeated in all other plots as the background); (b) Site 1; (c) Site 2; (d) Site 3; (d) Pump test water samples only - all boreholes at Cuningar Loop combined. 167

Figure 6.6 Plots from the deepest boreholes from each of Site 1, 2 and 3 within Cuningar Loop, showing **a**) $\delta^{34}\text{S}$ values with depth (m OD); **b**) sulfate concentration with depth; and **c**) $\delta^{34}\text{S}$ values plotted against sulfate concentration. Blue polygons highlight GGC02 anomalies with elevated sulfate concentrations and intermediate $\delta^{34}\text{S}$ values. Plot contains all sample types (A, B and C). 171

Figure 6.7 Standard $\delta^{18}\text{O}$ and $\delta^2\text{H}$ from all GGERFS water samples (including mains water), plotted against the global meteoric water line (Craig, 1961) and rainwater data collected at the University of Glasgow between December 2016 and February 2020 (Walls *et al.*, 2022), comprising the local meteoric water line. 173

Figure 7.1 Pourbaix diagram for iron with samples plotted from Chapters 3 and 5 to indicate their iron status. Figure adapted from Younger (2007). 188

List of Tables

Table 2.1 Minewater geothermal energy systems in the USA detailed by Korb (2012).	29
Table 2.2 (Overleaf) Issues reportedly encountered at the described MWG schemes. X = major difficulty, \diamond = some difficulty, * potential difficulty, but resolved. Grey cells = no information. HEX = heat exchanger. Be aware that there is a correlation between difficulties reported and detail of reporting.	32
Table 3.1 Sedimentary successions from the Carboniferous for the West Lothian area of the Midland Valley of Scotland. Other areas host variations within the Strathclyde Group. Modified from (Monaghan, 2014) and (Waters <i>et al.</i> , 2007)	53
Table 3.2 Coal authority treatment sites in Scotland (Bailey <i>et al.</i> , 2016)	57
Table 3.3 Results for all gravity mine drainages (not including the 4 pumped systems in Scotland). Data from TCA treated discharges available only for: Flow rate L/s, Temperature, Heat Available, Total Heat Delivery with COP of 4 and $\Delta T=4$ K, pH, Electrical Conductivity, Alkalinity and Fe (total). CTP – Calculated thermal potentials, LID – Laboratory isotopic data.	67
Table 3.4 Total iron loading of mine water into Scottish treatment sites based on total iron concentrations.	74
Table 3.5 Correlation of iron loading and heat available for the untreated discharges with the highest iron loadings, based on total iron concentrations.	75
Table 4.1 Description of the input layers for GIS analysis.	90
Table 4.2 Coverage area by the MiRAS in each of the affected Scottish local authority areas.	100
Table 4.3 Coverage area of the MiRAS and heat available from surface mine water resources, broken down into local authority areas.	107
Table 5.1 Details of coal seams present beneath the site. Depths as read from BH04, converted to metres above Ordnance Datum (m OD = effectively m above sea level).	120
Table 5.2 Median and inter quartile range (IQR) values for total (tot) and dissolved (dis) iron and manganese from sampling points across the field site. N, number of samples. Discharge 1 was sampled only once.	141
Table 5.3 Generic indicative costs for coupled ground stability (GSI) and mine water geothermal investigation (MWGI) for approximately 20 GSI boreholes, where three of these are completed as monitoring wells.	147

Table 6.1 Numbers of water samples collected and analysed by site and sample type. Number of samples analysed for $\delta^{34}\text{S}$ is in brackets.....	154
Table 6.2 Mains water quality supplied by Scottish Water to the Cuningar area of Glasgow via Milngavie treatment works, average of 2021 (Scottish Water, 2021); and the average of the two mains water samples taken from the office at the Dalmarnock drilling location (Shorter et al., 2021b). n.a. – not analysed.	156
Table 6.3 Sulfide-sulfur isotope data from pyrite separated from coal horizons at the GGERFS ('GGA' Cuningar boreholes – drill cuttings) and stratigraphic and seismic monitoring Dalmarnock borehole (GGC01 – core sample). Their stratigraphic level is also presented in relation to the mined coal-bearing horizons from which they were collected (see. Figure 6.3).....	165
Table 6.4 $\delta^{34}\text{S}$ isotope data from dissolved sulfate in fluids sampled during the drilling programme for the stratigraphic and seismic monitoring borehole (GGC01) at the Dalmarnock drilling location.....	167
Table 6.5 Arithmetic means of the pump test water samples as grouped by the screen horizon. Field and laboratory chemical data from Palumbo-Roe et al. (2021b) compared with seawater from Lenntech (2022). Arithmetic mean sulfur isotopic values are added from this study, and Tostevin et al. (2014) for seawater.	169
Table 6.6 $\delta^{34}\text{S}$ values from Cuningar pumping test water samples.	170
Table 6.7 $\delta^{34}\text{S}$ values of Ballagan Formation gypsum evaporite samples from Ballagan Glen. * - museum sample without record of fault side. Facies column indicates chronostratigraphical ordering of sample beds, where 1 is the oldest.	172

List of Supplementary Material

Appendices from each chapter are included in a separate document titled “How can optimal sites for mine water geothermal energy systems be identified and where are they in Scotland? Supplementary material.”

Chapter 3 - Heat recovery potential and hydrochemistry of mine water discharges from Scotland’s coalfields

Appendix 3A - *Literature sourced data on surface mine water, either from pumping or gravity drainage*

Appendix 3B - *Data collected as part of this study from untreated mine water gravity drainages*

Appendix 3C - *Quality Assurance Data and Results*

Appendix 3D - *Oxygen and hydrogen stable isotope data for Glasgow December 2016 to February 2020*

Chapter 4 - GIS analysis for the selection of optimal sites for mine water geothermal energy application: a case study of Scotland’s mining regions

Appendix 4A - *“Mine Water Geothermal Resource Atlas for Scotland” outputs for local authority areas with surface mine water resources*

Chapter 5 - Combining ground stability investigation with exploratory drilling for mine water geothermal energy development. Lessons from exploration and monitoring

Appendix 5A - *Field data*

Appendix 5B - *Analysis results*

Appendix 5C - *Flow Rate Estimates*

Appendix 5D - *Water Profiles*

Appendix 5E - *Borehole Completions*

Chapter 6 - The occurrence of elevated $\delta^{34}\text{S}$ in dissolved sulfate in a multi-level coal mine water system, Glasgow, UK

Appendix 6A - *Analysis results*

Acknowledgements

Firstly, I would like to thank my supervisors Dr Neil Burnside, Mr Dave Banks, and Prof. Adrian Boyce for continued inspiration, support and feedback over the last four years. Neil, I am grateful for how you always were available for meetings, in person originally, and more recently, online. Your effort and compassion when planning and refining my PhD project ideas is greatly appreciated, likewise your editing contributions and accompaniment in the field. Dave, thank you for consistent, expert advice and feedback throughout the PhD campaign. I am truly grateful that you continued as one of my supervisors following my move, granting me access to a great wealth of knowledge and reminders of the importance of succinctness. Adrian, thank you for your professional input and your endless enthusiasm to help bring my research to life.

I would like to extend my thanks to those who assisted me so generously in the laboratories of Glasgow and Strathclyde Universities and SUERC. Namely, Tatyana Peshkur for patience and teaching when planning my field endeavours and running analyses; Alison MacDonald for generous time donations to share data collection methods and run isotope samples, especially when covid-19 prevented lab access; Anne McGarrity and Jeanine Lenselink from my time at UofG, and Carla Lopez at UofS for teaching and helping me with chemical analysis. My thanks also go to other members of staff including John MacDonald at UofG for facilitating some early fieldwork and Yannick Kremer at UofS for being willing to share his GIS course, helping me to convert my datasets to tangible maps, and providing guidance through its write up.

I would like to acknowledge the funding I have received across the course of this project from the Environmental and Physical Science Research Council (EPSRC), thank you for funding my research and my experiences. To each of the additional funding awards I have received, or my PhD research has benefitted from, I am truly grateful:

- EPSRC IAA and Energy Technology Partnership for funding Dollar drilling programme, this was a phenomenal learning experience.
- NERC National Environmental Isotope Facility for funding analysis of O, H and S stable isotopes at the Scottish Universities Environmental Research Centre (SUERC).
- The John Mather Trust for a Rising Star Award which funded conference attendance and presentation; further assistance with my GIS work; funding a “video thesis” to aid

science communication; and partial funding for my “Giro di Geothermal” bicycle tour through Europe whereby I was able to visit over 20 operating geothermal sites.

Thanks also go to Nicholas Poett of Harviestoun Home Farm for agreeing to let the research team use private land for my project; to TownRock Energy for providing many learning and work experience opportunities, in particular to David Townsend for the continued feedback and inspiration to keep my PhD relevant and useful to the geothermal industry. Thanks to Dollar Museum for lend of their archival material for reference. I am also grateful to British Geological Survey team members for access collection of UKGEOS samples, and to The Coal Authority for provision of datasets which proved to be pivotal to completion of this research.

I extend thanks to other landowners who granted me access during my field sampling campaigns and the many field assistants who were willing to join in, rain or shine: Jura MacMillan, Laura Dozier, Pippa Wood, Dom James, Mike Schiltz, David Townsend, Sean Watson, Sally Jack, Dan Whittington, Mylène Receveur, Mohamed El Gheriani, Jennifer Roberts, Simon Theilen and Hannah Jukes; plus Ross Sloan for providing communication during independent field trips.

Thanks go to the other PhD students who have been present throughout my journey and have facilitated many moments of inspiration, reflection and laughter. In particular I would like to thank Mike Schiltz, Sean Watson, Iain Moore and Mark Stillings.

Finally, a word of thanks to my parents, brothers, and close friends, who have remained interested and encouraging throughout.

Chapter 1 - Introduction and Setting

1.1 Introduction and study area

Rising concerns over global greenhouse gas levels have put pressure on nations to curb their emissions in pursuit of carbon neutrality (Scottish Government, 2020a); it is imperative that we take advantage of renewable energy sources where possible. Heat energy in Scotland comprises over half of the nation's total energy consumption (50.3%); but in 2020 only 6.4% of heating was from renewable sources, totalling 5,008 GWh, and well shy of the 2020 target of 11% (Energy Saving Trust, 2021).

Water held in abandoned, flooded mines has been identified as a viable, low-carbon source of heating and/or cooling when coupled with heat pumps (Banks, 2008, Preene and Younger, 2014, Younger, 2016). Across the UK, 23,000 deep coal mines (NELEP, 2021) underly around 25,000 km² of land (Johnston *et al.*, 2008). The Midland Valley of Scotland (MVS) has long since been mined for its abundant mineral deposits, with the most widespread of these being coal (Gillespie *et al.*, 2013). Upon closure of mines and cessation of mining related dewatering measures, excavated void spaces were flooded by groundwater as it recovered towards the original pre-pumped levels. The temperatures of resulting mine waters are not typically high (10 – 20 °C) (Farr *et al.*, 2021); however, the heat available is a function of the flow rate achieved from boreholes, mine shafts or drainage discharges, and the temperature change across a heat exchanger (Bailey *et al.*, 2016). Stable year-round temperatures make mine water an attractive, constant thermal resource (Farr *et al.*, 2016) and the extensive and interconnected void spaces hosted by multiple mined horizons has created bedrock aquifers with greatly increased artificial porosity and permeability (Ó Dochartaigh *et al.*, 2015).

Use of mine water as a thermal energy source can be via a number of configurations, each selected to suit the size and form of the available resource (Banks *et al.*, 2019). Mine water geothermal (MWG) energy can be delivered on a multi-megawatt scale for heating or cooling, or can be developed as part of a district heating network where heating and cooling demands can utilise large volumes of mine water as a thermal buffer (Fraser-Harris *et al.*, 2022, Verhoeven *et al.*, 2014). Whilst Scottish MWG projects to date have been installed without extensive hydrogeological insight, they performed satisfactorily for around 20 years (Banks *et al.*, 2019, Banks *et al.*, 2009). Other potential projects have failed to progress beyond planning

stages (Townsend *et al.*, 2020) despite being designed on a case by case basis and including expert involvement from the outset (James Hutton Institute, 2016).

This thesis recognises that if the geothermal sector in Scotland is to grow, then clear communication of MWG resources is necessary. There are multiple factors which dictate the success of a MWG system, including mining geometries, public acceptance, project funding and maintenance burden, among others (Walls *et al.*, 2021). Therefore, communicating criteria for project appraisal, as well as the lifecycle challenges is important. Some challenges facing global MWG systems stem from water chemistry, including iron (oxy)hydroxide precipitation and corrosion from reducing or saline waters (Younger, 2001). Detailing water chemistry prior to project installation means that data can inform engineering solutions and will likely improve the longevity of the project.

Prominent knowledge gaps exist over MWG resource location and availability in Scotland. To identify best locations for MWG application and provide a rapid screening tool for non-expert stakeholders and decision makers, an evidenced resource map was required. Creation of such a tool could be influential to the overall renewable heating balance by facilitating uptake of MWG heating and cooling for domestic or commercial demands. By characterising mine water chemistry across the MVS, this thesis can contribute to successful installations by providing baseline data to inform engineering solutions (Bailey *et al.*, 2013, Farr *et al.*, 2016). Similarly, exploring a means to facilitate and expand roll-out of MWG investigation works where mines are believed to be shallow enough to merit ground stability investigation, could prove valuable to increase system uptake.

In this thesis the study area is geologically constrained by the extent of Scottish coal fields held within the MVS. The MVS terrane spans from the NE-trending Highland Boundary Fault between Stonehaven and Helensburgh to the parallel Southern Upland Fault between Girvan and Dunbar. Both site-specific case studies in this thesis are at a smaller scale, focussing on individual collieries, one in the SE of Glasgow, in the Central Coalfield and one from the Stirling and Clackmannan Coalfield in the town of Dollar, Clackmannanshire.

1.2 Aims and Research Questions

The principal aim of this thesis was to advance the MWG knowledge base to achieve real-world impact in the expanding renewable energy sector. Research approaches were guided by workflows believed to facilitate the uptake of MWG energy. Limiting the research area to the MVS helped to achieve a useful balance of wide-scale geographical dataset investigation and

comprehensive site-specific case study data collection. Although the research area is limited to Scotland, the best-practice methods outlined for phases of development and operation are applicable to MWG systems across the world.

Research questions (RQ) and research objectives (RO) were as follows:

- RQ1: What are the principal challenges for successful delivery of MWG systems, and how can these be overcome?
 - RO. 1.1: Explain existing knowledge on MWG application and describe available configurations.
 - RO. 1.2: Provide an account of the current status of global MWG heating/cooling systems.
 - RO. 1.3: Detail the challenges faced by existing and former MWG systems and explore relevant mitigations.
- RQ2: Where are the optimal locations for MWG application in the MVS?
 - RO. 2.1: Detail the scale of thermal resource hosted by mine water at surface across the MVS, quantifying individual thermal resources.
 - RO. 2.2: Explore which governing criteria are most influential for MWG developments (with a focus on abstraction-reinjection doublet systems).
 - RO. 2.3: Develop an interactive map of combined criteria to indicate optimal areas for MWG development.
- RQ3: What are the chemical properties of mine water across the MVS, and what implications do these have for MWG systems?
 - RO. 3.1: Determine the composition of mine waters from boreholes, shafts and gravity discharges across the MVS.
 - RO. 3.2: Explore concentrations of scaling and corrosive species for engineering impacts and polluting species for environmental impacts.
- RQ4: Can MWG investigation become more commonplace by inclusion of geothermal evaluations into routine ground stability investigations (GSI)?
 - RO. 4.1: Conduct field data collection and install MWG monitoring infrastructure during GSI work.
 - RO. 4.2: Explore the synergies between the requirements and limitations of GSI and MWG investigations.

- RQ5: How can stable isotope data contribute to understanding hydrogeology in MWG systems?
 - Collect stable isotope data from key minerals and mine water from across multiple horizons and outflow points associated with flooded mine workings.
 - Determine how measured isotopic ratios relate to interaction histories between mine waters and exposed workings and/or local lithologies.

1.3 Thesis Outline and Style

Chapters 2, 3, 5 and 6 have each been written as a standalone manuscript, and each has been published or accepted for publication by a peer-reviewed journal. Each manuscript consists of an independent abstract, introduction, and method section, with details of the respective study area and pertinent geological setting followed by sections for results, discussion, and conclusions. Contents of the published/accepted chapters inevitably contain some overlap, and findings from one chapter can feed into another. Since they were intended for publication, they were written as first-person plural. Whilst co-authors provided advice and assistance during field work, data analysis and interpretation, and with manuscript framing, structuring, and editing, I was the primary author responsible for the majority of the work within, and writing of, manuscripts. Funding awards that facilitated research activities are acknowledged in each manuscript where relevant.

Chapter 4 has been included as a standard thesis chapter whereby the context is explained by preceding chapters, but it maintains a minor introduction to accompany the results as a publicly available, interactive map tool. All necessary context and method statements are included within Chapter 4. Chapter 7 concludes the research and provides suggestions for future work.

Since each chapter was submitted to a different publisher, some formatting, spellings, and terminology are inconsistent throughout the thesis document. These include the spelling of *sulphur*, *sulphide* and *sulphate* for some chapters and *sulfur*, *sulfide* and *sulfate* in others; *minewater* as one word or *mine water* as two; and the labelling of figures, tables and equations is subtly different. The numbering scheme has been curated to ensure no two are labelled as the same, e.g., *Figure 3.1* is the first figure within Chapter 3.

Geothermal terminology describing size, accessibility and proven scale of geothermal energy in different settings is not as well established as the terminology in other sectors, e.g. mining. Whilst progress has been made to unify the sector's nomenclature, this has not been

widely adopted. As a result, some terms in the published papers of this thesis do not directly correlate with the terms outlined in the United Nations Framework Classification for Resources (Update 2019) to Geothermal Energy Resources (UNECE, 2022). Specifically, the term “resource” is used repeatedly in throughout the thesis. The term “resource” in this context is used to describe exactly that detailed by UNECE as a “source” i.e., “the thermal energy contained in rocks, sediments and/or soils, including any fluid contained underground or naturally discharging at the ground surface, which is available for extraction and/or conversion into energy products.” (UNECE, 2022).

Finally, it is noteworthy, that these “sources” are present as “known” or “potential” sources, where the former is an established, proven or harnessed source of energy. The latter describes a scenario whereby the existence or scale of thermal energy has not been demonstrated by direct evidence (i.e. boreholes). The phrase “surface mine water” is used as a catch-all term throughout the thesis to describe the “known resources” which are present as Coal Authority treatment schemes or untreated gravity drainage outflows at surface. The sources described in Chapter 4 are inherently “potential sources”.

Chapter 2 – This chapter was published in the MDPI Energies Journal.

Published as: Walls, D.B.; Banks, D.; Boyce, A.J.; Burnside, N.M. A Review of the Performance of Minewater Heating and Cooling Systems. *Energies* 2021, 14, 6215. doi: 10.3390/en14196215.

This chapter forms the overarching literature review for the thesis. Whilst data was obtained primarily from published articles, some was collected in the form of interviews, questionnaires, and site visits. This publication details mine water geothermal system configurations, gives accounts of global case studies with a particular focus on challenges they have faced, and systematically groups and digests each of these, suggesting mitigations for each. The configurations and challenges detailed in this chapter are used as a framework for subsequent chapters.

Chapter 3 – This chapter was published in the Earth Science, Systems and Society Journal of the Geological Society of London.

Published as: Walls D.B., Banks D., Peshkur T., Boyce A.J. and Burnside N.M. (2022) Heat Recovery Potential and Hydrochemistry of Mine Water Discharges from Scotland's Coalfields. *Earth Sci. Syst. Soc.* 2:10056. doi: 10.3389/esss.2022.10056

This chapter outlines heat available (derived from temperature and flow rate) from mine water outflows present at the surface across the Midland Valley of Scotland. These are grouped into: sites pumped and/or treated by The Coal Authority; and untreated gravity drainages from mine workings, which when combined can provide 48 MW of heat energy. Hydrochemical analyses provides a proxy for subsurface mine water chemistry, useful for planning and mitigation during geothermal system deployment. Each of the outflows has been photographed and documented in the chapter appendices.

Chapter 4 – This chapter consists of a guidance document for the publicly available Mine Water Geothermal Resource Atlas for Scotland (MiRAS) hosted on the Improvement Service's Spatial Hub website:

<https://www.spatialdata.gov.scot/geonetwork/srv/eng/catalog.search#/metadata/63ccef-ed-0165-461d-a5a5-025b0b2463c5>.

This chapter presents an interactive map which depicts optimal areas across the MVS for MWG development. It explains why such a screening tool is necessary, where the input datasets were sourced and what limitations they have. It details how the input data were processed and the rationale behind labelling properties as favourable or unfavourable. It indicates areas, that according to application of evidenced screening criteria, are best placed for MWG development. It draws on three practical MWG field experiences to provide quality assurance of map outputs. The appendix of this chapter presents subsurface (MiRAS) and surface (included from Chapter 3) MWG resources for each of the 19 affected local authority areas.

Chapter 5 – This chapter has been accepted for publication in the *Scottish Journal of Geology* of the Geological Society of London.

Accepted as: Walls, D.B.; Banks, D.; Boyce, A.J.; Townsend, D. H.; Burnside, N.M. Combining ground stability investigation with exploratory drilling for mine water geothermal energy development. Lessons from exploration and monitoring.

This chapter explores how ground stability investigation (GSI) boreholes can be adapted to include MWG investigation work. It details the findings of a case study project in Dollar, Clackmannanshire, where GSI work was necessary for a housing development in close proximity to flooded mine workings. It was recognised that a potential MWG resource could be explored through similar processes, without much additional budget. The results of drilling into flooded voids, water chemistry, and changes in hydrogeology are all presented to inform the MWG system which may be developed on site. The lessons learned, which could influence other similar sites, are shared to promote good practice.

Chapter 6 – This chapter has been accepted for publication in the International Journal of Coal Geology.

Accepted as: Walls, D.B.; Boyce, A.J.; Banks, D.; Burnside N.M. The occurrence of elevated $\delta^{34}\text{S}$ in dissolved sulfate in a multi-level coal mine water system, Glasgow, UK.

Some of the stable O, H and S isotope data have also been briefly presented in:

Monaghan AA, Bateson L, Boyce AJ, Burnside NM, Chambers R, de Rezende JR, Dunnet E, Everett PA, Gilfillan SMV, Jibrin MS, Johnson G, Lockett R, MacAllister DJ, MacDonald AM, Moreau JW, Newsome L, Novellino A, Palumbo-Roe B, Pereira R, Smith D, Spence MJ, Starcher V, Taylor-Curran H, Vane CH, Wagner T and Walls DB (2022) Time Zero for Net Zero: A Coal Mine Baseline for Decarbonising Heat. *Earth Sci. Syst. Soc.* 2:10054. doi: 10.3389/esss.2022.10054

This chapter focusses on mine water chemistry, in particular stable isotopes of sulphur alongside oxygen and hydrogen from the British Geological Survey's mine water geothermal UK Geo-Energy Observatories site at Cuningar, SE Glasgow. Stable isotope samples were taken from multiple boreholes, at various stages of drilling, and from superficial, bedrock and mined coal horizons. The isotopic signature of sulphate-sulphur in mine water is different to that of the sulphide-sulphur in the bedrock. This chapter explores the potential sources of the different signatures, and what this means with regards to water sources within mine water geothermal systems.

Chapter 2 - A Review of the Performance of Minewater Heating and Cooling Systems

This chapter was published as: Walls, D.B.; Banks, D.; Boyce, A.J.; Burnside, N.M. A Review of the Performance of Minewater Heating and Cooling Systems. *Energies* 2021, 14, 6215. <https://doi.org/10.3390/en14196215>. As of 20th March 2023, this article has 6580 views and 8 citations.

Abstract

As decarbonisation of heating and cooling becomes a matter of critical importance, it has been shown that flooded mines can provide a reliable source of low-carbon thermal energy production and storage when coupled with appropriate demand via an appropriate heat transfer technology. This paper summarises the potential resource represented by a long legacy of mining operations, the means heat can be extracted from (or rejected to) flooded mine workings, and then considers the risks and challenges faced by minewater geothermal energy (MWG) schemes in the planning, construction, and operational phases. A combination of site visits, interviews and literature reviews has informed concise, updated accounts for many of the minewater geothermal energy systems installed across the world, including accounts of hitherto unpublished systems. The paper has found that a number of previously reported MWG schemes are now non-operational. Key risks encountered by MWG schemes (which in some cases have led to decommissioning) include clogging of system components with mineral precipitates (e.g., ochre), uncertainty in targeting open mine voids and their hydraulic behaviour, uncertainty regarding longevity of access to minewater resource, and accumulated ongoing monitoring and maintenance burdens.

2.1 Introduction

From the early days of quantitative geoscience, measurement of temperature in underground mines has proved a powerful tool in estimating geothermal heat fluxes, involving scientists such as Lord Kelvin, James Clerk Maxwell, Archibald Geikie, Charles Lyell and Joseph Everett (e.g. (Prestwich, 1887, Thomson *et al.*, 1871)). Pačes and Čermák (1975) recognised the geothermal potential of mines in the Czech Bohemian massif and used their observations in the development of chemical geothermometric tools. Indeed, one of those Czech mines (Svornost Ag-Co-As-U mine at Jáchymov) is now equipped with a small-scale geothermal heat pump system to extract heat from the minewater (Jirakova *et al.*, 2015, Novák *et al.*, 2011).

The feasibility of extracting heat from (or rejecting heat to) flooded mine workings has been demonstrated by operational projects in the USA, Germany and Canada since the 1980s (Jensen, 1983, Jessop *et al.*, 1995, Wieber and Pohl, 2008). Although this promising low-carbon heating and cooling source is available in numerous countries with a strong mining

legacy, many are yet to exploit the potential. There are several configurations of minewater geothermal energy (MWG) systems; the fundamental design involves removing heat from the water in abandoned flooded mines to provide low-carbon heating for a variety of users, often through district heating networks. In a typical system, heat is transferred from minewater to a secondary heat transfer circuit via a plate or shell-and-tube heat exchanger. Heat pumps are typically employed to upgrade heat from the secondary heat transfer fluid and deliver it at a suitable temperature to a customer. The heat pumps can be centralised at one or a few “energy centres”, distributing high temperature fluid to customers. Alternatively, in a distributed system, individual customers use heat pumps to extract heat from (or reject heat to) the low-temperature secondary circuit. Many MWG systems are thus a subset of well-established Ground Source Heat Pump (GSHP) technology (Banks, 2008, Banks *et al.*, 2004, Yang *et al.*, 2010). The use of a heat exchanger and secondary fluid avoids potential corrosion and/or mineral scaling issues caused by direct contact between minewater and the heat pump evaporator/condenser (Burnside *et al.*, 2016b).

Minewater can also be used for commercial or industrial cooling, whereby “waste” heat is transferred from buildings or industrial processes to minewater. Active cooling can be via use of heat pumps (as described above), but cooling may also be achieved via a “passive” heat exchanger, since minewater is often cooler than the spaces or processes to be cooled and the temperature gradient is favourable. Former mining sites are often redeveloped as commercial or retail facilities, thus the provision of cooling may be more important to customers than provision of heating. Some of the most complex schemes incorporate elements of both heating and cooling, and also provide an element of thermal buffering or storage, e.g. that in Heerlen, Netherlands (Verhoeven *et al.*, 2014).

Several previous articles have presented accounts of global MWG case studies (Banks *et al.*, 2004, Farr *et al.*, 2016, Preene and Younger, 2014, Ramos *et al.*, 2015, Wieber and Pohl, 2008). This paper draws on these and also presents newly established schemes to generate an updated review of installed capacity of MWG schemes, and comments on the current status of some widely referenced schemes. However, it also focusses on the installation and operational challenges encountered by the reviewed MWG systems, identifies the most common challenges and offers suggestions for best practice to overcome these.

2.2 Low-Carbon Energy from Coal Mines

The mining industry, and the fossil fuels it produces, have been two of the foundations of industrial growth and economic well-being. The industry has historically also been responsible for slavery (Barrowman, 1897), endangerment of workforces (Younger, 2004), problematic industrial relations (Glyn and Machin, 1997) and environmental degradation. The last category includes contaminating mine drainage (CMD), acid rain, smog, greenhouse gas emissions (Finkelman *et al.*, 2002), subsidence (Donnelly, 2020) and seismic events (Bishop *et al.*, 1993). People working in coal-producing areas were endangered by exposure to the products of coal combustion, contamination of potable aquifers by minewaters (Headworth *et al.*, 1980) and inhalation of coal dust (Finkelman *et al.*, 2002). Closure of coalfields created new environmental and socio-economic problems (Younger and Robins, 2002) as the sites became derelict. Old workings became liable to dust, solute and debris release from abandoned tailings, increased erosion potential and contaminated soils, surface subsidence risks and negative impacts on the local flora and fauna (Laurence, 2006). Many towns, communities and work forces around the mines were left without their primary source of employment (Younger, 2016).

Underground mines usually required ongoing pumping of inflowing water to maintain dry mining conditions. Their closure, cessation of pumping, and recovery of minewater toward pre-mining levels has presented one of the greatest challenges associated with the industry's downturn (Younger, 1995a, Younger and Adams, 1999). Subsequent risks of contaminated aquifers (Bailey *et al.*, 2016), CMD (Robins, 1990), watercourse pollution and ground instability (Andrews *et al.*, 2020) require monitoring and mitigation. Such mitigation often involves the continued abstraction of minewater to maintain acceptable water levels. This is associated with considerable pumping and treatment costs, but the pumped water can also represent a low-carbon geothermal resource for heating and cooling, which can offset these costs and potential environmental liabilities (Banks *et al.*, 1997, Verhoeven *et al.*, 2014). A summary of progression from active coal production to repurposing for MWG is depicted in Figure 2.1.

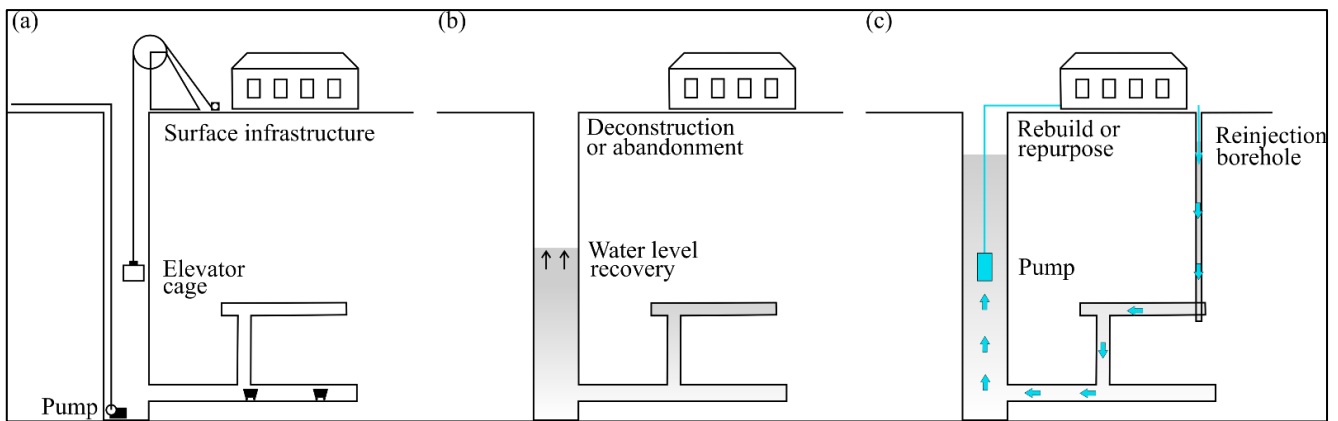


Figure 2.1 Schematic representation of the history of a mine, from (a) active mining with pumped dewatering; through (b) post-abandonment flooding; to (c) repurposed as a MWG system.

Minewater resources do not host high enough temperatures to generate electricity (Kaczmarczyk *et al.*, 2020), but they offer low enthalpy resources for space heating in new-build or retrofitted buildings, usually when coupled with heat pump technology and shared heat networks (Banks *et al.*, 2004). Minewater as a heat resource typically exhibits more stable year-round temperatures than other environmental heat pump sources – river, air or shallow soil (Banks, 2008). A comparison is shown in Figure 2.2, whereby minewater discharge temperatures from the South Wales coalfield are plotted against fluctuating atmospheric temperature from the nearby town of Neath, South Wales. The temperatures in shallow mines may be influenced by the ground/atmosphere interface and temperatures are often close to, or a little above, the annual average soil temperature (10-12°) (Banks, 2008). Deeper minewater is influenced by the geothermal gradient of surrounding rocks, which averages 28 °C/km in UK coal fields (Farr and Busby, 2020).

The use of minewater in heat exchange or heat pump systems presents its own set of hydrochemical challenges because of the water-rock interaction processes occurring in the mining environment. The pH of minewaters can vary widely (Banks *et al.*, 2002b), and some deep mines contain highly reducing (methane, hydrogen sulphide-rich), saline waters (Burnside *et al.*, 2016b). Many metal mines yield extremely acidic, metal- and sulphate-rich CMD, often due to the intensive oxidation of sulphide minerals. Coal mines can contain both these water types, but are often characterised by a more circumneutral water, typically with a high loading of dissolved iron (Fe^{II}) and manganese (Mn^{II}) which can precipitate as an oxyhydroxide sludge when exposed to oxygen (Burnside *et al.*, 2016a). Such oxidation and precipitation is often deliberately encouraged when coal minewater is treated prior to release in the environment (Younger, 1995a, Younger and Adams, 1999), but is undesirable within a heat exchanger or minewater borehole (Bailey *et al.*, 2016).

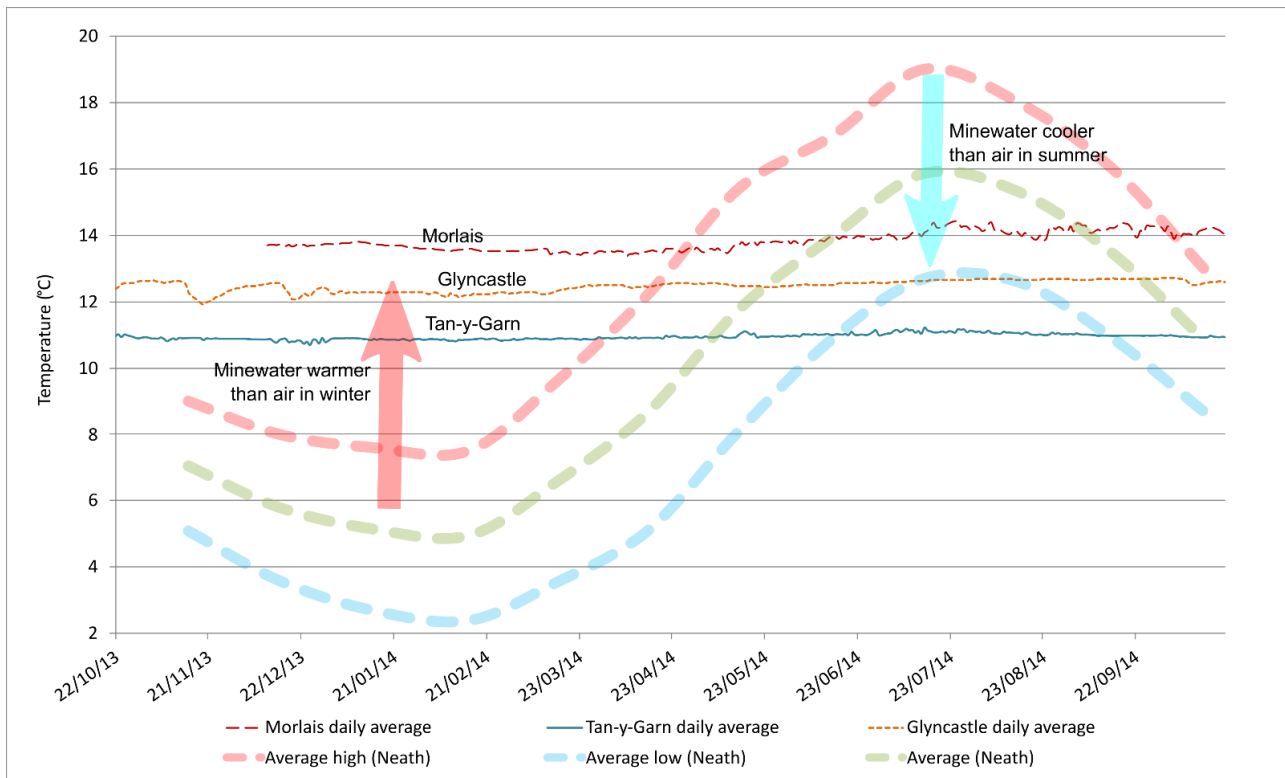


Figure 2.2 Temperatures of minewater in South Wales, presented as daily averages of half-hourly data recorded in surface outflow point, compared with monthly average high/low air temperatures for Neath in the period 1961-1990 (from <https://en.wikipedia.org/wiki/Neath>, based on Meteorological Office data). Note that the Tan-y-Garn minewater (3.9849°W 51.7696°N; (Taylor *et al.*, 2016a, 2016b)) temperature is a little higher than annual average air temperature, while the increasing temperatures at Glyncastle (3.6889°W, 51.7119°N) and Morlais (4.0680°W, 51.7004°N) and are believed to be due to increasing depth of minewater derivation. Minewater data provided by Gareth Farr of the British Geological Survey, with thanks, as reported in Farr *et al.* (2016).

By overcoming the challenges facing MWG systems and implementing widespread installation of these systems, the geothermal sector could provide a fitting new purpose for abandoned mines in pursuit of a lower carbon future (Adams *et al.*, 2019). Current challenges include: sourcing funding or capital investment; obtaining timely permissions for planning; abstraction and disposal from regulatory agencies; engineering technicalities around system design; the management of water chemistry and identifying just and sustainable economic and management models for selling heat and cooling. MWG systems can facilitate a significant drop in carbon emissions and beneficial economics (Preene and Younger, 2014) when compared to hydrocarbon-based heating alternatives (Jessop *et al.*, 1995), and present a sustainable heat supply if managed correctly (Verhoeven *et al.*, 2014).

2.3 Types of Minewater Geothermal Energy Systems

During planning and installation of a MWG system, consideration of physical and chemical parameters is important to determine the optimal mode of heat extraction. Open and

closed loop systems suit different scenarios depending on parameters including, size of the resource and demand, expected flow rate, water chemistry, and thermal conductivity of host rocks (Banks *et al.*, 2019). The configurations are presented in Figure 2.3 and explained below.

2.3.1 Open System

Open systems describe the practice whereby minewater is brought to the surface via gravity drainage or pumping. A shell-and-tube or plate heat exchanger transfers heat between the minewater flow and a secondary heat transfer fluid serving a thermal demand, often via a heat pump array (Korb, 2012). It is thus a type of groundwater-sourced heat pump system (Novák *et al.*, 2011). Flooded mine systems are especially attractive, as open and highly interconnected networks of mine workings create productive “anthropogenic” aquifers yielding large, pumped discharges. Because advection of heat with minewater flow is a highly effective form of heat recovery (50 L/s of cool minewater can readily yield 1 MW of heat energy), open systems typically offer higher potential thermal outputs than their closed loop alternatives (Banks, 2008). Open systems can be further subdivided as follows.

2.3.1.1 Open system with reinjection

Other geothermal systems (Hot Sedimentary Aquifers (HSA) and Hot Dry Rock (HDR) (Lund and Boyd, 2016)) use this concept as an efficient means of exploiting a thermal resource, as it conserves water resources and reservoir pressures by returning thermally “spent” water to the aquifer, and avoids the risk of contaminated discharge and the need to treat discharged water (Banks *et al.*, 2019). A system comprising an abstraction well – heat exchanger – reinjection well is termed a geothermal well doublet. A good understanding of subsurface flow pathways between the wells of a doublet, and of the potential for rock-water heat exchange along such pathways (Banks *et al.*, 2003, Loredó *et al.*, 2017a), is key to the sustainability of such systems. Potentially, the migration of a cold front from a reinjection well could be relatively rapid, and lead to thermal “feedback” if the abstraction and reinjection wells are located in the same worked seam (Harnmeijer *et al.*, 2017) (hence the desirability of separation). The rate of cold front advance will depend largely on the geometry and dimensionality of the mine void space and the degree of thermal exchange with the rock matrix (e.g., on whether voids are open or filled with waste). Long and tortuous flow pathways are preferred since mine roadways and voids can have low surface area-to-volume ratios and rapid water flow, with relatively low heat exchange per metre of flow pathway (Loredó *et al.*, 2017a). Conversely, if the intended flow pathway between wells is not of suitable permeability, the

minewater resource can become depleted around the abstraction wells, with elevated head and possible surface break-out around the reinjection well (Banks *et al.*, 2009). Abstraction and reinjection from different (but connected) mine horizons, or flow pathways via collapsed longwall goaf (Liu *et al.*, 2021, Yang *et al.*, 2018, Zhang *et al.*, 2016), can both be strategies for attaining protracted flow pathways in a well doublet with a high degree of thermal water-rock interaction, but both scenarios are subject to considerable predictive uncertainty. The capital costs of drilling abstraction wells into mine voids can be high (and increase disproportionately with depth), especially if multiple reinjection wells are required. Heat exchangers and injection boreholes can be highly susceptible to mineral precipitation and clogging and require good design, regular monitoring and a potentially costly program of ongoing maintenance to maintain injectivity.

2.3.1.2 Open system with discharge

In this case, following heat exchange, the thermally spent abstracted minewater is simply disposed of at surface to the ocean or local watercourse (Bailey *et al.*, 2013, Burnside *et al.*, 2016a, Loredó *et al.*, 2017b). Monitoring will usually be required to demonstrate that the water quality and temperature of the discharge comply with environmental regulations (Loredó *et al.*, 2017b). Often, to achieve a compatible quality with the local water bodies, the minewater will need to be passively or actively treated (Bailey *et al.*, 2016, Banks and Banks, 2001). Passive treatment usually employs gravity and natural materials in aeration cascades, settlement lagoons and aerobic wetlands to oxidise and remove iron and neutralise pH. Active treatment may have elements of the same infrastructure, but includes the use of electrical pumping, oxidising agents or alkalis to oxidise ferrous iron or raise pH (Bailey *et al.*, 2016) and filtration. Anaerobic treatment systems are also feasible. Open system with discharge avoids expenditure of drilling and maintaining reinjection boreholes, however, ongoing expenditure and/or large land areas may be required for treatment (Bailey, 2016, Banks, 2003). In arid climates, or where recharge to the mine is limited, there is also the risk that the minewater resource may be depleted with time. In countries (such as the UK, Poland or Spain) where minewater is deliberately pumped to manage water levels and avoid surface or aquifer contamination, the pumping and treatment costs may already be covered, and installing a MWG system becomes economically favourable, potentially recouping some of the expenditure on pumping and treatment (Hall *et al.*, 2011).

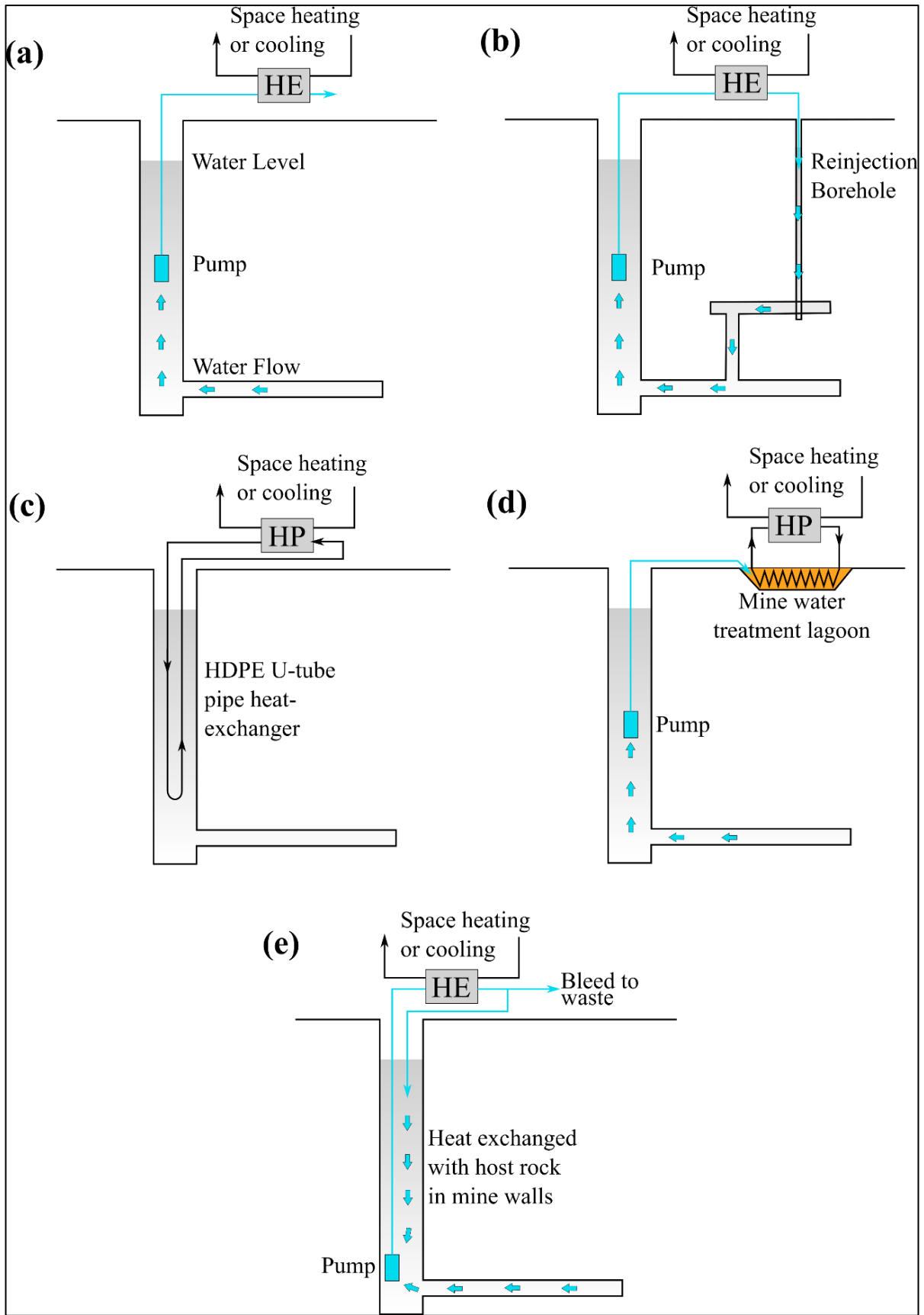


Figure 2.3 Configurations of Minewater Geothermal Energy Systems: (a) Open system with discharge; (b) Open system with reinjection; (c) Borehole closed loop; (d) Surface closed loop; (e) Standing column. Edited from (Banks *et al.*, 2019) with permission from © David Banks.

2.3.1.3 Gravity drainage systems

In 2000, Younger (2000a) highlighted that across the UK, there were over 400 ferruginous gravity discharges from coal mines. Bailey et al (2016) confirmed in 2016 that there are still several hundred discharges which are unmonitored in the UK. Of the monitored gravity drainage treatment sites in the UK ($n = 21$), the mean temperature is 11.5 °C, ideal for cooling purposes and also for heating via the use of a heat pump. Using such a gravity-fed minewater discharge, where it coincides with a thermal demand, avoids the capital expenditure required for drilling an abstraction well.

2.3.2 Closed Loop

Here, a secondary heat transfer fluid is circulated through heat exchange pipes submerged in minewater within a shaft, tunnel or borehole, absorbing available heat without abstracting the water. The heat transfer fluid is then typically circulated to a heat pump, where the heat is extracted and the newly chilled fluid returned to the submerged heat exchange network (Banks *et al.*, 2004).

Low maintenance or problematic minewater chemistry can be deciding factors for installation of closed loop over an open system. Accessing the heat reservoir without extracting the water leaves minewaters unable to corrode or clog any heat pump or heat exchanger (Banks *et al.*, 2004). A closed loop system typically requires fewer, if any, environmental permits. On the negative side, closed loop systems typically deliver relatively limited quantities of heat (maybe several 10s of kW; e.g. the 70 kW scheme at Auguste Victoria, Germany (Bracke and Bussmann, 2015)), due to the conductive heat processes limiting heat transfer from the minewater to heat transfer fluid. Open system minewater extraction, where heat is moved with water by advection, typically deliver far higher loads: pumped flows in excess of 100 L/s can deliver several MW of heating (e.g. at Mieres, Spain (Loredo *et al.*, 2017b)).

2.3.2.1 Surface Closed loop

Pumped discharge or gravity drainage sites, which employ passive minewater treatment, often host aeration cascades and lagoons which facilitate oxidation and precipitation of dissolved minerals (Bailey *et al.*, 2016). Closed loop heat exchange pipes or panels can be submerged within such treatment lagoons, as at Caphouse, UK (Banks *et al.*, 2019, Burnside *et al.*, 2016a). Consideration must, however, be given to whether such heat exchangers will allow maintenance or desludging of lagoons, or whether accumulated sediment or ochre will interfere with their heat exchange ability (Burnside *et al.*, 2016a).

2.3.3 Standing column

Standing column technology is a means to exploit an open mine shaft for removal of heat without high capital expenditure associated with borehole drilling. Pumping and reinjection of the minewater at separate depths within the same water column requires a modest abstraction rate to avoid thermal feedback, or sufficient groundwater throughflow to replenish the heat resource in the shaft (Burnside *et al.*, 2016b). Open shafts provide access to a large volume of water in the mine workings and are engineered to remain open indefinitely (Younger and Adams, 1999), which brings extended life to the source. Hybrid systems are also possible, where part of the pumped water flow is returned to the shaft, while part is “bled off” and discharged to a surface recipient (Banks *et al.*, 2017).

2.4 Data Collection Methods

The global uptake of MWG systems has been relatively slow (Preene and Younger, 2014). The first examples of installation were developed in the 1980s (Korb, 2012), but the authors found evidence for fewer than 50 known cases harnessing this resource, many of them only at pilot scale, and many are no longer operational.

To gain a global overview of the current status of MWG systems, we have systematically gathered information via the following methodologies:

- Literature review (Hall *et al.*, 2011, Preene and Younger, 2014, Ramos *et al.*, 2015, Watzlaf and Ackman, 2006)
- Where possible, written or telephone interviews with researchers, consultants or operators of MWG schemes
- Visits or personal experience of research on MWG schemes

For each scheme, the following information has been systematically collected:

- a) Location and name
- b) Type of mine
- c) Size of scheme (kW or MW peak/installed capacity)
- d) Purpose of scheme

- e) Current status of scheme and a description of main challenges encountered when developing or operating.

A short summary of each reviewed scheme is provided under the corresponding country sub-section in the Results, and the main challenges encountered have been abstracted, analysed and summarised in Table 2.2. For each scheme, the main source of information (L = literature, I = interview, V = personal visit / experience) has been identified.

2.5 MWG Systems Status Results

2.5.1 The United Kingdom

Shettleston Housing Association [L,V] constructed a coal minewater scheme in 1999 in eastern Glasgow, UK (4.1668W, 55.8504°N). A borehole abstracts up to an estimated 3 L/s minewater from relatively shallow coal workings and passes it directly through two heat pumps with a combined heating capacity of 65 kW, supplying heat to a 16-unit social housing complex (Banks *et al.*, 2009, SUST, 2006). The thermally ‘spent’ water is reinjected via a borehole, 37m away (Banks *et al.*, 2019), making it an “open system with reinjection” configuration. The abstraction and reinjection horizons and depths are not definitively known; the abstraction horizon is thought to be coal workings of the Glasgow Ell (or adjacent) seam (Banks *et al.*, 2019); the reinjection horizon may be coal workings, or permeable sandstones within the Carboniferous Coal Measures. The system initially used minewater as “grey water” for the apartments, but iron staining of sanitary ware led to this being discontinued. The heat pump system ran for much of its lifespan with few operational challenges. The inline filter required regular cleaning as the water occasionally contained ochre flocs and sediment already when abstracted, especially after heavy rainfall (Banks *et al.*, 2019). Currently, the Shettleston scheme is unused. Walls *et al.* (2020) explain that the accumulated burden of maintaining the system and identifying contractors who could manage a number of issues (clogging of the reinjection borehole, miscommunication between electrical control units, build-up of ochre in pipework and loss of pressure) proved to be a greater commitment than the Housing Association were ultimately able to sustain. The discontinuation of this system was thus not due to any single “fatal flaw” but to a combination of more minor issues (both physical and chemical in nature) and the perception that the maintenance requirements of such a small system were difficult to justify.

The **Lumphinnans** [L,I,V] minewater heating system was constructed in 2000 following success at Shettleston. Located at Ochil View, Lumphinnans, Fife, UK (3.3332°W, 56.1209°N), it supplied heat to a refurbished 18-unit social housing complex. Its design and size were similar to Shettleston. The open system with reinjection configuration abstracted minewater (estimated up to 3 L/s) from the Diamond/Jersey coal seam at 172.5 m depth, the reinjected waters were to a shallower borehole 100 m away. The system initially worked well; however, free cascading of thermally spent minewater into the reinjection borehole allowed oxygenation and precipitation of ochre that eventually clogged it up (Banks *et al.*, 2009). Lumphinnans minewater system has been decommissioned and has since been replaced by gas boilers.

The **Markham minewater scheme** [L,V] is located at Markham No. 3 shaft, near Bolsover, Derbyshire, UK (1.3285°W, 53.2424°N). It is a relatively small (20 kW) heat pump scheme, supplying heat to a small company office complex, and also pre-heating gas engines for rapid start-up, the purpose of which is to generate peak load electrical supply for the national grid (Athresh, 2017, Athresh *et al.*, 2015, 2017, Banks *et al.*, 2019). The heat source is minewater from a deep coal mine shaft, which is pumped through a shell-and-tube heat exchanger connected to the heat pump, and then returned to the same shaft at a different depth in a standing column arrangement (Burnside *et al.*, 2016b). The system has functioned well, with negligible problems of heat exchanger clogging noted (presumably due to the reducing, oxygen-free nature of the water) (Burnside *et al.*, 2016b). As minewater levels in the mine system are still rising rapidly post-closure, the abstraction – reinjection arrangement has been raised in the shaft as minewater levels have risen. The main challenge has been the high submersible pumping energy costs, due to the deep minewater level in the shaft, which has eroded the overall energy efficiency of the scheme (Banks *et al.*, 2019). As minewater levels continue to rise, however, energy expenditure on pumping would decrease and the overall efficiency improve. The current status of the scheme is unknown.

Two pilot (research) systems have been combined at the former **Caphouse** [L, V] colliery, now housing the National Coal Mining Museum of England, located at Overton, near Wakefield, Yorkshire, UK (1.6251°W, 53.6416°N). The 10 kW capacity heat pump could be coupled to one of two available heat exchanger systems: (i) direct shell-and-tube heat exchange with a portion of the minewater pumped from the Hope Shaft for the purposes of regional minewater level control (open system with surface discharge), (ii) a closed loop heat exchange unit submerged in the first aeration pond of the minewater treatment system (Burnside *et al.*, 2016a). These provided space heating to one of the nearby museum exhibit buildings. The iron

content of the pumped minewater had already begun to oxidise and form ochre flocs on abstraction. This meant that the in-line minewater filters on the open system required cleaning of ochre deposits up to several times per day (Banks *et al.*, 2019), although the shell-and-tube heat exchanger itself experienced remarkably little scaling (Banks *et al.*, 2019). The closed loop system operated without significant maintenance issues and was preferred by the operational staff. The system is current non-operational following the research phase.

The Coal Authority treatment site at the old **Dawdon** [L,I,V] Colliery, County Durham, UK (1.3313°W, 54.820114°N) pumps and actively treats minewater at rates up to 150 L/s before discharge to the sea, to prevent contamination of an overlying drinking water aquifer (Bailey *et al.*, 2013, The Coal Authority, 2018). In April 2011, a pilot system was installed where c. 1 L/s of treated (aerated) minewater was passed through a shell and tube heat exchanger, transferring heat to a 12 kW heat pump providing heating for the treatment facility building (Bailey *et al.*, 2013). Throughout the first year of operation, the in-line filter and heat exchanger clogged with ochre deposits which restricted flow and decreased efficiency, despite the water hosting <1 mg/L total iron. The system was reconfigured using the same hardware, but using untreated minewater, with 71-74 mg/L total iron. This was successful: the use of unaerated, reducing raw minewater prevented dissolved iron from oxidising and precipitating and, after seven months there were no reports of ochre clogging of the heat exchanger (Bailey *et al.*, 2013). The pilot system at Dawdon is currently operational. The Coal Authority (CA), Durham County Council and Tolent Construction are implementing ambitious plans to use the entire pumped minewater flow (150 L/s at 19 °C) to develop and supply up to 6 MW heat to a 1500 house ‘garden village’ (The Coal Authority, 2020).

At **Abbotsford Road, Gateshead** [I,V] (1.5557°W, 54.9544°N) an open system abstraction-reinjection scheme has been developed with the intention of heating a beverage warehouse facility, via 2.4 MW installed heat pump capacity (Steven, 2021b). It is thus a large private system with a dedicated customer. The scheme currently consists of three 110-120 m deep abstraction wells into Coal Measures sandstones (i.e. not mine voids) and three deeper (155 m) boreholes to reinject thermally spent water to the level of the High Main coal seam workings (Steven, 2021b). The scheme was intended to produce around 100 L/s water, but is only licenced for 49 L/s and is currently only able to produce 30 L/s at c. 11 °C from one of the three abstraction wells (the other two having low yields). Two of the three reinjection wells have sufficient capacity to accept the reinjected water. The scheme is, however, fully licensed and operational at this reduced capacity (Steven, 2021b). The main challenges faced by the scheme are as follows: (i) insufficient yield to operate at full capacity, (ii) slowly declining

yield during operation, requiring periodic cleaning of plate heat exchanger to remove precipitated ferric hydroxide, by circulation of either citric or oxalic acid to restore capacity (Figure 2.4), (iii) technical issues with maintenance of heat pumps, (iv) cessation of trading from the original consultant on the scheme, with loss of hydrogeological knowledge and information (Steven, 2021b).

Some 700 m to the NW, at **Nest Road, Gateshead** [I,V] (1.5635°W, 54.9584°N), the same operator has constructed another abstraction-reinjection scheme with the intention of heating a beverage warehouse facility, via 1.2 MW installed heat pump capacity (Steven, 2021b). The scheme currently consists of one 130 m deep abstraction borehole from the level of the High Main coal seam workings and one 280 m deep reinjection borehole accessing deeper workings down to the Harvey-Beaumont seam (Steven, 2021b). Two other drilled boreholes failed to access significant additional capacity. The abstraction well is capable of producing the required 60-70 L/s water, although the reinjection well has hitherto only been tested at c. 40 L/s. The scheme currently has a temporary licence to operate from the Environment Agency (Steven, 2021b). The main challenges faced by the scheme are as follows: (i) the reinjection capacity of the scheme has yet to be fully demonstrated, (ii) extended timeframe and requirements to obtain full licence from Environment Agency, and heat access agreement from The Coal Authority, (iii) cessation of trading from the original consultant on the scheme, with loss of hydrogeological knowledge and information. The degree of thermal interference between the two Gateshead schemes has yet to be empirically demonstrated (Steven, 2021b).

The minewater heating scheme in **Crynant** [L,I], employs a 35 kW heat pump to heat a large farmhouse, farm workshops and an adjoining physiotherapy centre in West Glamorgan, UK (3.7486°W, 51.7244°N). The abstraction borehole accesses mine workings from the Cwmnant Colliery at 63 m bgl, whereby water is pumped at c. 2 L/s at a constant 11.5 °C (Farr *et al.*, 2016, Manju, 2020). The system employs a 63.9 m deep reinjection borehole, approximately 60 m away from the abstraction borehole, to complete the open system with reinjection, (Manju, 2020). Data pertaining to water chemistry, temperature, water level, electricity consumption were all collected during onsite monitoring. Some cleaning of the heat exchanger was required after a winter cycle (Manju, 2020), since then the system has faced further ochre build up, partially blocking the submersible pump and pipework. As a result, the system has reported higher electricity consumption and subsequent costs (Hopkins, 2021). Following removal of the pump from depth, the system is currently non-operational (Hopkins, 2021).

Full scale test pumping at rates of up to 50 L/s and with heat extraction of over 100 kW heat was carried out at the 256 m deep Florence haematite mine shaft at **Egremont, Cumbria [L,V]** (3.5177°W, 54.4784°N). A hybrid standing column system was trialled with disposal of part of the thermally spent pumped minewater to a surface recipient and part being recirculated back to the pumping shaft. Significant (MW scale) thermal potential was suggested by the trial. No system has been commissioned at the shaft, due to lack of clearly identified heat demand, and pending the demonstration of acceptable environmental impact, safe water disposal and agreement between owning / operating parties. Dissolved iron did not occur in significant amounts in the pumped water and no scaling or clogging issues were noted (Banks *et al.*, 2017).

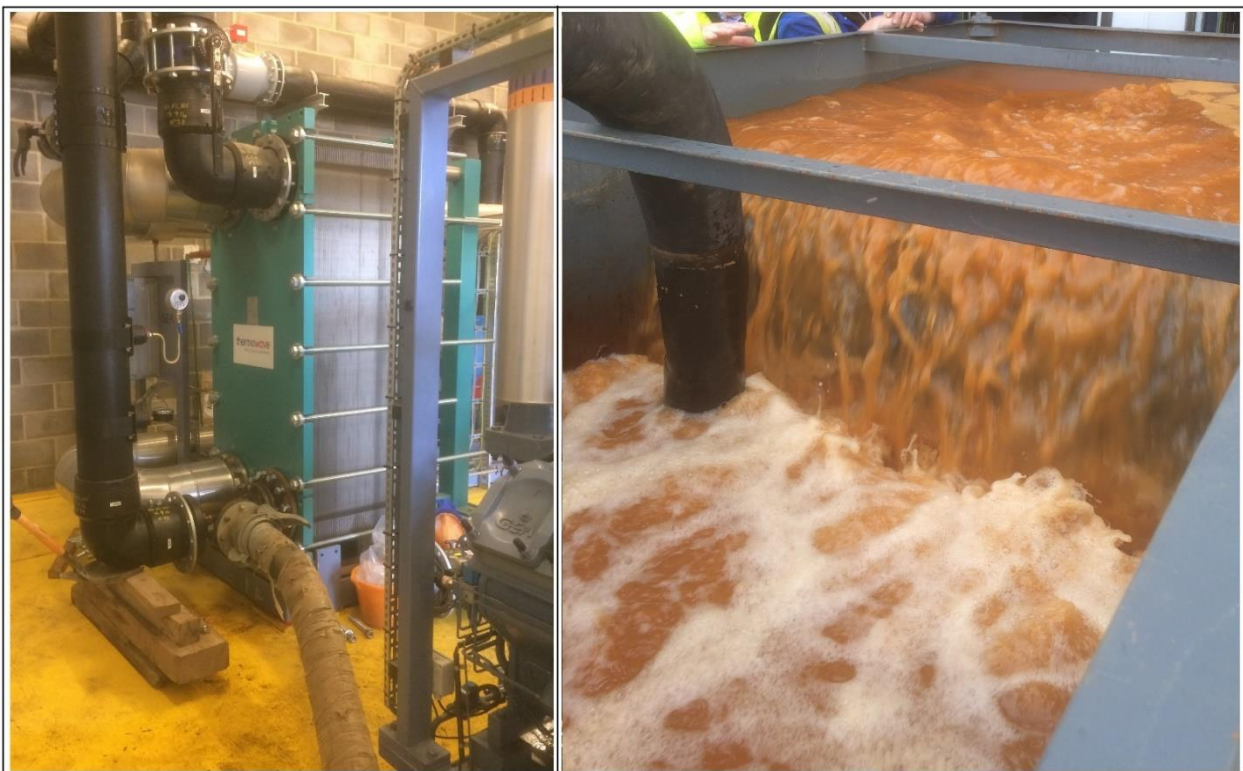


Figure 2.4 Periodic recirculation of citric acid solution through the plate heat exchanger at Abbotsford Road, Gateshead, UK (left), to remove accumulated ochre (which can be seen in the recirculation tank, right). Photos reproduced with permission of © David Banks, after (Banks, 2021)

2.5.2 Norway

At the historic **Folldal [L,I]** Cu-Zn-S mine in central Norway (Bjerkgard and Bjorlykke, 1996) (9.992°E, 62.1410°N) a closed loop system of 18 kW heating capacity was installed to provide heating for the underground Wormshall cavern, used for concerts and banquets. It would employ a 600 m long, 50 mm diameter pipe to collect heat from the 600 m deep flooded shaft, coupled to a heat pump to provide warm air at 22 °C (Banks *et al.*, 2004). The system came offline c. 2011, to be replaced by a standard air-to-air heating system (Johnsrud, 2021).

A similar system was installed as described by Banks *et al.* (2004) at the **Kongsberg** [L,I] silver mine in southern Norway (9.6004°E, 59.6302°N) (Banks *et al.*, 2004, Kotková *et al.*, 2018). The system can provide 12 kW of heating to the underground banqueting and concert hall (the 'Festsalen'), via a closed loop system whereby an anti-freeze solution is circulated through a 130-250 m long polyethene collector loop in the main shaft. The current status of this system is operational (Berg, 2021). The system is reported to have run unproblematically since installation, and the closed loop configuration was preferred (over an open system) due to the unfavourable chemical nature of the metal mine's water (Banks *et al.*, 2004).

2.5.3 Russia

Minewater was reportedly first used in Russia for heat production at **Osinnikovskaya mine** [L] (87.414°E, 53.646°N) near the Siberian city of Novokuznetsk, in the Kuznetsk coal basin (Kuzbas). A 130 kW heat pump was used to extract heat from minewater and supply it at 45 °C to the mine's administrative buildings (Gasho, 2017, Zakirov, 2013).

In the eastern Donetsk coal basin (Donbas) of southern Russia, several minewater drainage stations are in operation to control and treat coal minewater levels: Sholokhovskaya, Tatsinskaya (together 119 L/s or 430 m³/hr), Kirov (390 L/s or 1400 m³/hr), Glubokaya and Yuzhnaya (Oblast', 2014). The deep mines and relatively high minewater temperatures make heat recovery from the water in attractive option, though hitherto only implemented at a single locality - Novoshakhtinsk in Rostov oblast'.

Cherni (2011) describes the pilot heat pump scheme at **Novoshakhtinsk** [L], Rostov oblast' (39.9339°E, 47.7478°N) (Dmitrienko *et al.*, 2019). Here, minewater heat pumps are used to supply two hospitals, two schools and a kindergarten. Minewater is pumped from 390 m depth via a drilled well at 18-23 °C at a rate of around 28 L/s. Two heat pumps, each of capacity 384 kW, provide hot water at 65 °C to a 2.5 km district heating network. The minewater temperature is dropped by 5-8 °C and the water reinjected to a different horizon of the mine workings at 50 m depth (Fursova, 2012). Three 2 MW back-up gas boilers are available when outdoor temperatures fall well below zero (Dmitrienko *et al.*, 2019). The cost of the heat pump scheme is reported at 160 million rubles (5.7 million USD at 2011 rates), with a projected 7 year payback. The 2011 paper (Cherni, 2011) reports a significant planned expansion of the scheme.

Dmitrienko *et al.* (2019) indicate the potential of other mines in the area, for example the Glubokaya (Deep) mine, in Shakhty city (40.3244°E, 47.7244°N), which pumps up to 258

L/s water with a temperature in excess of 19 °C. To date, no investors have been forthcoming due to the mine being over 2 km from the nearest locus of demand.

2.5.4 Spain

The 3.9 MW system installed in **Mieres** [L,V], Asturias, Northern Spain (5.7747°W, 43.2428°N) is a well-functioning, well-reported example of the scale of heating and cooling provision which can be achieved through MWG energy. It delivers heating and cooling to public buildings via two 352 kW heat pumps at a university, one 652 kW and two 1.2 MW heat pumps at a hospital and a 100 kW heat pump operating at the Asturian Energy Foundation (FAEN) (Loredo *et al.*, 2017b). Water is pumped, using four submersible pumps, at a rate of around 100 L/s from the 362 m deep Barredo coal mine shaft, in order to control minewater levels in the regionally interconnected complex of workings (Lara *et al.*, 2017, Loredo *et al.*, 2017b). The pumped minewater temperature is around 23 °C (Banks, 2017, Banks *et al.*, 2019). The majority of the minewater flow is passed through an array of shell-and-tube heat exchangers (Figure 2.5), where heat is exchanged with an intermediate heat transfer fluid circuit, running around 1.9 km to the heat pumps in the plant room of the Álvarez Buylla hospital. The ratio (heating and cooling provided) / electricity consumed for the hospital system was reported as between 7.6 and 7.9 in the years 2015-16 (Fernandez, 2017). A smaller portion of the minewater is directed to the University plant room, where heat is exchanged via plate heat exchangers and thence to the University's "Edificio de Investigación" heat pump array. Following heat exchange, all the minewater is discharged to the Rio Caudal river, which classifies the scheme as "open system with discharge". The minewater chemistry is relatively mineral-rich (mean total dissolved solids 1200-1400 mg/L), but iron-poor (mean iron 1.1 to 1.6 mg/L depending on depth of pumping), and is consistent throughout the connected mine system (Loredo *et al.*, 2017b). The iron content has caused some minor issues with clogging of the University plate heat exchangers, which were able to be disassembled, cleaned and returned to service (Loredo *et al.*, 2017b). The shell-and-tube heat exchangers have hitherto appeared less prone to clogging issues. The mine system is being explored for Underground Pumped Hydroelectric Energy Storage and Compressed Air Energy Storage plants in addition to the established MWG scheme (Menendez and Loredo, 2020).



Figure 2.5 (left) Shell-and-tube heat exchangers between minewater and secondary circuit to hospital, Barredo shaft-top building; (right) minewater to secondary circuit plate heat exchangers. University plant room. Photos by © David Banks.

2.5.5 The Netherlands

The scheme in **Heerlen** [L,V], The Netherlands (5.9557°E, 50.9168°N) was developed in phases. In around 2005, five wells (two “hot” wells to 700 m depth with water temperatures of c. 28 °C, two “cold” wells to c. 250 m depth and 16 °C and one intermediate well to 350 m depth for return of thermally spent water) were drilled into abandoned, flooded workings of the Oranje Nassau collieries with the intention of supporting district heating and cooling in the suburb of Heerlerheide. The minewater, especially from the hot wells, was potentially corrosive due to its salinity (electrical conductivity at c. 7300 $\mu\text{S}/\text{cm}$) and reducing nature (Eh 45-65 mV), and also contained dissolved iron. Issues with water quality were overcome by excluding contact with oxygen, careful selection of materials and provision of pipeline “pigs” for scale removal (Minewater-Project, 2008). Modelling work (e.g. (Ferket *et al.*, 2011)) suggested, however, a significant potential for thermal feedback within the mine system, so the system was reconceptualised with a greater emphasis of thermal storage (i.e. reinjecting heat or “coolth” back to the mines at appropriate temperatures and depth). The system has evolved to become a 5th generation district heating and cooling network using the mine workings as a thermal buffer (Verhoeven *et al.*, 2014), thus greatly reducing the risk of over-abstraction and subsequent exhaustion of the heat resource (Verhoeven *et al.*, 2016). In such a concept, a (primary) minewater spine delivers warm or cool minewater to consumer clusters, where heat stations use passive heat exchange or heat pumps to supply (secondary) cluster-level district heating or cooling networks (DHCN). At each individual property, tertiary heat exchangers exchange heat or coolth between the building and the DHCN (Verhoeven *et al.*, 2014). Energy

recipients include more than 300 dwellings, a college, a hotel, a sporting centre, and several office buildings, one of which features a datacentre (Verhoeven *et al.*, 2016). Among some of the technical challenges reported were multiple failures of pressurised pipework buffers following installation, since incorrect nitrogen pressure was not recognised by the contractor; and the importance of this parameter had not been well communicated by the supplier. A flooding incident in April 2014 saw the cold-water production well cause significant water damage in the operations room basement. Pressure peaks and a leaking gasket were identified as the main cause, exacerbated by a lack of safeguards (Verhoeven *et al.*, 2016).

2.5.6 Poland

The pilot-scale scheme at the ARMADA housing development in **Bytom, Poland** [L,V] (18.9049°E, 50.3355°N) was constructed near the outfall of the discharge pipe for minewater pumped from the Ewa shaft of the Szombierki Colliery (Figure 2.6). The colliery required dewatering at a rate of at least 3,000 L/min at 24-25 °C to provide protection to neighbouring collieries (Hyria, 2017). A small proportion of the minewater was led off the main outfall pipe and through a plate heat exchanger coupled to a c. 9 kW heat pump, providing heat to the site offices of the ARMADA development company. The spent minewater was led back to the main discharge. The scheme was thus of the open, pump-and-discharge type, with minewater being discharged to a lake and thence to the Bytomka River. The water quality was relatively good and required no treatment (Hyria, 2017). The system's current status is operational (Janson, 2021). The main challenge faced by the scheme, and indeed the reason why it was not fully developed for the entire housing complex, was the lack of any guarantee from the mine dewatering agency of the continued supply of minewater from Szombierki mine (Janson *et al.*, 2017). The relocation of pumping from Szombierki to the adjacent Centrum mine has been delayed from 2020 to 2022-2023 (Janson, 2021). Additionally, there are some indications that the plate heat exchanger was under-sized, leading to significant temperature loss between the minewater and the secondary heat transfer fluid (Hyria, 2017).

At the offices of **CZOK** (the mine dewatering authority of the Upper Silesian coalfield in Poland) in **Czeladz** [L,I], a demonstration minewater heat pump project was installed around 2011-2013. The offices are located at the site of the shafts of the Saturn coal mine (19.0926°E, 50.3019°N), which requires dewatering to protect adjacent mines from flooding (Tokarz and Mucha, 2013). Water is pumped from the Pawel shaft of Saturn mine at a rate of around 416 L/s (Janson, 2021) at a temperature of 13-15 °C. The mine workings extend to 400 m below

sea level, but the pumps are located at around 210 m depth (c. +70 m OD). The water is derived from both mined coal strata in the Carboniferous sequence and roof leakage from the overlying Triassic aquifer. The low water temperature suggests that much of the water has a relatively shallow source. The water has a pH of 7.3 and a total mineralization of 1186 mg/L but does contain elevated iron and manganese (6 mg/L Fe and 1 mg/L Mn), which has caused issues with ochre precipitation in minewater pipes. A portion (5-6 L/s (Karpiński and Sowizdżał, 2018)) of the pumped water is, therefore, directed to a treatment plant (comprising aeration and filtration) to remove excess iron and manganese and thence to plate heat exchangers, connected to two 59 kW heat pumps, supplying heating and cooling to the CZOK offices, following which the pumped water is discharged to the Brynica river. The current status of the project is operational.



Figure 2.6 The pumped mine water discharge from Ewa shaft in Bytom, Poland (left), and its outfall into a lake within the ARMADA housing development complex (right). Photos reproduced with permission of © David Banks

A minewater heating system at the **Sobieski Mine** [L], Jaworzno, Poland (19.2821°E, 50.1919°N) has provided hot water for the mine bathhouse since 2015 (Karpiński and Sowizdżał, 2018). Minewater is pumped from 500 m depth at a rate of 21 m³/min (350 L/s) at a temperature of 15 °C (Karpiński and Sowizdżał, 2018). Of this, around 18 L/s is diverted to support five twin-compressor heat pumps and provide a total heating capacity of 420 kW (Janson, 2021). Intermediate heat exchangers are installed to protect the heat pumps from the

hydrochemical risks posed by the high mineral content (4990 mg/L), chloride (2270 mg/L) and sulphate (380 mg/L) (Karpiński and Sowizdżał, 2018). This system falls in the “open system with discharge” classification. The current status is operational, with an estimated payback period of 6 years and a design life of 18 years, with no major difficulties recorded since installation.

2.5.7 Czech Republic

The **Jeremenko mine** [L] shafts (18.2698°E, 49.8061°N) are used as a central pumping station for minewater in the Ostrava coal basin (Florčinská, 2014). The minewater temperature is reported as 26-29 °C. Since around 2006, heat pumps have been used to provide heating at around 55 °C to administrative buildings and employee baths. The total installed capacity is reported by Jirakova et al. (2015) to be around 91 kW.

Jirakova et al. (2015) and Novák et al. (2011) also report a modest heat pump scheme based on the **Svornost Ag-Co-As-U mine** [L] at Jáchymov (12.9115°E, 50.3726°N) in Krušné Hory, which has a history of balneological usage. Minewater temperatures of 29-36 °C are reported.

2.5.8 Germany

A number of MWG schemes are operational in Germany. These will not be reviewed further here, as they have been recently summarised by Ramos et al. (2015) and Oppelt et al. (2021). The authors of the present study have no special additional knowledge of these schemes and it is understood that a comprehensive review article is being prepared by German authors at this time.

2.5.9 Canada

The town of **Springhill** [L,I,V], Nova Scotia, Canada is underlain by seven worked coal seams dating from 1872-1958, hosting minewater with temperatures of up to 20 °C (Jessop, 1995, Jessop *et al.*, 1995). Minewaters are generally circum-neutral calcium sulphate-bicarbonate waters, with a few mg/L dissolved iron and often significant H₂S (Banks, 2017, MacAskill *et al.*, 2015, Michel, 2009). A mining museum at the former Syndicate Mine, south of the town (64.0739°W, 45.6339°N) pumps minewater to control water levels in the region. Studies of minewater thermal potential were carried out as early as 1984-85 and by the mid-1990s around eight independent MWG schemes had been established, delivering coolth and

heat to manufacturers, including Ro-Pak (plastic manufacturing 64.0681°W, 45.6456°N, since 1988) and Surette Batteries (64.0644°W, 45.6535°N from 1989), a restaurant, a dentist building, and a modest town district heating system (the “town loop”, from 1992). Most of the schemes are open abstraction-reinjection systems, typically using different worked seams for abstraction and reinjection, and typically dominated by summer cooling over winter heating (MacAskill *et al.*, 2015). The status of individual projects has changed over time, new systems have come online, and others have ceased: indeed, since 2004 a 12.5 L/s minewater doublet system has been installed at a Community Centre and provided, heating, space cooling and refrigeration for an ice rink. The systems have generally run efficiently, although challenges have included: the inadvertent introduction of oxygen causing iron clogging problems in one system (Surette Batteries) (Michel, 2009); possible thermal feedback effects in the Community Centre wells; and a trend to increasing abstraction temperatures, which may be due to upward migration of deep minewater or to the net excess rejection of summer heat from the systems (Michel, 2009).

2.5.10 The USA

Location	Recipient	Year
Scranton, Pennsylvania	Architecture Centre	2010
Carbondale, Pennsylvania	Cable Company Building	1980s
Kingston, Pennsylvania	Community Recreation Centre	1981
Kingston, Pennsylvania	Hospital Building	1980s
Pittsburgh, Pennsylvania	Church Building	2008
Kingston, Pennsylvania	Radio Studio	1979

Table 2.1 Minewater geothermal energy systems in the USA detailed by Korb (2012).

Korb’s (2012) publication is frequently referenced to convey a collection of minewater systems in the USA outlined in Table 2.1, others have been described by other authors (Banks *et al.*, 2004, Bao *et al.*, 2019, Jensen, 1983). Recent discussion with Mike Korb (2021) provides a brief but significant update on the status of the selection of American systems. The only operational system remaining from those originally described is the passive cooling system in the Architecture Centre at the Marywood University site in Scranton, Pennsylvania. Whilst the Cable Company Building had already been confirmed as decommissioned owing to design flaws and aeration of minewater, the other systems have each become disused or decommissioned since the publication in 2012. The Kingston Community Recreation Centre

required a rebuild in 2019, seeing the minewater heating system replaced by natural gas source. The Kingston Hospital scheme was shut down several years earlier following a history of backflushing with fine coal waste, and subsequent water fouling. The Radio Studio, also in Kingston, was demolished, and the Church in Pittsburgh, Pennsylvania became disused following bankruptcy (Korb, 2021).

2.6 Challenges

Challenges facing MWG systems are present throughout each stage of development – planning, installation and operation - the most prominent of these are captured in Figure 2.7.

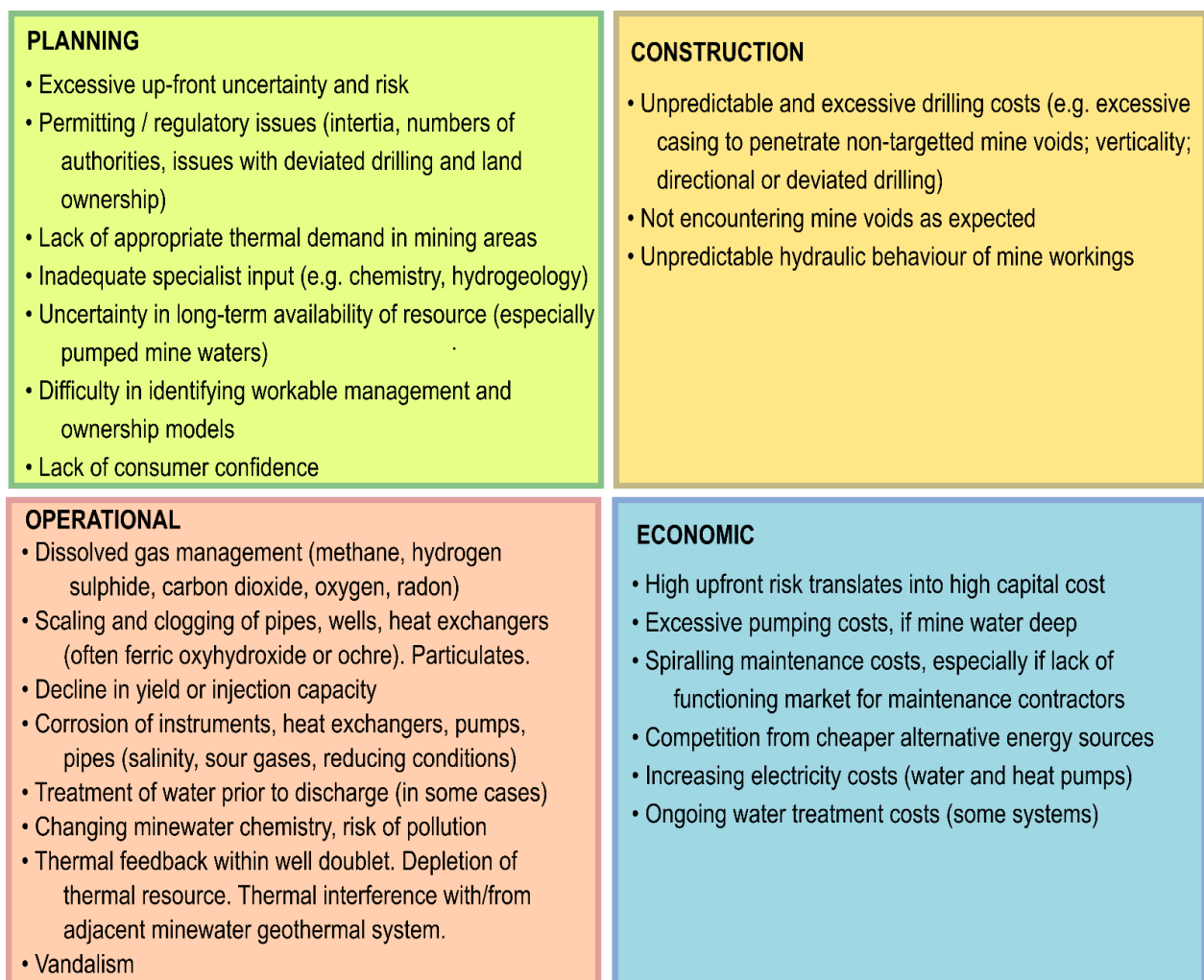


Figure 2.7 Identified issues which minewater geothermal energy systems may face throughout their project lifetime.

2.6.1 Planning and feasibility

Thorough feasibility studies covering hydrogeological, geometric, engineering and thermal characteristics of mine systems and adjacent aquifers usually precede successful

systems (Jardón *et al.*, 2013, Ordóñez *et al.*, 2012), and regular monitoring of water chemistry and temperature can extend their longevity. Good practice for feasibility studies involves consulting archival and historic mining data from sources such as mining owners and regulators (The Coal Authority (TCA) in the UK), local library archives and any independent historic collections held by local mining investigators (Harnmeijer *et al.*, 2017). These provide invaluable data on the type (longwall, pillar and room, total extraction), extent, dimensions, and connectivity of mined workings. The mine workings must be evaluated in the context of adjacent and regional aquifers. In addition to evaluating the available resource, other important factors must be considered, for example, proximity of a suitable and economically viable heat consumer (Bao *et al.*, 2018, Jardón *et al.*, 2013). As many systems perform optimally with balanced heating and cooling loads, one should ideally aim to identify a mix of heating and cooling customers. The minewater scheme at Heerlen is an indicator of a future direction: low temperature 5th Generation Heating and Cooling networks, where MWG is one of a number of possible sources of heating and cooling and can also be an important thermal store or buffer in the system (Boesten *et al.*, 2019).

Good practice generally requires investigation into the mining history and hydrogeology of the desired site, and a clear conceptual model of heat, solute and water movement within the unstressed (i.e., pre-pumped) and hydraulically stressed (i.e. pump-perturbed) mine system. Analytical or numerical modelling of mine systems may assist in understanding (Banks *et al.*, 2002a, Ferket *et al.*, 2011, Loredó *et al.*, 2017a), but should be approached with caution. The behaviour of many mine systems may be reliant on a few critical hydrogeological pathways (drifts, open shafts or roadways) and may be dramatically affected by unpredictable factors: is a ventilation door on a roadway open or closed; is a water dam intact, leaking or failed; has a section of workings collapsed and, if so, is it still transmissive; has a shaft been backfilled with permeable or impermeable material? Thorough hydrochemical and dissolved gas sampling of minewater can assist in identifying risks of corrosion or clogging, and inform selection of appropriate construction materials (Roijen *et al.*, 2007, Walls *et al.*, 2020). Such sampling should be carried out prior to construction and during initial operation to identify chemical changes induced by pumping and reinjection. In addition to water chemistry and temperature, sampling for stable isotopes (oxygen, hydrogen and sulphur isotopes) may aid understanding of minewater behaviours. For well doublet systems, chemical or thermal tracer tests may assist in understanding flow pathways and issues of thermal feedback and residence time (Harnmeijer *et al.*, 2017). For example, had thorough hydrochemical assessment been carried out prior to the construction of the Lumphinnans and

Shettleston schemes, issues with ochre staining by minewater being used as “grey water” could have been avoided, and risk clogging of injection wells could have been reduced (dissolved iron oxidises in contact with oxygen to precipitate ferric oxyhydroxide) (Banks *et al.*, 2019, SUST, 2006).

In most national systems, the operation of an MWG system will require a system of permits, which may include:

- Overall planning permission
- An environmental permit to abstract minewater
- An environmental permit to discharge or reinject minewater
- A mining permit or heat extraction agreement from a mining authority
- Approval from a renewable energy or subsidising authority

Managing this permitting process can be a discouraging experience; it is not unknown for some permits to expire before others have been negotiated. The unpredictable hydrogeological behaviour of mine systems means that permitting authorities can have a poorly developed conceptual model, and valuable time can be expended agreeing appropriate testing and monitoring. Due to the high up-front risk and capital expenditure of many MWG systems, long delays in permitting imply negotiating an economic “chasm” between expenditure and realisation of revenue.

Integration of minewater sourced heating and cooling into an efficient building thermal delivery system or district heating and cooling network involves a large, complementary expertise across the disciplines of engineering and geoscience, which should not be underestimated by scheme developers. A successful MWG system involves seamlessly integrating skills of hydrogeologists, mining engineers, chemists, HVAC and buildings services engineers, economists and planners.

Table 2.2 outlines the various difficulties that some of the MWG schemes discussed above have experienced (or, at least, admitted to experiencing!). Rather than engage in an in-depth discussion of each individual category of “problem”, a single example of a scheme that has encountered that problem will be selected to highlight the issues involved.

Table 2.2 (Overleaf) Issues reportedly encountered at the described MWG schemes. X = major difficulty, \diamond = some difficulty, * potential difficulty, but resolved. Grey cells = no information. HEX = heat exchanger. Be aware that there is a correlation between difficulties reported and detail of reporting.

	Not encountering mine voids as expected	Unpredictable hydraulic behaviour of mine voids	Inadequate or declining yield or injectivity	Dissolved gas issues	Clogging/ scaling of pipes, wells or HEX	Corrosion	Water treatment required	Thermal feedback	Excessive pumping costs / energy	Cumulative maintenance burden	Lack of long term minewater availability
UK											
Shettleston			◇		◇					X	
Lumphinnans			X		X					◇	
Markham				*					◇		
Caphouse closed loop											
Caphouse pumped minewater					X						
Dawdon pilot					*						
Abbotsford Road	◇		X		◇						
Nest Road	◇	◇				◇					
Crynant					X				X		
Norway											
Folldal											
Kongsberg											
Russia											
Novoshakhtinsk											
Spain											
Mieres					◇						
Netherlands											
Heerlen					*	*		*			
Poland											
Bytom											X
Czeladz							X				
Sobieski											
Czech Republic											
Jeremenko, Ostrava											
Svornost, Jachymov											
Canada											
Springhill	X				◇			◇			
USA											
Architecture Centre											
Cable Company Building					X						
Community Recreation Centre						*					
Hospital Building											
Church Building											
Radio Studio											

2.6.2 Technical Challenges

2.6.2.1 Striking Open Workings

Most nations where extensive mining was carried out have a tradition of precise underground surveying and the ability to produce excellent mine plans, as such maps were pivotal to minerals claims, taxation assessments, underground and surface safety. However, the quality, completeness and accuracy of such maps has evolved with time, and one must suspect that, in early days of private mining, maps *may* have underreported the true extent of mining activities, for economic and legal reasons. Legislation pertaining to recording the extent of coal mine workings in the UK was introduced in 1872 (Younger, 2007). Prior to this date, there were no obligations to communicate the method, extent or dates by which coal was extracted from the subsurface. Locations of stoops, rooms, roadways or other mine features were often poorly recorded. Following nationalisation of the coal mine industry in the UK in 1947, the quality of mapping evolved again, with a tendency to highly detailed maps with a consistent format.

The construction of an MWG system relies on a sound understanding of the interconnected workings which it exploits, both to understand the probable hydraulic behaviour of the workings and to be able to identify targets for drilling with accuracy. While historic techniques of underground surveying were surprisingly accurate, one must recognise that there may be an inherent uncertainty in the accuracy of subsurface mapping, which will be inferior in older plans. There may also be uncertainties in georeferencing historic mine plans to modern digital mapping. Where areas of pillar and room workings are shown in plans, the differentiation between voids and pillars may not be reliably shown, nor whether they have subsequently been “robbed” or collapsed. All of this leads to uncertainty of encountering a void when drilling, given that unworked to worked coal ratios in pillar and room workings may vary between 30 and 70% (Andrews *et al.*, 2020). Finally, even if a subsurface drilling target can be identified accurately, it is challenging to drill a completely vertical borehole, capable of penetrating, say, a 3 m wide roadway at depth of 300 m, and one should also consider whether a drill bit is likely to penetrate roadway supports and reinforcement. Rapid drilling techniques, such as down-the-hole hammer (DTH), typically have a poorer vertical accuracy than more expensive techniques such as wireline coring or directional drilling. For example, Nordell *et al.* (2016) documented an average lateral deviation of 16 m in 21 supposedly vertical, 150 m deep, DTH closed loop ground source heat boreholes in Sweden (although cost, rather than verticality was likely to have been prioritised in that case).

Small-diameter pilot boreholes, to prove a mine void target prior to drilling a full diameter borehole, provide a means to reduce the risk of loss of capital during drilling. Such pilot boreholes may allow measurement of water levels and even sampling before the hole is reamed out at full diameter and permanent casing installed. Identifying the precise locations of the roadways proved to be an issue at Springhill, Nova Scotia, where test drilling into the old mine workings was conducted by several consultants. These test drills were shallow, reaching down to less than 100 m depth (Ross and Kavanaugh, 1993), and any which intersected pillars instead of open workings did not provide water and were usually abandoned (Michel, 2009).

At the recently drilled UKGEOS minewater research site in Glasgow (4.2011°W, 55.8383°N (Monaghan *et al.*, 2021c)), where “*mine plans were examined by experienced geologists prior to drilling, 3 of the 6 target mine workings encountered a void*” upon drilling (Monaghan, 2021). These were, however, largely pillar and room workings and it was recognized at the outset that the georeferencing error on the mine plans was greater than the dimension of the room/void. One can probably assume, therefore, that the drilling outcome partly represents the statistical ratio of voids to pillars, possibly combined with subsequent extraction of pillars. Monaghan (2021c) thus reported that inaccuracy was experienced at the “metre scale”. Mine plans were examined by experienced geologists prior to drilling and targets chosen with great care, the rate of success of encountering voids as anticipated was good, but by no means perfect.

At a newly developed scheme in Caerau, Wales (3.6415°W, 51.6379°N), discussion is ongoing regarding uncertainty in the hydrogeological significance and connectedness of voids encountered by exploratory boreholes, as this will affect the overall sustainability of this system (Brabham *et al.*, 2020).

At Nest Road, Gateshead, despite good mine plans being available, boreholes did not necessarily encounter workings as expected. Workings were encountered where not explicitly shown on maps and, indeed, *vice versa*. Four boreholes were drilled to obtain one good abstraction and one good reinjection borehole.

2.6.2.2 Unpredictable hydraulic behaviour

Conventional hydrogeological theory has grown out of the assumptions of Darcy’s Law (laminar flow through a permeable granular medium) and the ideal Theis scenario (radial flow towards a well in a homogeneous, isotropic aquifer of infinite extent) (Theis, 1935). None of these assumptions are valid in an interconnected network of mine voids: indeed, there are many

aspects of minewater hydrogeology that are more similar to karst hydrogeology (Aldousa and Smartb, 1988, Elliot and Younger, 2014) than a conventional Darcian granular medium. Factors such as collapses, inter-seam shafts and boreholes, water dams and fracturing can dramatically influence hydrogeological behaviour. It should come as no surprise that the hydraulic behaviour of mine workings is poorly predictable and that conventional numerical modelling approaches should be treated with great caution (approaches based on network modelling have shown some potential, however (Ferket *et al.*, 2011)).

For example, the abstraction borehole at Nest Road, Gateshead, penetrated to the level of the worked High Main seam. The drawdown versus time response was rather flat, characteristic of a leaky / constant head recharge boundary, good lateral connectivity and high transmissivity. The reinjection borehole, at the same location but to deeper workings, showed almost an opposite response: a quasi-linear evolution of upconing with time at early time, more consistent with workings behaving as a “sealed reservoir” (Banks, 2021). Neither of these behaviours could have been readily predicted in advance, neither are Theisian and they may have implications for the subsequent operation of the scheme.

Rapid fluid pressure changes or elevated flow rates, especially in shallow mine workings, may theoretically lead to risk of geotechnical instability or erosion of unworked pillars (Todd *et al.*, 2019). A thorough assessment of geotechnical risk should be undertaken on evaluating any mine water thermal scheme (and is usually required by The Coal Authority in the UK). Having said this, most UK mines have been subject to very significant water head fluctuations caused by dewatering during their working life, followed by re-flooding on closure. InSAR (Interferometric Synthetic Aperture Radar) data clearly show small regional ground movements across wide areas related to re-flooding of workings (Bateson *et al.*, 2015, Sowter *et al.*, 2013). Water head fluctuations caused by MWG systems are likely to be modest in comparison.

2.6.2.3 Inadequate Yield and Injectivity

A lower production or reinjection yield than anticipated will limit the thermal output of the system. In many cases, the yield and injectivity of a borehole will be related to open mine voids being encountered, as discussed above. However, poor yield or injectivity may be related to unexpected hydraulic behaviour of flooded workings (see above), or to chemical or biological clogging of recharge boreholes (see below).

For example, at Lumphinnans and Shettleston in Scotland, the free cascading of water into injection boreholes (promoting iron oxidation and precipitation) has promoted clogging and decline in performance of injection boreholes and has contributed to the cessation of the systems (Banks *et al.*, 2019, Banks *et al.*, 2009, Walls *et al.*, 2020).

2.6.2.4 Dissolved Gas Issues

The management of dissolved gases in the minewater used in MWG systems can be critical for minimising the risk of clogging, scaling, odours, asphyxiation and corrosion. Contact between oxygen and an anoxic minewater containing dissolved ferrous iron or manganese can lead to oxidation of these metal cations and precipitation of oxidised manganese or ferric oxyhydroxides. This was observed in the reinjection borehole at the Lumphinnans scheme (Banks *et al.*, 2009) and, initially, at Dawdon (Bailey *et al.*, 2013). Degassing of excess CO₂ from minewater on exposure to the atmosphere can lead to an increase in pH and thus an increased tendency to precipitation of carbonates and hydroxides (Banks *et al.*, 2009). Degassing of CO₂-enriched, N₂-enriched or O₂-depleted gas mix in an enclosed wellhead chamber or building, especially at times of low atmospheric pressure, can also lead to a risk of asphyxiation (Gunning *et al.*, 2019, Hill, 2004). Dissolved methane can be present in minewater in significant quantities and can cause risk of explosion if allowed to degas in an uncontrolled manner, especially to enclosed spaces. Dissolved methane at the Markham No. 3 mine shaft was deliberately vented away to the atmosphere in a controlled manner (formerly it had been commercially produced from the shaft) (Banks *et al.*, 2019). Finally dissolved hydrogen sulphide (H₂S) in minewaters can prove a corrosion risk to a range of metals (corrosion of downhole sensors has proved to be an issue at the Nest Road site (Steven, 2021a)), and its uncontrolled release can cause an odour nuisance. In the case of the Dutch Heerlen scheme, understanding and management of dissolved gases was recognised at an early stage to be an important factor for success (Minewater-Project, 2008).

2.6.2.5 Clogging / scaling of pipes, wells and heat exchangers

Pumping a mine void increases water velocities and may induce turbulence. This can cause clastic particles to be suspended in the water and mobilised. Installing in-line filters prior to heat exchangers should remove large clastic fragments but may not remove smaller particles. Such filters can also prove to be a locus for ochre precipitation and accumulation. At the Mieres

site, Spain, particulate matter, including pyrite grains, were found to occur within a plate heat exchanger disassembled for cleaning (Loredo *et al.*, 2017b).

Arguably more problematic than mobilisation of particulate matter is the potential problematic chemistry of many minewater (Bailey *et al.*, 2013, Banks *et al.*, 2009, Banks *et al.*, 1997, Burnside *et al.*, 2016a). Most minewater from coal or metal sulphide mines contain high loadings of dissolved (ferrous) iron, derived from either pyrite oxidation or reductive dissolution of iron carbonates or oxides. Upon oxidation and precipitation, the accumulation of iron oxides, commonly known as ochre, is the most common issue when dealing with minewater. It can cause staining and clogging of pipework, heat exchanger surfaces and boreholes, as noted in the previous section. Accumulations in pipework or heat exchangers will restrict the apertures, increase system pressure gradients, and may reduce achievable flow rates (Loredo *et al.*, 2017b). At Shettleston, Scotland, ochre did accumulate slowly in pipes, but the system was able to operate for a considerable period without notable cause for concern (Banks *et al.*, 2019). At Abbotsford Road, ochre accumulates over a period of months within the plate heat exchanger, necessitate periodic flushing with solutions of citric or oxalic acid (Steven, 2021a). At Mieres, Spain, ochre slowly accumulates in the plate heat exchangers of the University system, requiring disassembly and cleaning, but the shell-and-tube heat exchangers of the Hospital system appear more resilient. This observation is arguably as one would expect, given the larger apertures of the tubes compared to the plates.

Accumulation of ochre in wells and pumps can cause a decline in borehole performance (injectivity of specific capacity) and place stress on submersible pumps. Coatings of ochre on metal surface can also allow reducing, corrosive niches to develop between the ochre and the metal surface.

Restricting access to oxygen is a key factor in controlling ferrous iron oxidation and ochre (ferric oxyhydroxide) precipitation. At Markham, where the water is anoxic and contact with atmospheric oxygen is avoided, scaling problems have been remarkably few, as was also the case when unoxygenated water was used at Dawdon (Bailey *et al.*, 2013, Banks *et al.*, 2019). In some cases, prevention of iron oxidation can be difficult, as oxygen can gain access to minewater in unsaturated mine workings, in mine shafts or even in pumped boreholes. For example, at Caphouse, analyses appeared to demonstrate that iron in the minewater had already begun to oxidise and form flocs prior to entry into the MWG system, possibly due to exposure to oxygen within the pumped Hope Shaft, or within the workings themselves. This led to rapid accumulation of ochre on the in-line filter prior to the heat exchanger (Banks *et al.*, 2019).

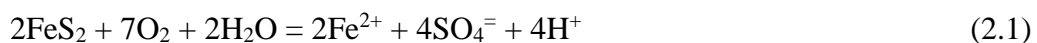
The risk of clogging can be reduced by: (a) careful management of dissolved gases and exclusion of oxygen for the pumping-heat exchange-discharge pipe work; (b) prevention of cascading in abstraction and reinjection wells; (c) monitoring of pressure differentials at key points in pipework systems and across heat exchangers; (d) visual or CCTV inspection; (e) a regular program of sampling of minewater chemistry.

In closed loop systems, accumulation of iron oxyhydroxide precipitates around heat exchange pipes or plates can hinder the free convection of water around the exchangers, restricting heat transfer and thus decreasing the overall efficiency of the system (Banks, 2008, Banks *et al.*, 2019). In cases where closed loop heat exchangers are mounted within minewater lagoons, protocols will need to be developed for desludging and cleaning the lagoons, which may involve the temporary removal of the heat exchange elements.

2.6.2.6 Corrosion

Corrosion of metallic components of wells, pumps, pipes and heat exchangers can take place by a variety of mechanisms, depending both on water chemistry and the metal in question (McLaughlan, 2014, Popoola *et al.*, 2013). However, as with scaling and precipitation, minewater possess a particular set of chemical characteristics which can enhance corrosion risk. Deep mines can contain highly saline waters, at elevated temperatures and of a highly reducing, sometimes H₂S-rich, nature (Anderson, 1945, Banks *et al.*, 1996). High concentrations of H₂S can enhance corrosion in all steel types (Twigg, 1984). Highly reducing, sulphide- / chloride-rich waters can prove very corrosive, even in stainless (high-Cr) steels traditionally regarded as corrosion-resistant, as the oxide layer that offers corrosion protection under normal circumstances can be disrupted, although a sulphide layer can develop in its place to limit the progress of corrosion (Burnside *et al.*, 2016b, Feng *et al.*, 2017, Finsås Wika, 2012, Ge *et al.*, 2003, Wang *et al.*, 2017). Copper and its alloys are very susceptible to corrosion in sulphide-rich conditions. At the Nest Road site, enhanced corrosion of downhole sensors in H₂S-containing, reducing minewater has necessitated their replacement with more robust titanium models (Steven, 2021a).

In shallower mining environments, the oxidation of pyrite typically releases dissolved iron, sulphate and acid.



The acid is often partially consumed by hydrolysis reactions with silicate or carbonate (e.g., siderite, ankerite, calcite, dolomite).



Acidity and elevated “free” carbon dioxide concentrations can prove corrosive to carbon- and mild steels (Koteeswaran, 2010, Li *et al.*, 2019). Finally, as seen above, the dissolved iron can oxidise and precipitate as ochre (ferric hydroxide) scales. Ochre (or limonite) gradually hardens over time, dehydrating and becoming redder, via ferrihydrite and goethite, towards a haematite composition (Houben, 2003). In some cases, biofilms may be involved. Although the overall environment may be oxidising, corrosion-promoting niches can develop under the iron oxyhydroxide scale or biofilm layers, where normal ionic diffusion is hindered and reducing conditions may develop. Given the prevalence of dissolved sulphate in minewater, sulphate-reducing environments could even develop below the scales, against the metal surface (de Romero, 2005, Larsen, 2020, Videla, 2005).

In cases of high corrosion risk, titanium can be used as an alternative to stainless steel in wells, pipelines or heat exchangers (Kaya and Hoshan, 2005) or of course, high strength plastics for wells and pipes.

2.6.2.7 Minewater treatment

In open systems with discharge to surface water, it is likely that regulators will require treatment of the minewater prior to discharge, to prevent contamination. In the UK, regulators are especially concerned about residual concentrations of iron and manganese discharged to watercourses, as precipitation of these can discolour stream beds and smother benthic fauna. Iron can be effectively removed either by passive (aeration, precipitation, settlement, wetland (Banks, 2003)) or active (oxidation, neutralisation, flocculation, settlement/clarification, filtration (Bailey *et al.*, 2013)) techniques. Most of these schemes in the UK were constructed to control the subsurface minewater levels, to prevent uncontrolled minewater discharges or to treat existing gravity discharges. Any heat recovery from such schemes via MWG schemes would be a beneficial by-product (e.g., the pilot schemes at Caphouse, or the Seaham Garden Village scheme under development at Dawdon). Consideration must be given, however, to the extent to which changes in temperature might impact the various stages of any treatment process.

In Poland, regulators are more concerned about discharge of salts (chloride and sulphate) in minewaters to rivers (Zgórska *et al.*, 2016); these are very challenging to remove by treatment (Ericsson and Hallmans, 1996). Other problematic parameters, such as barium or radium, can be more readily removed by treatment (Chałupnik *et al.*, 2020, Pluta, 2001).

In the case of a new pumped MWG scheme with discharge to the surface environment, where there was no pre-existing need to pump, the requirements for construction of water treatment plant, and the ongoing costs of pumping and treatment would likely be substantial.

At the Mieres MWG system in Spain, waters from deep mines are permitted to be discharged into the nearby Rivers Turón and Caudal (Loredo *et al.*, 2017b) with no treatment. Iron concentrations are modest, but the minewater discharges have been demonstrated to alter the river chemistry (increased concentrations of salinity, alkalinity and several solutes, including sulphate, altered temperature) (Loredo *et al.*, 2017b). These issues were most pronounced in the summer months of low river flow.

Bailey *et al.* (2013) initially used minewater treated by aeration and settlement as feed water for their pilot MWG scheme at Dawdon, UK. They found that although treatment removed much of the iron, it also introduced oxygen to the water: residual iron rapidly oxidised and clogged components of the heat exchange system. When they reverted to anoxic, untreated raw water, these clogging issues ceased. In the UK, there is thus a perception that oxygen exclusion is the optimal strategy for prevention of clogging (although there are circumstances where it may not be practical or wholly effective, see above).

In Poland, however, minewater is treated for iron removal by aeration and “filtration” prior to entry to the heat exchange system at the Czeladz MWG system. This appears to be successful, in the absence of reports to the contrary (Janson, 2021, Karpiński and Sowizdzał, 2018, Tokarz and Mucha, 2013).

2.6.2.8 Thermal feedback / depletion of heat resource

At the Heerlen scheme, the risk of possible thermal feedback between abstraction and reinjection wells was perceived to be relatively high (Minewater-Project, 2008). This led to the reconfiguration of the mine void more as a thermal store or buffer, than as a source of heating and cooling, with temperature changes within the subsurface minimised. At present, the prospect of a wholly reliable modelling approach to heat transfer in complex networks of subsurface mine voids seems distant, but the approach of (Ferket *et al.*, 2011), involving a conduit network approach coupled to tunnel heat exchange (Loredo *et al.*, 2017a, 2018), seems

promising. The use of empirical techniques – appropriate pumping test techniques, solute and heat tracer tests, and diligent ongoing monitoring of abstracted and reinjected water temperature and chemistry – are to be encouraged.

In the Gateshead area of North-East England, a number of MWG systems have been proposed and The Coal Authority are attempting to develop a system of Heat Access Agreements to prevent interference between systems and thermal depletion (GOV.UK, 2021). The two MWG systems at Nest Road and Abbotsford Road are only 700 m apart and there may exist some potential for thermal interference. The schemes will be carefully monitored into the future, but at present there seems no clear evidence of thermal conflict (Steven, 2021b).

At the Markham standing column (single shaft) scheme, no thermal feedback was observed; however, the flow and density regime within the shaft is not fully understood.

2.6.2.9 Excessive pumping costs

The energy expended in pumping minewater from a shaft or borehole is directly proportional to the pumping head (which will be the sum of the elevation difference between the dynamic water level in the shaft and the surface, plus frictional losses in pipes and heat exchanger) and is given by:

$$P = \frac{h \times \rho \times g \times Q}{\zeta} \quad (2.3)$$

The heat delivered by a minewater heat pump system is given by:

$$H = \frac{\Delta T \times c \times \rho \times Q}{(1 - 1/COP)} \quad (2.4)$$

Where P = electrical power consumption by submersible pump (W); h = pumping head overcome (frictional losses + elevation difference) (m); ρ = density of water = c. 1000 kg/m³; g = acceleration due to gravity = 9.81 m/s²; Q = pumping rate (m³/s); ζ = pump efficiency (dimensionless fraction); c = specific heat capacity = c. 4200 J/kg/K; ΔT = temperature drop at heat exchanger/heat pump (K); COP = coefficient of performance of heat pump.

For a pumping rate of 50 L/s (= 0.05 m³/s) and a pump efficiency of 65% (0.65), Equation 2.3 shows how 7.5 kW of electrical energy is expended when pumping the water against a head loss of 10 m (i.e., very shallow minewater). If the head loss is 100 m (deep minewater level), the pumping expenditure increases to 75 kW. The product of P (Equation

2.3), 3500 hr/yr pumping (assumed), and an electricity cost of £0.14 per kWh (typical UK price), gives annual pumping costs of £3700 and £37,000 for these two scenarios.

For a ΔT of 4 °C and a heat pump coefficient of performance (COP) of 4, 50 L/s would deliver 1.117 MW of heat (279 kW of which is derived from the heating effect of the electricity required to run the heat pump – a function of the COP and accounted for in Equation 2.4), with an annual heat pump electricity cost of £137,000 (279 kW x £0.14 per kWh x 3500 hr).

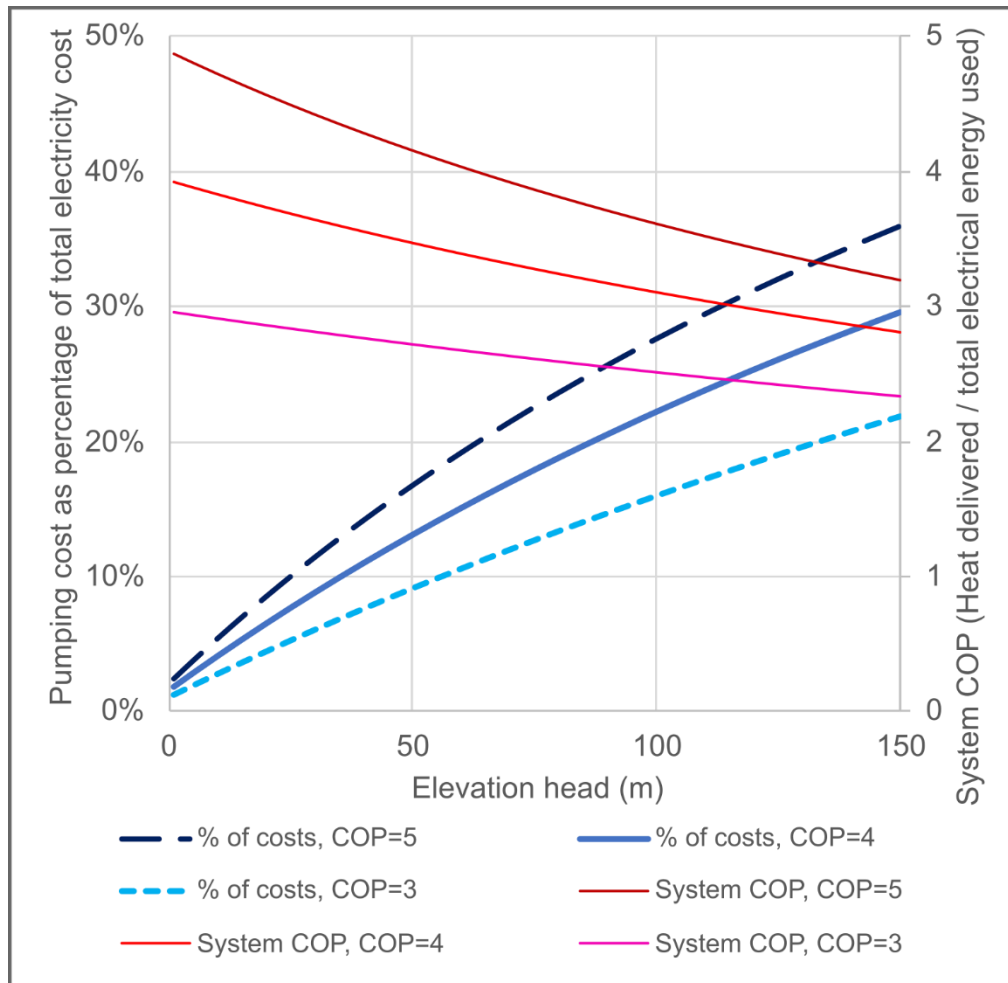


Figure 2.8 Hydraulic pumping costs, as a % of total electricity cost, and system COP, as a function of elevation head (elevation up which water is pumped). A constant frictional head loss of 6 m is added to the elevation head loss. Only water pumping and heat pump power and costs are considered. The heat pump COP is set at values of 3, 4 and 5. System COP is defined as Total heat output (kW) / Total electricity use (kW). Other assumptions: water density of 1 kg/L, temperature change across heat pump = 4 °C, volumetric heat capacity of water = 4.19 kJ/L/°C.

It can be seen that, for a minewater head of 10 m, the water pumping costs are almost negligible, but they are far from negligible for a head of 100 m. If we define the system COP (in a highly simplified manner) as total heat delivery divided by total electricity consumption,

we can see that, for a head of 10 m, the system COP is $1117 \text{ kW} / (279 + 7.5 \text{ kW}) = 3.9$. For a pumping head of 100 m, the system COP reduces to $1117 \text{ kW} / (279 + 75 \text{ kW}) = 3.2$. The relationships between pumping head, system COP and hydraulic pumping cost are shown in Figure 2.8.

This analysis was performed by Athresh et al. (2015) for the Markham heat pump scheme, where the water level in the shaft is still rising, following the colliery closures in the area. In 2011, the minewater was almost 240 m deep, but by 2015 had risen to within 150 m of the surface. The authors concluded that such deep water levels had a detrimental impact on the overall energy efficiency of the system but that, as minewater levels continue to rise, the energy efficiency will improve dramatically.

2.6.2.10 Cumulative maintenance burden

The Shettleston scheme, which has been used as a case study for many articles promoting the potential for MWG systems (Banks *et al.*, 2009), worked well for up to 20 years since being commissioned in 1999, despite minewater being passed directly through the heat pump evaporator. Walls *et al.* (2020) describe how physical and chemical issues contributed to the system recently being decommissioned. Since there were different contractors employed to service the separate components of the system, the housing association was unable to resolve the exact nature of the issue(s) but believed that several technical factors could have contributed (clogging of the reinjection borehole, miscommunication between electrical control units, slow build-up of ochre in pipework and loss of pressure (Walls *et al.*, 2020)), in addition to the challenge of supplying reliable, responsive heat to social housing customers at an affordable price. It is evident that with every extra stakeholder or contractor, the projects become more complex, and untangling cause and responsibility of issues becomes increasingly difficult. The lack of a mature market for maintenance of such systems (e.g. “one stop shop” contractors), makes it highly challenging for small operator on a limited budget to adequately maintain a MWG scheme (an observation that has been made in the context of many ground source heat schemes by Banks and Birks (2020)). Indeed, the array of potential technical (and regulatory) challenges associated with MWG systems means that the cumulative monitoring and maintenance burden can prove economically unviable for small-medium scale systems. One can speculate that, in the absence of a mature and competitive maintenance market, complex MWG schemes are only viable above a certain economic scale.

2.6.2.11 Lack of demand / lack of future minewater availability

For a sustainable MWG system, one requires not only favourable mining hydrogeological conditions (the resource), but also a demand and a means of conveying heat from source to consumer (heat / cooling transfer and distribution).

In Poland, abundant warm minewater resources and existing pumped minewater shafts are located beneath major conurbations (e.g. Katowice (Janson *et al.*, 2009)). In the UK, while flooded coal mine workings exist below several major cities (Newcastle, Gateshead, Manchester, Sheffield/Rotherham, Stoke-on-Trent, Glasgow), many (but not all) of the existing Coal Authority's pump-and-treat schemes are located outside conurbations in locations of sparse demand. Ideally, this should lead The Coal Authority, developers and planners to ask:

- Whether any future minewater pumping and treatment schemes could be more deliberately located in built-up areas, possibly using compact active treatment systems, rather than passive lagoons and wetlands in rural areas.
- Whether planners should be more pro-active in designating land in the vicinity of existing mine-water discharges as development zones.

Indeed, a recent feasibility study of minewater geothermal potential in the Fortissat area of Lanarkshire, Scotland, found favourable technical potential, but ultimately the density of heating / cooling demand in the vicinity was insufficiently favourable (Harnmeijer *et al.*, 2017).

It is one thing to identify a potential MWG resource, a potential demand and to obtain planning consent. It is quite another challenge to ensure that the regulatory permits (planning permission, environmental permitting, subsidy approval) can be acquired within a time frame that satisfies the development timetable. It is also essential, for a sustainable system, to be able to guarantee that the minewater resource will be available in the future. The resource may become unavailable if:

- The locus of any pumped minewater discharge changes, for example, because the dewatering authority believes the pumping should be moved elsewhere for economic or operational reasons (as occurred at the ARMADA development at Bytom, Poland).
- A gravity minewater discharge dries up due to dewatering, development or mining activities in the vicinity (as has reportedly happened at the Fordell Castle minewater discharge in Scotland, related to open casting at Muirdean (Rowley, 2013, Sparling, 2013)).

2.7 Conclusion

Lessons are still being learned about minewater heating and cooling resources and technology, first realised in the 1980s, by systems which have recently become operational. In many cases, solutions to risks posed to projects require thorough planning and ongoing monitoring and maintenance to ensure suitable operation. It is clear that even well-established systems, frequently used as case studies for proof of feasibility, have run in the face of some operational challenges. Evidently, MWG systems that have the ability to adapt and improve when faced with challenges or changes in demand are better placed to succeed, Heerlen being a good example.

The selection of a favoured MWG configuration to harness thermal energy from a flooded mine, from a range of design configurations, requires evaluating various pros and cons and is often a reflection of controlling factors such as available capital, minewater chemistry, mandatory pumping of coal seams and thermal energy demand, among others. However, upon investigating the feasibility of using minewater to provide heating and cooling, certain good practices prove to be invaluable for the longevity of the installation, including thorough (geological, hydrogeological, geochemical, thermogeological) mine characterisation and hydraulic/ geochemical testing to identify the optimum operational mode for efficient and sustainable extraction of heat or ‘coolth’. Characterisation and empirical testing can be supported by numerical or analytical modelling, provided that current limitations in modelling minewater environments are recognised. Following commissioning, many MWG schemes have continued to encounter significant operational challenges, which should ideally be identified at an early stage via ongoing monitoring (e.g., of minewater heads, pressure losses in pipework and heat exchangers, minewater chemistry). Fortunately, many of the technical and operational challenges can have mitigating engineering solutions. However, in addition to specific technical, hydraulic and chemical challenges, we would encourage potential MWG system operators to be aware of the less technical factors for successful implementation: spatial relationships between minewater geothermal resources (surface discharges or pumped minewater treatment schemes) and significant paired thermal demands (district heating networks in towns and cities); the seasonal balance between heating and cooling demand; the need to manage multiple parallel permits and contracts required for construction, abstraction and disposal of water and heat; competitiveness with other renewable heat sources; management and financial models for distribution and sale of heat and cooling to communities.

Author Contributions

Conceptualization, D.W., N.B. and D.B.; methodology, D.W., D.B., N.B. and A.B.; investigation, D.W. and D.B.; data curation, D.W. and D.B.; writing—original draft preparation, D.W.; writing, review and editing, D.W., D.B., N.B. and A.B.; supervision, N.B., D.B. and A.B.; funding acquisition, N.B. All authors have read and agreed to the published version of the manuscript.

Funding

This research was supported by NERC NEIF grant 2301.0920, EPSRC IAA grant EP/R51178X/1 and Energy Technology Partnership Scotland grant PR007-HE. N.M.B is funded by a University of Strathclyde Chancellor's Fellowship. A.J.B is funded by ICSF at SUERC (NERC Facility contract F14/G6/11/01).

Acknowledgments

We are grateful to the following people for providing information on many of the schemes described herein: Jonathan Steven of Groundwater and Geothermal Services Ltd. (Abbotsford Road and Nest Road), Ewa Janson (Central Mining Institute, Katowice, for the Polish schemes), Gareth Farr and Alison Monaghan of the British Geological Survey, Brian Herteis (Springhill), Mike Korb (USA schemes), Dr Manju of the University of Cardiff and Phil Hopkins (Crynant Plant) for information on Welsh MWG systems, Dr Bjørn Ivar Berg of Norwegian Mining Museum, Torstein Johnsrud of the Folldal Mines Foundation.

Chapter 3 – Heat recovery potential and hydrochemistry of mine water discharges from Scotland’s coalfields

This chapter was published as: Walls DB, Banks D, Peshkur T, Boyce AJ and Burnside NM (2022). Heat Recovery Potential and Hydrochemistry of Mine Water Discharges from Scotland’s Coalfields. *Earth Sci. Syst. Soc.* 2:10056. doi: 10.3389/esss.2022.10056. As of 20th March 2023, this article has 773 views and 1 citation.

Abstract

Prospective and operational mine water geothermal projects worldwide have faced challenges created by mine water chemistry (e.g., iron scaling, corrosion) and high expenditure costs (e.g., drilling or pumping costs) among others. Gravity fed or actively pumped drainages can be cheaper sources of low-carbon mine water heating when coupled with adequately sized heat exchanger and heat pump hardware. They also provide valuable chemical data to indicate mine water quality of associated coalfields. Field collection of temperature and flow rate data from mine water discharges across the Midland Valley of Scotland, combined with existing data for Coal Authority treatment schemes suggest that mine water heat pumps could provide a total of up to 48 MW of heat energy. Chemical characterisation of mine waters across the research area has created a valuable hydrochemical database for project stakeholders investigating mine water geothermal systems using boreholes or mine water discharges for heating or cooling purposes. Hydrochemical analytical assessment of untreated gravity discharges found that most are circumneutral, non-saline waters with an interquartile range for total iron of 2.0 - 11.6 mg/L. Stable isotope analysis indicates that the discharges are dominated by recent meteoric waters, but the origin of sulphate in mine waters is not as simple as coal pyrite oxidation, rather a more complex, mixed origin. Untreated gravity discharges contribute 595 kg/day of iron to Scottish watercourses; thus, it is recommended that when treatment schemes for mine water discharges are constructed, they are co-designed with mine water geothermal heat networks.

3.1 Introduction

Decarbonisation of heating and cooling is essential if we are to decrease anthropogenic emissions and combat climate change. For example, heat production accounts for 45% of energy use and 32% of CO₂ emissions in the UK (Crooks, 2018). Mirroring global efforts (United Nations, 2019), the UK government has committed to reaching net zero greenhouse gas emissions by 2050 (UK Government, 2021a, 2021b) and has mandated the end of fossil-fuel heating systems in all new build homes by 2025 (Committee on Climate Change, 2019). The Scottish Government has committed to net zero emissions by 2045 (Scottish Government, 2020b) and is proposing to ban fossil-fuel heating systems in new buildings by 2024 (Scottish

Government, 2022). Decarbonisation of heating and cooling has challenges different to that of other energy requirements (e.g., electrical power) since the former requires decentralised generation and consumption. Heating still has an overreliance on fossil fuels and is dependent on seasonal weather conditions. In 2020, only 6.4% of Scotland's overall non-electrical heat supply was from renewable technologies, far from the 2020 target of 11% (Energy Saving Trust, 2021).

The heating and cooling resource represented by abandoned, flooded mine workings has been portrayed as having significant thermal energy potential (Adams *et al.*, 2019). Flooded coal mines contain vast volumes of mine water in close proximity to housing and industry stock at between 10 °C and 36 °C (Farr *et al.*, 2021) which can be exploited to provide a thermal load via low-carbon heating and cooling networks (Verhoeven *et al.*, 2014). The Midland Valley of Scotland (MVS) alone has estimated mine water geothermal reserves of 12 GW, which given favourable conditions (accessibility and building stock quality) could provide over one third of Scotland's annual domestic heat demand (33 GW) (Gillespie *et al.*, 2013). There is no doubt that if these resources could be utilised in a cost-effective manner, they would be a major benefit in efforts to displace fossil fuels from heat production – turning former environmental liabilities into potentially valuable low-carbon assets.

Historically, removal of mineral material from underground coal mines in Scotland created void spaces at depths ranging from outcrop at surface to a little over 1000 m below ground level (bgl), with varying degrees of connectivity. As well as creating underground flooded void space (“anthropogenic karst” (Younger and Adams, 1999)) mining also enhances the porosity and permeability of adjacent aquitard and aquifer units by collapse and fracturing (Ó Dochartaigh *et al.*, 2015). Most of the abandoned mines in the MVS are former coal mines, but others include ironstone, limestone, oil-shale, and various metals (gold, silver, lead etc.) (Gillespie *et al.*, 2013).

The use of open loop abstraction-reinjection (well doublet) heat exchange systems based on shallow groundwater is globally widespread (Banks *et al.*, 2022, Jessop *et al.*, 1995, Monaghan *et al.*, 2021c, Ramos *et al.*, 2015, Verhoeven *et al.*, 2014, Walls *et al.*, 2021), and is similar to configurations found in other geothermal reservoir types such as hot dry rock and hot sedimentary aquifers (Limberger *et al.*, 2018, Reinecker *et al.*, 2021). However, there are alternative configurations by which mine water's thermal energy can be harnessed (Banks *et al.*, 2019, Walls *et al.*, 2021), each accompanied by varying drilling costs and project risks (Monaghan *et al.*, 2021c). Detailed understanding of mine water geothermal energy resource size and sustainability remains largely in its research phase, with increasing numbers of

projects being started (Banks *et al.*, 2022, Monaghan *et al.*, 2021c, Walls *et al.*, 2021). Owing to the heterogeneous nature of mine workings, each project has unique hydrogeological properties, thus uncertainty around the speed and extent of heat migration within mines and initial resource scale and availability are regarded as significant project risks during the planning stage (Walls *et al.*, 2021). Existing pumped or gravity mine water discharges, which do not require exploratory drilling or pumping tests are, therefore, appealing for development (Bailey *et al.*, 2016). Gravity discharges may emerge at the surface via mine adits or shafts (Younger and Adams, 1999), or ‘break out’ at the lowest hydrological point e.g., a river, even when there is no shaft or adit present. Their temperature, flow and estimated heat resource have either been recorded for ongoing environmental monitoring purposes or can easily be measured onsite (Wood *et al.*, 1999). In certain circumstances, mining authorities (such as The Coal Authority (TCA) in Great Britain) deliberately pump boreholes or shafts, where it is deemed necessary to prevent uncontrolled surface outbreak (Bailey *et al.*, 2016) or contamination of important water aquifers (Bailey *et al.*, 2013) above mine water systems. Further afield, other countries have similar pumping arrangements to protect adjacent mine workings (Janson *et al.*, 2016). The high loading of iron in many of the larger gravity and pumped discharges means that mine water treatment is required, often by passive aeration-precipitation-settlement-retention systems, involving lagoons and wetlands (Banks, 2003, Banks and Banks, 2001). Whilst this paper mainly focusses on gravity drainages from mines across Scotland, it includes the details of TCA pumping and treatment sites to improve the accuracy of potential heating estimates for mine water resources present at surface.

Water levels in UK coal mines were artificially lowered by dewatering throughout the 18th - 20th centuries (Younger and Adams, 1999). Initially, water “levels” or adits were used to drain mines by gravity to river valleys. As mining progressed deeper, pumping stations and engine houses were employed to keep the water table depressed at a safe level for mining activities, and manage water levels across interconnected coalfields (Wallis, 2017). The cessation of pumping following closure of collieries allowed groundwater to rebound to pre-mining levels. Interconnected mine voids remain the preferential flow pathway for groundwater where the water table has fully recovered following cessation of pumping, and these continue to drain mine water to the surface via shafts, drifts and adits (Younger and Adams, 1999). The network of coal mines which these pathways drain can be regional, with connections to numerous collieries, *e.g.* Fordell day level in Fife (Rowley, 2013). Younger and Robins (2002) predicted that the unmitigated impacts of mine water recovery and break out could include: risks of contamination of surface water bodies by high concentrations of iron,

manganese or sulphate (Younger, 2000a); flooding of agricultural, industrial or residential areas (Younger and LaPierre, 2000); and contamination of important aquifers overlying coal seams (Bailey *et al.*, 2013). Other impacts include an increased subsidence risk as the rising waters weaken previously dry, shallow workings (Smith and Colls, 1996), or transportation of mine gases to the surface, displaced from pore spaces by the rising waters (Hall *et al.*, 2005). The annual flow of some discharges may fluctuate (Environmental Agency, 2021), especially if associated with shallow workings or sink holes, responding immediately to rainfall and recharge events (Farr *et al.*, 2016). For example, the Jackson Bridge mine water discharge, in Holmfirth, Yorkshire, normally visually affects the local river with ferric iron for 5 km downstream, but after heavy rainfall the river turned orange for 60 km (Environmental Agency, 2021). Interception of these rising waters, before or following surface break out, is an opportunity to prevent impacts and engineer a local, renewable heating source.

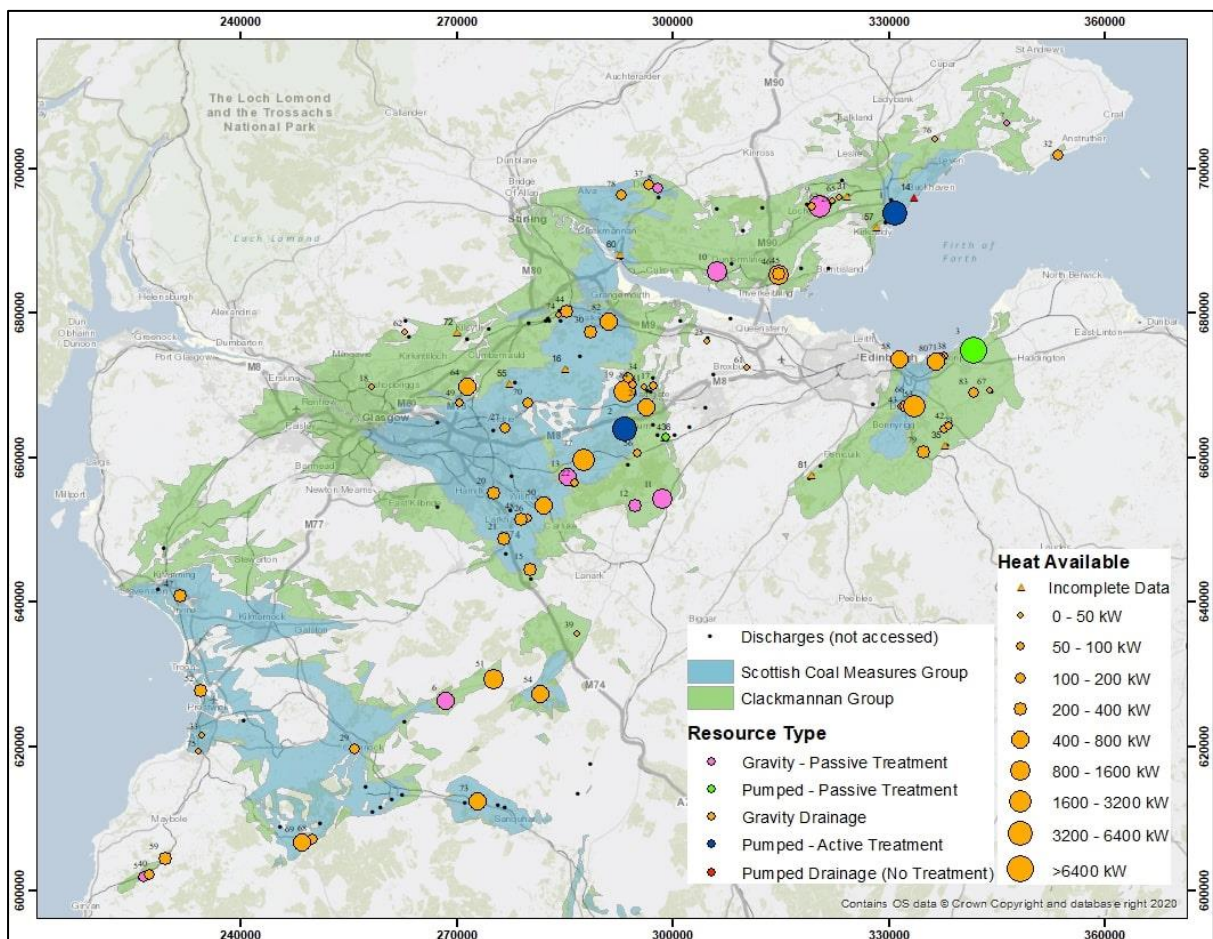


Figure 3.1 Map of Scotland's central belt coal-bearing strata with heat available from discharges and treatment sites. Contains British Geological Survey materials © UKRI 2022.

Gravity drainages can provide a source of low-carbon heating or cooling when coupled to appropriate thermal infrastructure in the form of heat exchangers and heat pumps. Since subsurface engineering is not required, gravity drainages represent a real opportunity for low-cost, low-risk resource utilisation when compared to schemes which require drilling of boreholes into multiple seams. For discharges which respond to seasonal rainfall, increased mine water fluxes fortunately correlate with periods of increased heating demand across colder months of the year (Farr *et al.*, 2016). Other discharges, which are often deeper sourced, show consistent flow rates independent of rainfall anomalies (Mayes *et al.*, 2021) which makes heat delivery consistent and reliable. This study presents heating potential and water chemistries, and therefore, the scale of an easily accessible low-carbon heating and cooling resource within the MVS. If sensibly harnessed, mine water gravity discharges can play a role in the decarbonisation of Scotland's heating infrastructure.

3.1.1 Geological Setting

This study focusses on the principal mining regions of Scotland, covering the Central, Lothians, Fife, Ayrshire and Douglas coalfields. The associated coal-bearing strata of the Carboniferous in the Midland Valley of Scotland terrane extend for approximately 150 km in an ENE trending block, 50 km wide, from Ardrossan and Girvan in the west to St Andrews and Haddington on the east coast (Cameron and Stephenson, 1985) (Figure 3.1). The MVS terrane is a graben structure bounded by the Highland Boundary Fault to the north and the Southern Upland Fault to the south (Bluck, 1984). As a sedimentary basin, it opened in the Lower Palaeozoic and preserves Silurian to Permian age sedimentary rocks (Cameron and Stephenson, 1985). The Carboniferous sedimentary successions and their relevant economic minerals are described in Table 3.1. Igneous activity across the area contributed to volcanic centres which now stand as elevated areas, e.g. the Kilpatrick, Campsie and Ochil hills; and subsurface activity cut the sedimentary sequences with a series of dykes and sills (Trueman, 1954). Depositional accommodation space, created as part of the transtensional strike-slip fault regime (Underhill *et al.*, 2008), generated several smaller basins which show syntectonic deformation thickness variations (Rippon *et al.*, 1996). Whilst coal seams across Scotland are found primarily in the Carboniferous successions within the MVS, the units extend into the Southern Upland Terrane, with further outliers hosted near Campbeltown in Kintyre, and in the Jurassic sedimentary successions of the Moray Firth at Brora (Trueman, 1954).

Table 3.1 Sedimentary successions from the Carboniferous for the West Lothian area of the Midland Valley of Scotland. Other areas host variations within the Strathclyde Group. Modified from (Monaghan, 2014) and (Waters *et al.*, 2007)

Age	Group	Formation	Dominant Lithologies	Economic Mineral
Westphalian	Scottish Coal Measures Group	Scottish Upper Coal Measures Formation	Sandstone, siltstone, mudstone, minor coal	Minor Coal
		Scottish Middle Coal Measures Formation	Sandstone, siltstone, mudstone, coal	Coal
		Scottish Lower Coal Measures Formation	Sandstone, siltstone, mudstone, coal	Coal
Namurian	Clackmannan Group	Passage Formation	Sandstone, conglomerate and mudstone	
		Upper Limestone Formation	Limestone, mudstone, siltstone, sandstone, coal	Coal
Visean		Limestone Coal Formation	Sandstone, siltstone, mudstone, coal	Coal
		Lower Limestone Formation	Limestone, mudstone, siltstone, sandstone	
	Strathclyde Group	West Lothian Oil Shale Formation	Oil-shale, sandstone, siltstone, mudstone	Oil-Shale
		Gullane Formation	Sandstone, mudstone, siltstone	
Tournasian	Inverclyde Group	Clyde Sandstone Formation	Sandstone	
		Ballaghan Formation	Siltstone, dolostone, minor evaporites	
		Kinnesswood Formation	Sandstone	

Early records of coal mining in Scotland date back to the 12th century, whereby monasteries were granted rights to extract coal, but the intensity of coaling increased significantly with the beginnings of the industrial revolution (Younger and Robins, 2002). Scottish coal was extensively mined in the Namurian Limestone Coal Formation of the Clackmannan Group and the stratigraphically higher Lower and Middle Scottish Coal Measures Formation of the Westphalian. Both the Limestone Coal and the Scottish Coal Measures host many workable coal seams amongst a cyclical stratigraphy of sandstones, siltstones, mudstones and shales (Cameron and Stephenson, 1985). Despite its name, the Limestone Coal Formation does not contain abundant limestone strata. The oil shales that are mined in some regions (e.g. West Lothian) are also held in Carboniferous strata (e.g. Visean), stratigraphically adjacent or subjacent to the coal-bearing formations (Monaghan, 2014).

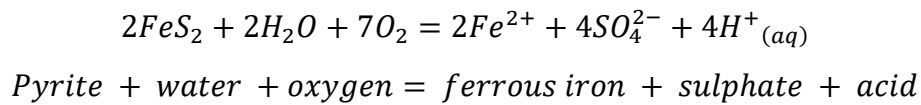
3.1.2 Hydrogeological Setting

The hydrogeological properties of unmined Carboniferous coal-bearing units in Scotland differ significantly to those of mined regions (Ó Dochartaigh *et al.*, 2015). The sandstone horizons of the sequences host the greatest permeabilities but tend to be fine grained, well cemented and interbedded with lower permeability mudstones, siltstones and coals (Ó Dochartaigh *et al.*, 2015). Groundwater movement in unmined regions is dominated by fracture flow, where host rock matrix permeabilities are in the range of 0.0003 to 0.1 m/d, and operational yields of 1.5 - 4.8 L/s are recorded by Ó Dochartaigh *et al.* (2015). Conversely, mined seams represent anthropogenic aquifers which have greatly increased aquifer transmissivity and can link formerly separate aquifer units laterally and vertically. The range of operational yields from boreholes and wells completed into mined strata in Scotland is large, from 0.5 L/s to 257.5 L/s (Ó Dochartaigh *et al.*, 2015), with flow regimes in the mined aquifers often being non-laminar (Younger and Adams, 1999). The common occurrence of a 1-2 m thick zone of significantly fractured or deformed rock mass above and below workings may have implications for overall hydraulic conductivity and storativity by creating preferential flow pathways and inducing adjacent porous media flow (Monaghan *et al.*, 2021c). As an example of the extent of mine working connectivity, the South Lanarkshire Farme Colliery, when active, was connected to other collieries over a scale of kilometres (Monaghan *et al.*, 2017, Monaghan *et al.*, 2021c). However, the groundwater flow properties in mine workings (Younger and Adams, 1999) and their response to pumping (Banks, 2021, Banks *et al.*, 2022) remain largely unpredictable before system installation and hydraulic characterisation. Similarly, temporal evolution of groundwater hydraulics in shallow mines may have implications for mine water thermal abstraction (Andrews *et al.*, 2020).

3.1.3 Mine water chemistry

The processes which influence coal mine water chemistry are well documented (Banks *et al.*, 2019, Banks *et al.*, 1997, Burnside *et al.*, 2016a, Younger, 2000b). Mine water discharges can be alkaline, acidic, ferruginous, saline, reducing, oxidising or relatively uncontaminated. Subsequent impacts of mine water chemistry on geothermal system infrastructure can include clogging and corrosion among others (Steven, 2021a, Walls *et al.*, 2021). Sulphide minerals which are present in coal-bearing strata or other mineral seams/veins, are susceptible to oxidation when exposed to air. Pyrite, in particular, is commonplace in coal-bearing strata and

when oxidised, reacts to release sulphate and soluble iron salts. The net processes are shown in Equation 3.1 (Banks *et al.*, 1997).



Equation 3.1

Mine drainage in Scotland typically comprises mineralised water with elevated concentrations of Ca, HCO₃⁻, SO₄²⁻, Fe and Mn (O Dochartaigh *et al.*, 2011). Circum-neutral pH values and high alkalinities suggest substantial dissolution of carbonate minerals by the acid derived from Equation 3.1 (Younger, 2001). Dissolution of carbonate minerals such as calcite (CaCO₃), dolomite (Ca,Mg(CO₃)₂), siderite (FeCO₃) and ankerite (Ca(Fe,Mg,Mn)(CO₃)₂) elevate concentrations of base cations and provide an additional potential source of dissolved iron (Banks *et al.*, 2019).

Groundwater rebound within mined voids dissolves sulphate and metal ions from rock faces and can carry resulting solutes to the surface. Extensive oxidation prior to water table rebound has historically induced ‘first-flush’ peak iron loads around one order of magnitude greater than long-term iron concentrations (Gzyl and Banks, 2007, Younger, 1997, Younger, 2000b). Discharged water is often clear at the outflow point since reducing conditions retain iron and manganese in solution. Following oxidation at surface, metal (oxy)hydroxides are precipitated and deposited, usually as orange “ochre” (ferric oxyhydroxide) on receiving channel beds. Ochre smothering in watercourses blocks sunlight and retards photosynthesis leading to serious deterioration in biological indices of water quality (Younger, 2000a).

Study of mine water discharges provides an inexpensive means to understand and monitor mine water properties across a region. Evidence for stratification of water chemistries in mined sequences (Loredo *et al.*, 2017b, Nuttall and Younger, 2004) means that sampled gravity discharges will tend to over-represent relatively shallow portions of mine water systems, however, the discharge chemistry provides a readily accessible proxy for the conditions in the mines. Dissolved ferrous iron in coal mine waters is often assumed to be predominantly derived from pyrite oxidation, but it may alternatively result from dissolution of iron-containing carbonates (Banks *et al.*, 1997) or conceivably even from reductive dissolution of ferric oxides or oxyhydroxides (Haunch *et al.*, 2021, Peiffer and Wan, 2016, Stumm and Sulzberger, 1992). Where dissolution of iron carbonate predominates, it can generate water chemistries with elevated iron and bicarbonate alkalinity, but relatively little sulphate (<100 mg/L) (Younger, 2000a). Oil shale mines, found primarily in West Lothian (Monaghan, 2014), and coal mines can both be influenced by dissolution of iron sulphides

(pyrite) and iron carbonates (siderite, ankerite). However, siderite tends to be more prominent in freshwater sedimentary sequences and pyrite in increasingly brackish or marine sedimentary sequences (Spears and Amin, 1981). It is recognised that much of the deposition of the West Lothian Oil Shales took place in fresh-brackish lacustrine environments and that siderite is an important component of the sequence (Dean *et al.*, 2018, Jones, 2007). One can thus speculate that iron carbonate dissolution may be more prominent in Scottish oil shale mines than coal mines – if so, one would expect lower sulphate contents in oil shale mine water.

Isotopic characterisation of water as measured by $\delta^{18}\text{O}$ and $\delta^2\text{H}$ (as ‰, against those ratios in the standard V-SMOW¹), can help decipher the age and interaction histories of the mine water (Burnside *et al.*, 2016b). Sulphur isotopic values, $\delta^{34}\text{S}$, give insight into the source and history of mine water sulphate (Banks *et al.*, 2020, Burnside *et al.*, 2016a, Janson *et al.*, 2016). Pyrite oxidation typically results in negligible S-isotopic fractionation in resulting sulphate relative to the source sulphide (Chen *et al.*, 2020). $\delta^{34}\text{S}$ values of pyrites (n=21) in East Ayrshire coals range between -26.3‰ and +18.4‰ with an overall mean (cleat and banded pyrite) of +2.7‰ (Bullock *et al.*, 2018). Studies have found that the mean values for deep mine waters in Europe can be around +20‰, and occasionally heavier (Banks *et al.*, 2020). Speculation of the controlling factors on sulphur fractionation contributing to the additional heavy sulphate has led to hypotheses including dissolution of sulphate-bearing evaporite horizons within overlying or adjacent strata (Chen *et al.*, 2020), residual marine waters, residual evaporative brines, and bacterial or thermal sulphate reduction reactions (Banks *et al.*, 2020). Seawater $\delta^{34}\text{S}$ values show a decreasing trend from +21‰ to +12‰ through the Carboniferous, where periods hosting the principal coal seams in Scotland (Namurian and Westphalian) show values of c. +14‰ to +16‰ (Kampschulte *et al.*, 2001).

¹ $(R_{\text{sample}}/R_{\text{standard}}) - 1) \times 1000 = \delta$ value; where $R = {}^{34}\text{S}/{}^{32}\text{S}$, ${}^{18}\text{O}/{}^{16}\text{O}$, ${}^2\text{H}/{}^1\text{H}$ – resulting in $\delta^{34}\text{S}$, $\delta^{18}\text{O}$ and $\delta^2\text{H}$ respectively.

3.2 Materials and Methods

3.2.1 Existing Data

Bailey *et al.* (2016) have compiled data and estimated thermal recovery potential for 12 mine water treatment schemes owned and operated by The Coal Authority in Scotland (Table 3.2). Additionally, there is a council operated treatment site near Allanton (55.7952°N, 3.8276°W) treating an overflow of water from Kingshill Colliery (James Hutton Institute, 2016). Data for each treatment site summarised from existing literature and data sources can be found in Appendix 3A.

Table 3.2 Coal authority treatment sites in Scotland (Bailey *et al.*, 2016)

Coal Authority treatment scheme	Ref No.	Treatment Type	Northing (°)	Easting (°)
Frances	1	Pumped – Active	56.1327	-3.1120
Polkemmet	2	Pumped – Active	55.8573	-3.7044
Blindwells	3	Pumped – Passive	55.9627	-2.9341
Cuthill	4	Pumped – Passive	55.8485	-3.6138
Dalquharran	5	Gravity – Passive	55.2799	-4.7308
Kames	6	Gravity – Passive	55.5121	-4.0843
Lathallan Mill	7	Gravity – Passive	56.2462	-2.8655
Mains of Blairingone	8	Gravity – Passive	56.1583	-3.6434
Minto	9	Gravity – Passive	56.1391	-3.2808
Pitferrane	10	Gravity – Passive	56.0549	-3.5077
Pool Farm	11	Gravity – Passive	55.7708	-3.6169
Wilsontown (Mousewater)	12	Gravity – Passive	55.7611	-3.6769

3.2.2 Identifying sample locations

At the start of the 21st Century, Scotland had 167 known mine water discharges in the MVS, with a total of 180 km of water courses affected by ochre (Younger, 2000a). We were provided with 153 records of mine water discharges sample locations of discharges believed to be associated with historic mining activities, which in 2000 were freely draining following coalfield-wide groundwater recovery towards pre-mining levels (Haunch, 2020).

Finding discharges relied upon identification of orange ochreous stream bed staining or a distinctive H₂S gas odour, indicative of potential microbial reduction of mine water sulphate. Any mine water discharges which may have been clear, colourless and without a smell or iron staining would have been overlooked, however, any streams or flowing water found near to the

original grid references were sampled for at least temperature and conductivity as indicative properties. Additionally, some natural groundwater discharges can be iron- or sulphide-rich, so the diagnostic criteria could not definitively confirm investigated waters as coal mine drainage. As a result, 66 of the 153 sites previously identified were analysed for this study. Some sites were identified but deemed unsuitable for sampling due to health and safety risk *e.g.*, Kincardine (#60²) which appeared as deep ochreous water within 5m of an active railway line; lack of clarity of where to sample a ‘pure’ mine water source; or cessation of flow. Five significant gravity discharges have been omitted due to access or safety reasons, in these instances data on flow rates, locations and iron concentrations has been taken from Whitworth *et al.* (2012) and their heating potential included in the results section, and shown in Appendix 3A.

Of the 66 sampled discharges, 64 are believed to be related to coal mines and 2 to oil shale mines, the latter typically associated with the Visean West Lothian Oil-Shale Formation. There are no discharges exclusively from limestone mines, but discharges related to coal seams may source water from adjacent worked limestone units, *e.g.* Wallyford Great (Watson, 2007). Of the 64 coal mine discharges, 26 are believed to be derived from mines or strata in the Westphalian Scottish Coal Measures Formation, while 38 are believed to be derived from mines in the Namurian Limestone Coal Formation.

3.2.3 Field sampling and onsite analysis

Throughout September and October of 2020, each of the 153 sites were visited with the primary aim to identify the precise location of the discharges, describe their source and characteristics, take initial physicochemical, temperature, and flow rate readings. The initial scouting exercise was to inform and streamline focused sampling trips for laboratory analyses. At each site the discharge was sampled as close to the emergence and as safely possible. A handheld Myron P Ultrameter was used to determine discharge pH, temperature, oxidation reduction potential (ORP) and electrical conductivity (EC). Recorded pH and EC values were automatically corrected to a standard temperature of 25 °C. ORP was measured in millivolts (mV) and read from a platinum sensor and a silver chloride (Ag/AgCl)-saturated KCl reference electrode. ORP values were 199mV lower than true Eh from a standard hydrogen electrode (Robinson pers. comm., 2022) but are presented here without adjustment. Equipment was

² The reference number preceded by the # symbol, aligns with the ordering system in Appendices A and B.

calibrated before each day's fieldwork and all water samples were refrigerated as soon as possible after collection.

Total alkalinity was determined as mg/L equivalent of CaCO₃ with a Hach Model 16900 digital titrator, using 1.6 N sulphuric acid and bromcresol green - methyl red pH indicator. Recorded values in mg/L CaCO₃ equivalent were then converted to meq/L (by dividing by 50.04 mg meq⁻¹). The alkalinity is assumed to be predominantly in the form of HCO₃⁻ at circumneutral pH values.

Separate aliquots were taken at site for different analyses. Filtration, to remove any particulate matter, was carried out using a hand-held, syringe mounted filter capsule. An aliquot for major anion analysis was filtered at 0.45 µm into 15 mL polypropylene screw-cap vials, with 2 mL decanted into custom vials for laboratory alkalinity analysis. An aliquot for dissolved elemental content was filtered at 0.45 µm into a 15 mL polypropylene screw cap vials and preserved using one drop of concentrated HNO₃ (68%, trace metal grade, Fisher Chemicals). An unfiltered aliquot for total (dissolved and undissolved) elemental content was collected using a clean 15 mL polypropylene screw cap vial. An aliquot for δ¹⁸O and δ²H analysis was taken using clean 15 mL polypropylene screw-cap vials, sealed with Parafilm to prevent sample evaporation. Three meteoric control δ¹⁸O and δ²H aliquots were taken monthly between December 2016 and February 2020 from the rooftop of the Rankine Building, University of Glasgow (55.8728°N, 4.2857°W). A 1 L unfiltered aliquot of sample water was collected in a plastic flask for sulphate-δ³⁴S analysis. Sulphate was subsequently precipitated as barium sulphate, using the method of Carmody *et al.* (1998): namely, the sample was acidified to pH 3–4 by dropwise addition of concentrated HCl (37% Trace Metal Grade, Fisher Chemicals) and then dosed with excess 5% BaCl₂ solution. A rapid cloudy reaction indicated the presence of sulphate via BaSO₄ precipitation.

Flow rate was calculated by measuring each stream channel's dimensions. The flow rate Q (cm³/s) is estimated from Equation 3.2, where depth and width are in cm, and V is velocity, measured in cm/s. The correction factor of 0.5 is applied to account for the irregular flow cross section and slower flow at the channel edges.

$$Q = Depth \times Width \times V \times 0.5$$

Equation 3.2

The width of the flow channel at the surface (cm) and the depth of the flow channel (cm) were measured with a ruler or tape measure. The flow speed of the channel (cm/s) was measured by dropping a buoyant item (normally leaf or grass) into the flow and measuring

distance covered in 1 second. Flow rates in cm^3/s were then multiplied by 0.001, to obtain a discharge in L/s. In other instances where the flow was from a discrete source and of a low flow rate, it was measured by timing the filling of a 1 L flask.

Finally, notes and photographs were recorded to detail each individual sample point. Notes included: the presence/intensity of H_2S gas smell; the source of the drainage (identified as closely as safely possible); the colour and turbidity of the mine water; and the size and colour of flocs suspended in the water. Each of these additional data points can be found alongside images of the discharges in Appendix 3B.

3.2.4 Laboratory hydrochemical analytical methods

Of the 66 discharge samples identified, 57 were sampled for chemical analysis. All hydrochemical analyses were completed in the laboratories of the Department of Civil and Environmental Engineering (CEE), University of Strathclyde.

A Metrohm 850 Professional ion chromatographer was used for determination of five anions (F^- , Cl^- , SO_4^{2-} , Br^- , NO_3^-). The separation utilised a Metrosep A Supp 5 anion analytical with Guard column (Metrosep A Supp 5 Guard/4.0) at 24 °C and an eluent comprising of 1 mM NaHCO_3 and 3.2 mM Na_2CO_3 prepared in ultra-pure water ($18.2 \text{ M}\Omega \text{ cm}^{-1}$) (Triple Red water purification system). The flow rate was 0.7 mL/min. Calibration standards were 0.1, 0.5, 1, 5 and 10 mg/L and prepared in ultra-pure water. Samples with elevated concentrations were diluted with ultra-pure water to a level within a calibration range. Anion concentration was chosen on an individual basis, when the least diluted sample version fitted the calibration range. The IC method was developed according to British Standards Institution (2009) and Metrohm customer support recommendations.

Determination of 12 dissolved and total elements (B, Ba, Ca, Fe, K, Mg, Mn, Na, S, Si, Sr and Zn) used an Inductively Coupled Plasma Optical Emission Spectrometer (ICP-OES) iCAP 6200 Duo View ICP Spectrometer, Thermo Fisher Scientific model equipped with an autosampler (Teledyne CETAC Technologies, ASX-520) and Thermo i-TEVA Version 2.4.0.81, 2010. The operating conditions are presented in Appendix 3C.

For determination of total elemental content, the samples were acid digested using a Microwave Assisted Reaction System (MARS-6, CEM). 10 mL of thoroughly mixed, unfiltered sample was transferred into MARS Xpress Plus 110 mL Perfluoroalkoxy alkane (PFA) microwave digestion vessels. Samples were digested with reversed “*Aqua Regia*” mixture of hydrochloric and nitric acids (1:4, HCL - 37 %, and HNO_3 - 68 %, Trace Metal

Grade, Fisher Chemicals). The following microwave operating parameters were utilised: maximum power - 1800 W; ramp time - 20 minutes; hold time - 20 minutes; temperature – 170 °C. Samples digests were brought up to 50 mL with ultrapure water using volumetric flasks, then filtered through 0.45 µm for ICP-OES analyses.

Multi-element 3-point calibration standards were prepared from 1000 mg/L element stock standard solutions (Fisher Scientific) using ultrapure water. Addition of 68% trace metal analysis grade nitric acid (Fisher Chemicals) to a final acid concentration of 5% for dissolved content analyses, and addition of reversed “*Aqua Regia*” to 20% for total elemental content analyses. Yttrium (5 mg/L) was used as internal standard (IS) solution (Fisher Chemicals), to account for any matrix effects due to differences between samples and standards. The IS was added through automated online addition with an internal standard mixing kit. A brief method validation study found the following linear ranges: 0.01 to 1 mg/L for barium and strontium, 0.5 to 50 mg/L for calcium, magnesium, potassium, sodium, iron and sulphur and 0.1 to 10 mg/L for boron, manganese, silica and zinc. Analyses proceeded when calibration curves generated correlation coefficients (R^2) >0.9980. Instrument equilibration and system’s suitability were checked according to CEE labs Standard Operating Procedure for ICP-OES and Quality Control and Assurance procedure. CEE methods of analyses were mainly based on British Standards Institution (2018).

Elemental method quantification limits were based on instrument-predicted method quantification limit values (Appendix 3C), obtained from the calibration parameters for each element.

In addition to field analyses of alkalinity, the decanted portion of the anion aliquot was analysed for laboratory-based alkalinity using an automated discreet KoneLab Aqua 30 (Thermo Scientific Aquarem 300; Clinical Diagnostic). Methyl orange buffer solution approach was used, with the intensity of colour measured spectrophotometrically at 550 nm. All relevant data is included in Appendix 3B.

3.2.5 Laboratory isotopic analytical methods

Isotopic determinations for all 57 sampled mine water discharges were carried out at the National Environmental Research Centre (NERC) National Environmental Isotope Facility (NEIF) Stable Isotope Laboratory based at the Scottish Universities Environmental Research Centre (SUERC), East Kilbride.

For $\delta^{18}\text{O}$ analysis, samples were over-gassed with a 1% CO_2 -in-He mixture for 5 min and left to equilibrate for a further 24 hours. A sample volume of 2 mL was then analysed using standard techniques on a Thermo Scientific Delta V mass spectrometer set at 25 °C. Final $\delta^{18}\text{O}$ values were produced using the method established by Nelson (2000). For $\delta^2\text{H}$ analysis, sample and standard waters were injected directly into a chromium furnace at 800 °C (Donnelly *et al.*, 2001), with the evolved H_2 gas analysed on-line via a VG Optima mass spectrometer. Final values for $\delta^{18}\text{O}$ and $\delta^2\text{H}$ are reported as per mille (‰) variations from the V-SMOW standard in standard delta notation. In-run repeat analyses of water standards (international standards V-SMOW and Greenland Ice Sheet Precipitation (GISP), and internal standard Lt Std) gave a reproducibility better than $\pm 0.3\text{‰}$ for $\delta^{18}\text{O}$ and $\pm 3\text{‰}$ for $\delta^2\text{H}$. For sulphate- $\delta^{34}\text{S}$ isotope analysis, barium sulphate precipitate was recovered from the sampling vessel, washed repeatedly in deionised water and dried. SO_2 gas was liberated from each sample by combustion at 1120 °C with excess Cu_2O and silica, using the technique of Coleman and Moore (1978), before measurement on a VG Isotech SIRA II mass spectrometer. Results are reported as per mille (‰) variations from the Vienna Canyon Diablo Troilite (V-CDT) standard in standard delta notation. Reproducibility of the technique based on repeat analyses of the NBS-127 standard was better than $\pm 0.3\text{‰}$.

3.2.6 Quality Assurance

The ion balance errors (IBE) were deemed acceptable after they returned 31 results within $\pm 5\%$, 20 within $\pm 10\%$, 5 within $\pm 15\%$, and one outlier at 17%. Despite the outlier having an IBE of 17%, the disparity between cations and anions was 0.23 meq/L, reflecting a very low margin for error for samples with low mineralisation.

Since sulphate (SO_4^{2-}) was run via IC, and sulphur elemental analysis was run via ICP-OES, correlation between the two for sulphate (meq/L) is possible (on the assumption that all sulphur is present as sulphate). These show a very strong correlation (Appendix 3C), but sulphate concentrations derived from measured ICP sulphur were selected for use in IBE and presentation. The correlation between field and laboratory alkalinity was good (Appendix 3C). The laboratory analyses are preferred and cited since a colorimetric endpoint was sometimes difficult to judge in the field for mine waters tinted with turbidity, iron flocs or changing daylight.

‘Field blanks’ were collected in parallel to discharge samples, ultrapure water was carried into the field and analysed subject to the same collection and processing methods as the

discharge samples, e.g., filtration, acidification, digestion. This was done to monitor for any contamination of samples during collection. Laboratory blanks were created from ultrapure water and subjected to the same laboratory processes as the discharge samples to check for contamination. All field and lab blanks returned acceptable values which concluded there was no, or minimal interference from the process of field sampling, sample preparation and/or laboratory analyses.

3.2.7 Thermal resource estimates

The thermal resource potential of discrete mine water flows present at the surface was calculated using two different methods. Firstly, as a function of flow rate and temperature, the **heat available (G)** was calculated in Equation 3.3.

$$G = Q \cdot \Delta T \cdot S_{VCwat}$$

Equation 3.3

Where, Q is flow rate (L/s), ΔT is temperature change in K, S_{VCwat} is volumetric heat capacity of water ($4180 \text{ J L}^{-1} \text{ K}^{-1}$). The ΔT value is the temperature change in the mine water that can be effected by a heat exchange or heat pump device and will also depend on the raw temperature of the mine water. For **G**, the ΔT will vary since the warmer the source water, the greater the temperature drop that can be accomplished without risk of freezing in the heat exchanger. We selected $6 \text{ }^\circ\text{C}$ as a suitable return temperature following heat exchange, therefore, ΔT values are defined as the difference between the mine water temperature and the postulated return temperature of the “thermally spent” mine water ($6 \text{ }^\circ\text{C}$). Note that absolute temperature values e.g., discharge source or return temperatures, are in $^\circ\text{C}$, whereas relative temperatures and changes (ΔT), for use in equations, are in K.

Alternatively, we can estimate the total **heat pump delivery (H)** (Equation 3.4) from a heat pump system, the principal differences being that: a) additional heating is added from the electrical input of the heat pump, and b) the value of ΔT is set at an assumed constant value of 4 K (as opposed to fluctuating with source temperature). We assumed a uniform coefficient of performance (COP) of 4, though it should be noted that heat pump COP can vary depending on the temperature of the heat source. The only variable for **H** in Equation 3.4 is flow rate (Q), therefore resources with high temperatures do not generate higher values, as they would for **G**.

$$H = \frac{Q \cdot \Delta T \cdot S_{VCwat}}{1 - \left(\frac{1}{COP}\right)}$$

It should be noted that, while a small ΔT of 4 K is a reasonably typical figure for a heat pump evaporator, larger ΔT values can be achieved by manipulating flow rates across a secondary heat exchanger, although larger ΔT will typically be at the expense of COP.

3.3 Results and Discussion – Thermal Resources

A catalogue of discharge descriptions and images is available in the supporting material Appendices 3A and 3B. Since the original mine discharge data was two decades old, it was clear that in some instances, more recent developments had altered the presence or form of the discharges. Some locations had treatment sites established by TCA, whilst others were near new housing developments, where shallow mine voids may have been thoroughly grouted for ground stability.

Heat available (G) from each of the locations of the discharges or treatment sites is plotted in Figures 3.1 and 3.2. The greatest single source of mine water heat available at the surface is 6.9 MW (Blindwells - pumped, passive treatment site - #3). With a source temperature of 11.6 °C ($\Delta T = 5.6$ K), and an average discharge of 294.6 L/s (Bailey *et al.*, 2016), Blindwells hosts the highest available surface mine water heating resource in Scotland. The two Coal Authority sites with pumping and active treatment (Frances - #1; Polkemmet - #2), host the next highest values of available heat, 3.6 MW and 3.9 MW respectively. One treatment site with gravity drainage and passive treatment has a heating capacity over 2 MW (Minto - #9), whilst two others of the same nature host available heat above 1 MW (Pitfirrane - #10; Pool Farm - #11).

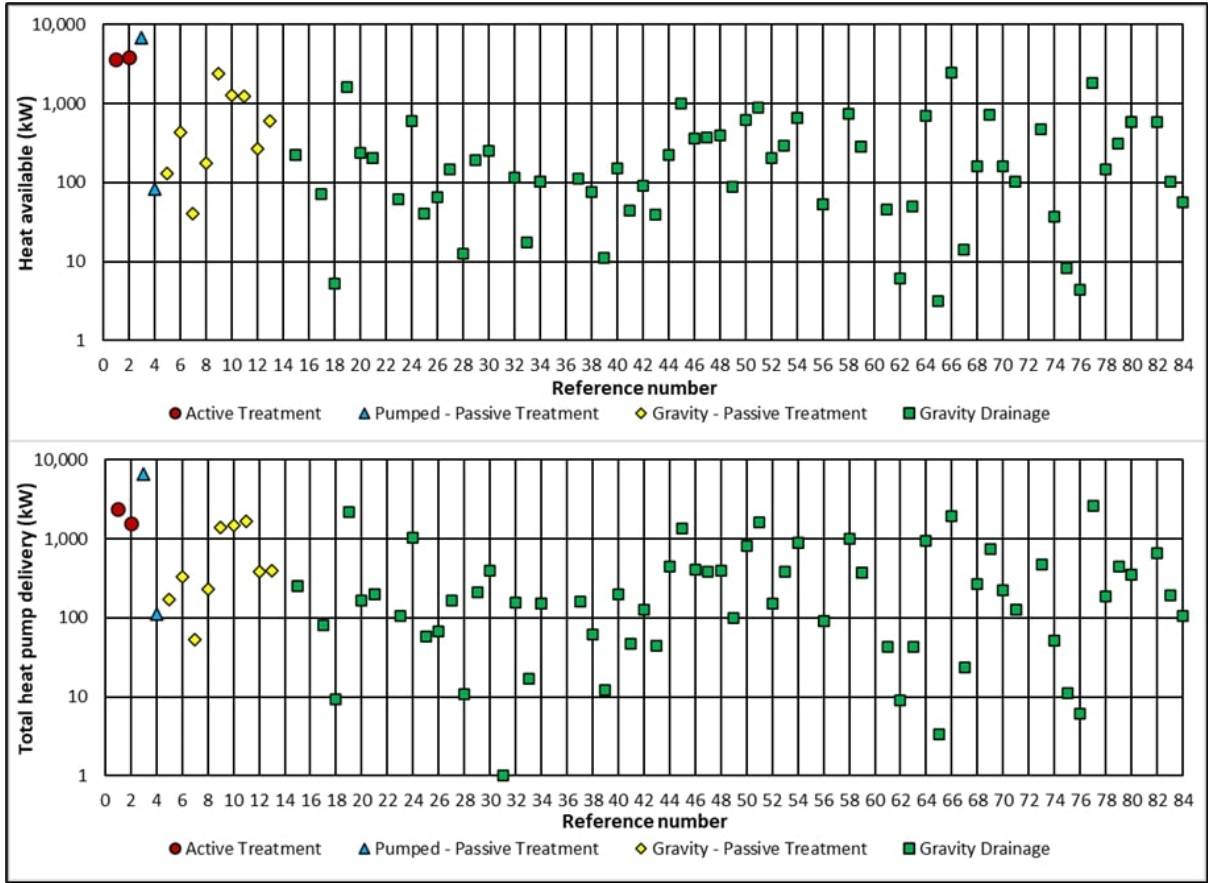


Figure 3.2 Thermal outputs of treatment sites and gravity drainages. Heat available (top) and total heat pump delivery (bottom).

The potential heating resource of treatment or pumping stations is already understood by TCA (Bailey *et al.*, 2016), where 34 billion litres of water was treated by TCA in Scotland during 2020-2021 (The Coal Authority, 2021a). The total estimated volume of water across the year equates to c. 1078 L/s estimated flow rate, which when used for **total heat pump delivery (H)** (Equation 3.4), with a ΔT value of 4 K and a COP of 4 gives a total potential heat delivery of:

$$H = \frac{1078 \text{ L s}^{-1} \cdot 4 \text{ K} \cdot 4180 \text{ J L}^{-1} \text{ K}^{-1}}{1 - \left(\frac{1}{4}\right)}$$

$$H = 24 \text{ MW}$$

Equation 3.5

Combining temperature and flow rate data from other sources (Bailey *et al.*, 2016, James Hutton Institute, 2016, Whitworth *et al.*, 2012), suggest that the **total heat pump delivery (H)** from treatment sites across Scotland (TCA and Council operated) is a more modest 16.8 MW, from a total flow rate of 754 L/s. **Heat available (G)** (Equation 3.3) derived from the same dataset for the Scottish treatment sites produces a higher overall total of 21 MW

since this reflects larger ΔT values than the standard 4 K for **H** (in some cases ΔT is as high as 13.2 K from a discharge temperature of 19.2 °C (Polkemmet, #2)), however, the additional heating contribution from the heat pump is absent.

In addition to TCA pumping or treatment sites, the untreated gravity drainages found as part of this study are estimated to have a collective **total heat pump delivery (H)** (with ΔT value of 4 K and a COP of 4) of 23.9 MW, which doubles potential heat delivery from surface mine water in Scotland. **Heat available (G)** from untreated gravity drainages is 19.3 MW. Untreated discharges reported in (Whitworth *et al.*, 2012) which feature in Appendix 3A (i.e. not sampled in this study) were assigned a temperature of 10 °C, and therefore, the true value for **G** may be slightly higher.

Treated and untreated mine water combine to present a heating potential of up to c. 48 MW available at the surface. Surface resources provide the ‘lowest hanging fruit’ when planning mine water heating and cooling development. These resources can be harnessed without significant capital expenditure for drilling and with greatly reduced pumping costs as part of the operational expenditure. Visualising heat units (W - watts) can be simplified by assigning an average 2 bed house/flat a thermal peak demand of 4 kW (BoilerGuide, 2022). With this generalised assumption, we can state that up to 12,000 two-bedroom homes could be heated by surface mine water resources. This optimistic viewpoint should be tempered by the fact that many of the discharges are distant from urban areas and other loci of heat demand, meaning that the potential thermal resource has no obvious user at present. Prior to harnessing the thermal energy of a mine water discharge, regular sampling and monitoring should be performed to establish environmental baselines and seasonal temperature variability. These data are imperative for assessing overall heating/cooling delivery before installation of any associated infrastructure.

Table 3.3 Results for all gravity mine drainages (not including the 4 pumped systems in Scotland). Data from TCA treated discharges available only for: Flow rate L/s, Temperature, Heat Available, Total Heat Delivery with COP of 4 and $\Delta T=4$ K, pH, Electrical Conductivity, Alkalinity and Fe (total). CTP – Calculated thermal potentials, LID – Laboratory isotopic data.

		Units	Maximum	75th percentile	Median	Mean	25th percentile	Minimum
Field data	Flow rate	L/s	117	20.0	8.93	19.5	3.0	0.15
	Temperature	°C	15.1	11.2	10.2	10.6	9.70	7.80
	pH	pH units	8.00	6.99	6.80	6.73	6.52	4.01
	Electrical Conductivity	$\mu\text{S/cm}$	6515	1238	932	1104	578	146
	Oxidation-Reduction Potential	mV	330	14	-10	-3	-39	-103
	Alkalinity	meq/L	22.1	8.43	5.45	6.26	3.02	0
CTP	Heat Available (G)	kW	2487	426	154	358	50.7	0.71
	Total heat pump delivery (H)	kW	2606	438	197	429	63.5	1.00
Laboratory chemical data	F ⁻	mg/L	0.620	0.147	0.116	0.143	0.093	0.060
	Cl ⁻	mg/L	900	43.7	30.5	65.6	17.9	7.31
	SO ₄ ²⁻	mg/L	1170	250	148	223	72.7	6.71
	Br ⁻	mg/L	13.1	3.16	1.26	1.92	0.354	>0.02
	NO ₃ ⁻	mg/L	11.6	1.03	0.215	1.10	0.022	>0.01
	Na	mg/L	1345	44.9	23.9	69.4	16.0	4.36
	Ca	mg/L	256	121	94.7	97.5	54.7	5.10
	Mg	mg/L	158	63.0	40.7	47.3	22.2	2.38
	K	mg/L	38.3	14.5	7.48	9.87	3.87	0.830
	Fe (total)	mg/L	74.8	11.2	4.23	10.1	1.98	0.416
	Fe (Diss)	mg/L	56.0	7.30	3.41	8.64	1.52	0.024
	Mn (Total)	mg/L	6.61	1.63	0.770	1.31	0.371	0.030
	Mn (Diss)	mg/L	6.72	1.76	0.853	1.43	0.499	0.013
	Sr	mg/L	3.04	1.36	0.616	0.89	0.243	0.016
	Si	mg/L	14.7	6.73	4.75	5.73	4.09	2.06
	B	mg/L	0.838	0.152	0.074	0.140	0.032	0.002
	Zn	mg/L	0.194	0.024	0.008	0.021	0.004	0.001
Ba	mg/L	0.231	0.071	0.039	0.054	0.026	0.013	
Chemical ratios	Cl/Br mass ratio		1904	98.6	26.1	125.0	10.8	2.42
	SO ₄ ²⁻ /Cl ⁻ molar ratio		16.72	3.22	1.61	2.74	0.655	0.080
	Na/Cl ⁻ molar ratio		11.97	1.43	1.06	1.88	0.902	0.426
	(Ca+Mg)/SO ₄ ²⁻ meq ratio		16.8	3.72	2.51	3.11	1.45	0.525
	Ca/Mg molar ratio		7.32	1.717	1.340	1.601	1.036	0.752
	Ca/Alkalinity meq ratio		1879	1.28	0.760	35.1	0.591	0.242
LID	$\delta^{34}\text{S}$	per mille	+48.0	+13.3	+9.9	+10.7	+5.3	+0.3
	$\delta^{18}\text{O}_{\text{vsmow}}$	per mille	-6.8	-7.4	-7.6	-7.6	-7.8	-8.5
	$\delta\text{D}_{\text{vsmow}}$	per mille	-43.7	-48.0	-49.2	-49.6	-52.0	-57.0

Results and Discussion – Hydrochemical Data

3.3.1 Physicochemical properties

The physicochemical results for every gravity drainage (#5-84) including those treated by TCA (Bailey *et al.*, 2016) or local council (James Hutton Institute, 2016) are presented as box and whisker plots in Figure 3.3 and listed in Table 3.3. The box portion contains the middle 50% of the data points (between the 25th and 75th percentiles), representing the interquartile range (IQR) (Tukey, 1977). The central line represents the median value, whilst the cross locates the arithmetic mean. The ‘T’ shaped whiskers extend towards the maximum and minimum values of the dataset. Their extent is capped at 1.5 times the length of the box (Reimann *et al.*, 2008), and reach as far as the most extreme value within this range. Beyond the extent of the whiskers, individual extreme outlier data points are plotted. Any samples with values below detection limits have been set to 0 for the purposes of plotting.

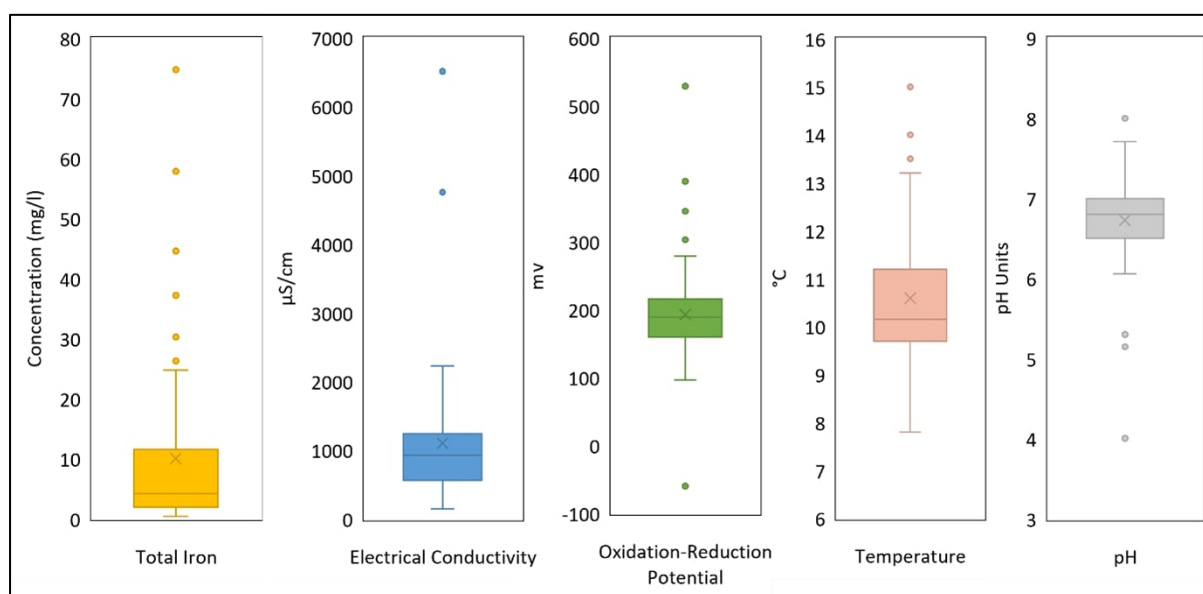


Figure 3.3 Box and whisker plots for total iron and physicochemical properties for all gravity drainages in Scotland including those treated by TCA (Bailey *et al.*, 2016) or the council (James Hutton Institute, 2016), and the untreated discharges sampled in this study.

Water temperatures range between 7.8 °C and 15.1 °C. Very shallow coal mine drainages with short groundwater flow pathways can be influenced by thermal variations at surface or percolating rainfall temperatures, causing discharge temperature to fluctuate across the seasons (Farr *et al.*, 2016). Higher temperatures reflect mine water source depth and the geothermal gradient of an area (Farr *et al.*, 2021), buffered from surface temperature fluctuations by tens to hundreds of metres of bedrock. The highest overall discharge

temperature is from TCA's treatment site at Minto (#9) gravity drainage (15.1 °C) (56.1391°N, 3.2808°W) where the coordinates of the discharge location correlate with the disused No.1 and No.2 shafts of Minto Colliery, reaching 184 m BGL and 302 m BGL respectively (The Coal Authority, 2022). The highest temperature discharge sampled as part of this study (15.0 °C) is Wallyford Great (55.9475°N, 3.0167°W) (#80). Watson (2007) explains the arrangement of the Wallyford Great 'engineered' discharge, which flows from an artesian borehole. The borehole was recently drilled (in 2005) to c. 190 m BGL, where it is understood to drain artesian waters from unrecorded limestone workings, connected to Wallyford colliery. Temperature seasonality was not measured in this study, but accounts of mine water discharges from Wales in Farr *et al.* (2016) show a variety of temperature responses throughout the year. Deep sources demonstrated greater stability (subset reported in Walls *et al.* (2021)), whilst shallow sources or rapidly recharging systems, showed greater temperature fluctuation, some displaying an IQR of around 3 °C (Farr *et al.*, 2016).

Electrical conductivity (EC) ranges between 146 µS/cm and 6515 µS/cm, with an interquartile range of 564 – 1242 µS/cm. EC reflects total ionic solute content and is influenced by groundwater residence time, influence of marine or connate water, soil zone processes (e.g., rainfall evapotranspiration and CO₂ generation) and rock mineral suite and degree of weathering. In coal mines, one potential determining reaction is sulphide oxidation which not only releases iron and sulphate, but also protons, which hydrolyse other minerals and release base cations and alkalinity. Consumption of protons (acid) by carbonate (and silicate) weathering explains the circumneutral pH values observed in many of the mine waters, and their alkalinity content (Wood *et al.*, 1999). However, it is also known that deep coal mines sometimes host naturally saline formation water (Anderson, 1945, Younger *et al.*, 2015). The two elevated EC outliers are Glenburn (#52) (6515 µS/cm) and Douglas (#39) (4756 µS/cm). Associated elevated Na and Cl⁻ values for the Glenburn discharge (55.5145°N, 4.6223°W) and an immediate proximity to the coast, reasonably suggests marine influence on chemistry and EC. The Douglas discharge (55.6008°N, 3.7994°W) also contains elevated Na and Cl⁻ values but is sited c. 50 km from the coast. The recorded mine adit appears to drain workings associated with Douglas colliery's main shafts (both 238 m deep (Oglethorpe, 2006)) and to be overlain by spoil heaps (binges) from the mine. It is known that deep mines throughout the UK are characterised by highly saline formation waters (Younger *et al.*, 2015). The sodium chloride content in the Douglas mine water (721 mg/L sodium and 900 mg/L chloride) could thus be due to a component of saline water either in the mine water itself or in leachate from the spoil tips percolating into the adit.

Highly variable redox conditions in shallow mine waters are reflected by ORP ranges between -103 mV and +330 mV, with a median value just below zero (-10 mV). 23 of 58 discharges (39.7%), not including those treated by TCA, had an H₂S odour.

Total iron present in Scotland's mine water discharges ranges from 0.4 mg/L to 74.8 mg/L, with an interquartile range of 2.0 - 11.6 mg/L. The Dalquharran (#5) discharge (55.2799°N, 4.7308°W) hosts the highest total iron concentration, after infamously having one of the highest ever recorded peak iron concentration (c. 1500 mg/L) during the 'first flush' phase of mine water rebound and surface breakout (Younger and Adams, 1999). Peak and long-term iron concentration are often linked and may correlate with total sulphur content of the worked coal seams (Younger, 2000b). The Dalquharran discharge is currently intercepted by a passive treatment arrangement operated by TCA, before outflow to the local watercourse (Water of Girvan).

3.3.2 Elemental properties

The following figures and hydrochemical interpretations consider only the 57 sample sites of this study. TCA treatment sites have been omitted since they are partially characterised elsewhere (Bailey *et al.*, 2016), and sampling access was limited. Figure 3.4 shows box and whisker diagrams for mine water chemistry. Bicarbonate and sulphate are the dominant anions in the mine water. Chloride is a dominant anion in two discharges (discussed above). Elevated sulphate in the mine waters is usually assumed to reflect the products of sulphide oxidation processes, but interpretation of $\delta^{34}\text{S}$ may also suggest other possible sulphate sources including marine inundation, evaporites, evaporitic brines or carbonate associated sulphate (CAS).

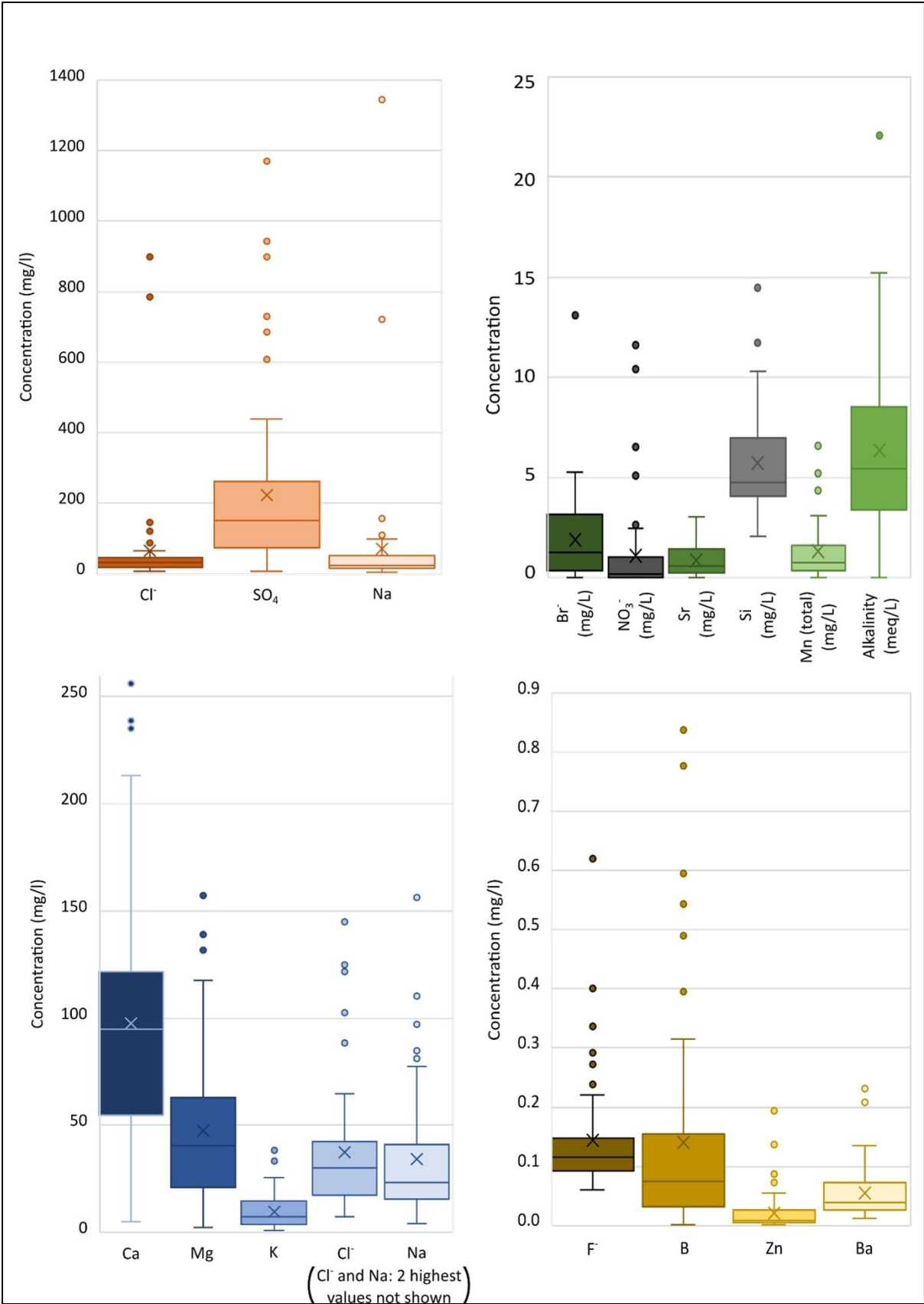


Figure 3.4 Box and whisker plots following water chemistry analysis of the untreated gravity discharges sampled in this study (not including treated discharges by TCA or council). All values in mg/L except alkalinity in meq/L.

The most common mine water type is calcium-bicarbonate. Calcium is the dominant cation for 18 of the 57 samples (>50% meq/L contribution) and for a further 23 samples is the highest percentage (meq/L) cation. Bicarbonate is the dominant anion in 34 of the 57 samples (>50% meq/L contribution) and has the highest percentage (meq/L) for another 2 samples. 18 of the sampled waters have sulphate as the highest percentage anion (in meq/L). A Durov plot with total dissolved solid (TDS) concentration is shown in Figure 3.5. Cation meq/L values mostly cluster in an area around 35-65% Ca, 15-55% Mg and 0-40% Na+K, with a few outliers more dominated by Ca or Na. Anion meq/L plots spread between sulphate and alkalinity, with the majority <20% Cl. There is a slightly higher density skewed towards higher percentages of alkalinity. The central plot suggests that, when excluding the high concentration saline outliers, greater TDS values correlate with sulphate-dominated anion balances.

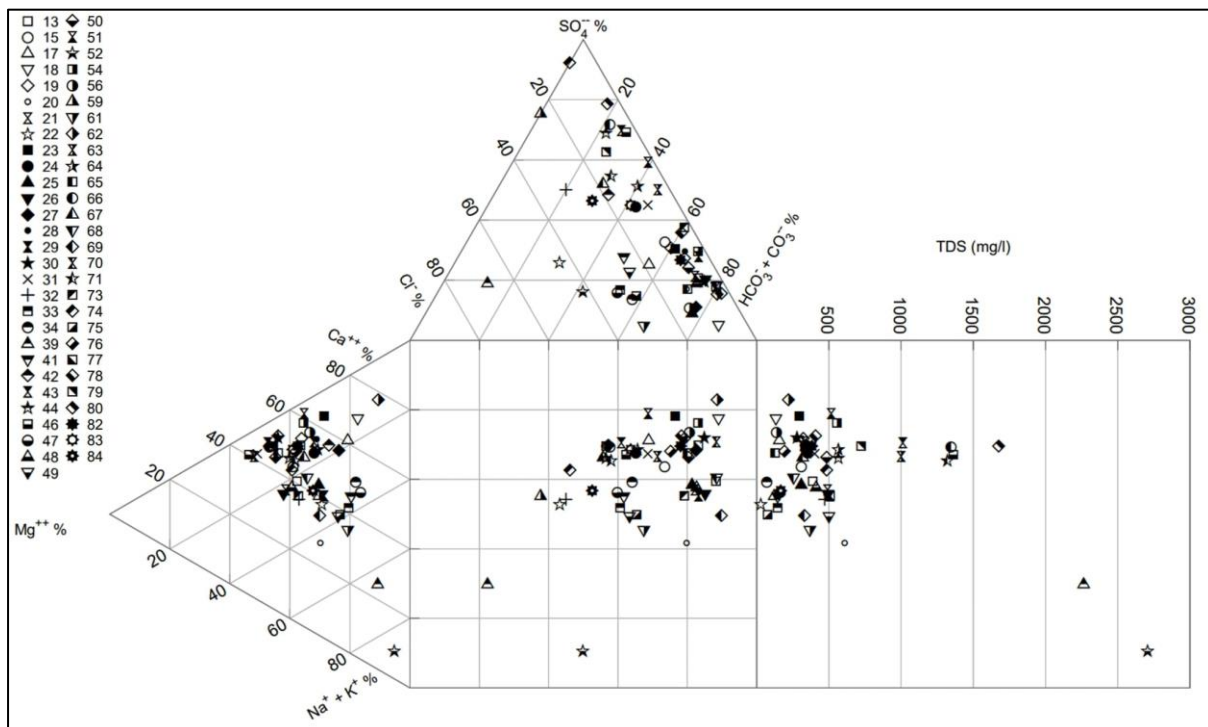


Figure 3.5 Durov plot for untreated gravity discharges sampled in this study, with total dissolved solids (TDS) shown on right hand extension plot.

The Younger diagram (Figure 3.6) was designed to plot groundwaters which have been affected by pyrite oxidation and to interpret their source and history (Younger, 2007). Plotting Younger diagrams requires total acidity. This is calculated using the method outlined in (Younger, 2007) whereby total acidity in meq/L is defined as:

$$\text{Total Acidity} = 1000(10^{-pH}) + \{Fe^{2+}\} + \{Fe^{3+}\} + \{Mn^{2+}\} + \{Zn^{2+}\} + \{Al^{3+}\} + \{Cu^{2+}\}$$

Equation 3.6

where each of the values in parentheses is the concentration of the dissolved ion in meq/L. To make this calculation, it is assumed that the dissolved iron in the water is in ferrous form (ferric iron is generally insoluble in all but the most acidic waters). The main mineral contributors to acidity are almost exclusively ferrous iron and manganese.

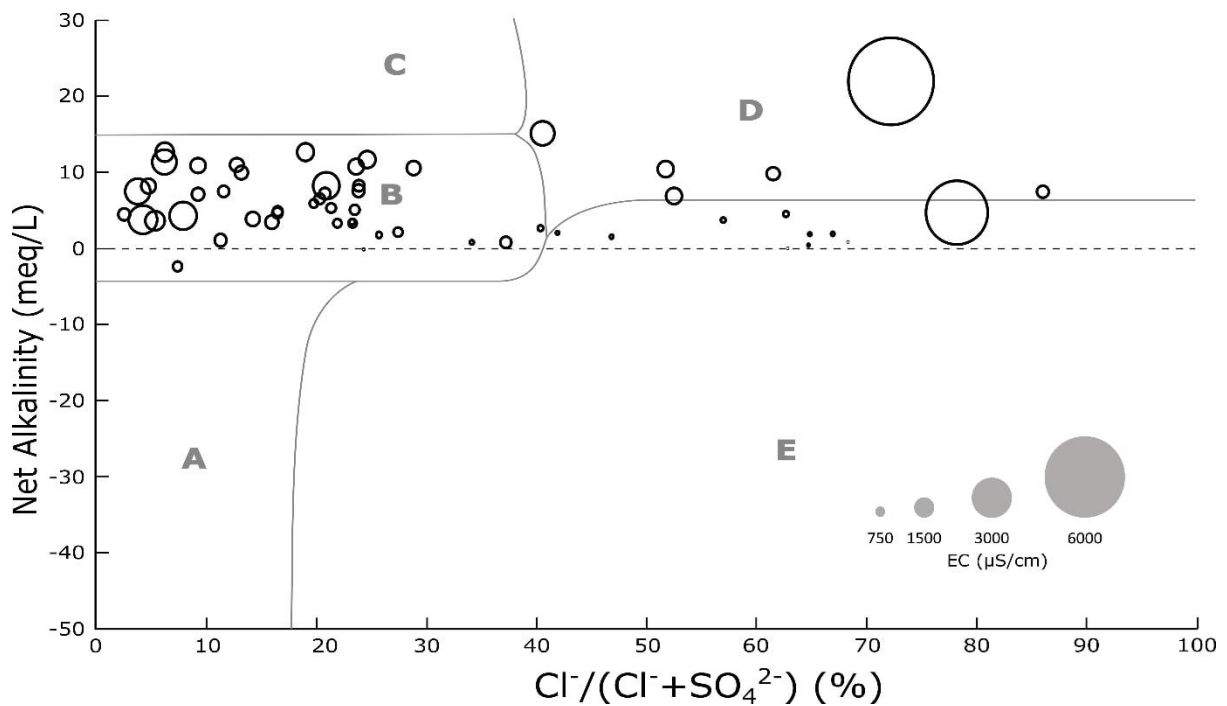


Figure 3.6 Younger diagram with untreated discharges from this study, where bubble sizes reflect the EC value. The Cl^- and SO_4^{2-} on the x-axis are both meq/L. The typical plotting fields are: A – Acidic spoil leachates, tailings/bing drainage, and shallow oxygenated workings in pyrite rich strata; B – Majority of fresh, shallow, ferruginous coal mine waters; C – Previously acidic waters, since neutralised; D – Deep-sourced pumped, saline mine waters; E – Field in which few mine waters plot.

Net alkalinity has been plotted on the Y-axis by subtracting the total acidity from the total alkalinity (both in meq/L). The majority of the mine waters plot in field B, i.e., “typical” British coal mine waters, whose chemistry is assumed to be controlled by the processes of pyrite oxidation and neutralisation. For comparison to the X-axis plots, average seawater has a $Cl^-/(Cl^-/SO_4^{2-})$ value of 90.7% (Lenntech, 2022), infiltrating rainfall is 85.4% (O Dochartaigh *et al.*, 2011), and mean values for groundwater from Carboniferous aquifers which have not been extensively mined for coal plot at 56.4% (Ó Dochartaigh *et al.*, 2015). This diagram was created for understanding mine waters but is less useful when plotting waters with low mineralisation (i.e., waters not affected by pyrite oxidation), plotting the conductivities of the

discharges as circle sizes shows the low EC samples (small circles) which may not be best characterised by a Younger diagram. In the instance where there is a distinct saline influence on the mine waters (#39; #52), the $\text{Cl}^-/(\text{Cl}^-/\text{SO}_4^{2-})$ ratio increases, despite both having sulphate concentrations in the highest 25% (335.9 mg/L and 405.1 mg/L respectively).

3.3.3 Iron loading

The iron loading value (kg/day) of a mine water discharge is a function of flow rate (L/s) and total iron concentration (mg/L). The mine waters entering Scottish treatment sites have a combined iron loading of 1032 kg/day (Bailey *et al.*, 2016, James Hutton Institute, 2016). The mine water is intercepted and treated to remove most of the total iron (Table 3.4) and as a result, the treatment sites prevent 960 tonnes of iron (solids) from entering Scottish water courses each year (The Coal Authority, 2021a). The discharges sampled in this study show a combined iron loading of 595 kg/day. Since these discharges are yet untreated, the total iron content currently flows, without interception, into streams and rivers or directly into the ocean.

Table 3.4 Total iron loading of mine water into Scottish treatment sites based on total iron concentrations.

Treatment Site	Type	Flow rate (L/s)	Total Iron (mg/L)	Iron Loading (Kg/Day)
Frances	Active Treatment	109	57.1	537
Polkemmet	Active Treatment	70	24.7	149
Blindwells	Pumped - Passive Treatment	295	4.4	112
Cuthill	Pumped - Passive Treatment	5	24.5	10.6
Median from Gravity Passive Treatment (n=9)		17.0	11.9	23.3

Table 3.5 shows the top seven untreated discharges ranked in order of iron loading. They have iron loadings close to or significantly above the median values of the gravity passive treatment sites (Table 3.4), hence a treatment site may become necessary for each of them. Importantly, since flow rate has a positive correlation with both iron loading and heat available (G), the discharges with the highest iron loadings represent high heating potential. Table 3.5 shows that six of the seven highest iron loadings have greater than 0.5 MW heat available, with the greatest at Old Fordell (Junkie's Adit: #66) on the River South Esk having 2.49 MW. Old Fordell causes extensive ochre smothering along the river in the centre of Dalkeith, Midlothian (Figure 3.7). There is reason, therefore, for future mine water treatment systems to incorporate a means to harness and distribute the heating capacity of the mine water discharges.

Table 3.5 Correlation of iron loading and heat available for the untreated discharges with the highest iron loadings, based on total iron concentrations.

Discharge	Flow rate (L/s)	Total Iron (mg/L)	Iron Loading (Kg/Day)	Heat Available (MW)
Old Fordell	88	26.8	202	2.49
Marnock	43	26.7	98.9	0.70
Wallyford Great	16	44.6	60.6	0.59
Falkirk	20	26.3	45.4	0.22
Shotts	117	2.5	25.5	1.81
Boghead	46	5.1	20.3	0.60
Barbauchlaw	99	2.0	17.0	1.61



Figure 3.7 Images of Old Fordell (“Junkie’s Adit”) mine water discharge (top), which hosts the highest iron loading of the untreated discharges (1L bottle for scale), and the resulting downstream ochre precipitation on the River South Esk (bottom).

3.3.4 Stable isotope data

3.3.4.1 Oxygen and Hydrogen

O and H isotopic values for discharges of this study (outlined in Appendix 3B) are plotted in Figure 3.8. The results from the University of Glasgow meteoric control samples (Appendix 3D) are plotted alongside, with their trendline generating the mean Local Meteoric Water Line (LMWL). All the mine discharge samples plot close to the mean Global Meteoric Water Line (GMWL) and the LMWL. The arithmetic means for the mine water discharges (Figure 3.8) ($\delta^{18}\text{O} = -7.6$; $\delta^2\text{H} = -51$) overlap within one standard deviation of the arithmetic means for the meteoric controls ($\delta^{18}\text{O} = -7.2$; $\delta^2\text{H} = -48$). This demonstrates that the mine waters' H_2O component is likely derived from relatively recent meteoric water and has not undergone significant isotope exchange with minerals or evaporative processes: thus, no trace of deep, interacted, more ancient groundwaters are detected.

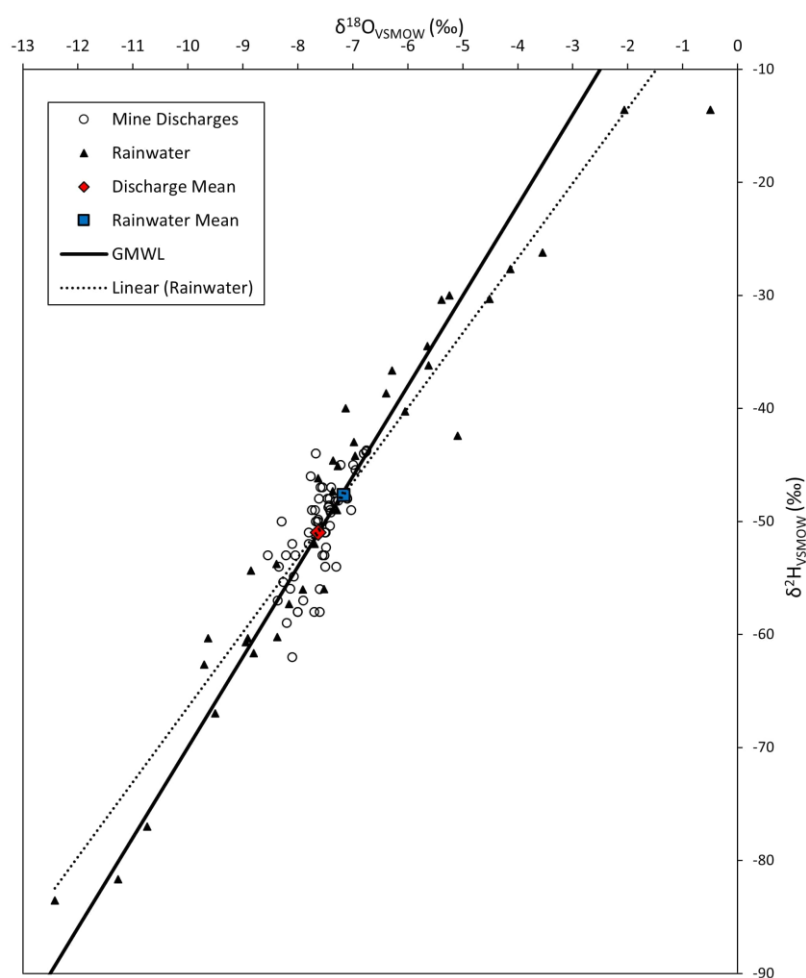


Figure 3.8 Oxygen and hydrogen isotope plot for the untreated MVS mine water discharges against the global meteoric water line (solid) and a local meteoric water line (dashed) derived from rainwater samples at the University of Glasgow.

3.3.4.2 S Isotopes

A histogram with sulphur isotope $\delta^{34}\text{S}$ values for the gravity drainages sampled in this study show a range between 0‰ and +48‰ (Figure 3.9). 52 of the 56 measurements plot between 1‰ and 20‰, but without a clear mode. The factors controlling the sulphate sulphur isotopic composition of the mine waters remains unclear. Banks *et al.* (2020) suggested that high $\delta^{34}\text{S}$ (around or above +20‰) might reflect a contribution from marine-derived salts (although elevated chloride would distinguish these), from evaporite dissolution in overlying or adjacent strata (however, this might be reflected by elevated Cl^-/Br^- ratios if halite was present), or from residual evaporitic brines. They also suggested that sulphate reduction processes might serve to elevate mine water $\delta^{34}\text{S}$ in some cases.

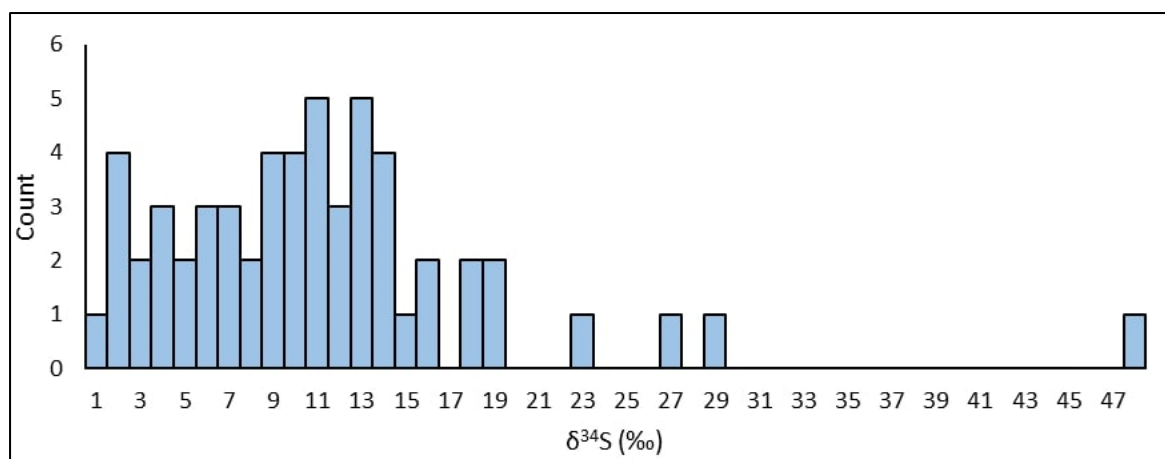


Figure 3.9 Histogram of $\delta^{34}\text{S}$ values collected from the untreated mine water discharges in this study.

The dominant signature of the mine waters has $\delta^{34}\text{S}$ between +2‰ and +20‰ (Figure 3.9). Typical Coal Measures pyrite values range from -26.3‰ and +18.4‰ (Bullock *et al.*, 2018), thus, the majority of mine water $\delta^{34}\text{S}$ are at least compatible with the hypothesis of predominant sulphide oxidation derivation. However, there is a disparity between the distributions of the two sample groups. The Coal Measure pyrite values have a mean of +2.7‰ (Bullock *et al.*, 2018), whilst the mine waters show a heavier mean $\delta^{34}\text{S}$ value of +10.7‰ and have no samples with negative $\delta^{34}\text{S}$, suggesting there remains isotopically heavy sulphate entering the system adding to the value expected from oxidation of pyrite minerals.

Scottish contaminated mine drainages' (CMD) neutrality is ascribed to a pH buffering effect caused by dissolution of carbonate minerals in the host rocks as outlined above (Farr *et*

al., 2016, O Dochartaigh *et al.*, 2011, Wood *et al.*, 1999). Resulting groundwaters have increased (and in many cases, dominant) concentrations of hardness minerals (Ca and Mg) and alkalinity. A Limestone Coal Formation core sample from the British Geological Survey's (BGS) Glasgow Geothermal Energy Research Field Site (GGERFS) shows elemental calcium and magnesium present at average concentrations of 12,700 ppm (1.27%) and 6928 ppm (0.69%) respectively from X-ray Fluorescence (XRF) readings at 2 cm intervals across 168 m of bedrock (Monaghan *et al.*, 2021b). The median value for the Ca/alkalinity ratio of the mine water discharges is close to one, suggesting that calcite dissolution is a predominant source of Ca and alkalinity to the water. Evidence from these sources shows that carbonate minerals are present throughout coal-bearing rocks, found most densely in marine (fossiliferous) limestone units and tidal deposited mudstones with a range of biotic fossil remains (Monaghan *et al.*, 2021b).

Figure 3.10 shows that an increase in the equivalent ratios of alkalinity or Ca and Mg versus sulphate correlate somewhat with increasing $\delta^{34}\text{S}$ values between zero and the quoted $\delta^{34}\text{S}$ value for Namurian and Westphalian seawater (c. +14‰ and +16‰), and beyond towards modern seawater (+21.2‰) (Tostevin *et al.*, 2014). Carbonate associated sulphate (CAS) in limestones and marine bands host $\delta^{34}\text{S}$ values reflective of Carboniferous seawater (Wu *et al.*, 2014) and, given the evidence for extensive carbonate dissolution could reasonably be a factor explaining the heavier $\delta^{34}\text{S}$ in discharge waters. Where mine waters contain sulphate sourced only from oxidised coal seam pyrites the ratio of alkalinity to sulphate would be expected to be <1. With progressive dissolution of carbonate minerals and incorporation of both alkalinity and CAS, the ratio moves well beyond 1 and, in this study, as high as 17.4. During dissolution of carbonate minerals, the CAS, which is present as structurally substituted sulphate ions within the carbonate lattice (Kampschulte and Strauss, 2004), can be released. However, abundances of CAS in modern biogenic carbonates average around 600 ppm, and in most carbonates around 100 ppm (Fichtner *et al.*, 2017). It is unlikely that heavy $\delta^{34}\text{S}$ contribution from CAS could be the sole controlling factor on the groundwater overall $\delta^{34}\text{S}$ value, but a potential contribution should not be ignored. If the alkalinity increase relative to sulphate is indicative of sulphate reducing bacteria, often found in anoxic groundwater (Brown *et al.*, 2002), then the CAS hypothesis could be dismissed.

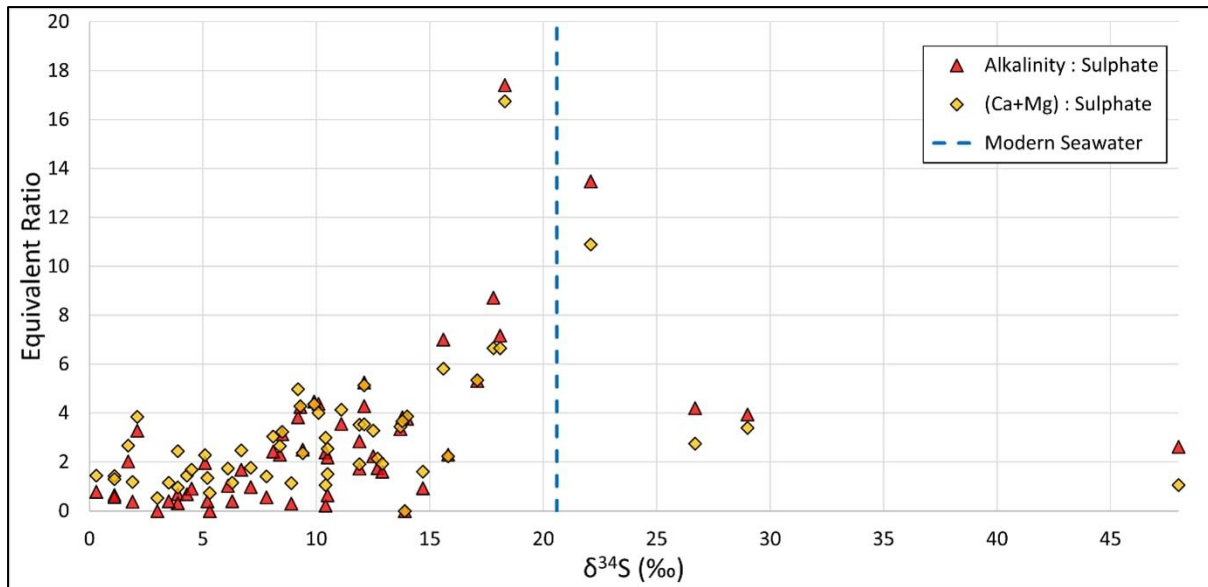


Figure 3.10 $\delta^{34}\text{S}$ plots against alkalinity to sulphate ratio, and calcium and magnesium (combined) to sulphate ratio (both as meq/L ratios).

The Banks et al. (2020) hypothesis whereby recent marine inundation leaves a seawater $\delta^{34}\text{S}$ footprint (circa +21‰) on the groundwaters can be confidently excluded since chloride concentrations are too low (median = 35 mg/L). The two exceptions to this are Douglas and Glenburn, where the hypothesis may fit since they show elevated salinity. All sampled mine waters have $\text{SO}_4^{2-}/\text{Cl}^-$ molar ratios which exceed modern seawater (0.052) (Lenntech, 2022) and suggest contribution of sulphate without additional chloride, likely derived from lithological sources (pyrite) (Banks *et al.*, 2020). Likewise, the median Na^+/Cl^- molar ratio is 1.06, (max 12, min 0.43), which exceeds modern seawater (0.858), and suggests some additional lithological sources of sodium (felsic minerals) beyond marine derived salinity (Banks *et al.*, 2020). The Cl^-/Br^- mass ratios of most of the sampled mine waters (median 26.1) show values lower than that of seawater (292) (Lenntech, 2022) (Figure 3.11). The majority also plot lower than typical shallow groundwater ratio values (from 100 to 200) (Davis *et al.*, 1998). Significantly lower values for groundwater, which have reached as low as 4, are attributed to the degradation of humic material in peat deposits (Davis *et al.*, 1998). Organic materials are known to concentrate bromide without concentrating chloride, therefore the authors speculate that overall low Cl^-/Br^- ratios reflect influence of contribution of bromide from organic matter in coal seams and no additional chloride from marine inundation.

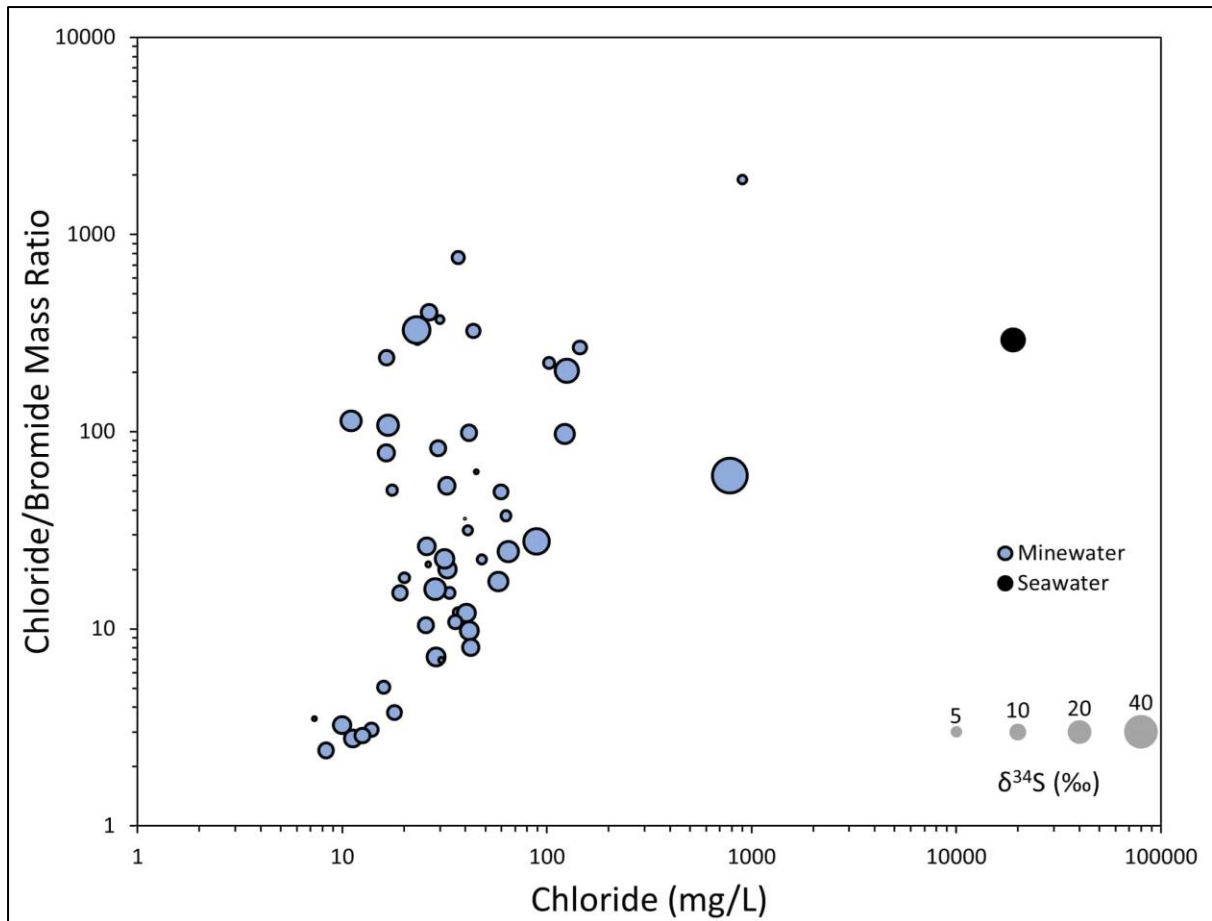


Figure 3.11 Plot of the chloride : bromide ratio against chloride concentration, with circle sizes proportionate to $\delta^{34}\text{S}$ value. Seawater in black.

Evaporites of the Ballagan Formation, primarily gypsum with some anhydrite and pseudomorphs of halite, are detailed in Millward *et al.* (2018), found in abundance amongst fluvial, overbank deposits and saline–hypersaline lake deposits, with the latter hosting the majority of the evaporite minerals. Since the Ballagan Formation is of Tournaisian Age, it correlates with seawater $\delta^{34}\text{S}$ values of early Carboniferous at c. +20‰ (Present *et al.*, 2020), thus dissolution of the sulphate bearing minerals (gypsum and anhydrite) could introduce these heavy isotopic values to the groundwater. Douglas (#39) is the only mine water to have a Cl^-/Br^- above 1000 (value=1904), which suggests mixing with a groundwater which has interacted with halite deposits. However, the hypothesis whereby heavy $\delta^{34}\text{S}$ values are derived from evaporite mineral dissolution does not fit well with this data since the data points with concentrated Cl^- and high Cl^-/Br^- (especially Douglas) do not show heavy $\delta^{34}\text{S}$ values (Figure 3.11). Ca and Mg in the mine water is not consistent with that of SO_4 , generating $(\text{Ca}+\text{Mg})/\text{SO}_4$ equivalent ratios which range between 0.5 and 16.8, with a median value of 2.5, making gypsum/evaporite dissolution unlikely to be a controlling factor for most of the samples.

Sulphate concentrated in residual saline brines or paleo-evaporites remains a potential explanation for the elevated $\delta^{34}\text{S}$ values. Following deposition of the coal-bearing strata in the Carboniferous, the MVS created depositional environments for sediments through the Permian to the Cretaceous. Whilst arid desert aeolian conditions dominated in the west through the Permian (Cameron and Stephenson, 1985), the preserved rocks off the coast of the Firth of Forth show evaporite deposits including gypsum and anhydrite from the hypersaline Zechstein Sea (Thomson, 1978). In the late Cretaceous, tropical seas submerged all but the highest areas of Scotland and deposited chalk layers (Harker and Trewin, 2002) during the probable Phanerozoic sea level peak, which may have been 150-300 m higher than present (Rawson, 2006). Arid climates following transgressions may have induced evaporation and concentration of saline waters, leading to brines or evaporites left behind. Whilst the associated rocks have since been eroded (Harker and Trewin, 2002), leaving sparse existing bedrock from the Permian – Cretaceous, the brines may have percolated into the bedrock beneath carrying sulphate with an isotopically heavy seawater/evaporite signature, and, whilst unlikely on geological grounds to be a major source, their contribution cannot be ruled out.

The heavy $\delta^{34}\text{S}$ outliers include Glenburn (#52) at +48‰, described for its elevated EC above, is likely influenced by modern seawater, although this would only raise the $\delta^{34}\text{S}$ to c. +21‰. The process by which the signature reaches +48‰ is unknown and is far heavier than any value from coal mine water elsewhere. Another very heavy $\delta^{34}\text{S}$ value (+29‰) is from Rozelle Park (#75). Whilst Rozelle Park discharge has no recorded mine workings beneath it (The Coal Authority, 2022), the site (55.43896°N, 4.62201°W) is underlain by Lower Scottish Coal Measures rocks hosting ironstone seams and thin coals (British Geological Survey, 2008). Small, shallow, unrecorded workings may be present beneath the site and form the source of the 0.5 L/s discharge. The final heavy $\delta^{34}\text{S}$ value of +26.7‰ is from the Baron discharge (#20 - 55.7724°N, 3.9925°W) believed to be derived from the 32m deep Broomside-Haugh Shaft (The Coal Authority, 2022) accessing workings of the abandoned Dalziel-Broomside Colliery on the River Clyde, near Motherwell. These samples (Glenburn, Rozelle Park and Baron) are not associated with especially deep mines and would not be expected to exhibit mixing with deep brines or reducing conditions (of the three, only Glenburn had odours of H_2S). There are also no obvious evaporite sources for sulphate in the vicinity of these discharges (and in any case there are no evaporites likely to have $\delta^{34}\text{S}$ higher than around +20‰ for Carboniferous seawater sulphate, e.g., Present et al., 2020). Since the $\text{SO}_4^{2-}/\text{Cl}^-$ ratios do not suggest current

or palaeomarine influence, elevated $\delta^{34}\text{S}$ does not support the hypotheses of Banks *et al.* (2020).

Evidently, the isotopic signature of dissolved sulphate in these mine waters is not homogeneous. Whatever the source of the dissolved sulphate, it is clear that their origin is not from a simple oxidation of pyrite in coals, particularly when considering the significant elevated $\delta^{34}\text{S}$ values seen across the MVS. The origin of this sulphate is complex and unpredictable, likely involving the interplay of several sources. This is echoed by the review of Banks *et al.*, (2020), and in Clackmannanshire Scotland which suggests that the signature may indeed be variable *within* any given mine water system (unpublished data).

3.4 Conclusion

Although mine water chemistry sampled at mine water discharges may not be representative of chemistry at depth in mine systems, this research provides a useful dataset as an entry point for stakeholders looking to install mine water geothermal systems across the Midland Valley of Scotland. Overall, the mine waters are circumneutral with dominant calcium-bicarbonate type, although many have sulphate as the dominant anion. Carbonate (and silicate) minerals are assumed to have been hydrolysed by protons released by oxidation and dissolution of sulphide minerals, in turn releasing base cations and alkalinity. Intriguingly, increasing $\delta^{34}\text{S}$ values correlate somewhat with mineralisation from carbonate dissolution. An exclusive origin of sulphate from oxidation of pyrite in exposed coals is unlikely on the basis of the highly variable $\delta^{34}\text{S}$ (mostly between 0 and 20‰) which is typically isotopically heavier than source pyrite across the Midland Valley of Scotland: this suggests an interplay of several sources. Inclusion of isotopically heavy sulphate released during the dissolution of marine carbonates is proposed as an influence on the $\delta^{34}\text{S}$ values of the mine waters, however, its absolute concentrations make it unlikely to be the controlling factor. Marine inundation is unlikely to be the source of heavy isotopic sulphate, but ancient evaporites / evaporitic brines are implicated. The complex origin of the sulphate contrasts with the relatively simple origin of the host water, being dominated by local meteoric water.

Gravity fed or actively pumped drainage from coal mines has been shown to host significant heating potential for circulation in district heating networks if harnessed by heat exchanger technology and converted to useable heat using a heat pump. Using mine water which is present at the surface removes drilling capital expenditure and is less restricted by subsurface risks, however, the discharges are location-dependent, and any heat consumers

would have to be proximal. In the Midland Valley of Scotland, the mine water brought to the surface via gravity or pumping for treatment has been calculated to provide a total heat pump delivery of 48 MW, corresponding to the peak heating demand of 12,000 two-bedroom houses. Where gravity discharges are not treated by The Coal Authority to remove the dissolved and suspended iron, ochre pollution and smothering reduces natural water quality and oxygen availability in the receiving watercourses. Untreated discharges contribute 595 kg/day of iron to Scottish watercourses and the largest untreated gravity discharge polluters show a strong correlation with high heating potential. The most obvious of these is Old Fordell (Junkies Adit) in the centre of Dalkeith, Midlothian, which hosts 2.49 MW heating potential. It is thus recommended that any future treatment sites consider installation of heating infrastructure to harness the low-carbon mine water thermal resource, provided a demand exists in the vicinity.

Author Contributions

Conceptualization, DW, NB, and DB; Methodology, DW, TP, DB, NB, and AB; investigation, DW; Data curation, DW and TP; Writing—original draft preparation, DW; Writing, review and editing, DW, DB, TP, NB, and AB; Supervision, NB, DB, and AB; Funding acquisition, NB. All authors have read and agreed to the published version of the manuscript.

Acknowledgements

We are grateful to the following people for contributing their time to assist with field data collection: Jura MacMillan, Laura Dozier, Michael Schiltz, Dominic James, David Townsend, and Philippa Wood. We would like to thank landowners who granted access to their land for sampling. We would also like to thank Alison McDonald for her help with isotopic analysis at SUERC.

Funding

This research was supported by NERC NEIF grant 2301.0920, EPSRC IAA grant EP/R51178X/1 and Energy Technology Partnership Scotland grant PR007-HE. N.M.B is funded by a University of Strathclyde Chancellor's Fellowship. A.J.B is funded by the NERC National Environmental Isotope Facility award at SUERC (NEIF-SUERC, NE/S011587/1) and SUERC.

Chapter 4 - GIS analysis for the selection of optimal sites for mine water geothermal energy application: a case study of Scotland's mining regions

This chapter forms a guidance document for the Mine Water Geothermal Resource Atlas for Scotland which can be found on the Improvement Service's Spatial Hub platform:

<https://www.spatialdata.gov.scot/geonetwork/srv/eng/catalog.search#/metadata/63ccfed-0165-461d-a5a5-025b0b2463c5>

4.1 Introduction

Mine water geothermal (MWG) energy describes the practice of using water held in abandoned flooded mines to heat or cool surface thermal demands (Banks, 2016, Banks *et al.*, 2004, Hall *et al.*, 2011, Jessop *et al.*, 1995, Ramos *et al.*, 2015, Walls *et al.*, 2021, Younger, 2016). The low temperatures (as low as 10 °C) require heat pump technology to upgrade thermal energy to usable temperatures for heating homes or industrial applications (Athresh *et al.*, 2016). For cooling purposes, a heat pump may (active cooling) or may not (passive cooling) be required. The use of mine water as a thermal source is becoming increasingly popular but has had a slow overall uptake since its inception in the 1980s (Bracke and Bussmann, 2015). Global case studies are presented and discussed in Hall *et al.* (2011), Ramos *et al.* (2015) and Walls *et al.* (2021). The available configurations of MWG systems, detailed in Banks *et al.* (2019) and Walls *et al.* (2021) are tailored to local factors such as presence of open shafts, existing discharge and treatment requirements, and mine water head. One of the most common configurations is “open loop with reinjection” detailed in Banks *et al.* (2019) and employed in Heerlen (Verhoeven *et al.*, 2014), Gateshead (Banks *et al.*, 2022) and Springhill, Canada (Jessop, 1995, MacAskill *et al.*, 2015).

Heating and cooling remains the principal energy use in Scotland (greater than 50%) (Scottish Government, 2020c) but has not yet made notable changes towards decarbonisation (Energy Saving Trust, 2021). Renewable sources contributed 6.4% in 2020, failing to meet the target of 11% for the same year (Energy Saving Trust, 2021). These minor contributions reflect

the fact that when compared to the status quo of hydrocarbon-based heating sources, renewable thermal energy is challenging to store, transport, and manage. Any new low-carbon heating system must find a means to source local and reliable heat with clear agreements for sustainable production and usage. MWG can face high capital costs of drilling and heating infrastructure and can be subject to significant operational costs if chemical fouling is problematic or water requires pumping from great depth (Walls *et al.*, 2021). There is a need for more MWG projects in Scotland to further prove the resource and reassure investors that these systems can operate successfully over many years. Selecting suitable locations for development would be greatly assisted by a new approach which allows stakeholders to perform initial resource screening and find optimal locations for siting MWG systems.

Coupling a sub-surface thermal resource with a suitable surface heat or cooling user is imperative for MWG to reach installation and operation stages. Investigations involving specific existing or future surface thermal demands e.g., Dollar Community Sustainable Housing (Townsend *et al.*, 2020), can place land ownership constraints on the locations of flooded mine borehole access points. Conversely, if the subsurface is well understood and the thermal energy resource is well characterised, a lack of sufficient surface heating demand could render a project unnecessary e.g., Fortissat (James Hutton Institute, 2016). Such mismatches give merit to a workflow which couples appropriate subsurface thermal resources to surface heating and cooling requirements as early as possible. Since characterisation of a mine water geothermal resource is often a specialist process performed by professional consultants, this thesis has developed a subsurface screening tool to make knowledge of MWG potential in Scotland more accessible to non-specialists. This study has combined over 100,000 data points pertaining to coal mines in Scotland (Table 4.1), relying heavily on The Coal Authority’s (TCA) archive of digitised mine abandonment plans, to produce the Mine Water Geothermal Resource Atlas for Scotland (MiRAS). It is envisaged that this will allow stakeholders (including landowners, council representatives, developers and project champions), who

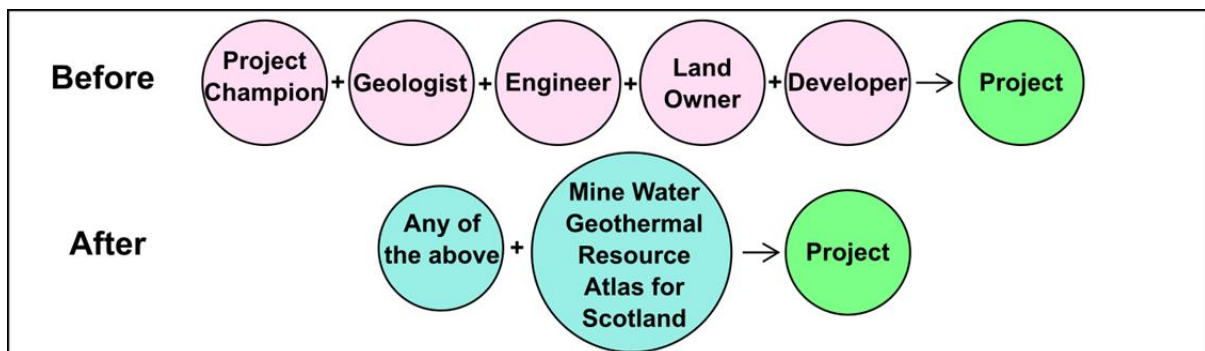


Figure 4.1 Necessary parties for conception of a mine water geothermal project before and after development of the Mine Water Geothermal Resource Atlas for Scotland.

typically have little technical or geological background, to perform rapid early appraisal of the mine water resource in their location of interest without needing to submit TCA information requests or obtaining data that requires additional expert interpretation. Figure 4.1 indicates the necessary parties required to instigate a MWG project before and after the introduction of the MiRAS.

The intention of the MiRAS is to highlight optimal areas to exploit MWG energy in Scotland. The analysis has been tailored to find locations suitable for mine water geothermal systems as “open loop with reinjection” (see Walls *et al.* (2021) for details), which require at least two boreholes completed into overlapping seams, where one abstracts, and one reinjects water. This was selected since it is typically the configuration which can be scaled up to provide multi-megawatts of thermal energy with less risk of thermal feedback or excessive dewatering (Walls *et al.*, 2021). Since it does not have a net abstraction of water, there are no associated treatment costs or increasing pumping costs with lowering mine water head.

If the scale of Scotland’s mine water thermal resource, estimated at 12 GW (Gillespie *et al.*, 2013), becomes better communicated, it is envisaged that the MiRAS will prove influential for increasing the rate and success of MWG deployment. Ideally, the provision of optimal MWG sites will influence stakeholder decisions i.e., where to invest and develop land to make the best use of the low-carbon resource, resulting in MWG potential included as part of a standard appraisal for a residential or industrial development plan. Whilst it is acknowledged that focused expert input would be required to integrate surface heat demand and subsurface resources in detail, the MiRAS provides non-experts and decision makers with a first-pass high-level summary of the potential MWG resource located within their area of interest. The Scottish Heat Map (heatmap.data.gov.scot) can be used in parallel to the findings of this study as a means to compare the two side by side. It shows heat demand from Scottish buildings alongside existing or planned heat networks and areas with high density social housing.

The four criteria for site selection are summarised below and explained fully in the Data and Methodology section. These criteria define areas where:

1. There are more than one (overlapping) worked coal seams - to allow for abstraction and reinjection to different seams.
2. The coal seams are deeper than 30 m to minimise subsidence risk (Abbate, 2016).
3. The mine water head (i.e., mine “water table”) is not excessively deep (< 60 m below ground level) to avoid excessive pumping head, thus minimising amount and cost of electricity required to lift water to surface (Athresh *et al.*, 2015, Walls *et al.*, 2021).
4. The mines are shallower than 250 m below ground level to minimise drilling costs (Diamond, 2022).

The study area spans the principal coalfields of the Midland Valley of Scotland (MVS), covering the Central, Ayrshire, Lothian, Fife, Sanquhar, and Douglas coalfields. It also includes the West Lothian Oil Shale field. The areas of interest are shown in Figure 4.2, reflecting the extent of the Scottish Coal Measures Group (Westphalian Coal), Clackmannan Group (Namurian and Visean Coal) and the Strathclyde Group (Visean West Lothian Oil Shale Formation) (Monaghan, 2014). This study has prioritised overall cost (capital and operational expenditure, CAPEX and OPEX) in response to the challenges of acquiring funding for MWG systems, and for consultancies to generate a business case with competitive CAPEX and OPEX against counterfactuals.

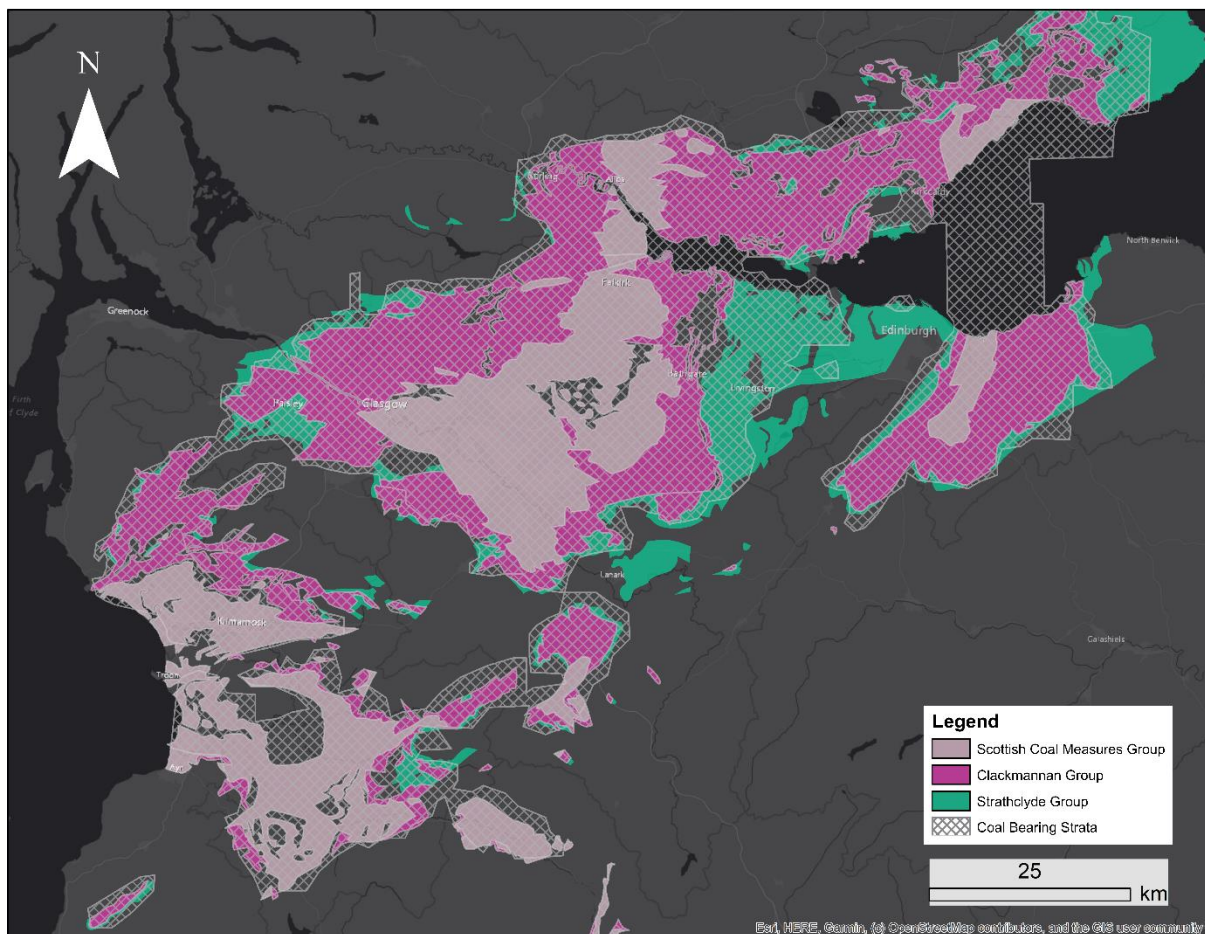


Figure 4.2 Map of the study area, broken down into its comprising shapefiles. Coloured sections denote the Carboniferous bedrock outcrop, whilst the hatched area represents areas of coal workings from Jones *et al.* (2004). Coal workings exist outside the outcrop areas since the coal-bearing strata are concealed in these areas by younger strata. Contains British Geological Survey materials © UKRI 2022.

4.2 Data

In this study, six datasets were obtained and prepared using Geographic Information System (GIS) software to visualise the four criteria. The datasets are summarised in Table 4.1 and discussed below. The processes by which the four criteria were created are detailed in a

flow diagram (Figure 4.3), where Criteria 1 and 2 are combined. Following the processes in Figure 4.3, the four output criteria layers were created, and when combined, identify optimal areas for open loop mine water geothermal systems with the most favourable economics.

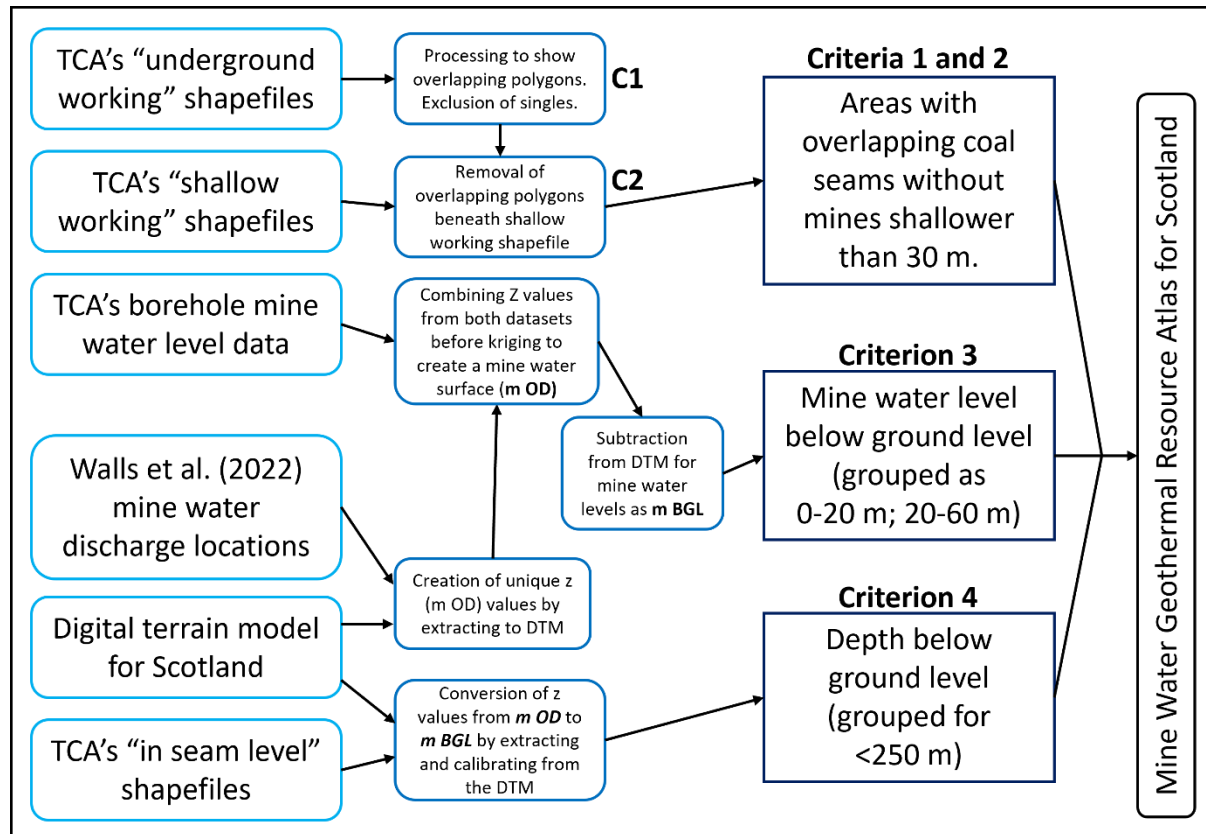


Figure 4.3 Flow diagram showing the overall processing from input datasets to reach the suitability map. Each of the 4 criteria are indicated, or abbreviated to C.

4.2.1 Dataset 1 - Underground workings

The “Underground working” vector dataset consists of polygons which represent the geographical extent of worked mines. It is a digital version of spatial data from mine abandonment plans. As a part of TCA’s GIS archive of mining data, this dataset was created for automated provision of coal mining reports, used by organisations wishing to identify possible ground instability and potential mining hazards (Tipper, 2015b). The geographical extents of mined areas were plotted by TCA following scanning and georeferencing of paper copy abandonment plans. Accuracy issues arise from several processes involved with creation of the data. There can be slight geographical uncertainties from human error during original surveying, and following this, some further uncertainties following georeferencing of the plans onto GIS. It is also accepted that not all mines in Scotland are recorded, e.g., the age of the first

workings (12th century) greatly pre-date legislation to ensure documentation (1870's) (Younger and Adams, 1999), leaving some shallow mines undocumented. Mine abandonment plans in the UK became more reliable, and of uniform quality after nationalisation in 1946. Whilst the polygons in this dataset define the areal extent of mining excavations, they do not show any detail concerning the layout of shafts, roadways or worked panels which may influence preferred locations for drilling and accessing mine water.

4.2.2 Dataset 2 - Shallow workings

The “Shallow working” vector dataset consists of polygons which represent worked portions of mined seams within 30 metres of the surface. TCA created this derived dataset by extraction from the “Underground working” shapefiles and keeping only polygons (or portions of polygons) which were within 30 m of the surface, however, the surface model from which the depths were extracted is not known. The uncertainties inherent to the “underground working” shapefiles are carried over, and many old shallow workings are likely to be absent from the dataset since they originate from a time when documentation was not mandatory.

4.2.3 Dataset 3 – In seam level

The “In seam level” vector dataset comprises of a series of point elevations, each correlating to a certain location within a worked seam (longitude value X and latitude value Y) and host a Z value (elevation) relative to Ordnance Datum. These are spot elevations copied from their original plots on abandonment plans. The X and Y coordinates of each point is subject to the same challenges as the previous two datasets (surveying and georeferencing errors). The Z values also depend on the precision of the original survey. Digitisation of this dataset required conversion to metric units, some typographical errors may generate incorrect digital values. The nature of the dataset means that information on depth is not uniformly distributed, and some areas have sparse “In seam level” points.

4.2.4 Dataset 4 – Monitored mine water head

The mine water head (i.e., mine “water table”) relative to Ordnance Datum was obtained for each of TCA's monitoring stations (n=48) in the Midland Valley of Scotland. The data are multipoint vector data with X, Y and Z values. These are transcribed following regular measurement by TCA and are available as part of the environmental data packages. The coordinates of the monitoring boreholes or shafts are precise, and the mine water head readings

have accuracies of 0.01 m. The spatial distribution of the monitoring stations is poor, since there are many monitoring points in the Lothian and Fife coalfields, but few in Central or Ayrshire. In coalfields that are actively managed by mine water pumping (or other dewatering), it should be recognised that mine water heads can vary as the dewatering regime changes. Moreover, mine water heads will often vary seasonally and with groundwater recharge events. The inputs for Dataset 4 are dated Autumn 2020 for surface discharges (Walls *et al.*, 2022) and Autumn 2021 (current data for when this analysis was performed) for TCA mine water head data in shafts and observation boreholes. This means that head levels may fluctuate above and below current measured mine water head with seasonal addition or removal of groundwater, but ultimately will not significantly affect optimal locations highlighted in this study. Further work would be required to include changes to mine water head near MWG systems as they come online. It would be expected that an “open loop with reinjection” configuration would have less of an effect on mine water head than the equivalent “open loop with discharge” since the latter has a net-removal of groundwater.

Input Layer	Summary	Quantity	Source
Underground workings	Polygons representing worked portions of mined seams. Converted to GIS format from mine abandonment plans.	33,651 polygons (104 MB)	The Coal Authority (Tipper, 2015b)
Shallow workings	Derived from the ‘underground workings’ dataset by extracting all workings, or parts whose depth is 30 metres or less from the surface.	12,222 polygons (25 MB)	The Coal Authority (Abbate, 2016)
In seam level	Point data representing the level of underground working at a specific point, in a specific seam, relative to Ordnance Datum (sea level)	82,794 points (39 MB)	The Coal Authority (Tipper, 2015a)
Monitored mine water head	X and Y data of TCA monitored mine water head observation points from boreholes or shafts, with Z values relative to Ordnance Datum	48 locations	The Coal Authority (Pers comms, 2022)
Mine water discharge locations	X and Y data of unmonitored mine water discharges, Z values created by extraction from DTM	81 locations	Walls et al. (2022)
Digital terrain model (DTM)	Raster layer of surface elevation for 5m grid squares	2.8 GB	Crown copyright and database rights 2022 Ordnance Survey.

Table 4.1 Description of the input layers for GIS analysis.

4.2.5 Dataset 5 – Mine water discharge locations

The mine water discharge locations (n=81) are X and Y coordinates of locations where mine water drains from associated workings under gravity. Locations were recorded using a GPS device by Walls *et al.* (2022), alongside other properties of discharging mine water. The accuracy of the X and Y values varies with GPS error, which is usually ± 3 m. The dataset is not exhaustive. There remain unmonitored discharges in the MVS which exist but were not captured as part of this research.

4.2.6 Dataset 6 - Digital terrain model

The digital terrain model (DTM) was compiled from 370 tiles of Ordnance Survey Terrain 5 at scale 1:10,000, July 2021 version. The raster tiles are 5 km by 5 km with 5 m post spacing (the distance between points which make up the elevation grid). The data is converted from a triangulated irregular network (TIN), which was created by editing with mass points, breaklines and height data collection by automated techniques (e.g., LIDAR, INSAR). This dataset was calibrated against known GPS points, and a root mean square error (RMSE) was calculated for the multiple samples in each area. The reported RMSE is 1.5 m for Urban areas, and 2.5 m for rural, moorland and mountainous areas (Ordnance Survey, 2017).

4.2.7 Other factors

The resource potential of a MWG site is influenced by more than the four criteria generated in this study, although these are seen as the principal factors. Other controlling “geofactors” were identified which may be included in a subsequent version with a multi-criteria evaluation technique:

- Method of working. If unknown, then the age of workings may be used as a proxy for the mining method or likelihood of subsidence and collapse (Andrews *et al.*, 2020);
- Yearly rainfall and surface topographic gradient, as proxies for hydrogeological controls on hydraulic gradients and throughflow rates
- Depth intervals of individual mine water blocks, as a proxy for expected abstraction temperature (Farr *et al.*, 2021)
- Hydrochemistry – using surface discharge data as an indication of subsurface chemistry – to highlight areas with ‘good’ or ‘bad’ properties (Walls *et al.*, 2022)

4.3 Methodology

For this study, the four core criteria were created via the following methods.

4.3.1 Criterion 1 - Areas with overlapping mined seams, and Criterion 2 - without mines shallower than 30 m

4.3.1.1 Method

The underground working shapefiles were analysed to determine the number of overlapping polygons in each area using the processes outlined in the flow diagram of Figure 4.4. Up to 22 overlapping polygons were returned, this may reflect 22 overlapping mined seams or (more likely) reflect some overlapping inaccuracies which exist at the edges of the original shapefiles. Once overlapping seams were identified, the ‘shallow workings’ layer was used to remove unsuitable, shallow areas (Figure 4.4). Figure 4.5 represents the starting and resultant shapefiles in a simplified schematic diagram. The resulting polygons were rasterised in preparation for combination with rasters from other criteria. Figure 4.6 shows locations associated with Criteria 1 and 2 - overlapping workings across the MVS where locations with shallow workings have been removed.

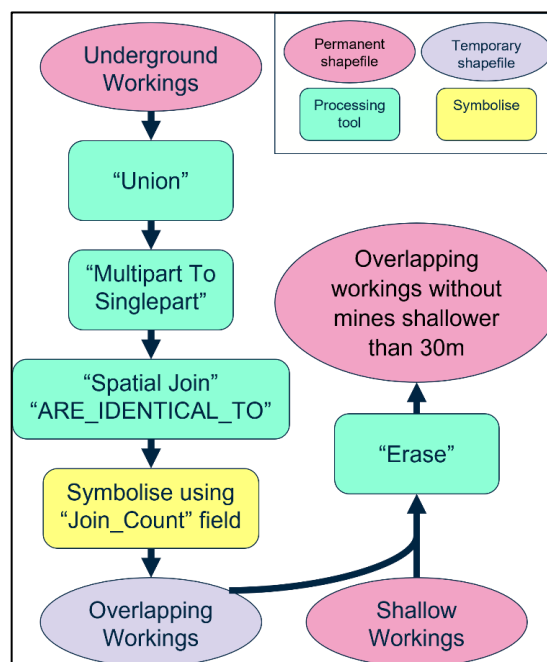


Figure 4.4 Flow diagram showing GIS processing of “underground workings” to reach “overlapping mined seams without mines shallower than 30 m”.

4.3.1.2 Rationale

In places where mining affected multiple mineral seams (in this case mostly coal), horizons with increased permeability (mined voids or extensive fractures) result at multiple depths beneath the ground, e.g., the Heerlen MWG scheme in The Netherlands (Verhoeven *et*

al., 2014). Overlapping mined seams are a favourable property of an open loop MWG system since they create vertical separation between locations of reinjection and abstraction. They contribute to long, tortuous flow pathways, lessening the risk of thermal feedback and hence improving heat longevity (Loredo *et al.*, 2017a, 2018). On the contrary, using a single mined seam for abstraction and reinjection would present short flow pathways, perhaps without ample host rock interaction for the cooled water to return to its original temperature, thus increasing the chance of thermal feedback and reduced efficiencies. This analysis, therefore, excludes areas which have only one seam present, screening for only those with overlapping seams. If there were to be two worked seams which overlap, whereby one was less than 30 m below ground level (BGL), the area would be excluded on the premise that there are shallow workings present.

Areas underlain by shallow mined workings may have an inherent subsidence or ground instability risk (The Coal Authority, 2017). Further to this, rising mine water head levels can result in mm-scale uplift across coal workings which may induce deformation at pillar edges. This process, along with thermal oscillations may deteriorate workings enough to induce localised collapse (Todd *et al.*, 2019). A commonly used ‘rule of thumb’ states that for every meter of coal abstracted, 10 m of overlying rock is potentially affected by subsidence (Bell, 1986, Healy and Head, 1984). Thus, with some 3 m tall roadways and some coal seams greater than 2 m thick, a 30 m value is prescribed by TCA as ‘at risk shallow workings’ (Abbate, 2016). The actual zone of collapse and compression above a longwall seam is a function of the width of the panel, but this can vary (Younger and Adams, 1999). Moreover, shallow workings may already have been grouted for stability and are hence unsuitable as a geothermal resource. This study has thus provisionally excluded areas where workings are less than 30 m below ground level. It is recognised, however, that there may be areas with shallow workings, where the hydrogeology and ground stability issues are sufficiently understood as part of more detailed studies to allow the operation of MWG schemes. It stands to reason that development of sites

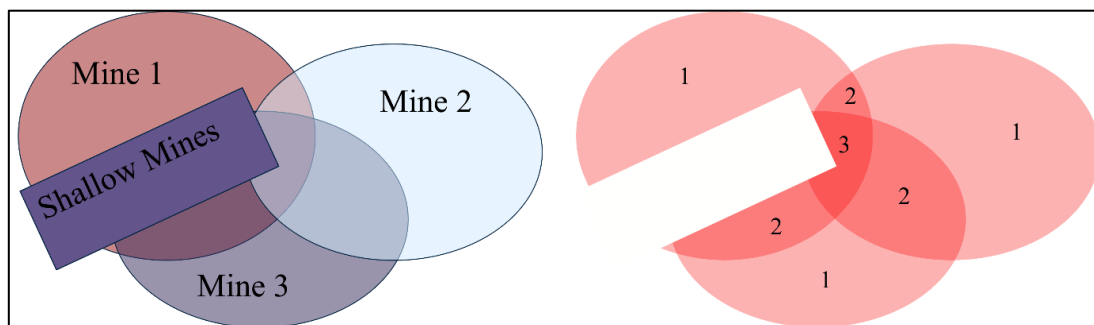


Figure 4.5 Schematic representation of conversion from “underground workings” and “shallow workings” (left), to “overlapping mined seams without mines shallower than 30 m” (right).

affected by old, shallow mining works could be screened for MWG heating or cooling via a different technique, such as the processes outlined in Chapter 5.

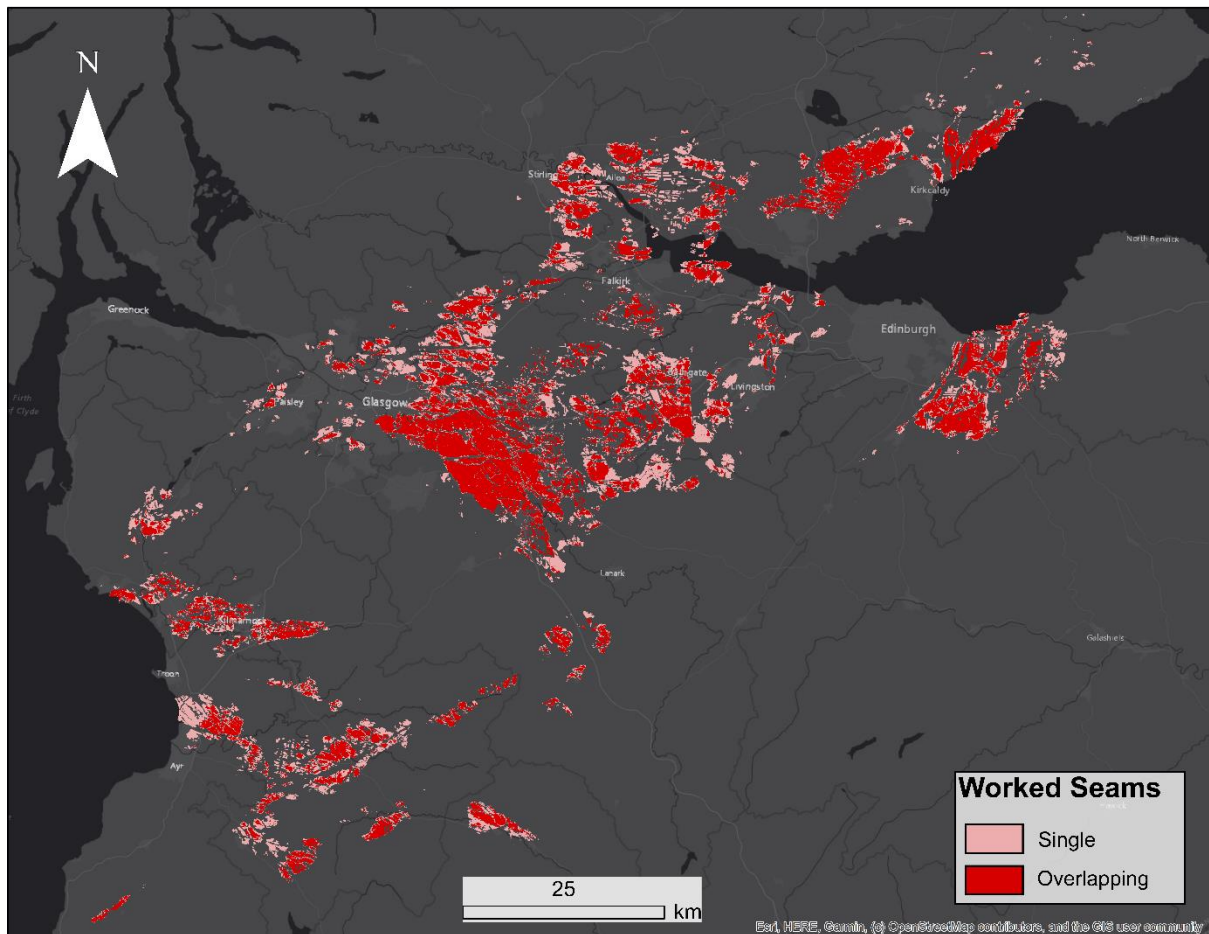


Figure 4.6 Map of central Scotland showing areas of overlapping coal seams, without shallow seams (<30 m BGL). Reproduced with the permission of © The Coal Authority. All rights reserved.

4.3.2 Criterion 3 - Areas where mine water head is predicted to be between 0 m and 60 m below ground level (grouped as 0-20 m BGL and 20-60 m BGL)

4.3.2.1 Method

Elevations in metres above Ordnance Datum (m OD) (which in the UK is mean sea level) were extracted from the DTM for each of the mine water discharge locations detailed in Walls *et al.* (2022). They were combined with data for mine water head (m OD) in TCA's monitoring locations. Together, these were control points for creation of a mine water surface elevation vector layer (Figure 4.7). The mine water surface across the MVS, was interpolated using Empirical Bayesian Kriging. Kriging (Matheron 1960, Chung *et al.*, 2019) estimates the value of unsampled locations as the weighted average of surrounding points. The Kriging equation determines a weighting factor for each of the influencing points to minimize variance.

It produces a surface which is the best linear interpolation for the available data. As a result, it lacks local or small-scale heterogeneities that could be present in the real potentiometric surface. The accuracy is more reliable in locations where there is a greater density of control points (e.g., East- and Mid-Lothian), and less so where points are few and distal. The resulting raster has been clipped to the extent of Carboniferous mined strata in Scotland (Figure 4.2).

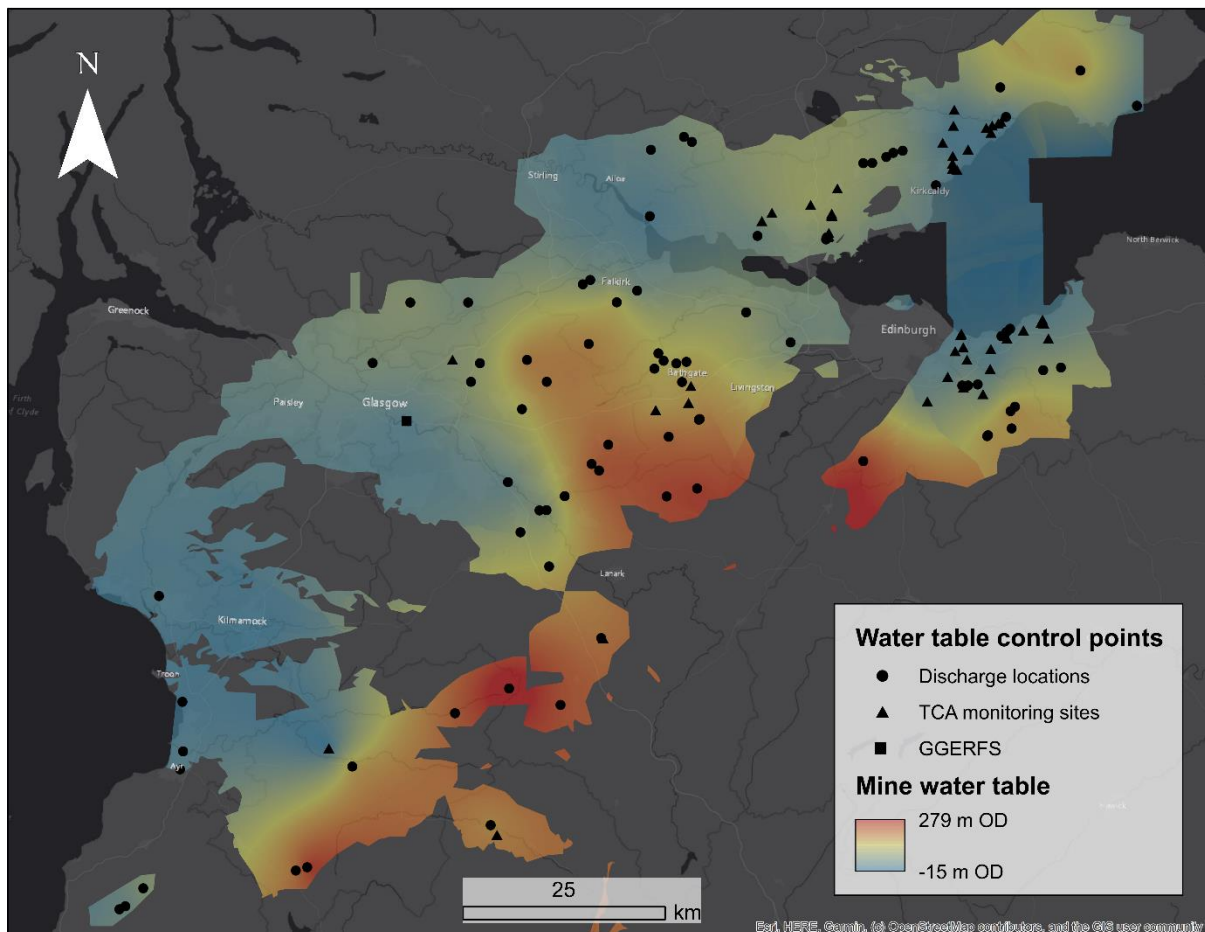


Figure 4.7 Map of predicted mine water table (m OD). GGERFS: Glasgow geothermal energy research field site. Contains data from © The Coal Authority. All rights reserved.

Once the mine water surface (m OD) was produced as a raster layer, the vertical difference between it and the surface level (DTM) was calculated. This formed a ‘depth to mine water head (m BGL)’ raster layer. The calculated depths for mine water head are mapped in 10 m increments in Figure 4.8, with shallower values (0 m – 20 m BGL) shown in shades of pink and deeper values (20 m - 60 m BGL) shown in shades of blue. Depths greater than 60 m BGL are not shown, the raster has been clipped to the same extent as above.

4.3.2.2 Rationale

Mine water head is not inherently linked to the depth of coal seams, for example, the UK Geo-Energy Observatories (UKGEOS) site observes a resting head level of only 0.5 m – 3 m BGL despite mine depths of c.45 m and c.85 m BGL (Palumbo-Roe *et al.*, 2021b). Mine water head described here is a potentiometric surface – where the water level would rise to in boreholes which intersect workings, often above the upper limit of the mine. It is possible that resting mine water head corresponds to the mine depth, or that the shallow worked seams are dry in areas with a deep water level.

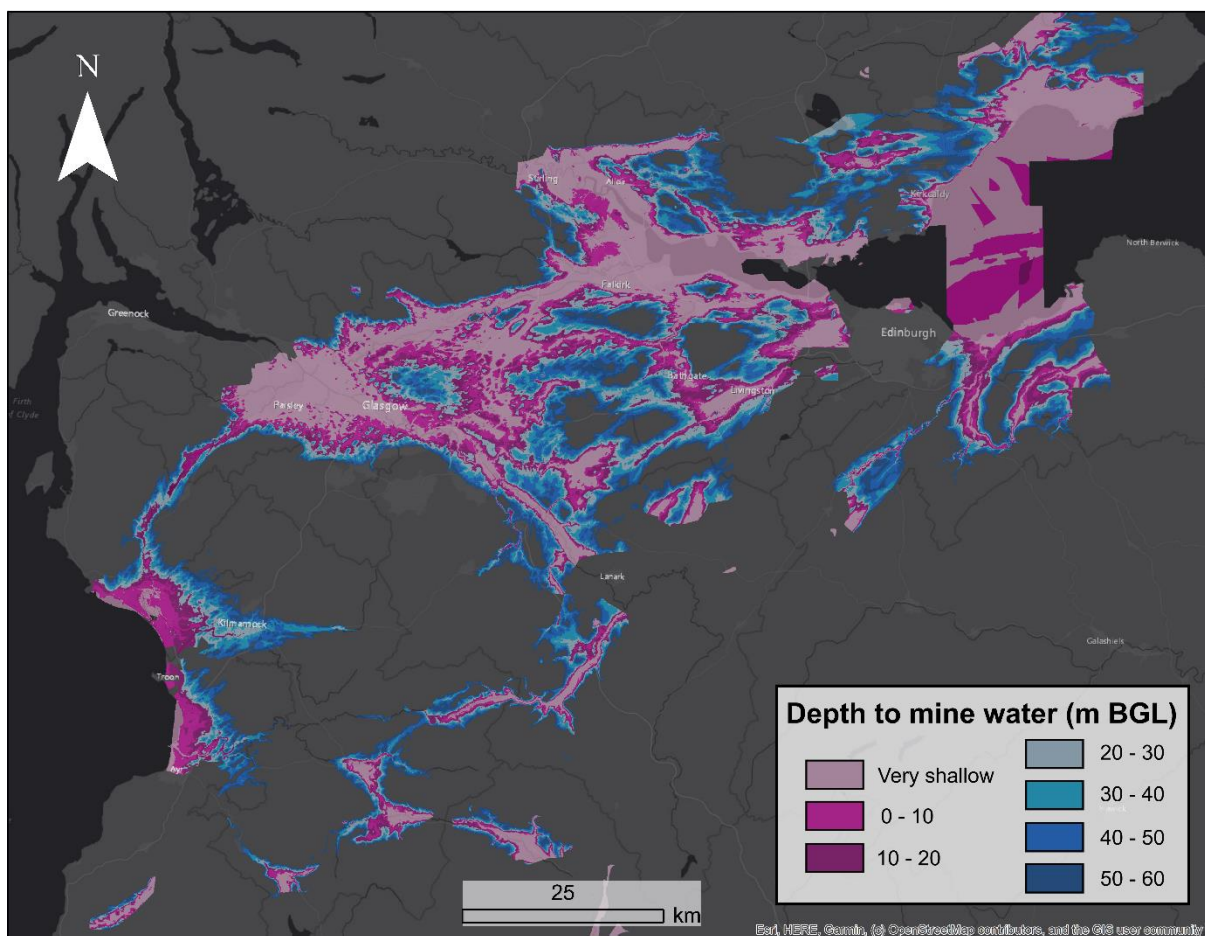


Figure 4.8 Map of predicted depth to mine water level (head) (m BGL). Contains data from © The Coal Authority. All rights reserved. Crown copyright and database rights 2022 Ordnance Survey.

Depth to mine water head is a crucial factor when considering the cost effectiveness of a MWG system since the energy expended for pumping is directly proportional to the pumping head depth. In their analysis Athresh *et al.* (2015) found that for 50 L/s, a dynamic pumping head of 10 m BGL gives annual pumping costs of £3700, compared to £37,000 for 100 m BGL. Areas with shallow resting head levels therefore present the most promising economic settings

when considering pumping costs. Boreholes across the sites of UKGEOS (Palumbo-Roe *et al.*, 2021b) and Lanchester Wines (Banks *et al.*, 2022) observed dynamic heads 0.5 m to 30 m deeper than respective resting head during pumping rates of 20 to 30 L/s. It is feasible therefore, that a site with a resting head of 60 m BGL may observe a dynamic head close to 100 m BGL if pumping higher flow rates, incurring costs close to £37,000 per annum as described. In this study, the authors have presented 10 m incremental increases for predicted depth to mine water head, as far as a cut-off of 60 m BGL.

It is important to remember that this study was performed to focus on locations suitable for mine water geothermal systems as “open loop with reinjection” (see Walls *et al.* (2021) for details), which require at least two boreholes completed into overlapping seams, where one is reinjecting water. There is a risk during reinjection that mine water induces localised water level rise in the borehole, causing a surface breach and flooding of the area. Similarly, reinjection could lead to a more regional mine water head increase and induce new discharges or flood susceptible areas. The Lanchester Wines Abbotsford Road site in Gateshead observed a dynamic head up to 25 metres higher during reinjection at c. 30 L/s (Banks *et al.*, 2022). This could limit the reinjected flow rate or require portions of the water to be disposed of at the surface. The zones with mine water head between 20 and 60 m BGL therefore define the areas where open loop with reinjection should work optimally with acceptable pumping costs and a small risk of up-coning challenges. Where mine water head is shallow (0 to 20 m BGL) there may be some risk that reinjection causes mine water heads to approach the surface, depending on the transmissivity of the workings. “Open loop with discharge” *may* be more feasible for areas with very shallow mine water (0-20 m BGL), but in turn, may require additional permitting (discharge consents) and available land for treatment depending on water chemistry (Walls *et al.*, 2021).

4.3.3 Criterion 4 - Depth to mined seams beneath ground level

4.3.3.1 Method

“In seam level” point values were converted from metres OD to metres BGL by subtraction from surface level values of the DTM. The depth (m BGL) points were symbolised differently for those equal to or less than (\leq) 250 m BGL, versus greater than ($>$) 250 m BGL, as seen in Figure 4.9.

To create a final map showing all four criteria, a raster surface was required. A continuous surface which depicts depth (m BGL) was created by kriging “in seam level” points.

Inverse Distance Weighting (IDW) was used, whereby values are calculated using a weighted average of the nearest points. The weights are proportional to the inverse of the distance between the data point and the prediction location raised to the power of two. As a result, as the distance increases, the weights decrease rapidly and thus, only the 12 nearest points were considered for each IDW. In areas where seams overlap, as described in Criterion 1, there can be depth differences of tens of metres or more. If, within a given area, a grouping of mine workings has elevation points above and below the 250 m BGL cut-off, the weighted average produced by the IDW raster layer dictates whether the area is deemed above or below the cut-off. This raster is useful to produce a final output combined with the rasters from the other criteria, but the raw data is also valuable since it hosts information on each of the seams.

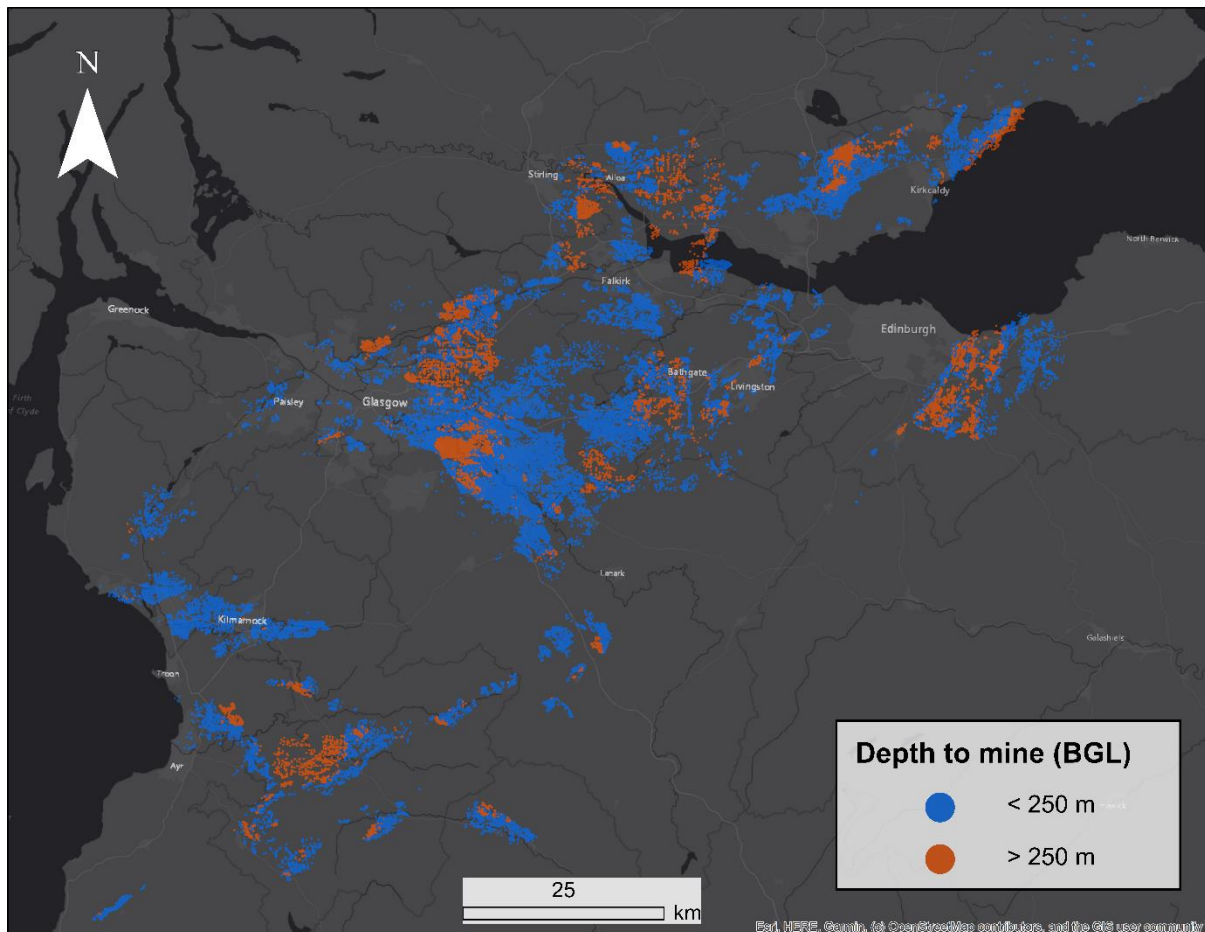


Figure 4.9 Map of coal mine elevation points, coloured to reflect depth relative to the 250 m BGL cut-off. Reproduced with the permission of © The Coal Authority. All rights reserved. Crown copyright and database rights 2022 Ordnance Survey.

4.3.3.2 Rationale

Selection of a suitable drilling range between surface and c. 1000 m BGL is subjective and depends on the intended outcome of a given MWG project. For example, if targeting maximum potential temperature, then it is likely that the deepest mine in each area would be identified. For this study, depths shallower than 250 m BGL were classed as suitable, and deeper than this, unsuitable. Predictions of drilling costs performed by TownRock Energy (not available in the public domain) have found that drilling cost per metre increases significantly beyond 250 m. This is largely due to the higher mobilisation cost and day rate for a drill rig required to reach such depths (Diamond, 2022). This does not mean to say that projects deeper than 250 m are unfeasible, but this cut-off was selected to meet the original intentions of this study: to improve uptake rate of MWG system deployment by highlighting the most economically optimal areas. The shallower mine workings are associated with lower capital expenditure estimates and thus are progressed as the most economical.

Mine water heating and cooling systems can operate at depths greater than this, and often these will bring elevated temperatures, e.g. Heerlen, The Netherlands (Verhoeven *et al.*, 2014) which has a source temperature of 28 °C from 700 m BGL. The capital costs of construction and the project risks can be unattractive and, as is the case with Heerlen, these projects may only be able to operate in receipt of significant subsidies. Since Scottish mine water blocks were found to have mean geothermal gradients of 29.8 °C/km in Central Scotland, 26.8 °C/km in Ayrshire, 24.2 °C/km in Lothian, 22.2 °C/km in Douglas and 21.9 °C/km in Fife (Farr *et al.*, 2021), there is an argument that the MiRAS could be modelled in parallel for maximum temperatures, and somewhat irrespective of capital spend, but this was beyond the scope of this study. Fortunately, for a system coupled with a heat pump, the controlling factors on heat delivery is the temperature change (ΔT) (Banks, 2008) and flow rate (Bailey *et al.*, 2016). Temperature change (ΔT) is independent of source temperature, however, a higher starting temperature does make a heat pump more efficient.

4.3.4 Mine Water Geothermal Resource Atlas for Scotland

The raster layers from criteria 1-4 (C1-4) were combined to form a final raster later. The ‘raster calculator’ tool was used to find areas which met the study requirements. The input equation required the following:

- If C1 has overlapping seams and C2 has no workings <30 m BGL, then assign value 1, otherwise assign 0.
- C3 remained with “depth to mine water” values in 10 m increments to 60 m BGL.

- If $C4 \leq 250$ (m BGL), then assign value 1, otherwise assign 0

$$\text{Raster Output} = C[1,2] (1 \text{ or } 0) \times C3 (\text{value of depth m BGL}) \times C4 (1 \text{ or } 0)$$

Equation 4.1.

Equation 4.1 generated a value representative of the predicted mine water head only where there are overlapping seams and an average depth to mines less than or equal to 250 m BGL.

4.4 Results

Having detailed the four criteria in the section above, the resulting MiRAS allows identification of areas which meet the criteria.

To be selected as an optimal site, the area must have each of the following:

- Overlapping seams, without shallow workings
- Mine water head between 0-60 m BGL
- Average depth to workings less than or equal to 250 m BGL

The total area underlain by the MiRAS in each of the Scottish local authority areas can be seen in Table 4.2, where North Lanarkshire comfortably hosts the largest area at 90.9 km². Cumulatively, there is a total of 370.3 km² across 19 local authority areas which are most suitable for MWG development.

Local Authority	Area of optimal sites on MiRAS (km ²)	Local Authority	Area of optimal sites on MiRAS (km ²)
North Lanarkshire	90.9	Midlothian	10.7
South Lanarkshire	52.2	Stirling	8.2
Fife	46.4	East Dunbartonshire	7.6
East Ayrshire	30.3	East Lothian	6.3
West Lothian	28.9	Dumfries and Galloway	5.6
Glasgow City	23.3	Renfrewshire	1.4
Falkirk	17.9	City of Edinburgh	1.2
North Ayrshire	16.9	East Renfrewshire	0.4
Clackmannanshire	11.1	Perth and Kinross	0.2
South Ayrshire	10.7		
Total = 370.3 km²			

Table 4.2 Coverage area by the MiRAS in each of the affected Scottish local authority areas.

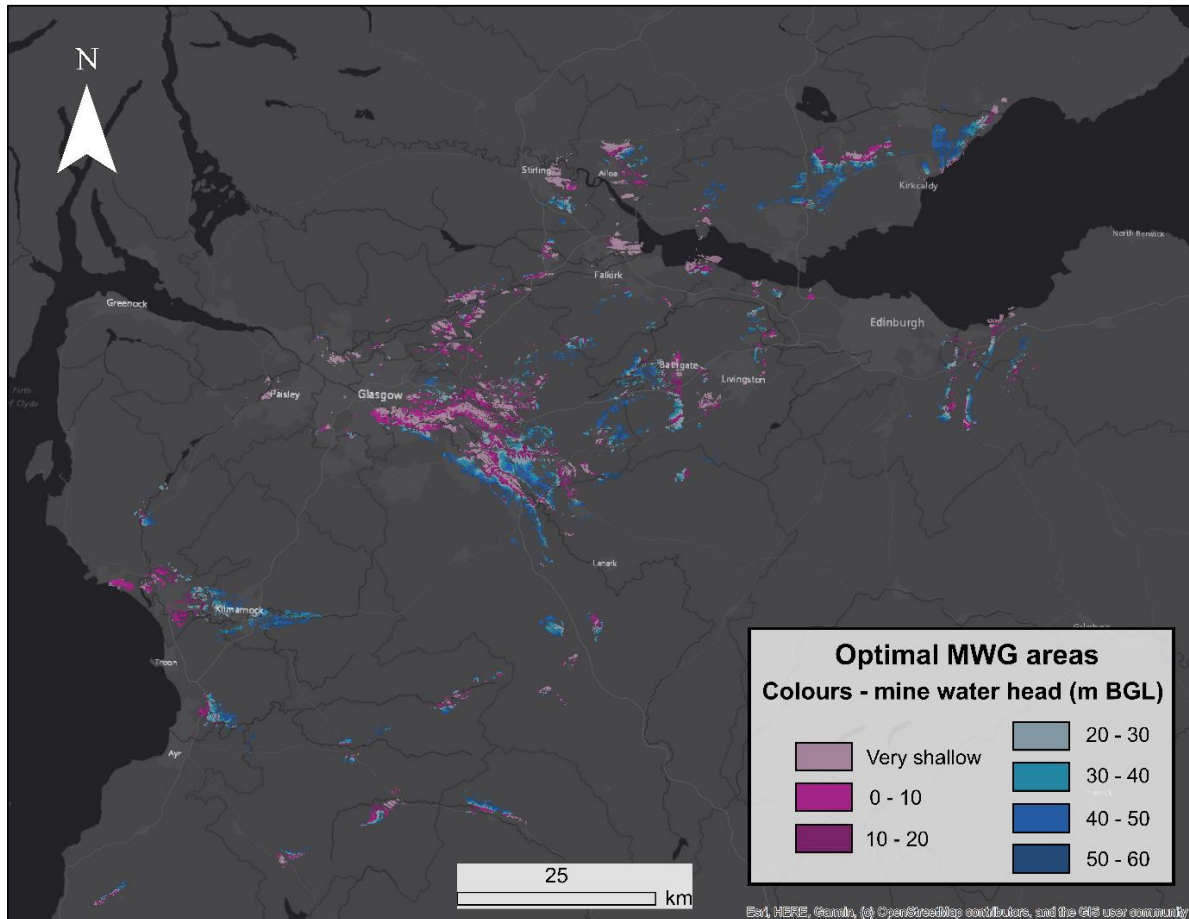


Figure 4.10 Mine Water Geothermal Resource Atlas for Scotland with optimal areas coloured corresponding to the depth to mine water (m BGL). Reproduced with the permission of © The Coal Authority. All rights reserved. Crown copyright and database rights 2022 Ordnance Survey.

The areas which result will briefly be described here, however, the results are best viewed in Appendix 4A for each local authority area. Alternatively, the final MiRAS can be viewed online:

<https://www.spatialdata.gov.scot/geonetwork/srv/eng/catalog.search#/metadata/63ccef-ed-0165-461d-a5a5-025b0b2463c5>

The optimal sites are presented in Figure 4.10, where the colour scheme corresponds to the predicted mine water head. Pink shaded areas reflect shallower depth to mine water head (0 – 20 m BGL), and blue shaded areas reflect 20 – 60 m BGL. The areas with suitable conditions for MWG open loop systems span the width of the MVS. The most densely populated area of potential stretches between SE Glasgow, Wishaw and Airdrie, but these resources are largely 0 – 20 m BGL. The best sites, with depths of 20 – 60 m BGL, are primarily located beneath more condensed population centres including Ayr, Kilmarnock, Bathgate, Stirling, Alloa, Cowdenbeath and Lochgelly, plus smaller clusters of towns in Mid- and East Lothian, and along the Fife coast to the NE of Kirkcaldy. The central portion shown in Figure 4.11, depicts extensive areas optimal for mine water geothermal beneath Hamilton, Wishaw

and Motherwell. Areas which would be well suited, albeit with a shallower mine water head, extend beneath Airdrie and Coatbridge.

4.5 Discussion

The identification of suitable sites for mine water geothermal energy systems is a first step towards increasing uptake of the resource across Scotland. Whilst the MiRAS is not a perfect interpretation of subsurface conditions, it is an excellent tool for stakeholders and decision makers who are involved in efforts to decarbonise heating in Scotland. The interactive, online MiRAS allows rapid screening of any site across the MVS for its mine water geothermal feasibility, bypassing the requirement to involve professional services at the earliest (screening) stage. Similarly, by hosting relevant data together on one map, professional services can use it as a valuable starting point when performing a complete site appraisal or feasibility study. Ideally, this tool will help MWG become a more widely understood resource, and one that will help the public understand its potential.

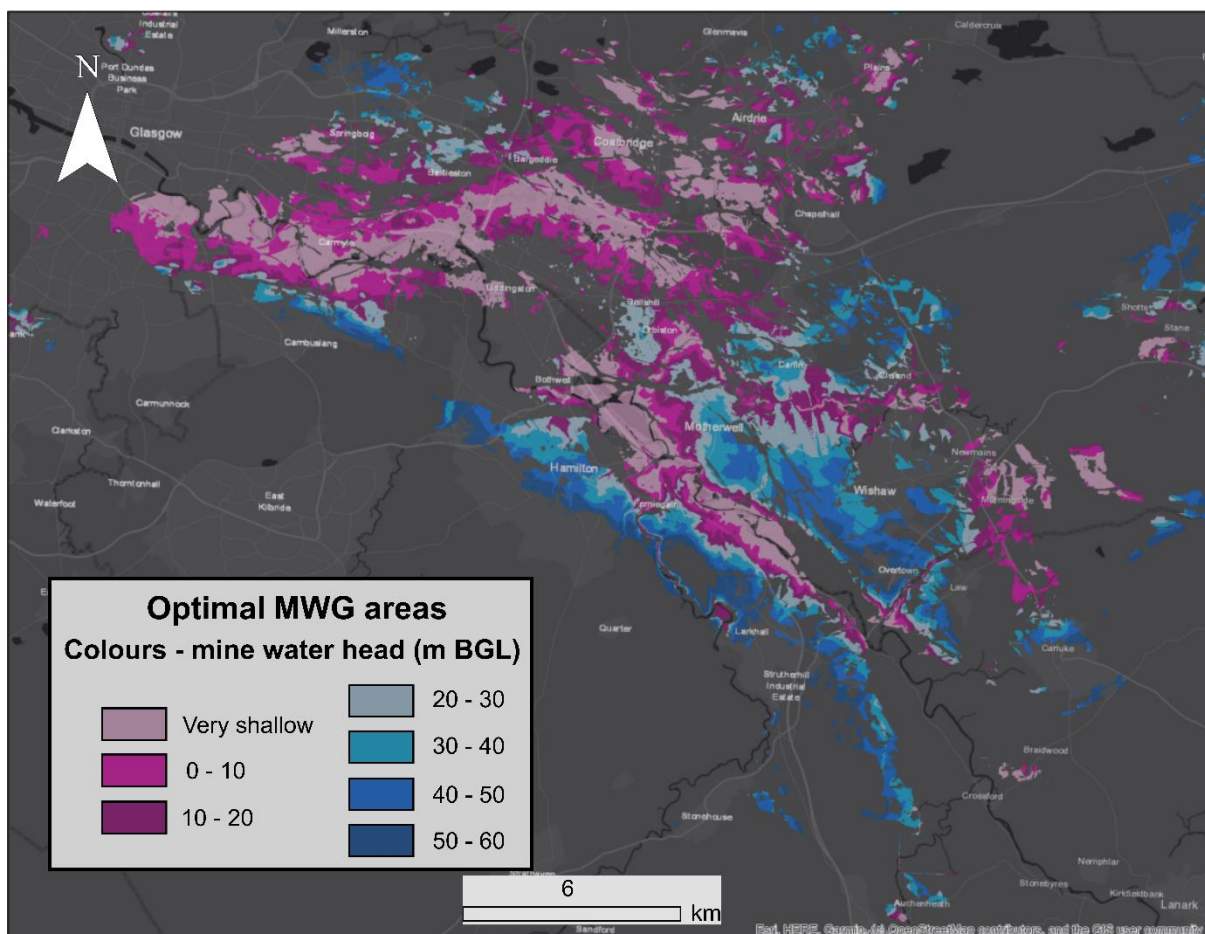


Figure 4.11 Enlarged Mine Water Geothermal Resource Atlas for Scotland, with optimal areas coloured corresponding to the mine water head (m BGL). Reproduced with the permission of © The Coal Authority. All rights reserved. Crown copyright and database rights 2022 Ordnance Survey.

The results should be viewed in the light of source data limitations. Firstly, it is recognised that a low density of mine water head data points in some locations means that the predicted mine water head has some inherent error. Figures 4.7 and 4.9 show areas where the water is predicted to be above ground level. Whilst this is what causes gravity discharges, absent data from unfound discharges means that the interpolated mine water head may be too high in some places. Hence these areas are labelled as “very shallow mine water”.

Secondly, predicting total available void space using the MiRAS is challenging since it has extracted locations where seams overlap, but does not indicate how many overlap, or their dimensions. The actual number of overlapping polygons range between 1 and 22, as described above, and this range will influence the mine water resource size. Similarly, there may be large extents of mined seams which do not overlap for much of their footprint but overlies for a small portion (see Figure 4.12). In these instances, the total available resource is underrepresented by the final selected areas. It is therefore necessary to ensure all mine workings are explored in full, following selection of suitable development areas by this study.

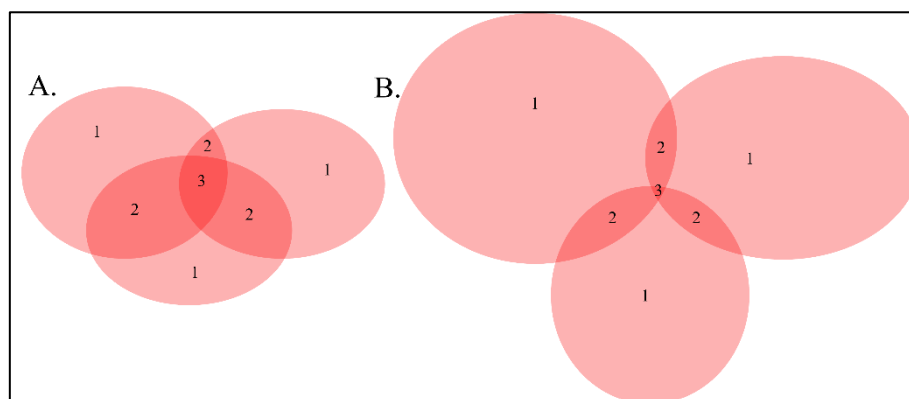


Figure 4.12 Schematic representation of difference between A) smaller total mined area but larger overlapping area; and B) larger total mined area but smaller overlapping area.

Thirdly, the MiRAS has only characterised mine water geothermal resource, not complementary heat loads. As described in the introduction, it is recognised that the resource and a thermal demand must be paired at an early stage of development to ensure a project can progress. The MiRAS has not included a map of the heating/cooling demand at the surface, similarly, it has not included a map of building development plans for Scotland. Whilst these are possible, the temporary nature of thermal demands and regular updates to development plans mean our findings would soon become obsolete.

Fourthly, the economic viability of MWG systems relies on more than just the four criteria outlined. As mentioned in the introduction other “geofactors” can have an influence

(e.g., water chemistry can greatly influence operation expenditure (Walls *et al.*, 2021)). Therefore, it may be feasible to incorporate a layer which reflects the spatial variation of total iron to predict areas where ochre clogging risk is most prominent. However, this is very likely to be three-dimensional and inherently difficult to represent on a two-dimensional map. In addition to “geofactors” there are political and infrastructural factors which can affect the economic feasibility of a MWG system, for example: government incentives for low-carbon heating, or costs of materials e.g., steel. Similarly, whilst it indicates where MWG systems are most economic to develop, the MiRAS does not go as far as calculating their performance against other heat sources (e.g., natural gas, or air-source heat pumps).

Penultimately, and as alluded to briefly above, there are some configurations of mine water geothermal systems which are not highlighted by the MiRAS. For example, open mine shafts throughout the MVS have potential to be significant assets for the MWG sector, providing a means of thermal storage or at the very least an access point for mine water abstraction. The MiRAS was primarily constructed for “open loop with reinjection” arrays, and therefore the feasibility or favourability of a “standing column” array within an open shaft cannot be interpreted from the MiRAS. However, the predicted mine water head output of this work may prove useful for estimating likely water level in an open shaft.

Finally, the resource detailed in this study provides a valuable first-pass screening tool for interested individuals prior to, or at an early stage of project development. What it cannot do however, is replace the necessary expertise required for development of a MWG system. Successful project development requires integrating skills of hydrogeologists, mining engineers, chemists, HVAC and buildings services engineers, economists and planners (Walls *et al.*, 2021). Since the MiRAS provides no internal detail on mined areas it cannot inform borehole locations, probable underground flow pathways or resource size. It is strongly recommended that following initial identification of an optimal location for a MWG project, relevant professionals are engaged to execute planning and installation correctly.

4.6 Integration of resource maps

Chapters 3 and 4 have indicated locations across Scotland which are best for development of surface and subsurface mine water thermal resources respectively. In this section they have been combined and arranged as simple map outputs for each local authority. As a result of integration of the surface and subsurface MWG resources of Scotland, the figures in Appendix 4A show “optimal areas” – which are the resulting areas from the raster layer of

the MiRAS produced in this chapter. These are coloured in the same fashion throughout, where a shallow mine water head is pink, and the optimal mine water head for open loop with reinjection is shown in blue. Overlaid are the point data from Chapter 3, indicating the heat available from the different types of surface resources. Heat available (G) is a function of the flow rate from boreholes, mine shafts or drainage discharges (Q), and the temperature change across a heat exchanger (ΔT) (Bailey *et al.*, 2016) and the specific volumetric heat capacity of water ($S_{VC_{wat}}$), explained in Chapter 3 in full, and calculated using Equation 4.2. These values are symbolised corresponding to their origin, e.g., existing treatment schemes (active, passive; gravity fed or pumped). Their number corresponds to the reference number in the supplementary material of Chapter 3 (Appendices 3A and B).

$$G = Q \cdot \Delta T \cdot S_{VC_{wat}}$$

Equation 4.2

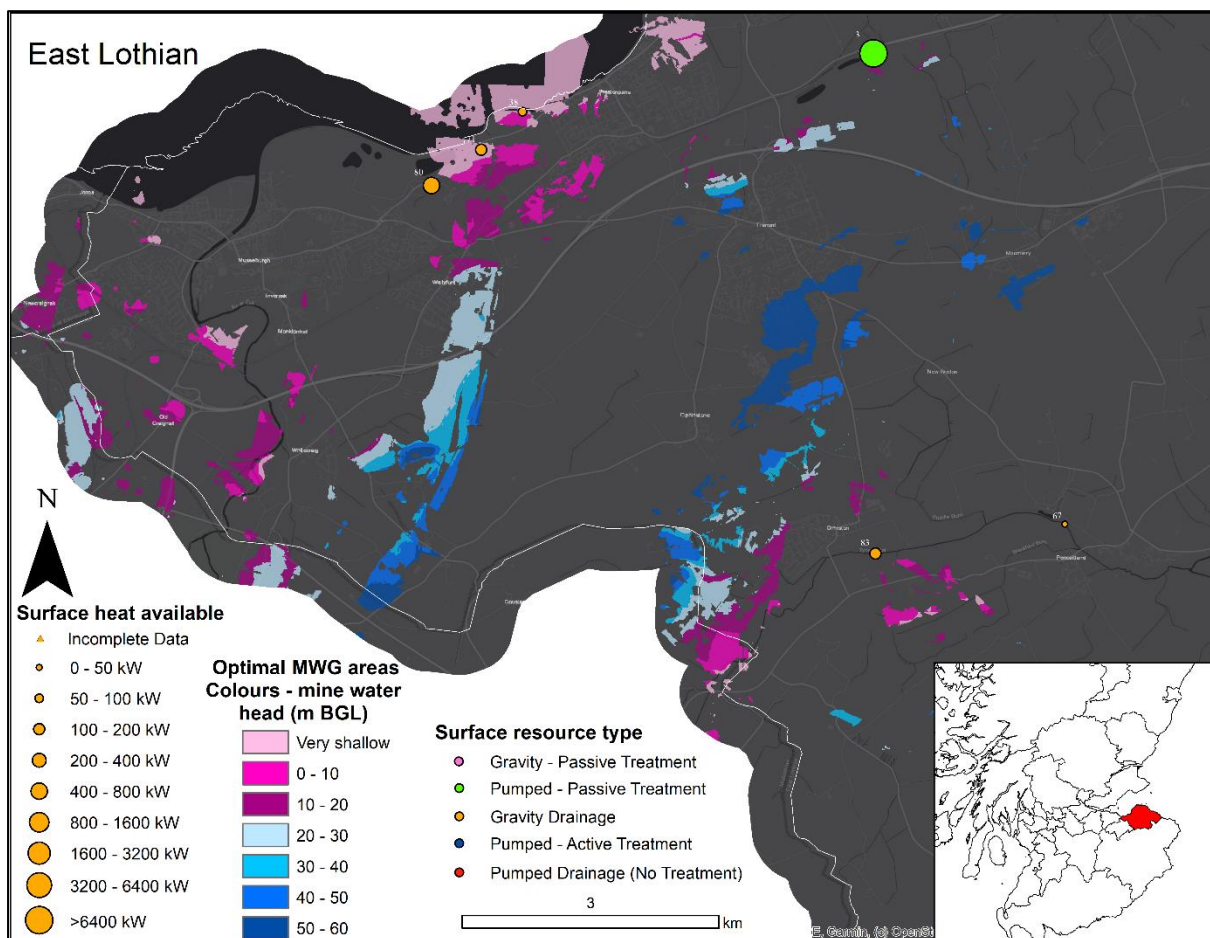


Figure 4.13 The western portion of East Lothian which hosts the Mine Water Geothermal Resource Atlas for Scotland with surface thermal resources included. Reproduced with the permission of © The Coal Authority. All rights reserved. Crown copyright and database rights 2022 Ordnance Survey.

It is envisaged that these maps (exemplified by Figure 4.13 and presented in full in Appendix 4A) can be circulated widely to communicate the thermal potential of mine water geothermal heating and cooling in Scotland. The example of East Lothian in Figure 4.13 shows the western extent of the local authority area, hosting Blindwells treatment scheme (#3 from Chapter 3) with 6.9 MW heat availability, comfortably the best mine water geothermal resource in Scotland. Whilst many of the large gravity discharges and TCA treatment schemes make good sense to develop and harness thermal energy, Blindwells is highly regarded because of the very large heat availability (Bailey *et al.*, 2016, Walls *et al.*, 2022), good proximity to adjacent urban areas and extensive local development plans (Optimised Environments Ltd., 2020).

4.6.1 Breakdown of best resources in local authority areas

Since the MiRAS does not include data pertaining to the number of overlapping seams; thickness of seams; type of workings; or expected extent of collapse, it cannot provide volume estimates of mine workings. Whilst there is not a direct correlation between coverage of the MiRAS “optimal areas” and the resource volume, it can be used as a useful proxy. Total optimal subsurface area from the MiRAS and total heat available (G) from the gravity discharges and Coal Authority treatment schemes (as published in Walls *et al.* (2022)) are useful to understand the Local Authorities with the greatest potential for MWG development. The results are shown in Table 4.3. North Lanarkshire comfortably hosts the largest area beneath which MWG systems could optimally be sited, at 90.9 km², however, the local authority areas of Fife, East Lothian and West Lothian have the highest heat available at surface. These three areas have large Coal Authority treatment schemes, including the pumping sites of Frances, Blindwells and Polkemmet, which are responsible for 14.4 MW of combined heat availability.

4.6.2 Quality Assurance

Decommissioned or existing mine water geothermal systems or research sites in Scotland can provide some quality assurance for the MiRAS since the details of the coal seams in each site are known in more detail. Each of the following has been assessed using the MiRAS and will be compared to the collected field data: The Shettleston Housing Association (SHA) mine water geothermal system which operated for c. 20 years from 1999 in eastern Glasgow (4.1668° W, 55.8504° N) (Walls *et al.*, 2021); the UKGEOS Cuningar Site, Glasgow (4.2008° W, 55.8383° N), which is a facility for monitoring, testing and innovation of mine water geothermal energy systems (Monaghan *et al.*, 2021c) which is covered in detail in Chapter 6;

and the Dollar field site (3.662° W, 56.165° N,) presented in Chapter 5, where ground stability investigative techniques were combined with mine water geothermal investigation to characterise an area of shallow (<60 m BGL) mine workings on the eastern edge of Dollar, Clackmannanshire.

Local Authority	Area underlain by the MiRAS (km²)	Total heat available at surface (kW) (from Walls <i>et al.</i> (2022))
North Lanarkshire	90.9	4489
South Lanarkshire	52.2	3018
Fife	46.4	8903
East Ayrshire	30.3	2395
West Lothian	28.9	6572
Glasgow City	23.3	5.3
Falkirk	17.9	1103
North Ayrshire	16.9	372
Clackmannanshire	11.1	261
South Ayrshire	10.7	795
Midlothian	10.7	3279
Stirling	8.2	N/A
East Dunbartonshire	7.6	6.1
East Lothian	6.3	7758
Dumfries and Galloway	5.6	470
Renfrewshire	1.4	N/A
City of Edinburgh	1.2	752
East Renfrewshire	0.4	N/A
Perth and Kinross	0.2	176
Total	370.3	40,354

Table 4.3 Coverage area of the MiRAS and heat available from surface mine water resources, broken down into local authority areas.

4.6.2.1 Shettleston

The area surrounding the SHA site has portions which meet all four MiRAS criteria, but the MiRAS does not select the area precisely beneath the abstraction and reinjection boreholes (Figure 4.14). The MiRAS is controlled by Criterion 1 here, which indicates that there are not overlapping worked coal seams beneath the SHA boreholes (Figure 4.15). This conforms with the findings of Banks *et al.* (2009) and Banks *et al.* (2019) who state that the abstraction borehole is likely completed into the workings of the Ell Coal Seam of Westmuir Pit from the period 1845–1862, but postulate that the reinjection borehole may not have entered mine workings, and instead may be completed into an adjacent Carboniferous (Westphalian)

Coal Measures aquifer sequence. It should be stated that the working dates from the Westmuir Pit are from before the mandatory requirement to record mine workings (Younger and Adams, 1999), and thus, some worked seams may be unaccounted for in the original TCA dataset. The mine water head data from 2016 (Walls *et al.*, 2020) beneath Shettleston Housing Association was not used as a data point for mine water head interpolation (Criterion 3) since the input data was to be true of 2020/2021. The mine water head is predicted by the MiRAS to be between 0 m to 10 m BGL beneath SHA, which is shallower than Walls *et al.* (2020) found in 2016, where mine water levels were between 12 m and 13 m BGL.

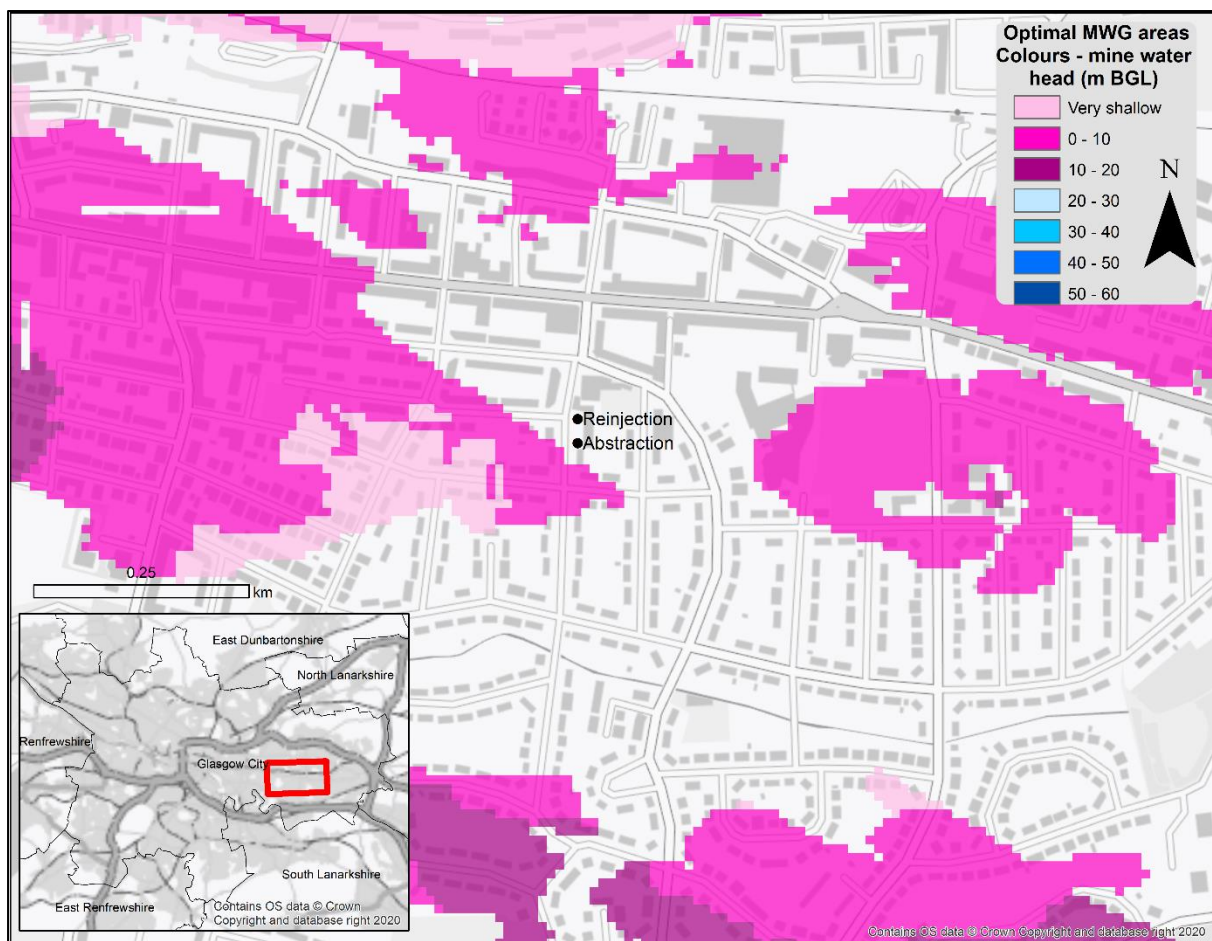


Figure 4.14 The Mine Water Geothermal Resource Atlas for Scotland applied to Shettleston Housing Association abstraction and reinjection boreholes, Glasgow. Reproduced with the permission of © The Coal Authority. All rights reserved. Crown copyright and database rights.

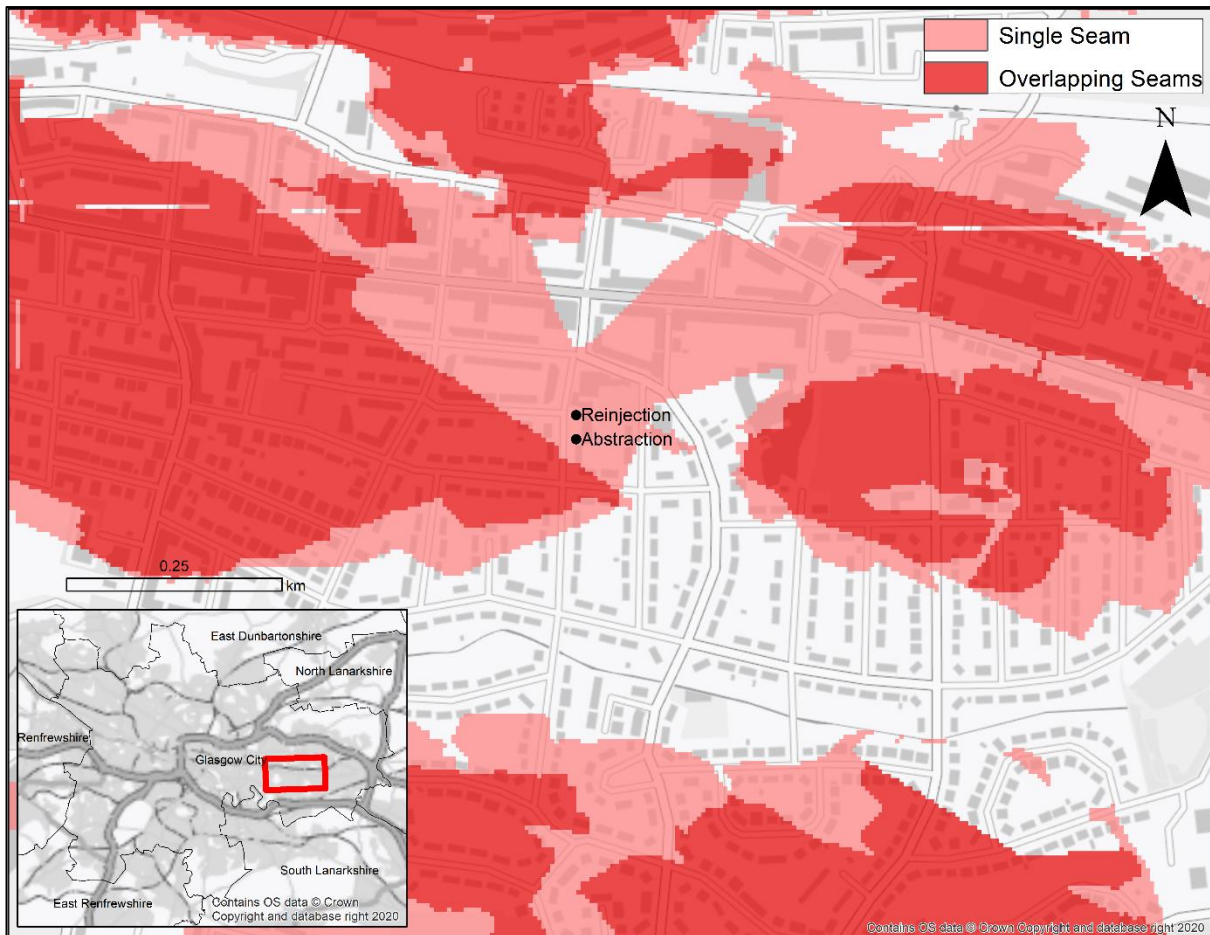


Figure 4.15 Single and overlapping coal seam locations near Shettleston Housing Association abstraction and reinjection boreholes, Glasgow. Reproduced with the permission of © The Coal Authority. All rights reserved. Crown copyright and database rights

4.6.2.2 UK Geo-Energy Observatories

The UK Geo-Energy Observatories (UKGEOS) Cuningar site is extremely well documented and hosts seven worked coal seams from the Farme Colliery dating between 1805 and 1928 (Findlay, 2020). There are 5 boreholes which intersect mine workings of the Glasgow Upper and Glasgow Main Coal Seams (Monaghan *et al.*, 2019). The resting mine water head in these boreholes was used as a datapoint for the mine water head level interpolation, with levels close to the surface (0.5 m to 3 m BGL). There are no shallow coal seams (<30 m) since the highest seam is c. 45 m BGL. The MiRAS highlights the Cuningar site as an optimal location for a MWG system, but since there is a shallow mine water head, it is recommended that the hydrogeology is well characterised before the site is used for open loop with reinjection (Figure 4.16).

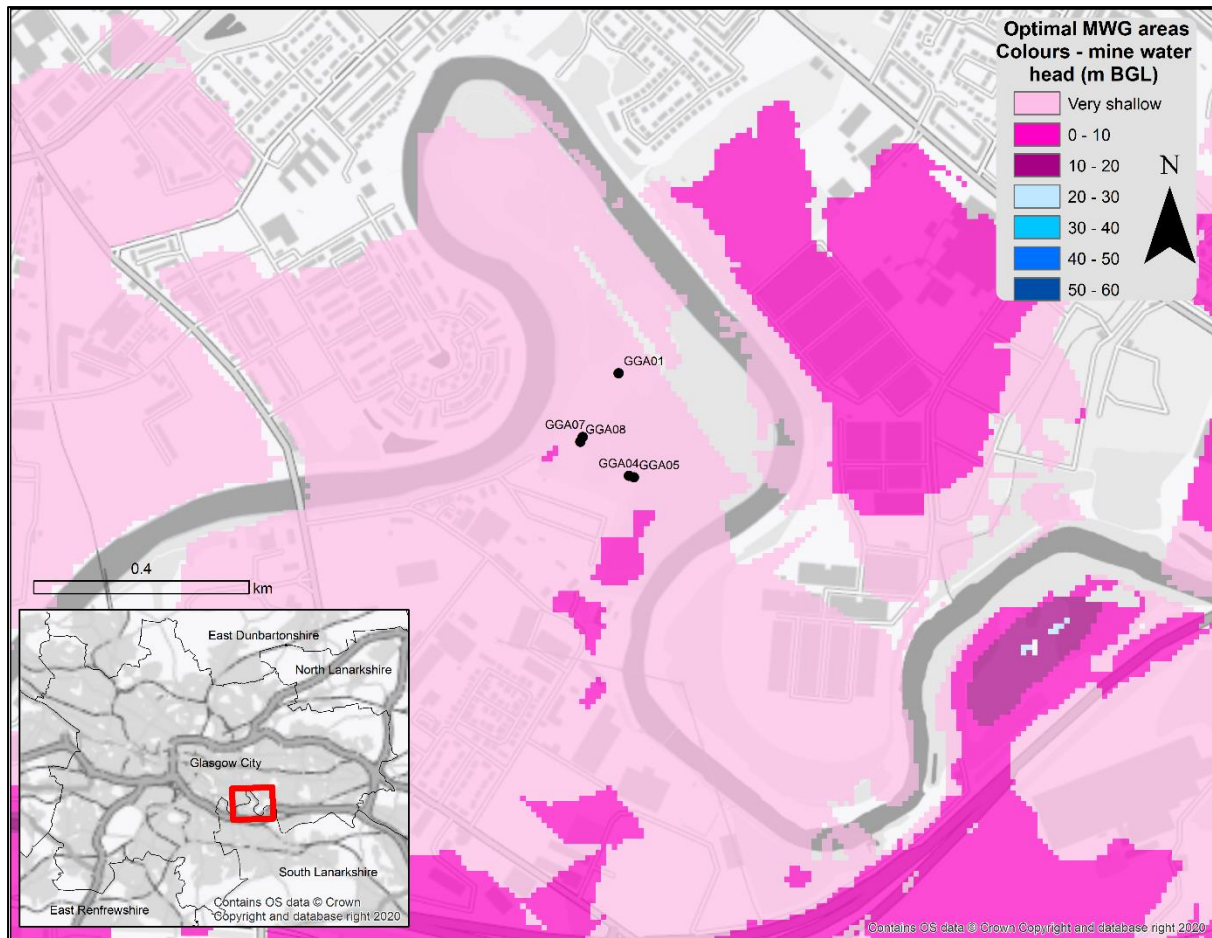


Figure 4.16 The Mine Water Geothermal Resource Atlas for Scotland applied to the UKGEOS Cuningar Site, Glasgow. The 5 boreholes which are completed into coal mines are shown in black. Reproduced with the permission of © The Coal Authority. All rights reserved. Crown copyright and database rights. Contains NERC materials ©NERC 2020.

4.6.2.3 Dollar

The Dollar research site, detailed in Chapter 5, has four seams worked across the last few centuries with the most recent forming part of the Dollar Colliery in 1950s and 60s. The depths range from surface outcrop to 50 m BGL, extending to greater depths north of the site in a small, isolated syncline. The mine water discharge was used as a controlling data point for the mine water head interpolation (Criterion 3) thus, the mine water head in Dollar Colliery are predicted with good accuracy. Since much of the site is underlaid by shallow workings (<30 m BGL) or single coal seams (Figure 4.17), the MiRAS has removed these areas and leaves only a small fraction of the site with overlapping workings which hosts all four criteria of the MiRAS (Figure 4.18).

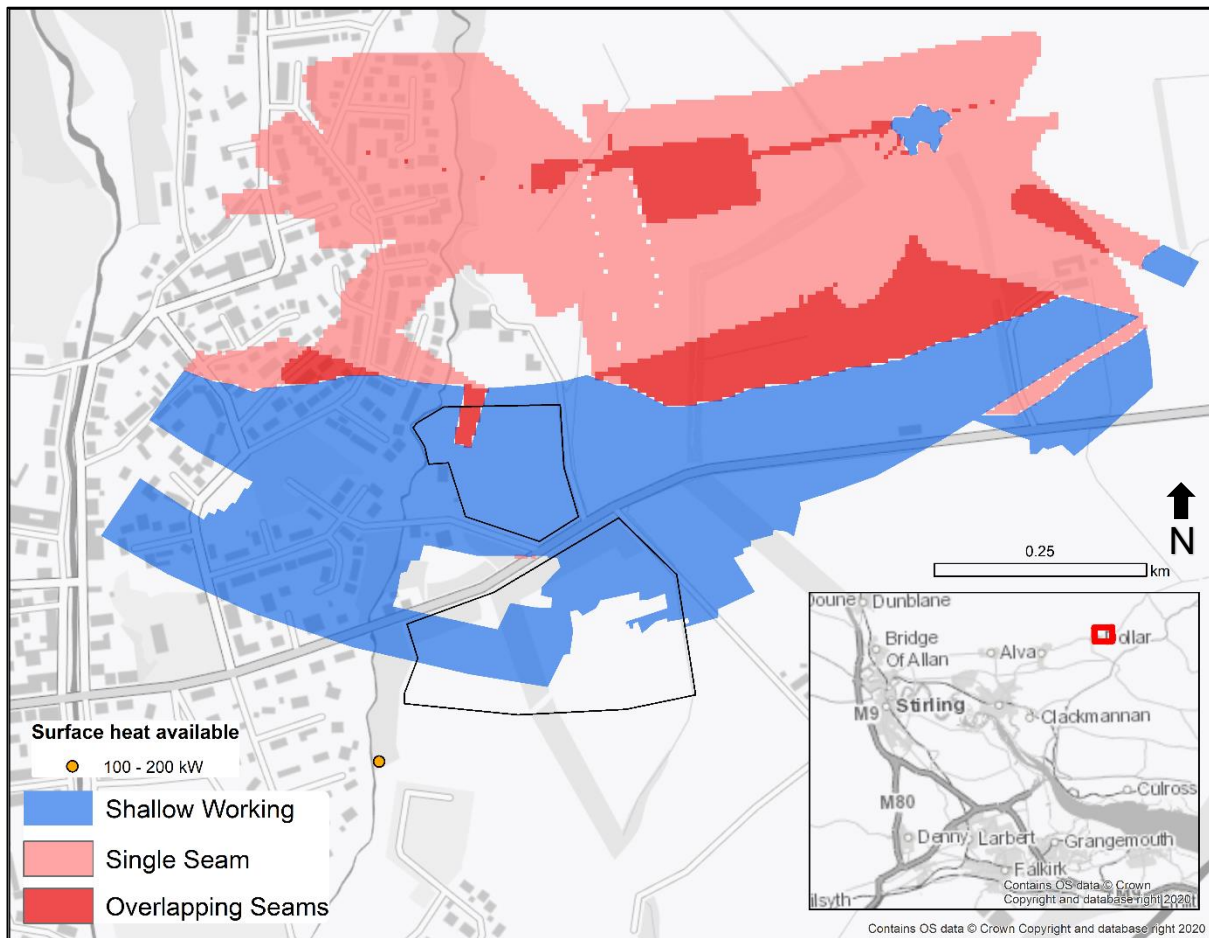


Figure 4.17 Areas of shallow (<30 m), overlapping and single coal seams beneath the Dollar Site, Clackmannanshire. The study area for Chapter 5 is shown by the black polygon. Shallow workings are shown as seen on TCA’s interactive map viewer (The Coal Authority, 2022). Reproduced with the permission of © The Coal Authority. All rights reserved. Crown copyright and database rights.

The workings in the area which do not meet the MiRAS requirements can contribute to the overall mine water resource volume, and this is exactly why the MiRAS can be used for indicative screening purposes only. The MiRAS is useful to identify optimal drilling locations for MWG systems, however, in order to characterise the resource in full, greater scrutiny of site-specific mine abandonment plans would be required. Similarly, since much of the site is not highlighted by the MiRAS because of shallow workings, the field site has proven to be an ideal testing location for the techniques detailed in Chapter 5 exploring shallow workings for MWG potential.

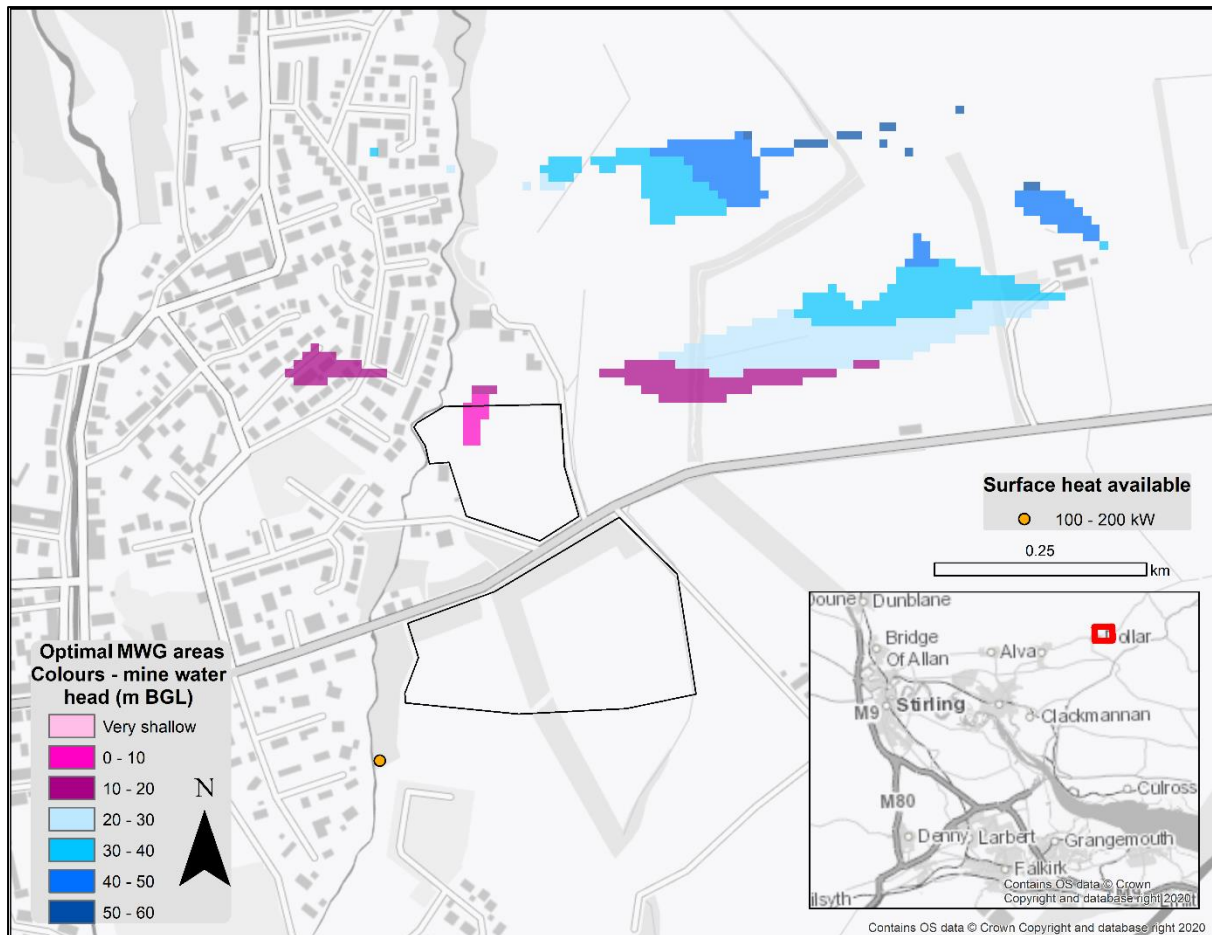


Figure 4.18 The Mine Water Geothermal Resource Atlas for Scotland applied to the Dollar Site, Clackmannanshire. The study area for Chapter 5 is shown by the black polygon. Reproduced with the permission of © The Coal Authority. All rights reserved. Crown copyright and database rights.

4.6.3 Considerations and Limitations

The risk of thermal feedback is present in “heating or cooling only” open loop MWG systems (MacAskill *et al.*, 2015). Whilst there are modelling techniques which predict the rate and timing of thermal feedback (Ghoreishi Madiseh *et al.*, 2012, Loredo *et al.*, 2016, van Hunen *et al.*, 2022), development of heating and cooling networks using mines as a thermal buffer (Fraser-Harris *et al.*, 2022, Verhoeven *et al.*, 2014) would be preferable in many locations, owing to their increased thermal longevity. This means that in the same way that the MiRAS can be used to site buildings for heating, it can also be used for those which have inherent cooling demands to facilitate future MWG systems becoming a 5th generation heating and cooling network. It should be stated that gravity discharges or TCA treatment schemes can be heating or cooling only, since there is no reinjection of cooled/warmed waters to the subsurface, but there should be consideration of SEPA regulations for temperature change of receiving water bodies (SEPA, 2016, 2022).

Other limitations of the MiRAS are that it follows only the guiding principles laid out at the beginning of this chapter. It screens only for overlapping coal seams deeper than 30 m BGL but shallower than 250 m BGL, and where the mine water head is predicted to be less than 60 m BGL. Whilst these are sound parameters for MWG systems and will remain useful for the majority, there are some aspects which are not accounted for.

- a) The deepest mine workings often correlate with the highest temperatures of the mining area. By removing mined seams deeper than 250 m BGL, there are some areas where the highest available temperatures are not presented.
- b) Screening primarily for open loop with reinjection systems means that overlapping seams are a necessity. Where projects could be executed as open loop with surface disposal, then there is no longer a requirement for overlapping seams. Single mined seams, provided adequate connection to a suitably sized mine water resource, would suffice as an abstraction point.
- c) Existing access points to the mine workings - open shafts or boreholes - which could be adapted for mine water abstraction are not shown. These situations could function as part of an open loop system which avoid significant drilling CAPEX, or open shafts can function on a more moderate thermal scale as a “standing column”, e.g. 20 kW provision at Markham (Burnside *et al.*, 2016b)

There remain some factors which the MiRAS does not account for, including the age of the workings. The hydraulic properties of legacy mines have been shown to be somewhat time dependent, with old mines displaying collapse breccias following pillar and stall failure, some of which show accumulation of low hydraulic conductivity clay minerals (Andrews *et al.*, 2020). Whilst the void locations and flow pathways may be representative at the time of abandonment and recording, evolution of the hydraulic condition may impact connectivity and sustainable yields (Monaghan *et al.*, 2021c).

4.7 Conclusions

Data pertaining to abandoned mines in the Midland Valley of Scotland from The Coal Authority and Walls *et al.* (2022) have been combined with surface elevation data from Ordnance Survey to create a Mine Water Geothermal Resource Atlas for Scotland (MiRAS). Processing of the available datasets produced interim GIS layers which show overlapping coal seams where there are no shallow (<30 m BGL) workings; mine water head in m BGL as predicted by kriging mine water elevation points; and depth to mine workings. The four criteria

were combined, and the resultant map indicates an area of 370.3 km² optimal for mine water geothermal development. Optimal resource areas span the Midland Valley of Scotland, with the greatest footprint of potential sites in North Lanarkshire.

It is by using the MiRAS that areas can be screened for mine water geothermal (MWG) potential, improving on the existing system which often requires involvement of technical experts from an early stage, and generally assumes that a project champion/developer is aware of the concept of MWG energy during planning stages. Areas which are denoted for residential, industrial or commercial development can be simply cross-referenced with the MiRAS, to instantly understand whether or not MWG is a potential thermal supply. Alternatively, the MiRAS can be used as a siting tool for stakeholders, influencing site selection for development. It is envisaged that this new means of rapid site appraisal will prove to be a useful tool for local authorities, landowners, and other stakeholders when exploring low-carbon heating opportunities and as a result, expand the awareness and increase the uptake of MWG resources. Future versions of the MiRAS could be expanded to include other factors, such as water chemistry or depth intervals, and have its impact improved by adding information regarding current and future heating and cooling demands.

Author Contributions

David B Walls: Conceptualization (Equal), Data curation (Lead), Formal analysis (Lead), Investigation (Lead), Methodology (Lead), Project administration (Lead), Writing – original draft (Lead), Writing – review & editing (Equal). David Banks: Conceptualization (Equal), Methodology (Supporting), Supervision (Equal), Writing – review & editing (Equal). Yannick Kremer: Methodology (Supporting), Supervision (Supporting), Writing – review & editing (Equal). Adrian J Boyce: Supervision (Equal), Writing – review & editing (Supporting). Neil M Burnside: Conceptualization (Supporting), Methodology (Supporting), Supervision (Equal), Writing – review & editing (Equal).

Chapter 5 - Combining ground stability investigation with exploratory drilling for mine water geothermal energy development. Lessons from exploration and monitoring.

This chapter has been accepted for publication as: Walls, D.B.; Banks, D.; Boyce, A.J.; Townsend, D. H.; Burnside, N.M. Combining ground stability investigation with exploratory drilling for mine water geothermal energy development. Lessons from exploration and monitoring. To the Scottish Journal of Geology of the Geological Society of London.

Abstract

Mine water geothermal's potential for decarbonisation of heating and cooling in the UK has led to increased national interest and development of new projects. In this study, mine water geothermal exploration has been coupled with ground investigation techniques to assess ground stability alongside seasonal mine water hydrogeology and geochemistry. Drilling operations in late 2020 at Dollar Colliery, Clackmannanshire, Scotland, encountered mined coal seams with varying conditions (void, intact, waste, etc.), reflecting different techniques used throughout a protracted mining history. We found that time and resources spent grouting casing through worked mine seams (ensuring hydraulic separation) can be saved by accessing deeper seams where those above are unworked. Continued assessment of existing water discharges and completion of boreholes with slotted liners into mined coal seams and fractured roof strata allowed chemical and water level changes to be monitored across a 1-year period. Mine water heads and mine discharge flow rates vary seasonally and are elevated between late autumn and early spring. The mine water has a low dissolved solute content. Dissolved sulphate-³⁴S isotope data suggest increased pyrite oxidation during lower water levels. These findings can inform future building decisions, whereby housing developments on site could use the mine water for heating.

5.1 Introduction

Ahead of a potential new-build housing development on the outskirts of Dollar, Clackmannanshire, Scotland, project stakeholders were required to conduct a ground stability investigation (GSI) drilling programme since the study area is a "Development High Risk Area" (The Coal Authority, 2022). Such activities explore the state and depth of the coal seams and workings associated with the abandoned Dollar Colliery beneath the development site. The developer wishes the new-build project to approach operational carbon neutrality and thus

instigated exploration of the potential for mine water contained in these partially flooded coal workings to provide low-carbon heating to the houses, via the use of heat pumps.

A previous, confidential TownRock Energy pre-feasibility study, dated March 2018, had identified that mine water geothermal energy extraction could be feasible for heating 25-35 new-build houses in this location, owing to the presence of overlapping, flooded coal seams (TownRock Energy, 2018). Since then, the 25-35 houses have been included in a larger application for up to 200 houses, which extends south beyond the area underlain by coal mines (Clackmannanshire Council, 2022) where the total heat demand is uncertain. Mine water geothermal investigation (MWGI) often involves significant upfront capital expenditure, but inclusion as part of necessary GSI work may present a means to reduce capital expenditure whilst screening sites for potential. Thus, since GSI was necessary for the planned housing development to proceed, it was postulated that the investigation could be adapted to include geothermal appraisal. This research programme was funded by the Energy Technology Partnership (ETP) and the Engineering and Physical Sciences Research Council (EPSRC) with the aim to explore the subsurface and assess the depth, stability and condition of the coal seams and workings below the site (GSI); simultaneously assessing the mine water characteristics and their geothermal potential.

5.1.1 Mine water geothermal energy

Mine water geothermal energy is a low carbon heating and/or cooling resource which uses abandoned and flooded mine workings coupled with ground source heat pump technology (Banks *et al.*, 2004, Jessop *et al.*, 1995, Ramos *et al.*, 2015, Younger, 2016). This resource has been implemented since the 1980s (Jensen, 1983, Korb, 2012, Michel, 2009, Wieber and Pohl, 2008), but has seen an increase in interest and uptake over recent years (Walls *et al.*, 2021). In the UK, projects are being established at locations where there are existing thermal resources brought to the surface, such as pumping and treatment sites (Banks *et al.*, 2019, The Coal Authority, 2018, 2020). Similarly, projects which access abandoned roadways or workings at depth to form “open loop with reinjection” mine water heat pump systems are being researched and deployed (Banks *et al.*, 2022, Monaghan *et al.*, 2021c). The need for low carbon heat is becoming increasingly important during the climate crisis and will be a crucial challenge to overcome if the UK is to reach net-zero by 2050. Plans to terminate installation of gas boilers in new build houses in the UK by 2025, and in Scotland by 2024 (Scottish Government, 2019), means that heat pumps and district heating networks are imperative to achieve this goal. Mine

water can provide a source of low-grade heat (and even “coolth”) for large scale heating networks (Verhoeven *et al.*, 2014). Challenges associated with the uptake of mine water geothermal systems, determined by a global assessment of case studies (Walls *et al.*, 2021), indicate that there are key decisions and practices during the planning, construction and operational stages which can optimise system longevity. In some cases, poor management of mine water chemistry has been a contributing factor to system or component failure, including corrosion and iron oxyhydroxide scaling (Korb, 2012, Steven, 2021a). A sound understanding of mine water chemistry prior to system installation is therefore beneficial since it can inform engineering solutions to mitigate operational risks and help avoid premature decommissioning (Walls *et al.*, 2021).

Mine water geothermal systems have mine water brought to the surface via pumping from shafts or boreholes (Banks *et al.*, 2019), or by gravity drainage through engineered structures (e.g., adits or shafts). In these locations mine water can have its thermal energy transferred to a heat demand via appropriately sized heat exchangers and heat pumps (Athresh *et al.*, 2016, Farr *et al.*, 2016). Understanding the available thermal resource, and therefore the scale of heating/cooling capacity, requires a sound understanding of the resource volume, potential flow rates from abstraction wells (James Hutton Institute, 2016), or from gravity drainages (Farr *et al.*, 2016, Walls *et al.*, 2022) and subsurface flow pathways. Good practice during resource assessment includes sinking pilot MWGI boreholes into mine voids to assess openness and condition and to construct monitoring wells during hydrogeologic analysis from pumping tests (Palumbo-Roe *et al.*, 2021a, Walls *et al.*, 2021).

5.1.2 Ground stability investigation

Ground stability investigation (GSI) describes localised invasive data collection via trial pits or boreholes, sunk to provide details of subsurface conditions prior to construction on a development site (British Standards Institution, 2020, Healy and Head, 1984). For this study area, GSI was initiated since the site is considered to be a “Development High Risk Area” (The Coal Authority, 2022) due to shallow workings. Standard GSI operations provide details of the groundwater heads and flows, rock or sediment thicknesses, the nature and depth of faults and voids, and the risk of gas migration (The Coal Authority *et al.*, 2019). Importantly for this study, they also provide insight into stability, thickness of overburden and need for grouting of mine voids (or other ground stabilisation actions) prior to development. Investigating the condition of coal seams, in areas where they are predicted to be close to the surface, requires

GSI of bedrock often to a depth of around 30 m. The pattern of collapsed overlying strata depends on the mining method and dimensions of coal extraction: longwall mining may involve complete collapse of roof structure, while methods such as pillar and stall may result in localised, uneven or asymmetric subsidence and settlement (Andrews *et al.*, 2020, Younger and Adams, 1999). Since construction of buildings typically increases surface loads, it also increases the likelihood of collapse and subsidence issues. GSI data interpretation identifies areas of land which are unsuitable for construction without remediation by consolidation or stabilisation methods. Changes in fluid pressures resulting from abstraction and reinjection of mine water for thermal exploitation may also result in additional risks of ground movement (Todd *et al.*, 2019).

5.1.3 Synergy between GSI and MWGI

Common estimates use a “1 in 10” rule-of-thumb to estimate the height of strata which may collapse following removal of material when mining (Bell, 1986, Healy and Head, 1984). Assuming a maximum subsurface void height of 3 m (for major underground roadways), workings within 30 m (3 m x 10) of the surface are identified as a risk (Abbate, 2016). Realistically, the affected height will often be less, since there are relatively few coal seams in the UK greater than 1.5 m thick. Younger and Adams (1999) describe a different approach whereby the affected height above longwall seams is more closely related to the width, depth and thickness of the worked panel.

Shallow flooded coal mines are both a subsidence risk and a potential thermal resource for new developments, but a depth boundary where subsidence risk from mine voids becomes significant is not absolute. The methods of MWGI and GSI have broad overlaps since both require drilling through bedrock in search of fractures, voids or coal seams. As mentioned, MWGI often carries a significant upfront capital, but inclusion in necessary GSI work, may present a means to reduce capital expenditure whilst screening sites for geothermal potential.

Some crossover differences between methods remain, crucially the ideal diameter of the boreholes. The default diameter of GSI boreholes in this study was 5” (127mm), restricting any installed polyethylene liners to 50 mm internal diameter (ID), leaving space for an adequate annulus for hydraulic sealing. MWGI pilot boreholes can prove presence or absence of a hydraulically productive horizon with boreholes of this diameter, but their application is limited to water sampling and water level monitoring. Wider diameter boreholes would be required for installation of electrical submersible pumps (minimum 100 mm ID), capable of undertaking

test pumping to prove suitability of workings for mine water geothermal application. Falling head tests would be feasible in narrower diameter boreholes, but would provide less accurate transmissivity data for the responsive horizon. Similarly, the restricted borehole diameter may only accommodate slimline geophysical probes or CCTV surveys, limiting the additional borehole characterisation.

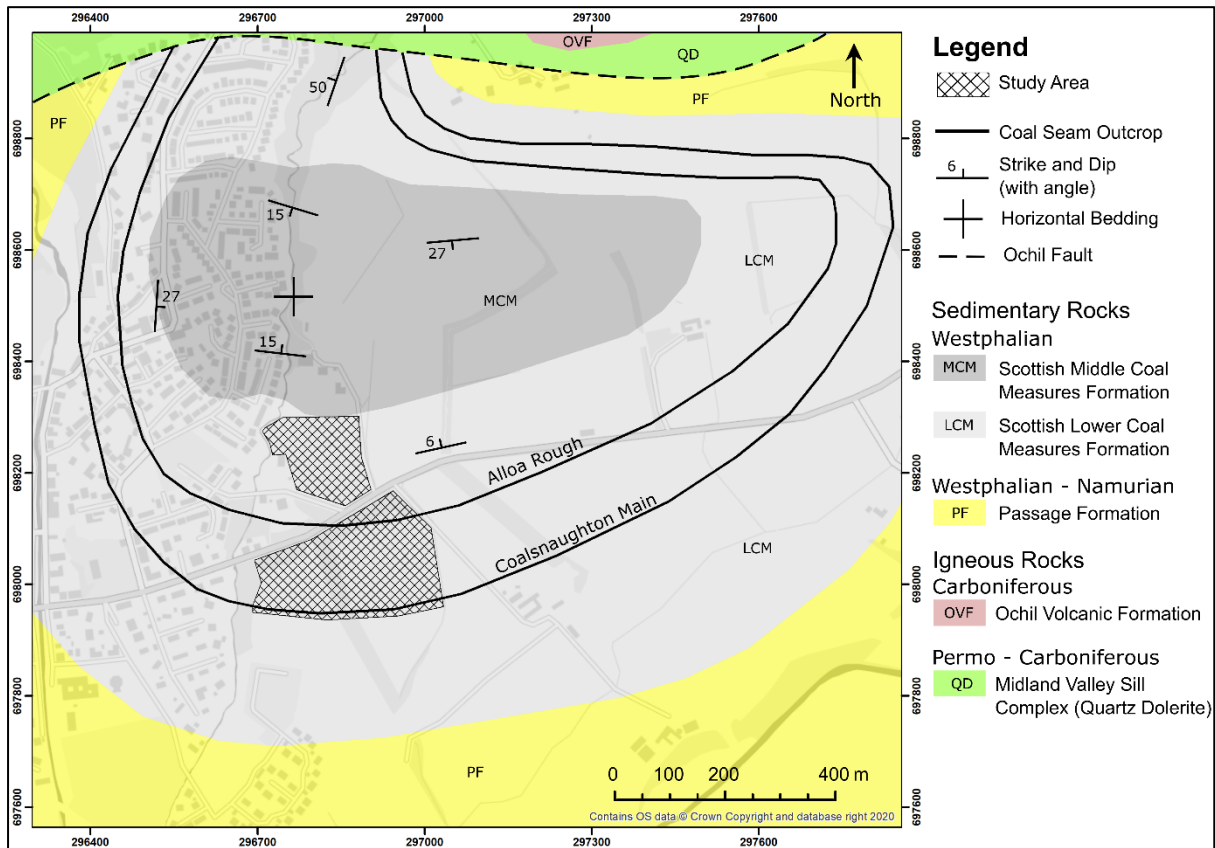


Figure 5.1 Simplified geological map of the eastern extent of Dollar, Clackmannanshire. Geological information derived from British Geological Survey (Armstrong *et al.*, 1974a). Contains OS data © Crown copyright and database rights 2022.

5.1.4 Geological setting

The study area on the outskirts of Dollar, Clackmannanshire, lies above coal seams from the Scottish Lower Coal Measures (LCMS) formation of the Westphalian Age (Figure 5.1). The coal seams of this study are part of a syntectonic synclinal structure with dip (in the study area) of up to c. 13° to the north (Armstrong *et al.*, 1974a). The sequence of major coal seams found at the site are detailed in Table 5.1. During deposition in the Carboniferous Period, development of the sedimentary basin was controlled by normal movement on the east-west trending Ochil fault immediately to the north of the syncline (Rippon *et al.*, 1996). Superficial deposits are 2.5 m to 10 m thick, present as horizons of glacial till and glacio-fluvial sands and gravels. In some portions of the study area, the sands and gravels are absent (Armstrong *et al.*, 1974b).

Scottish Lower Coal Measures' seam	Status	Working method	Elevation from BH04 (m OD)
Coal Mosie / McNeish Coal Seam	Unworked	N/A	53.7
Alloa Rough/Cherry	Worked across the site, extent unrecorded	Pillar and Stall	44
Alloa Splint	Extensively worked, older areas recorded in poor detail	Mostly pillar and stall. Small portion of longwall from Dollar drifts 1-3	40.5
Wallsend	A short distance above (and mostly grouped with) the Coalsnaughton Main	Panels of longwall working, likely grouped with Coalsnaughton elsewhere.	Grouped with Coalsnaughton
Coalsnaughton Main	Extensively worked, details accurately recorded in most areas.	Panels of longwall workings. Areas of old workings are likely pillar and stall	12.2

Table 5.1 Details of coal seams present beneath the site. Depths as read from BH04, converted to metres above Ordnance Datum (m OD = effectively m above sea level).

5.1.5 Mining history

Within the area of the coal-bearing syncline, some workings have detailed accounts of coal extraction (Coalsnaughton and Wallsend Seams mined in the 1940s and 50s (National Coal Board, 1954, 1955)), some merely record the outline of old workings without internal detail (Alloa Splint and old portions of Coalsnaughton (Bald, 1838)), and some workings are entirely unrecorded on mine plans (Alloa Rough). Workings of these seams date back many centuries, with the earliest record of mining in Clackmannanshire from the Church Legate Aeneas Silvus, who later became Pope Pius II, during the reign of James I. On a visit to the area at the beginning of the 15th century he reported seeing “poor people begging in rags at Church doors given pieces of black stone, with which they went away happy” (Dollar Museum, 2014).

Initially, working was via a number of vertical shafts on and around the site, many of which were connected to a horizontal drainage adit (the Day Level) running subparallel to the Kelly Burn, shown in plan view in Figure 5.2 and cross-sectional view in Figure 5.3. The Day Level was driven into the hillside for mine water drainage, to allow dry working conditions for miners (Younger and Adams, 1999). Many of these early mines are to the west of the site and have little detail recorded except for the outer extent and locations of at least eight shafts, with more elsewhere in the coal-bearing syncline (National Coal Board, 1955). To facilitate additional mining, developments first saw completion of a water wheel engine to drain the mines via a deeper pit and allow access to workings as deep as 28 m below ground level. Later,

the Day Level was extended to reach a new steam engine in a pit at Kelly Bank whereby water was raised from a working level of 36 m depth (Dollar Museum, 2014). These developments were prior to a legal dispute in 1840, which saw the cessation of mining in Dollar until re-opening in 1943 (Dollar Museum, 2014).

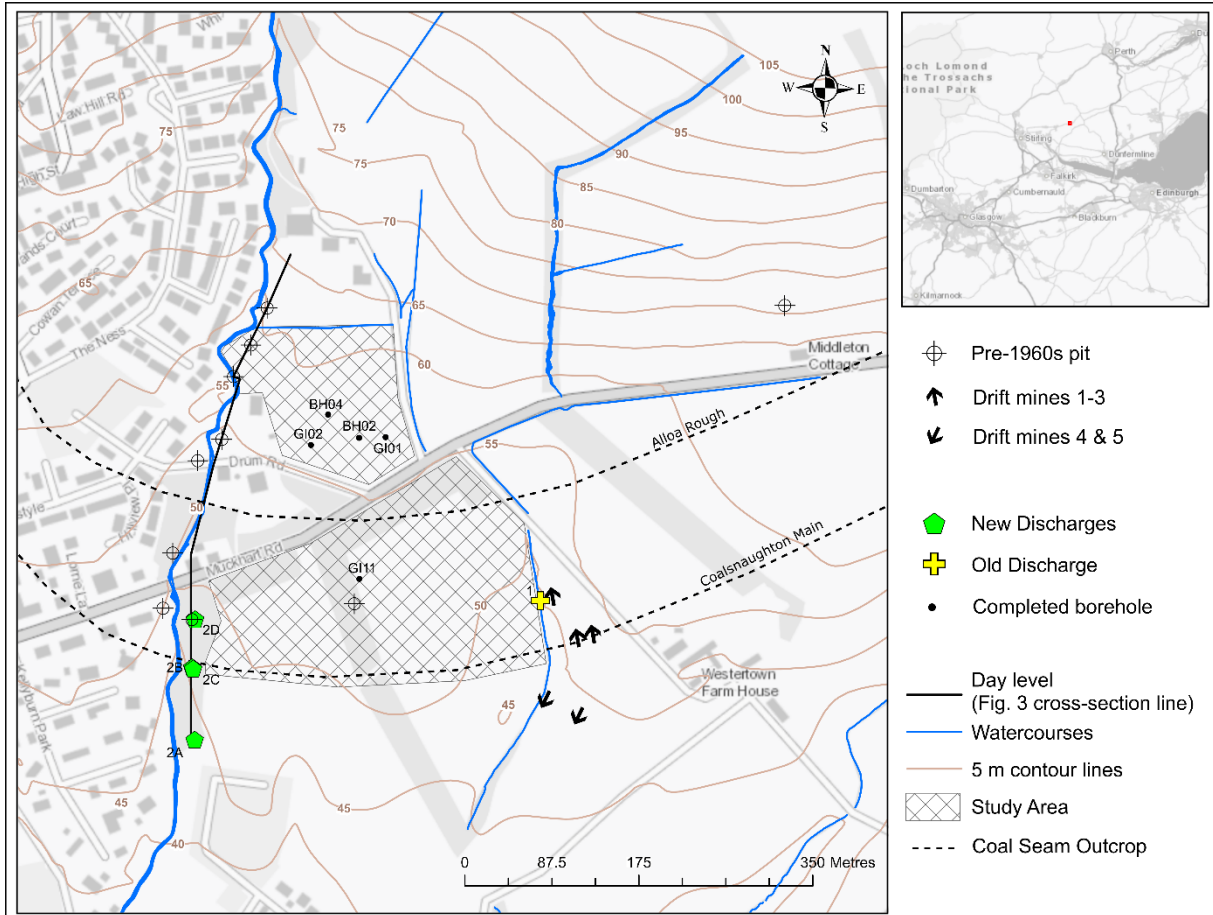


Figure 5.2 Topographic and hydrological map of the study area and surroundings with notable locations pertaining to the coal seams shown. Numbers correlate with discharge sample names. Arrows indicate orientation of drift mines from Dollar Colliery. Pit names can be seen in Fig. 5.4. Contains OS data © Crown copyright and database rights 2022.

Much of the total area of worked coal in the syncline was from the Dollar Colliery at West Pitgober [56.1632°N, 3.6587°W], which produced via three drift mines (Dollar 1, 2 and 3). These were mine roadways which were driven northwards towards the Ochil Hills following the Coalsnaughton Main Coal Seam at c. 13° from horizontal from 1943 as a response to the increase coal demand during World War II (Dollar Museum, 2014). Most of the coal extraction by Dollar Colliery was from the Coalsnaughton Main Seam but active workings in the Wallsend and Alloa Rough Seams were also accessed from the same drift mines. Three years after the operations from these drifts stopped in 1953, Dollar Colliery opened a new, separate, coal prospect between 1956 and 1960, with the driving of two new drifts (Dollar 4 and 5) south-

southwestwards into stratigraphically lower and hydraulically separate seams. These southern drift mines remained active until 1973 (Dollar Museum, 2014).

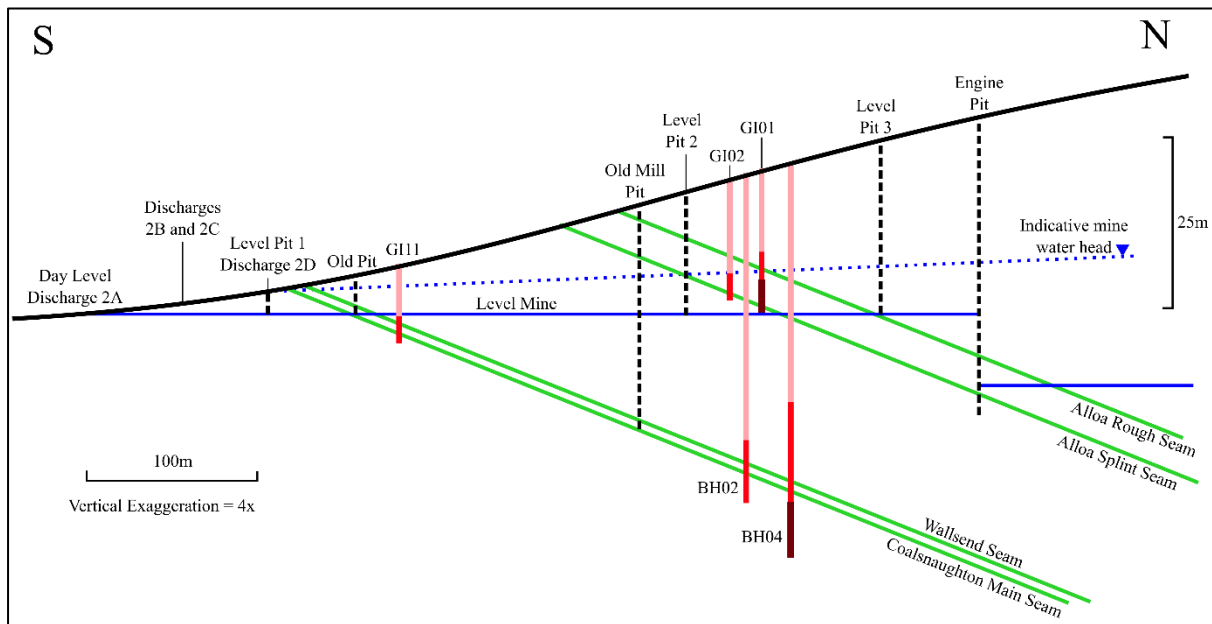


Figure 5.3 Schematic cross section through the coal seams with pit locations, along the line of the Day Level (shown in Figure 5.2) in the western part of the study area. The five completed boreholes have been projected onto the cross section from their locations 100 m to 150 m along strike, to the east. Pink reflects plain screen liner and red reflects slotted screen liner. Vertical brown sections at the base of GI01 and BH04 depict where each borehole was backfilled before completion with liner.

5.1.6 Hydrogeological setting

The Kelly Burn is the principal watercourse adjacent to the study area, defining its western boundary. It flows from the north as one of many streams which drain water from the Ochil Hills into the River Devon, south of the study area. The Kelly Burn was the recipient watercourse for the water discharged from the Day Level during mining operations. A small, perennial, un-named burn defines the eastern extent of the study area, similarly flowing southwards into the River Devon. It was the recipient of Discharge 1, detailed below.

Despite the Dollar Colliery expanding southwards into a deeper coal prospect via Dollar Drifts 4 and 5, the northern workings (accessed via Dollar 1-3 and the Day Level) in the local syncline remain hydrogeologically separate. This is demonstrated by mine water discharges at the southern margin (lowest elevation) of the northern workings, and the absence of worked coal seams spanning the separating anticline. Whilst the early Day Level was designed to be the lowest elevation access point to the surface for mine water drainage, there remain other locations across the site which connect the workings to the surface and present potential flow pathways for discharging mine water.

Interpretation of mine abandonment plans, and other historical data available in the Dollar Museum, suggested that the Day Level has the potential to drain water from all existing mine workings beneath the site and is the potential overflow point with the lowest elevation. However, upon investigation, no open mine entry at the site of the Dollar Level was found, despite its position being identified. On multiple site visits, and after a small pit was dug prior to drilling, no significant mine water flow was identified from the Day Level. Any water which pooled there was indicative of fresh meteoric water (i.e. not mine water). We therefore hypothesise that the Day Level flow ceased following mine closure, likely due to a subsurface blockage, most likely due to, e.g., obstruction of flow paths by collapsed strata or waste debris, or accumulations of iron (oxy)hydroxide “ochre” or swollen clays from mudstone.

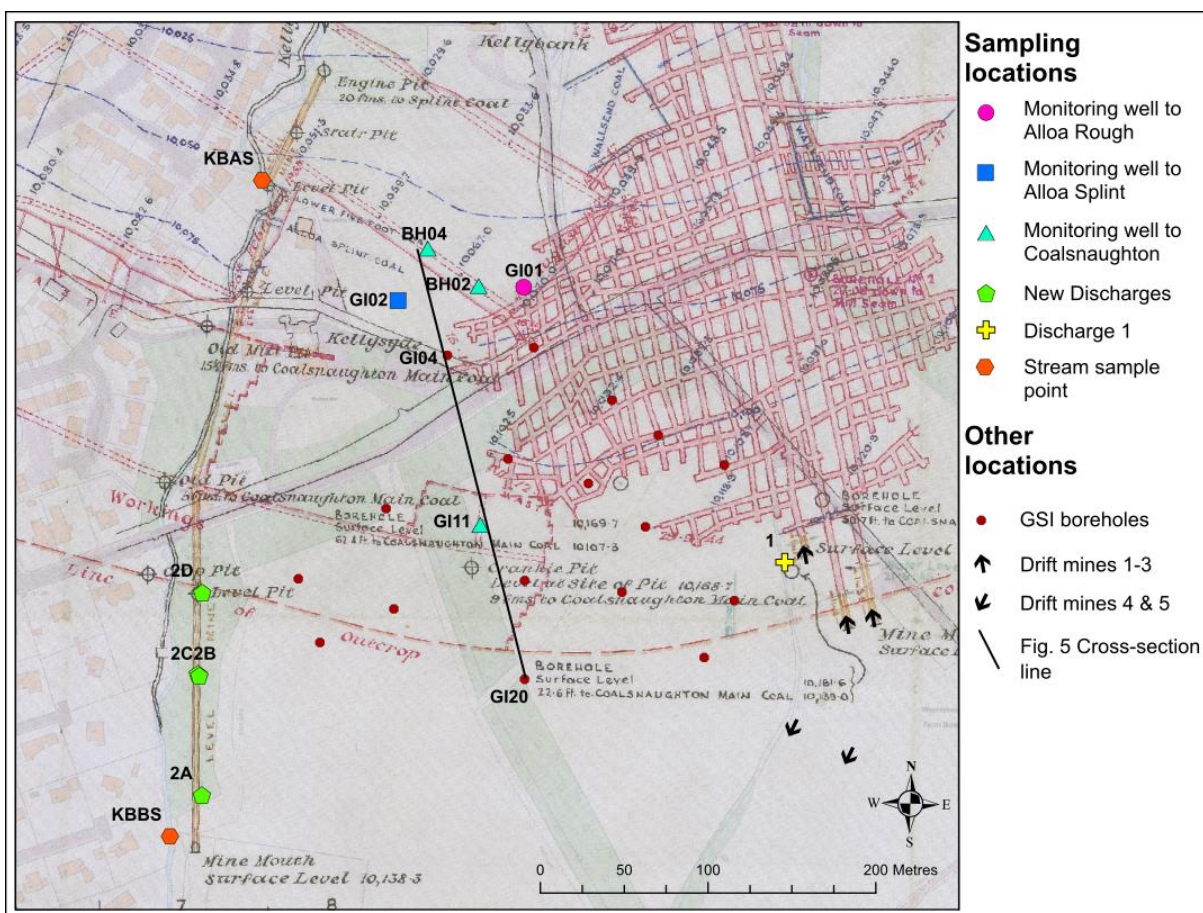


Figure 5.4 Borehole and sampling locations overlain on the mine abandonment plan for the Coalsnaughton Main Seam (National Coal Board, 1955), where red outlines extent and details of workings. Numbers correlate with discharge sample names. KBAS, Kelly Burn above site; KBBS, Kelly Burn below site. Arrows indicate orientation of drift mines from Dollar Colliery. Mine Plan as base map: Copyright Coal Authority. All rights reserved 2022.

An existing ochreous discharge (Discharge 1) was identified in November 2020 on the eastern side of the site [56.163739°N, 3.659694°W], located close to the Dollar No. 2 drift mine (National Coal Board, 1955), and the National Coal Board’s Dollar Mine No.1 bore (most

likely an exploratory borehole dating from 1953; Figure 5.4 depicts it encountering intact Coalsnaughton Main coal at 22.6 ft (6.9 m) below surface level). The flow from Discharge 1 was reported to be related to a collapse of land near the backfilled Drift 1, 2 and 3 entrances, most likely between 1960 and 1973 (and when Dollar No. 4 and 5 drifts were operating). Tim MacInness recalls that:

“When the shafts [drifts] 1, 2 and 3 were closed at the Dollar mine, the shaft entrance was filled in. When the shafts 4 and 5 were opened a car park was made, where the entrance to the old mine shafts 1, 2 and 3 had been. Unfortunately, insufficient filling material had been put over the old entrance. One day, when the men had finished their shift, and went to collect their cars, they found that the ground covering the car park had collapsed, taking several cars into the abyss” (Dollar Museum, 2014).

According to Harry Chalmers, former miner, interviewed in 2006 by Val Toon:

“A field collapsed, right, a big hole, just caved in.... they drive lorry loads of rubble and tip it in into the hole to fill it in...It’s still there and the overflow from the mine is down in the field” (Dollar Museum, 2014).

5.2 Methods

5.2.1 Desk Study

The study area was derived from an existing project between TownRock Energy and Harviestoun Home Farm (Figure 5.1, 5.2), where there are existing plans to develop housing. Scrutiny of available mine abandonment plans and local museum archives informed understanding of operation dates and extent of the mine workings. Georeferencing of mine plans on GIS software allowed identification of drilling locations to satisfy surface restrictions and subsurface drilling targets. The project team obtained a permit “to enter or disturb Coal Authority mining interests” to access coal seams with up to 24 boreholes using air-mist flush drilling.

5.2.2 Ground investigation

Compressed air and water mist were used to flush drill cuttings to the surface, whilst providing lubrication and temperature regulation at the interface between the drill bit and the bedrock. This method was selected in preference to water flush drilling since there were not easily accessible, reliable water supplies on site. Since none of the boreholes were to be cored,

interpretation of subsurface conditions relied on drilling penetration rates, water strikes, and cuttings returned to the surface with the air-mist flush.

All drilling was completed using a 23 ton (20.9 tonne) top driven rotary drill rig suited to open hole or coring applications, primarily for mineral exploration, water well drilling, geothermal and civil engineering applications. Drilling used a selection of three drill bits, depending on purpose:

- 6" (152mm) tricone rock roller – used to progress through superficial deposits to create a large enough diameter hole for 6" temporary steel casing to be emplaced, and for the 5 5/8" tricone bit to be subsequently deployed in bedrock.
- 5 5/8" (140mm) tricone rock roller – used for drilling in bedrock in boreholes to be completed with 75mm diameter polyethylene liners.
- 5" (127mm) downhole hammer – used for fast progression through bedrock in all ground investigation boreholes. 5" ID steel casing was used in the respective superficial deposits. Since these were smaller diameter boreholes, only 50 mm internal diameter (ID) polyethylene liners could be installed to complete the borehole as a monitoring piezometer, if required.

Stratigraphic logging of cuttings was performed to describe the depths and state of the coal seams beneath the site as accurately as the drilling methodology permitted. Beyond a hydraulically responsive coal seam, the water which was returned to surface along with the rock chips was used to aid borehole logging. For example, clear and colourless returning water indicated quartz rich horizons (sandstone); brown/pale grey cloudy water indicated mudstones or siltstones; and black/dark grey water with oily films indicated coal seams or very organic rich units (shale). Alongside water and rock interpretation, the following were recorded: the penetration rate of the drill bit; any episodes of fast drilling or "drops"; odour (e.g. of hydrogen sulphide gas). A gas monitor was used by the drilling contractor to monitor at the borehole head for mine gases including methane, carbon dioxide, hydrogen sulphide and total oxygen concentration. The geologist's observations were subsequently integrated with the drillers' factual daily logs to produce integrated borehole logs showing construction and geology.

5.2.3 Monitoring well completion

Five boreholes were completed as monitoring wells (Figure 5.4). Detailed completion diagrams can be found in Appendix 5E.

- BH02 [NS 96847 98188] and BH04 [NS 96815 98211] were completed with slotted screens into the areas of longwall panels in Coalsnaughton Main and Wallsend Seams. The boreholes are presumed to access compacted longwall mining waste (goaf).
- GI02 [NS 96798 98181] was completed with a slotted screen in the stall of presumed pillar and stall workings of the Alloa Splint Seam.
- GI11 [NS 96845 98047] was completed with a slotted screen into a void in the “old workings” of the Coalsnaughton Main and Wallsend Seams; this is understood to be a stall of pillar and stall workings.
- GI01 [NS 96873 98189] was drilled through the Alloa Rough to the Alloa Splint. The lowermost portion of the hole was backfilled, sealed and the well was completed with a slotted screen in the stall of presumed pillar and stall workings of the Alloa Rough Seam.

Since a sustainable mine water geothermal system depends upon long and/or diffuse flow pathways between loci of abstraction and reinjection (Walls *et al.*, 2021), it is poor practice to create potentially “short-circuiting” flow pathways between seams, thus efforts were made onsite to seal potential hydraulic short circuit connections between horizons. Hydraulic connections between superficial and bedrock aquifers were also avoided since connection of these hydraulically separate aquifer units could lead to pollution of superficial aquifers with contaminated mine drainage. Similarly, introduction of oxidising, lower temperature superficial groundwater to coal mine aquifers, can contribute to oxidation and precipitation of iron as iron (oxy)hydroxides and a lowering of the mine water temperature. Boreholes intersecting multiple responsive coal seams were sealed using a combination of packers, shale traps, bentonite, and cement-based grout. This is a time- and material-consuming exercise, suggesting that the simplest future strategy for mine water wells might be to target only one coal seam with each borehole; thus, if targeting a deeper seam, it is beneficial to find a location where the upper seam(s) is unworked.

The borehole liners comprised 3 m lengths of polyethylene (75 mm ID in BH02, BH04 and GI02; 50 mm ID in GI01 and GI11); slotted screens of the same material with 5 mm slots were selected to span the responsive horizon of each borehole. For voids in worked coal seams, a 3 m slotted length was adequate, whereas evidence for fracture networks above the mined horizons in BH02 and BH04 meant 6 m and 9 m of slotted screens, respectively, were selected. Over each of the slotted screen lengths, a “geosock” was secured, providing a membrane which

limits the size of particles which can flow into the borehole liner, whilst allowing inflow of water. In GI01, there was some degree of borehole wall collapse between withdrawal of the drill bit and the installation of the casing string. This prevented the installation of the liner to the full depth of the borehole.

5.2.4 Borehole monitoring of mine water

The mine water head in each completed monitoring well was logged at 10–15-minute intervals across a 15-month period using Schlumberger “CTD-Diver ®” submersible sensors with electrical conductivity, water level (collected as pressure data) and temperature sensors. A Schlumberger “Baro-Diver ®” barometer was deployed in the surface headworks of GI01 to record atmospheric pressure and temperature, and to allow groundwater pressures to be barometrically compensated and converted to groundwater head. The water levels were calibrated using manual Solinst ® TLC meter “dip-meter” measurements each month. The dip-meter was also used to generate vertical profiles of the water column in each borehole by taking monthly readings of electrical conductivity and temperature at intervals of 2-5 m between the mine water head and the base of the borehole. The results are shared in Appendix 5D.

5.2.5 Discharge estimation

Standard flow rate techniques could not be employed since this study did not have access to a flowmeter or material to construct weirs, and the diffuse nature of the discharges did not suit collection with a bucket and stopwatch. As an alternative, indicative flow rates from mine water discharges were estimated using measurements of each channel’s dimensions. The flow rate Q (cm^3/s) is estimated from Equation 5.1, where depth and width are in cm, and V is velocity, measured in cm/s. The correction factor of 0.5 is applied to account for the irregular flow cross section and slower flow at the channel edges.

$$Q = \text{Depth} \times \text{Width} \times V \times 0.5 \quad (5.1)$$

The width of the flow channel at the surface (cm) and the depth of the flow channel (cm) were measured with a ruler. The flow speed of the channel (cm/s) was measured by dropping a buoyant item into the flow and measuring distance covered in 1 second. Flow rates in cm^3/s were then multiplied by 0.001, to obtain a value in L/s.

5.2.6 Water sampling

Water samples were collected from the drilling return fluid as flooded mine voids were encountered during the drilling period (18th November 2020 to 4th December 2020 – samples 03-01 to 03-10). Following drilling, monthly sampling was conducted between the 16th of January 2021 and the 17th of December 2021 (samples 03-11 to 03-133) at the following locations (Figure 5.4):

- the five monitoring wells: BH02, BH04, GI01, GI02 and GI11;
- five locations of surface mine water discharge, designated Discharges 1 and 2A to 2D;
- two samples of streamflow from the Kelly Burn, from above and below the study area.

During monthly sampling, boreholes were sampled using a Waterra Inertial Pump, consisting of a high-density polyethylene (HDPE) 25 mm outer diameter pipe with a VS5 stainless steel internal foot valve, inserted to the depth of the monitored mine water horizon. The borehole was purged for at least five minutes prior to collection of the water sample at an estimated flow rate of 15 L/min (Waterra, 2022), indicating that c. 75 litres of water was purged before sampling.

Field determinations of pH, temperature, oxidation-reduction potential (ORP) and electrical conductivity (EC) were determined using a handheld Myron P Ultrameter. This meter automatically corrects values of pH and EC to a standard temperature of 25 °C. ORP values were measured in millivolts (mV) and read from a platinum sensor and a silver chloride (Ag/AgCl)-saturated KCl reference electrode. ORP readings are 199 mV lower than true Eh - the standardised measure for oxidation reduction potential derived from a standard hydrogen electrode (Robinson pers. comm., 2022) - but are presented here without adjustment. In the field, total alkalinity was determined as mg/L equivalent of CaCO₃ with a Hach Model 16900 digital titrator, using 1.6 N sulphuric acid and bromcresol green - methyl red pH indicator. Recorded values in mg/L CaCO₃ were then converted to meq/L (by dividing by 50.04 mg meq⁻¹). The alkalinity is assumed to be predominantly in the form of HCO₃⁻ at circumneutral pH values. Where required, equipment was calibrated before each day's fieldwork and all water samples were refrigerated as soon as possible after collection.

As regards samples of surface discharges and streams, samples were taken directly from as close to the discharges' source as safely possible, and from the centre of the Kelly Burn.

Separate aliquots were taken for different analyses, as detailed below. Filtration, to remove any particulate matter, was carried out using a hand-held, syringe mounted filter capsule.

1. An aliquot for major anion analysis was filtered at 0.45 μm into clean 15 mL polypropylene screw-cap vials.
2. An aliquot for dissolved elemental content was filtered at 0.45 μm into clean 15 mL polypropylene screw cap vials and preserved using one drop of concentrated HNO_3 (68%, trace metal grade, Fisher Chemicals).
3. An unfiltered aliquot for total (dissolved and undissolved) elements was collected using clean 15 mL polypropylene screw cap vials and preserved using one drop of concentrated HNO_3 (68%, trace metal grade, Fisher Chemicals).
4. An aliquot for $\delta^{18}\text{O}$ and $\delta^2\text{H}$ analysis was taken using clean 15 mL polypropylene screw-cap vials, sealed with Parafilm to prevent sample evaporation.
5. A 1 L unfiltered aliquot of sample water was collected in a plastic flask for sulphate- $\delta^{34}\text{S}$ analysis. Sulphate was subsequently precipitated as barium sulphate, using the method of Carmody *et al.* (1998): namely, the sample was acidified to pH 3–4 by dropwise addition of concentrated HCl and then dosed with excess 5% BaCl_2 solution. A rapid cloudy reaction indicated the presence of sulphate via the precipitation of BaSO_4 crystals.

5.2.7 Rock chip collection

Upon delivery of rock chips to the surface via the drilling flush, organic-rich (shales and dark brown/black mudstones) and coal horizons were selected for sulphur bearing mineral collection. The rock chips were washed using de-ionised water and sulphide bearing minerals were extracted using a scalpel or mineral drill. Only one sample of coal (CM1), from the Coalsnaughton Main Seam hosted enough collectable pyrite for analysis.

5.2.8 Chemical and isotopic analysis

5.2.8.1 Chemical analysis

Ion chromatography (IC) was used for determination of five anions (F^- , Cl^- , SO_4^{2-} , Br^- , NO_3^-) in the laboratories of the Department of Civil and Environmental Engineering (CEE), University of Strathclyde. An 850 Professional IC by Metrohm ion chromatograph was used. The separation utilised a Metrosep A Supp 5 anion analytical with Guard column (Metrosep A

Supp 5 Guard/4.0) at 24 °C with eluent comprising of 1 mM NaHCO₃ and 3.2 mM Na₂CO₃ prepared in ultra-pure de-ionised water. The flow rate was 0.7 mL/min. Calibration standards were 0.1, 0.5, 1, 5 and 10 mg/L prepared in ultra-pure water. The IC method was developed according to British Standards Institution (2009) and Metrohm customer support recommendations.

Determination of 12 dissolved and total elements (B, Ba, Ca, Fe, K, Mg, Mn, Na, S, Si, Sr, Zn) used an Inductively Coupled Plasma Optical Emission Spectrometer (ICP-OES) iCAP 6200 Duo View ICP Spectrometer, Thermo Fisher Scientific model equipped with an autosampler (Teledyne CETAC Technologies, ASX-520) and Thermo i-TEVA Version 2.4.0.81, 2010. The operating conditions are presented in the supporting material of Walls *et al.* (2022) (Appendix 3C).

For determination of total *Aqua Regia*-digestible elemental content of the water samples, they were acid digested using a Microwave Accelerated Reaction System (MARS-6, CEM). 10 mL of thoroughly mixed, unfiltered sample was transferred into MARS Xpress Plus 110 mL Perfluoroalkoxy alkane (PFA) microwave digestion vessels. Samples were digested with reversed “*Aqua Regia*” mixture of hydrochloric and nitric acids (1:4, HCL - 37 %, and HNO₃ - 68 %, Trace Metal Grade, Fisher Chemicals). Following the microwave operating parameters: operating power 800-1200-1800 W; ramp for 20 mins up to 170 °C; hold time 20 mins at 170 °C. Sample digests were brought up to 50 mL with ultrapure water using volumetric flasks, then filtered through 0.45 µm for ICP-OES analyses.

Multi-element 3-point calibration standards were prepared from 1000 mg/L element stock standard solutions (Fisher Scientific) using 18.2 MΩ/cm ultrapure water (Triple Red water purification system). 68% trace metal analysis grade nitric acid (Fisher Chemicals) was added to reach a 5% final acid concentration in the standard solutions for dissolved content analyses, similarly, reversed aqua regia was added to reach 20% in the standard solutions for total aqua regia-digestible elemental content analyses. Yttrium (5 mg/L) was used as internal standard (IS) solution (Fisher Chemicals), to account for any matrix effects due to differences between samples and standards. The IS was added through automated online addition with an internal standard mixing kit. A brief method validation study found the following linear ranges: 0.01 to 1 mg/L for barium and strontium, 0.5 to 50 mg/L for calcium, magnesium, potassium, sodium, iron and sulphur and 0.1 to 10 mg/L for boron, manganese, silica and zinc. Analyses proceeded when calibration curves generated correlation coefficients (R^2) >0.9980. Instrument equilibration and system's suitability were checked according to Civil and Environmental Engineering (CEE) labs Standard Operating Procedure for ICP-OES and Quality Control and

Assurance procedure. CEE methods of analyses were mainly based on British Standards Institution (2018). Elemental method quantification limits were based on instrument-predicted method quantification limit values (Walls *et al.* (2022) Appendix 3C), obtained from the calibration parameters for each element.

5.2.8.2 Isotopes

For $\delta^{18}\text{O}$ analysis, each sample was over-gassed with a 1% CO_2 -in-He mixture for 5 minutes and left to equilibrate for a further 24 hours. A sample volume of 2 mL was then analysed using standard techniques on a Thermo Scientific Delta V mass spectrometer set at 25 °C. Final $\delta^{18}\text{O}$ values were produced using the method established by Nelson (2000). For $\delta^2\text{H}$ analysis, sample and standard waters were injected directly into a chromium furnace at 800 °C (Donnelly *et al.*, 2001), with the evolved H_2 gas analysed on-line via a VG Optima mass spectrometer. Final values for $\delta^{18}\text{O}$ and $\delta^2\text{H}$ are reported as per mille (‰) variations versus Standard Mean Ocean Water (V-SMOW) in standard delta notation. In-run repeat analyses of water standards (international standards V-SMOW and Greenland Ice Sheet Precipitation (GISP), and internal standard Lt Std) gave a reproducibility better than $\pm 0.3\%$ for $\delta^{18}\text{O}$, $\pm 3\%$ for $\delta^2\text{H}$. For sulphate- $\delta^{34}\text{S}$ isotope analysis, the barium sulphate precipitate was recovered from the sampling vessel, washed repeatedly in deionised water and dried. SO_2 gas was liberated from each sample by combustion at 1120 °C with excess Cu_2O and silica, using the technique of Coleman and Moore (1978), before measurement on a VG Isotech SIRA II mass spectrometer. The single pyrite (CM1) analysis was similarly run, following the technique of Robinson and Kusakabe (1975). Results are reported as per mille (‰) variations from the Vienna Canyon Diablo Troilite (V-CDT) standard in standard delta notation. Reproducibility of the technique based on repeat analyses of the NBS-127 sulphate standard was better than $\pm 0.3\%$, and was $\pm 0.2\%$ for internal chalcopyrite standard CP1, run in conjunction.

5.2.8.3 Quality Assurance

Since sulphate (SO_4^{2-}) was run via IC, and sulphur elemental analysis was run via ICP-OES, correlation between the two for sulphate (meq/L) is possible (on the assumption that all sulphur is present as sulphate). These showed a strong correlation, but the ICP derived sulphate values were selected for use in IBE and presentation. The ion balance errors (IBE) were determined for a total of 127 water samples based on anion analysis of F^- , Cl^- , Br^- , NO_3^- , plus field-determined alkalinity and ICP derived sulphate (SO_4^{2-}); and ICP-OES analysis of

dissolved concentrations of Ca, Fe, K, Mg, Mn, and Na. Of these, 73 returned IBE's within $\pm 5\%$, 36 within $\pm 10\%$, 15 within $\pm 15\%$, and 3 outliers beyond $\pm 15\%$.

“Field blanks” were collected in parallel to discharge samples; ultrapure deionised water was carried into the field and analysed subject to the same collection and processing methods as the discharge samples, e.g., filtration, acidification, digestion. This was done to monitor for any contamination of samples during collection. Laboratory blanks were created from ultrapure deionised water and duplicates of some mine water samples were collected (Appendices 5A and 5B), these were subject to the same laboratory processes as other samples to check for contamination and reproducibility. The blanks and duplicates returned acceptable values which concluded there was minimal interference from field sampling or laboratory equipment.

5.3 Results and Discussion

5.3.1 Borehole Locations

The GSI boreholes were positioned by mining engineers, irrespective of areas with anticipated voids or intact coal. Their distribution was even across the site, as far south as the Coalsnaughton Seam's projected subcrop. Figure 5.4 shows the GSI borehole locations above the mine abandonment plan for the Coalsnaughton Seam. Four borehole locations were initially chosen by the authors as locations for MWGI boreholes, constrained by the footprint of the projected housing development since. Therefore, if they were successful, they could have been upgraded to full-scale production or injection boreholes. They were sited to have the greatest chance of connecting to open workings in the deepest seam, the Coalsnaughton. For example, BH02 was sited directly above the SE-NW longwall access roadway in the Coalsnaughton Seam, which may have remained open. BH04 was also projected to intersect the longwall access roadway in the Coalsnaughton, but it also penetrated the worked area of the Wallsend Seam above it. BH02 and BH04 were both above the highlighted area for “old workings” in the Splint/Rough Seams, and therefore, it was unclear whether they would intersect intact coal pillars, voids, or collapsed workings.

5.3.2 Drilling

Of the 24 boreholes outlined, 18 were drilled during November and December 2020. Five of these were completed as monitoring wells into coal seams which had good evidence for responsive mine water horizons (GI01, GI02, GI11, BH02 and BH04), 13 were drilled as

standard GSI boreholes and subsequently backfilled, and the remaining six were not drilled. Of these six, MWGI boreholes BH01 and BH03 were not required since their intended purpose of monitoring flooded coal seams was fulfilled by GI01, GI02, GI11, BH02 and BH04. The remaining GSI boreholes (GI05, GI06, GI07 and GI18) were not drilled, following events outlined in the “Changes in flow regime” section. The GSI boreholes were drilled as far as the first coal seam, which varied depending on location, whereas BH02 and BH04 were deepened to penetrate all coal seams.

The results and interpretations of the GSI study have been produced by professional mining engineers and their comments on building limitations or ground remediation works have been included in a non-public domain document and thus will not be discussed here. There are areas denoted as stable, thus the housing development can progress with mine water geothermal heating as a potential option worthy of further consideration. A series of SSE-NNW trending boreholes (GI20, GI14, GI11, GI04, BH02, GI02 and BH04) generate a cross-sectional representation of the coal seams (Figure 5.5) along the line of section is shown in Figure 5.4. It reflects measured depths at which rockhead and coal seams were encountered, with interpretation added to show the state of workings. Detailed geologic units of sandstone, mudstone and minor coals between principal coal seams are not shown.

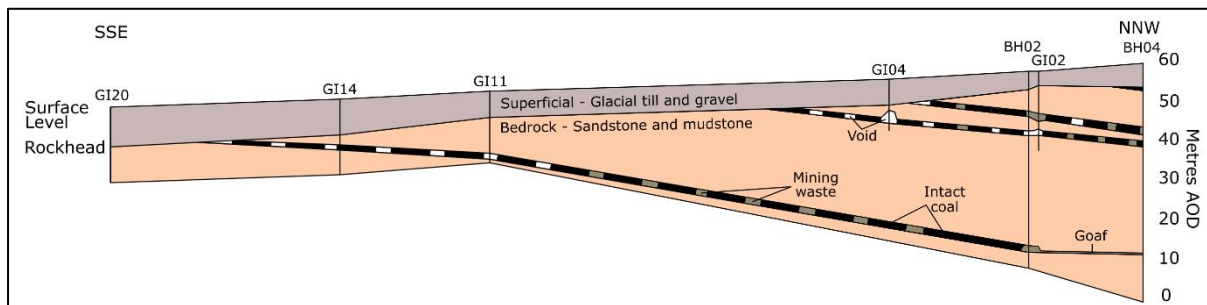


Figure 5.5 Cross sectional interpretation of borehole logs between the southernmost (GI20) and northernmost (BH04) boreholes along line of section shown on Fig. 5.4. No vertical exaggeration. AOD; above Ordnance Datum.

Upon reaching the depth at which the coal seams were present, drilling apparatus responded differently to varying conditions. The findings are detailed below.

5.3.2.1 Intact Coal

Where intact coal seams were encountered, drilling penetration rate showed no change. The air-mist flush returned rock chips (up to 5 mm) to the surface (the same size as had been returned from other lithologies). They remained dry, and a clear change from pale grey/brown (sandstone) chips to black vitreous (coal) chips was observed. Once the coal seam had been

passed, the rock chips reverted to pale grey reflecting a change in lithology. The intact coal seams are indicative of unworked regions or pillars in the pillar and stall workings.

5.3.2.2 Void

When entering a void, the drill bit lost all resistance from the bedrock and “dropped” the height of the void space in the workings. This response most likely reflects entering a “stall” of pillar and stall workings which had not been backfilled with waste material, however, voids can migrate upwards if roof strata fall to the base of the stall. The voids also produced mine water, flushed back to surface. In one case (GI02) the flush of air and mine water was lost altogether.

5.3.2.3 Mining Waste

Mining waste can be used to describe the material left behind in mine voids following mineral extraction. This can be adjacent horizons of sandstones or organic rich mudstones and shales which are deliberately packed into voids; or fallen debris from roof strata or supporting coal pillars. Mining waste may contain fragments of wood or metal. When encountering mining waste in a coal seam, the penetration rate of the drill bit was faster than the standard penetration rate. The air-mist drilling which had previously been returning dry or damp rock chips, began moving large volumes of water to the surface. Within the water there were clasts of rock, much larger than those made by drilling intact rock. The clasts of mudstone and shale, and sometimes coal, were as large as 100 mm. They often showed oxidised iron staining on their surfaces, indicating exposure to oxidising conditions.

5.3.2.4 Goaf

The term “goaf” can be used simply to refer to mining waste within void spaces. However, in this paper, it is used in a more specific sense, of the structure that results from the collapse of a mine working, either by pillar collapse, pillar robbing or longwall working with deliberate controlled collapse. Goaf can thus comprise a layer of compressed roof collapse strata, but sometimes (in the case of total extraction) a distinct horizon of collapse material can be difficult to identify. This may be the case, for example, where roof sandstone collapses “cleanly” onto pavement sandstone, as found at the Glasgow Geothermal Energy Research Field Site (GGERFS) (British Geological Survey, 2020). When drilling, no change in penetration rate necessarily occurs, and therefore, the goaf must be identified by other means,

e.g., the colour of the backwash of water, the presence of wood or oxidised rock fragments in the rock chip samples, or by down hole camera observations. Interpretation of goaf at the base of BH04 was based on field observations including: return fluids with a surface film of black oil and an organic matter smell; a tightly constrained prediction for depth from BH02; and evidence for open fractures above the seam location, including slight increases in drilling rate for up to 100 mm at a time and detection of H₂S gas at surface. The secondary permeability of the fracture network in the collapsed roof strata likely forms part of the productive response zones, and hence borehole screens were designed to include these regions.

5.3.3 Changes in flow regime

Discharge 1 was first visited on 19th November 2020, when it was found to have clear and colourless flowing water at approximately 7 L/s at 9.7 °C. It flowed out of an old pipe, nestled in the bank of the small stream. The cascading nature of the discharge meant that dissolved iron had been oxidised at surface and deposited orange ochre on the bank of the stream. A distinct smell of H₂S was present. A sample from the discharge was collected for chemical analysis and is discussed later.

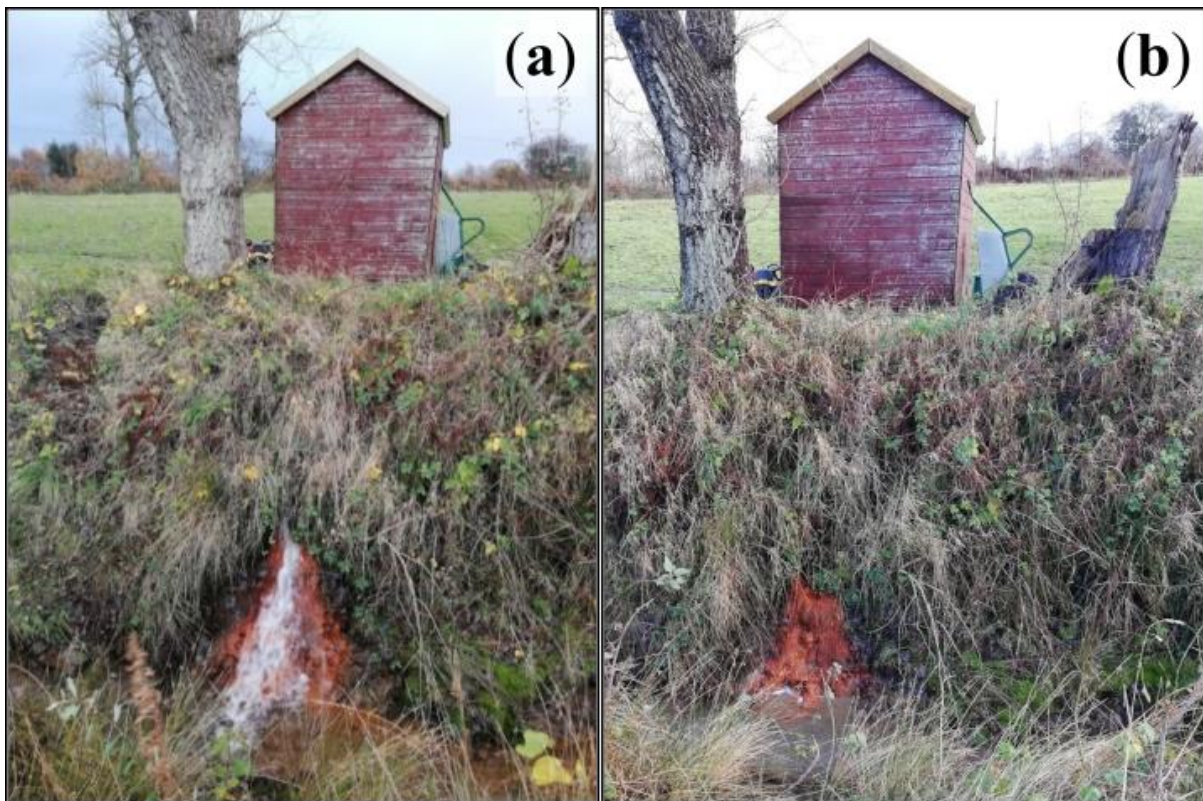


Figure 5.6 (a) Discharge 1 before (13/11/2020) and (b) after (05/12/2020) it ceased to flow.

During the latter stages of the drilling period in December 2020, Discharge 1 ceased to flow (Figure 5.6). At the same time, the Day Level outflow commenced flowing into the Kelly

Burn on the western extent of the site. Other discharges were identified at other locations further upstream along the course of the Day Level (e.g., possibly other historic shafts). The flooding and discharges can be seen in Figure 5.7. Following these observations on site, accounts of the activities and results were detailed and communicated to the Coal Authority adhering to the project completion guidelines. Similarly, the discharges were sampled and analysed for reporting to The Scottish Environmental Protection Agency (SEPA); these water chemistry results have been included in Appendices 5A and 5B.

The timing of the change is believed to be associated with drilling GI11, the first borehole to penetrate the old portion of the Coalsnaughton Main Seam. It seems that the act of drilling removed or cleared some form of underground flow obstruction, permitting the mine to recommence discharging to its original (lowest elevation) outflow point, the Day Level. The details of the subsurface barrier which was preventing flow at the Day Level remain unclear, and the permanence of the new flow regime is not known.



Figure 5.7(a) Day Level site prior to drilling period, digging to access fresh water (13/11/2020); (b) Day Level location following flooding and flow of mine water (Discharge 2A, 05/12/2020); and (c) the area north of the Discharge 2A upon first flooding, which since lowered to marshy ground and Discharges 2B and 2C (05/12/2020).

The recommenced outflow in the vicinity of the Day Level can be separated into 4 individual discharges, with their locations shown in Figure 5.2.

- At Discharge 2A, clear colourless water pools and flows into the Kelly Burn from the exit of the Day Level. It does not show any ochre precipitation along the channel bed but does have small numbers of iron flocs amongst the organic matter which can be seen when the channel base is disturbed. It flows at approximately 3-6 L/s depending on recent rainfall and seasonal changes.
- 75 metres further north from the day level there are two discharges (2B and 2C) which combine to flow into the Kelly Burn, distinguished as two separate discharges in March 2021. They were differentiated by several factors: the source location of each of the flows are approximately 5 m apart; the electrical conductivity is around 14 to 0 $\mu\text{S}/\text{cm}$ different; and finally, the channel beds of the discharges have significantly different ochre precipitation (Figure 5.8).
- There is a low flow (<1 L/s) from an old pond at the highest point of the woodland (Discharge 2D), just south of the road, which discharges through an artificial drain into the Kelly Burn.



Figure 5.8 Meeting of two discharges from 5 m apart. Discharge 2C (from the left) has a channel base with mostly organic matter, whilst discharge 2B (from top of image) coats the channel base in orange ochre. 30 cm ruler for scale.

The flow rates of all discharges were measured between November 2020 and March 2022 and are plotted in Figure 5.9 with supporting data in Appendix 5C; the figure captures the seasonal nature of the total discharging flow rate following a peak during at the end of

2020. Immediately following the change to the flow regime and the commencement of Discharges 2A-D they had a combined total flow rate of 27.6 L/s; much greater than the 7 L/s from Discharge 1. As mine water head lowered, Discharge 2D decreased to a negligible flow with rates far below 1 L/s, hence its omission after January 2021. The total flow rate from Discharges 2A-D decreased through the first half of the year and dropped below the original Discharge 1 flow rate in early June 2021. Following a minimum across July, August and September of 5.6 to 5.8 L/s, the combined flow rate from Discharges 2A-D rose and exceeded 7 L/s in November 2021 in response to seasonal recharge and reached 8.9 to 9.1 L/s between the end of November 2021 and March 2022. It is therefore suggested that the “draining down” of the mine system from the elevation of Discharge 1 to that of the Discharges 2A-D resulted in a temporary increase in the rate of mine water discharge. Following this, the total (2A-D) discharge flow rate restabilised to a range between 5.6 L/s in summer months and 9.1 L/s in winter, i.e. similar to the original flow rate of Discharge 1 (7.2 L/s).

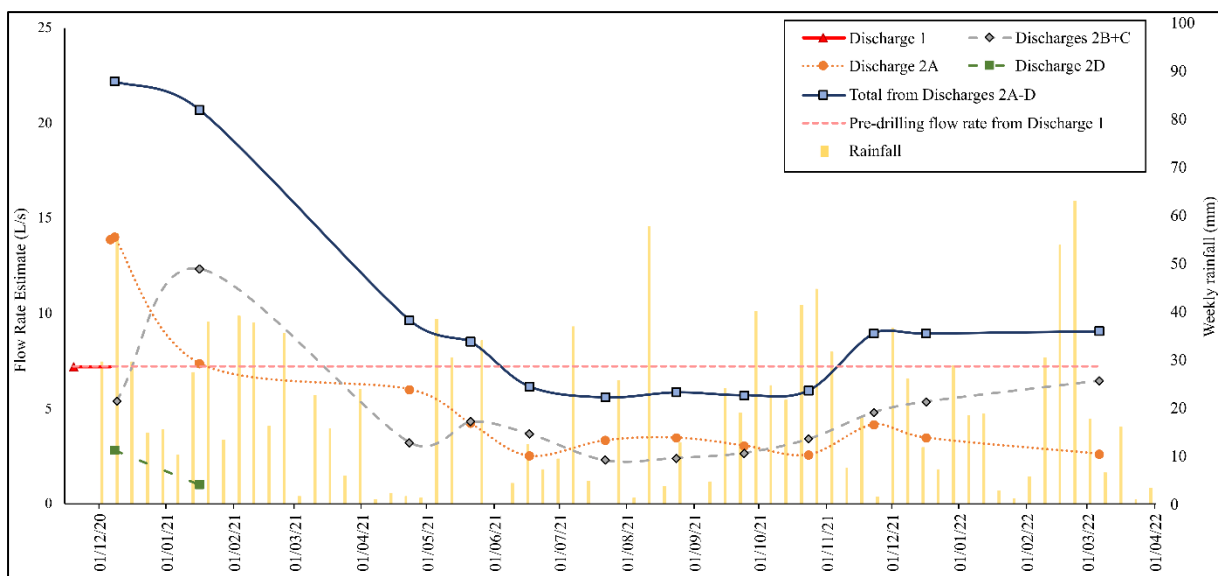


Figure 5.9 Total and component mine water discharge flow rates plotted against projected extrapolated flow rate from the ceased discharge (Discharge 1), and weekly rainfall data for Tillicoultry (Scottish Environment Protection Agency, 2022). Contains public sector information licensed under the Open Government Licence v3.0.

5.3.4 Borehole monitoring

Following drilling in November and December 2020, a declining mine water head was observed in the monitoring wells and corresponded with the maximum in total discharge flow rates discussed above, this is most likely a result of the draining down of the mine system from mine water head elevations controlled by Discharge 1 to the elevation of the original Day Level

(Discharge 2A) (Figure 5.10.). We discuss data from GI01 since it was one of the earliest boreholes to have mine water head data collected and shows the best correlation between the manual dips and the electronically logged data. Following the change in flow regime described above, all boreholes exhibited a sharp mine water head decrease between the 26th of November 2020 and the 16th of January 2021, in GI01 this was from 50.96 m OD to 47.36 m OD. Mine water head continued to fall throughout the spring and summer months to a minimum of 46.93 m OD on the 24th of September 2021. Throughout autumn and winter, mine water head increased with aquifer recharge to a maximum of 48.58 m OD at the end of February 2022 in response to major rainfall events and decreased evapotranspiration.

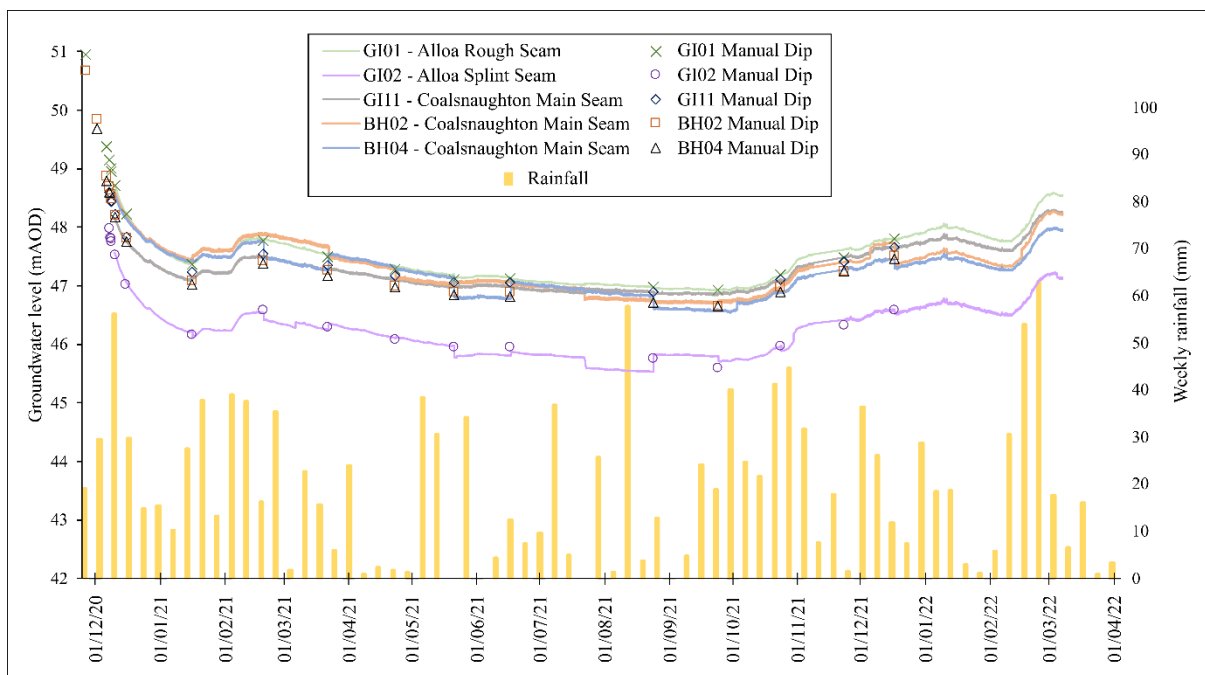


Figure 5.10 Manual dip and diver data for mine water levels, plotted against weekly rainfall data for Tillicoultry (Scottish Environment Protection Agency, 2022). Note that monthly sampling displaces the probes. Best efforts were made to ensure they were inserted at the same level as they were removed from, but discrepancies were due to adhesion between the probe string and the borehole liner. Contains public sector information licensed under the Open Government Licence v.0. Note that absolute elevation values are only accurate to c. 1 m OD as each wellhead elevation is derived from a digital elevation model.

The rate and magnitude of water level fall during initial de-watering (Figure 5.10) is greatest in GI01, where between midday on the 10th of December 2020 and midday on the 15th of January 2021 it falls 1.35 m from 48.73 m to 47.38 m OD, compared with 1.34 m in GI02, 1.03 m in GI11, 1.12 m in BH02 and 1.13 m in BH04. The approximately parallel hydraulic response of each seam reflects an overall hydraulic connectivity. Since the elevation of the boreholes was extracted from a digital elevation model (DEM), the absolute accuracy of the water level data cited above is poor (1 m accuracy), but the resolution (incremental change) of the loggers is excellent (1 mm). Thus, the head in GI02 appears to be c. 1 m lower than the

other boreholes, but this could merely reflect uncertainty in absolute elevations, or could equally reflect a lower mine water head due to proximity to the Kelly Burn discharges.

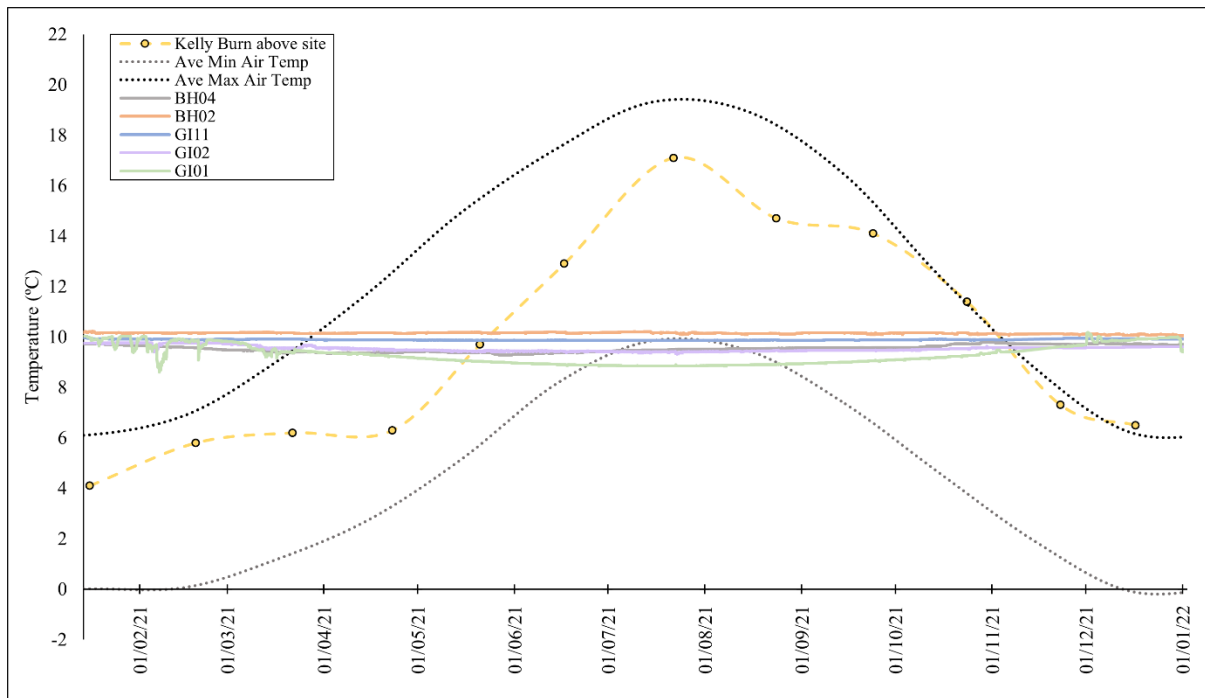


Figure 5.11 Seasonal temperature data for mine water in 2021, plotted against monthly measured Kelly Burn stream temperature data and average maximum and minimum air temperature between 1991-2020 (Met Office, 2022) calculated using the methods outlined in Hollis and Perry (2004). Mine water probes are at depths (below ground level) of 10 m in GI01, 16 m in GI02, 15 m in GI11, 16 m in BH04 and 42 m in BH02; which equate to depths below water level of c. 1-2 m in GI01, 6 m in GI02, 9-10 m in GI11, 6 m in BH04 and 31 m in BH02. Contains public sector information licensed under the Open Government Licence v3.0.

Mine water temperatures vary far less seasonally than air temperatures or on-site surface water temperatures (Figure 5.11), although individual temperature trends vary for each of the mine water monitoring points. GI01 shows an overall inverse trend to the average air data, whereby the lowest temperatures are observed at 8.86 °C in July and the highest are 10.03 °C in January, perhaps reflecting low thermal diffusivity and delayed seasonal thermal extremes relative to those observed at the surface. Similar temperature fluctuations are observed in each of the vertical water profiles between surface and 15-20 m BGL (Appendix 5D), however, the months which show the most extreme values are not consistent across each borehole. In the winter months, GI01 exhibits sudden increases or decreases of temperature by up to 1 °C. These are likely associated with rapid percolation of infiltrating rainfall since GI01 accesses the shallowest worked coal seam at a depth of 10 m BGL and has a mine water head less than two metres above the mined coal seam. BH02 and BH04 are the deepest boreholes, each reaching 50 m BGL; thus BH02 exhibited the highest annual mean temperature of 10.15 °C, with little variance. It should be noted that BH04’s diver was only set at a shallow depth of

16 m BGL. GI11 showed the most constant temperatures with only 0.12 °C of difference between the maximum and minimum. This is assumed to be a result of its southerly location in the deepest coal seam, suggesting that it has the greatest separation from infiltrating rainfall and run-off from the Ochil Hills on the northern edge of the coal-bearing syncline.

Sample Location	N	Statistic	Fe (dis) mg/L	Fe (tot) mg/L	Fe (tot – dis) mg/L	% Fe Dis mg/L	Mn (dis) mg/L	Mn (tot) mg/L
BH02 (Coalsnaughton)	11	Median	0.092	2.2	2.11	4.2	0.236	0.583
		IQR	0.145	1.69			0.377	0.198
BH04 (Coalsnaughton)	11	Median	1.53	4.27	2.74	35.8	0.338	0.369
		IQR	0.275	5.88			0.033	0.058
GI11 (Coalsnaughton)	12	Median	0.709	1.48	0.771	47.9	0.438	0.415
		IQR	0.38	1.06			0.109	0.114
GI01 (Alloa Rough)	11	Median	0.064	1.33	1.27	4.8	0.39	0.392
		IQR	0.065	1.41			0.069	0.082
GI02 (Alloa Splint)	11	Median	0.152	0.729	0.577	20.9	0.312	0.353
		IQR	0.075	0.278			0.031	0.079
Kelly Burn above site	12	Median	0.059	0.236	0.177	25.0	0.008	0.018
		IQR	0.053	0.36			0.01	0.011
Kelly Burn below site	12	Median	0.045	0.156	0.112	28.5	0.062	0.066
		IQR	0.027	0.179			0.049	0.044
Discharge 1	1	Value	1.23	0.916	-0.314	134	0.336	0.314
		IQR	N/A	N/A			N/A	N/A
Discharge 2A	13	Median	0.014	0.098	0.085	13.8	0.006	0.011
		IQR	0.01	0.226			0.002	0.012
Discharge 2B	11	Median	0.099	0.189	0.09	52.4	0.35	0.345
		IQR	0.016	0.036			0.013	0.036
Discharge 2C	10	Median	0.096	0.173	0.077	55.5	0.375	0.377
		IQR	0.055	0.14			0.095	0.126

Table 5.2 Median and inter quartile range (IQR) values for total (tot) and dissolved (dis) iron and manganese from sampling points across the field site. N, number of samples. Discharge 1 was sampled only once.

5.3.5 Water chemistry

All water chemistry results are presented in Appendices 5A and 5B. The Piper diagrams (Figure 5.12) show that all sampled mine and stream waters are Ca-HCO₃⁻ type, with minor variations between boreholes and respective coal seams. The spread across the Ca-HCO₃⁻ region reflects an overall shallow, fresh groundwater signature. However, the tendency for some of the samples to move towards the boundary with Ca-SO₄²⁻ suggests the influence of sulphide oxidation. The low dissolved solute content, with an EC range across all boreholes and discharges of 367 – 626 µS/cm, most likely reflects a short residence time in the mined aquifer. The different boreholes and discharge samples create a continuous spread on the Piper

diagram, indicating that samples are chemically related or evolved. The absence of clearly differentiated hydrochemical “facies” in the mined system suggests overall hydraulic connectivity.

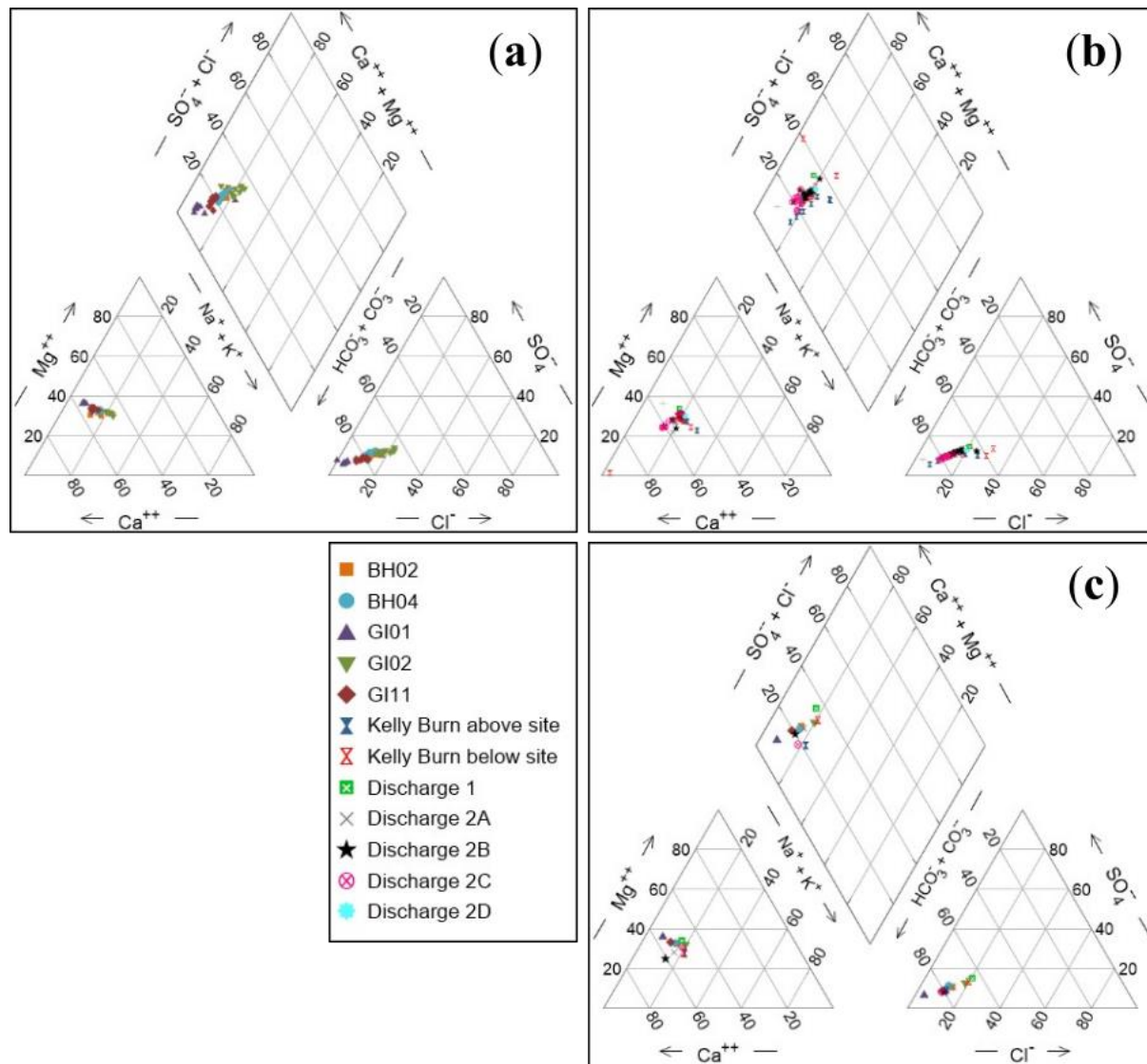


Figure 5.12 Water chemistry data from sample locations presented using Piper diagrams; (a) borehole and (b) discharge water chemistry data from the entire year; (c) data from all points for October 2021 (including the Discharge 1 from Nov 2020 for comparison).

Monitoring of total and dissolved iron provides a means to understand the risk of iron (oxy)hydroxide (ochre) scaling on mine water geothermal infrastructure pipework or heat exchangers. Overall, lower iron concentrations are preferred, but crucially, good practice seeks to maintain iron in its dissolved, ferrous state by isolating host mine water from oxidising environments prior to heat offtake (Bailey *et al.*, 2013). Iron concentrations are presented in Table 5.2 and show that samples from GI02 have both the lowest median total iron concentration (0.73 mg/L) and the lowest concentration of iron which is not dissolved (0.58 mg/L), i.e., total minus dissolved iron. GI11 has the greatest percentage of total iron in a

dissolved state (47.9%), which overall as a proportion of total iron is still quite low. This may suggest that there is some degree of in situ oxidation (or rapid oxidation during sampling) which may pose a risk of ochre scaling. There appears to be no clear correlation between iron concentration and host coal seams. The range of median values for total and dissolved iron between multiple boreholes of the Coalsnaughton Main Seam (Table 5.2) is greater than the range between the different seams. Similarly, manganese has a narrow range across the boreholes, around 0.2 to 0.5 mg/L, providing no means to differentiate dissolved or total metal signatures from each coal seam. Notably, the iron (total and dissolved) concentration in the new monitored discharges (2A-2C) is lower than it was from Discharge 1 in Nov 2020 (Table 5.2) and an order of magnitude lower than the water samples from boreholes.

Elevated sulphate and iron likely reflect iron sulphide (pyrite) oxidation and dissolution, but circumneutral pH values and alkalinity-dominated water types support the common consensus that Scottish mine waters are buffered by dissolution of carbonate minerals in adjacent strata or by alkalinity in the ambient groundwater (Farr *et al.*, 2016, O Dochartaigh *et al.*, 2011).

5.3.6 Isotopic composition

Quarterly isotopic data for water sampling locations indicate a seasonal fluctuation of dissolved sulphate $\delta^{34}\text{S}$ (‰) values (Figure 5.13). The broad trend from the boreholes and discharges is towards isotopically lighter values in the spring and summer, with heavier values in autumn and winter. GI11 shows the greatest variability of $\delta^{34}\text{S}$ with values typically isotopically heavier than other boreholes or discharges, reaching +22.2‰ in winter 2021. The CM1 sample of sulphide from coal pyrite from the Coalsnaughton Main Seam yielded a $\delta^{34}\text{S}$ value of +1.7‰. Other studies have shown sulphide from Scottish Carboniferous coal seams to have a wide range of values from -26.3‰ and +18.4‰, with an overall mean (cleat and banded pyrite) of +2.7‰ (Bullock *et al.*, 2018). All data points in this study are isotopically heavier than both CM1 and Bullock *et al.*'s (2018) arithmetic mean, but the majority fall within the dominant range of values from Scottish pyrite (Bullock *et al.*, 2018). Therefore, it is likely that the sulphate in the mine water is predominantly derived from pyrite oxidation, a derivation which results in negligible fractionation from the parent pyrite.

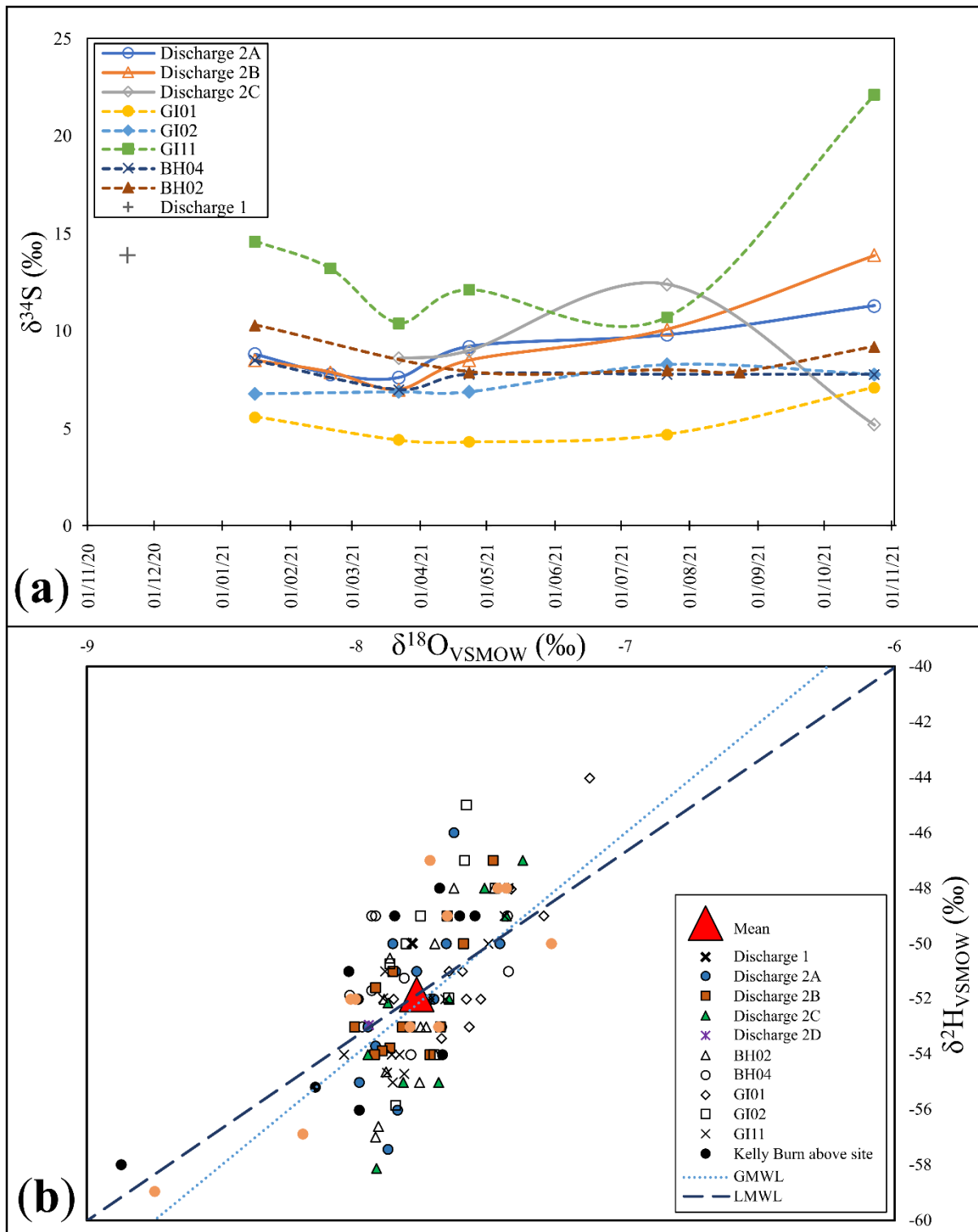


Figure 5.13(a) Dissolved sulphate $\delta^{34}\text{S}$ data for sampling points plotted across the sampling year (2021). (b) $\delta^{18}\text{O}$ and $\delta^2\text{H}$ stable isotope data plotted against global and local (Glasgow) meteoric water lines (GMWL (Craig, 1961); LMWL (Walls *et al.*, 2022)).

Nonetheless, there appears to be a minor component of isotopically heavy sulphur in the system – especially so, in relation to GI11. Such heavy sulphate has been increasingly found in mine water systems e.g., (Banks *et al.*, 2020, Burnside *et al.*, 2016a, Walls *et al.*, 2022). Potential sources of this sulphate include: evaporite dissolution, ancient brines, carbonate associated

sulphur (CAS), or reduction and fractionation of sulphate by sulphate-reducing bacteria in a closed system (Banks *et al.*, 2020, Monaghan *et al.*, 2022, Walls *et al.*, 2022). However, the former two (evaporites and brines) seem unlikely in a shallow, fresh mine water system with no Permian overburden, or indication of evaporites in the local stratigraphy. Similarly, limestone in the local stratigraphy is limited, and therefore CAS seems quantitatively inadequate given the relatively modest alkalinities in the mine water. Thus, further work is needed to explore this heavy end-member, but this should not detract from an isotopic signature in the Dollar mine water system which reflects dominant derivation from pyrite oxidation. Seasonal fluctuation may reflect higher rates of pyrite oxidation during low groundwater levels of spring and summer, when more sulphide bearing minerals become exposed to oxidising conditions. With greater pyrite oxidation, more sulphate with a low mean value (see Bullock's mean of c. +2.7‰) would be added to the system and lower the overall signature towards the mean.

Oxygen and hydrogen isotopic values from all borehole and discharge samples plot closely to the Global- and (Glasgow's) Local- Meteoric Water Line (GMWL (Craig, 1961); LMWL (Walls *et al.*, 2022)), and the mean of all of the samples falls essentially within error of the population on the meteoric water lines (mean $\pm 1\sigma$ as follows: $\delta^{18}\text{O} = -7.8 \pm 0.3\text{‰}$; $\delta^2\text{H} = -52 \pm 3\text{‰}$). This indicates that the mine waters' H₂O component is derived from modern meteoric water and has not undergone significant isotope exchange with minerals or modification by evaporative processes.

5.4 Reflections

The findings of this work have been condensed into practical lessons which may apply to other exploratory programs.

1. One of the principal challenges at the planning and investigation stages of mine water geothermal projects is sourcing capital funding for exploration. Hybridising GSI boreholes in areas where there are suspected shallow mine workings offers the opportunity for monitoring wells to be completed into the mine water geothermal reservoir. As our study shows this allows for the measurement of water level, temperature and hydrochemical monitoring. The overall budget is greater than that of GSI work alone, but less than separate campaigns of GSI and geothermal investigation. Indicative costs of combined GSI and MWGI have been included for a situation which completes three GSI boreholes as monitoring wells but are controlled by the scale of

the additional MWGI work (Table 5.3). A depth cut-off for when this technique becomes unattractive will likely depend on individual project economics.

2. Prior to operations beginning on site, data must be collected on existing mining related features in order to plan investigation works and to evaluate whether investigation works have the potential to alter the hydrogeology of the investigated system.
3. The extracted coal seam is not always the primary aquifer target, and for collapsed longwall mining there exists a fracture network above the depth of remnant material. Whilst the range of flow rates obtainable from longwall goaf is unclear, the screened horizon of the borehole should extend across the worked seams and height of any overlying hydraulically active fracture zone. This can be identified by using core logging or proxies from open hole drilling: minor drops/faster penetration rates, H₂S odour from fracture pockets.
4. In locations of overlapping worked coal seams, care must be taken to avoid creating new hydraulic and thermal short circuits between them via borehole annulus pathways. To avoid time- and resource-consuming operations to isolate seams within boreholes, it is advised to drill to deeper target seams in places where shallower seams are unworked.
5. Ensure water levels and throughflow rates are monitored to allow the scale of the thermal resource to be estimated. Water level and flow rate of shallow collieries can be expected to change with the seasons, reflecting periods with more intense rainfall and lower evapotranspiration. This could be reflected in higher flow rates and thus greater heat availability at specific times of the year.
6. Chemical analyses allow an improved understanding of source and history of mine waters, whereby certain parameters can influence the potential for scaling (and thus engineering design) of a mine water geothermal system. Full analysis of major and minor cations, together with iron and manganese, and field analysis of temperature, pH and a redox indicator, is regarded as a minimum initial chemical suite for MWG allowing an assessment of scaling and/or corrosion potential.

Item	Sum
Mobilisation	£3,200
GI borehole drilling and sealing	£15,300
Completion of three monitoring wells with 50 mm screen and liner	£2,600

Table 5.3 Generic indicative costs for coupled ground stability (GSI) and mine water geothermal investigation (MWGI) for approximately 20 GSI boreholes, where three of these are completed as monitoring wells.

5.5 Limitations

Following on from the reflections and recommendations made by the authors, we feel it is necessary to summarise some of the limitations of this technique, which may render such an approach challenging or unattractive.

1. The depths of any boreholes are likely limited by budget constraints of the project funder. Whilst it may be reasonable to extend boreholes an extra few tens of metres beyond the initial target depths, the maximum depth will likely be governed by funding and time allocation. Similarly, if mine workings are at a greater depth than GSI boreholes are mandated to reach, extending only one or two may be feasible, rather than expecting to complete multiple (e.g., 5 in this study).
2. The additional time and financial resources required to upgrade GSI boreholes to monitoring wells, with liners and standpipes as a minimum, is often cost effective. However, it is accepted that there is a significant time commitment required to subsequently monitor and sample the boreholes on a monthly basis. A private investor may view work of this nature beneficial only if they are serious about considering mine water as a thermal resource.
3. Comprehensive mine water test pumping programmes cannot be performed on boreholes with GSI diameters (50 mm ID completion) due to sizing, but falling head tests for indicative transmissivity values and aquifer response remains feasible.
4. A 5" (127 mm) diameter GSI borehole may be too narrow for some enhanced borehole characterisation or may at least require slimline probes e.g. downhole geophysical logging or CCTV.

5.6 Conclusion

Ground investigation boreholes were drilled into the strata and workings of Dollar Colliery, Clackmannanshire, Scotland. Five were completed as mine water geothermal monitoring wells to inform a mine water conceptual model and to collect geochemistry and

temperature data. The coal-bearing syncline provides a relatively small, isolated worked basin with mine workings dating back many hundreds of years, but the majority of coal extraction was in the decade following 1943. The associated ground stability report is confidential, but the use of shallow mines for mine water geothermal energy application remains plausible, provided ground stability recommendations are adhered to. The encountered coal mine conditions included voids, intact coal, mining waste and goaf, which were interpreted on the basis of wellhead observations during drilling. The Coal Authority and SEPA were informed that a change in the mine water flow regime was noted, whereby the previously established discharge ceased, and water began discharging from the original Day Level. Boreholes were completed into each of the worked coal seams beneath the site, with impermeable seals installed in annuli to ensure these did not create new hydraulic connections between mined horizons. Monthly sampling of boreholes and discharges provided insight into the mine water regime within these coal workings. The mine water regime appears unstratified and hydraulically connected across the different seams and areas of working. Mine water has a low dissolved solute content and shows only minor temperature fluctuations, relative to local air and stream temperatures. Following conceptual modelling, chemistry and temperature analysis, the progression of this site towards a housing development utilising mine water geothermal should be subject to further detailed investigation including pumping and re-injection tests. A suitable mine water geothermal configuration must consider the inherent ground stability risk, with utmost consideration for adequate monitoring and mitigation.

Acknowledgements

We would like to thank Nicholas Poett for provision of the study area and financial contribution to the project; Tatyana Peshkur for her help with chemical analysis at the University of Strathclyde; and Alison McDonald for her help with isotopic analysis at SUERC. We would also like to thank Dollar Museum for provision of historic materials. We are grateful to the following people for contributing their time to assist with field data collection: Mike Schiltz, John Naismith, Jura MacMillan, Laura Dozier, Sean Watson, Sally Jack, Dan Whittington, Maëlle Brémaud, Mylène Receveur, Mohamed El Gheriani, Jennifer Roberts, Simon Theilen and Hannah Jukes

Author Contributions

DBW: conceptualisation (supporting), project administration (equal), methodology (equal), investigation (lead), data curation (lead), formal analysis (lead), writing – original draft (lead), writing – review and editing (equal);

DB: conceptualisation (equal), methodology (equal), writing – review and editing (equal);

AJB: methodology (supporting), writing – review and editing (supporting);

DHT: conceptualisation (equal), investigation (equal);

NMB: conceptualisation (equal), methodology (equal), project administration (equal), writing – review and editing (supporting).

Funding Information

This research was supported by EPSRC IAA grant EP/R51178X/1, Energy Technology Partnership Scotland Knowledge Exchange Network Phase 3 - Industry Engagement Fund (PR007-HE) and NERC NEIF grant 2301.0920. N.M.B is funded by a University of Strathclyde Chancellor's Fellowship. A.J.B is funded by the NERC National Environmental Isotope Facility award at SUERC (NEIF-SUERC, NE/S011587/1).

Chapter 6 The occurrence of elevated $\delta^{34}\text{S}$ in dissolved sulfate in a multi-level coal mine water system, Glasgow, UK

This chapter has been accepted for publication as: Walls, D.B.; Boyce, A.J.; Banks, D. and Burnside, N.M. The occurrence of elevated $\delta^{34}\text{S}$ in dissolved sulfate in a multi-level coal mine water system, Glasgow, UK, to the International Journal of Coal Geology.

Highlights

- Dissolved sulfate- $\delta^{34}\text{S}$ in water interacting with unmined strata matches that of host sulfide minerals.
- Dissolved sulfate- $\delta^{34}\text{S}$ in coal mine water has elevated $\delta^{34}\text{S}$ compared to host sulfide minerals.
- $\delta^{18}\text{O}$ and $\delta^2\text{H}$ of coal mine water reflect meteoric origin.
- Evaporite dissolution, saline brines and microbial reduction may contribute to elevated dissolved sulfate $\delta^{34}\text{S}$ in water.

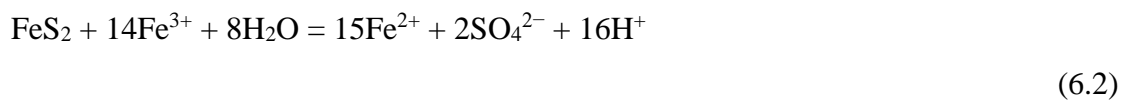
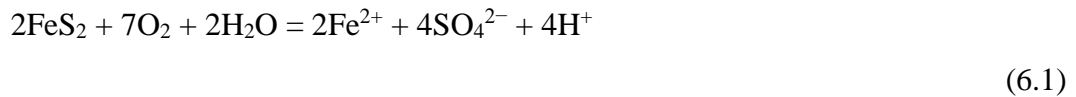
Abstract

Stable isotopic compositions of $\delta^{18}\text{O}$, $\delta^2\text{H}$ and dissolved sulfate $\delta^{34}\text{S}$ in water from abandoned and flooded coal mines are used to interpret the water's and solutes' origin and interactive history. These isotopic ratios have been determined in mine water from a shallow (<100 m) series of overlapping coal mine workings at the UK Geoenergy Observatories Glasgow Geothermal Energy Research Field Site (UKGEOS GGERFS). Comparison has been made between dissolved sulfate $\delta^{34}\text{S}$ of water in mined Carboniferous coal-bearing strata, that of water which had interacted with equivalent unmined strata, and $\delta^{34}\text{S}$ in sulfide-bearing minerals (pyrite) in the host sedimentary rocks and local evaporite (gypsum) of the Lower Carboniferous Ballagan Formation. $\delta^{18}\text{O}$ and $\delta^2\text{H}$ confirm a meteoric origin for coal mine waters. The $\delta^{34}\text{S}$ arithmetic mean and standard deviation of the pyrite ($+5.0 \pm 15.5\%$) and water from unmined strata ($+0.3 \pm 2.1\%$) were found to be similar, whereas the mine water exhibited elevated isotopic values ($+20.3 \pm 1.1\%$), plotting closer to that of modern-day seawater ($+21.2\%$) and Ballagan Formation gypsum ($+18.9 \pm 0.5\%$). Whilst the origin of dissolved sulfate in the mine water remains unclear, it is unlikely to be wholly due to simple pyrite oxidation. Influence of evaporite dissolution, fractionation associated with microbial sulfate reduction, and mixing with saline formation waters of marine, evaporitic or of another origin, cannot be ruled out.

6.1 Introduction

The origin of dissolved sulfate in flooded coal mine waters has typically been considered the result of dissolution of iron sulfide minerals (pyrite) following their oxidation

to form dissolved metals and sulfate, often via secondary hydroxysulfate mineral phases (Hammarstrom *et al.*, 2005, Younger, 1995b, 1997). Sulfide oxidation occurs during mining operations and groundwater flooding following mine closure, whereby the latter dissolves the products of oxidation (Banks *et al.*, 1997, Burnside *et al.*, 2016a). The electron acceptor for oxidation may be oxygen (Equation 6.1) or ferric iron (Equation 6.2) as oxidants.



The natural variability of the stable sulfur isotope ^{34}S , relative to the most common isotope ^{32}S (measured as $\delta^{34}\text{S}$), provides insight into the source and history of mine water sulfate (Banks *et al.*, 2020, Janson *et al.*, 2016). Oxidation reactions typically proceed with negligible sulfur isotopic fractionation (Chen *et al.*, 2020), meaning produced sulfate should be isotopically similar to the source sulfide, thus, the sulfate produced by reactions 6.1 and 6.2 should closely reflect the weighted isotopic average of the oxidised pyrite.

It has been shown that $\delta^{34}\text{S}$ values of cleat and banded pyrite in regional Carboniferous coals (East Ayrshire) range between -26.3‰ and +18.4‰ with an overall arithmetic mean and standard deviation of $+2.7 \pm 9.5\%$ (n=21) (Bullock *et al.*, 2018). Thus, oxidation-controlled generation of Scottish mine water sulfate would give a similar $\delta^{34}\text{S}$ value, provided this mean is broadly representative of Scottish Carboniferous coals. Previous studies, however, have published data showing significant difference between the isotopic signatures of mine water and of sulfide minerals, whereby deep mine water sulfate $\delta^{34}\text{S}$ reaches +20‰ and occasionally higher (Banks *et al.*, 2020, Burnside *et al.*, 2016b, Loredó *et al.*, 2017b). Shallower mine waters commonly exhibit lower sulfate $\delta^{34}\text{S}$ closer to the sulfide range (Banks and Boyce, 2023, Banks *et al.*, 2020, Walls *et al.*, 2022). Some researchers have assigned explanatory narratives to the origins of the elevated S isotopes in mine waters from specific study areas. For example, Chen *et al.* (2020) conclude that mine waters of the Anhui Province, China obtained elevated sulfate concentrations and dissolved sulfate enriched in $\delta^{34}\text{S}$ through the complex influence of high $\delta^{34}\text{S}$ evaporite gypsum in the coal-bearing sequence. Since seawater and derived evaporite deposits from throughout the Carboniferous period typically have $\delta^{34}\text{S}$ values between +13‰ and +21‰ (Kampschulte *et al.*, 2001), resultant $\delta^{34}\text{S}$ signatures of groundwaters affected by dissolution of evaporites of that age should match this range. The values associated with Carboniferous sea water are distinctly more enriched in ^{34}S than the mean Carboniferous pyrite

from East Ayrshire. More broadly, in Europe, evaporites are notably present in Permian and Triassic strata overlying coal-bearing sequences, with typical values between 10‰ and 20‰ (nearer 10‰ in Permian Zechstein period of massive evaporite deposition (Claypool *et al.*, 1980)). Elevated dissolved sulfate $\delta^{34}\text{S}$ in Polish and German coal mine waters has been ascribed to the influence of Triassic or even Miocene evaporites (Banks *et al.*, 2020, Rinder *et al.*, 2020).

This work reports the detailed monitoring of dissolved sulfate in a series of boreholes drilled into abandoned coal mine workings at the Glasgow Geothermal Energy Research Field Site (GGERFS), which is part of the British Geological Survey's (BGS) UK Geoenergy Observatories (UKGEOS). The GGERFS is a unique facility for monitoring, testing and innovation focused on understanding processes within mine water thermal energy systems (Monaghan *et al.*, 2021c) and its setting typifies the geothermal potential in abandoned, flooded coal mines that are widespread beneath many of the UK's towns and cities (Farr *et al.*, 2021). The samples taken in this study effectively represent a baseline for the GGERFS system, taken during initial drilling before any large-scale hydraulic testing. They thus approach being representative of the state of the system following abandonment of the last mine in 1928 (Findlay, 2020). This has allowed the structure of the S isotope distribution across a series of mine water boreholes to be explored for the first time.

6.2 History and description of the mine system

The GGERFS was developed to allow scientific observations of subsurface processes associated with mine water geothermal energy systems, and monitor their effect on the environment (Monaghan *et al.*, 2019). Situated primarily within the Cuningar Loop of the River Clyde, bordering Glasgow City and South Lanarkshire, the location has similarities with many post-industrial areas across the UK including land use, geology and coal mining history (Monaghan *et al.*, 2021c). The GGERFS is located above the western side of Scotland's extensively mined Central Coalfield (Clough, 1926) and hosts a ~300 metre thick succession of Scottish Upper, Middle and Lower Coal Measures formations of Westphalian age (British Geological Survey, 1992b). This sequence hosts seven worked coal seams from the Farme Colliery (main shaft 55.8356°N, 4.2021°W) dating between 1805 and 1928 (Findlay, 2020).

There are 12 boreholes at the GGERFS, spread between two locations (Figure 6.1): Dalmarnock and Cuningar Loop. The ground elevation is typically c. 10-12 m relative to Ordnance Datum (OD), around 6-8 m higher than the elevation of the River Clyde at Cuningar.

Dalmarnock has one seismic observation borehole - GGC01 (55.8411°N, 4.2227°W), drilled to 199 m below ground level (bgl) (Monaghan *et al.*, 2021a). GGC01 spans the entire stratigraphic section covered by the remaining 11 Cuningar Loop boreholes but, importantly, the coal seams encountered by GGC01 are unworked and intact (Kearsey *et al.*, 2019).

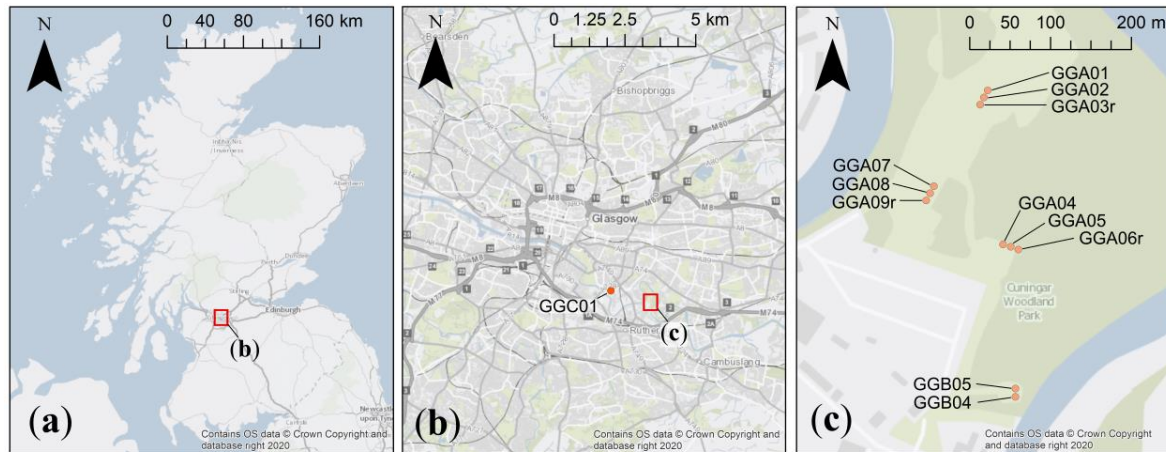


Figure 6.1 Maps showing a) UKGEOS location within Scotland; b) GGC01 borehole and the Cuningar Loop location (red box) in Glasgow's east end; c) The borehole array at Cuningar Loop on the River Clyde. Contains NERC materials ©NERC 2020. Contains OS data © Crown Copyright and database right 2020 (Monaghan *et al.*, 2019).

The 11 Cuningar Loop boreholes target various geological intervals at a range of depths (Figure 6.2), including:

- Five mine water boreholes which access abandoned, flooded workings of the Glasgow Upper Coal or Glasgow Main Coal seams, screened at depths of c. 49 m and c. 85 m bgl respectively. GGA01, GGA04, GGA05, GGA07, and GGA08 (Barron *et al.*, 2020a, Barron *et al.*, 2020b, Monaghan *et al.*, 2020a, Starcher *et al.*, 2020a, Starcher *et al.*, 2020b).
- Five environmental baseline monitoring boreholes, completed into superficial deposits or bedrock above mine workings, drilled to between 16 m and 45 m bgl. GGA03r, GGA06r, GGA09r, GGB04 and GGB05 (Elsome *et al.*, 2020, Shorter *et al.*, 2020b, 2020c, Walker-Verkuil *et al.*, 2020a, Walker-Verkuil *et al.*, 2020b).
- One sensor testing borehole (GGA02) which penetrated abandoned, flooded coal seams during drilling to a maximum depth of 94 m bgl (Monaghan *et al.*, 2020b).

	Dalmarnock GGC01	Cuningar Site 1 GGA01 GGA02 GGA03r	Cuningar Site 2 GGA04 GGA05 GGA06r	Cuningar Site 3 GGA07 GGA08 GGA09r	Cuningar total
Borehole fluid samples	14 (2)	11 (11)	14 (8)	22 (19)	47 (38)
Return fluid (routine daily)	12 (6)	10 (7)	13 (6)	14 (9)	37 (22)
Return fluid (rockhead)	N/A	1 (1)	1 (0)	2 (0)	4 (1)
Return fluid (mine water)	N/A	2 (2)	2 (2)	4 (4)	8 (8)
Return fluid total	12 (6)	13 (10)	16 (8)	20 (13)	49 (31)
Pumping test	N/A	3 (3)	5 (5)	5 (5)	13 (13)

Table 6.1 Numbers of water samples collected and analysed by site and sample type. Number of samples analysed for $\delta^{34}\text{S}$ is in brackets.

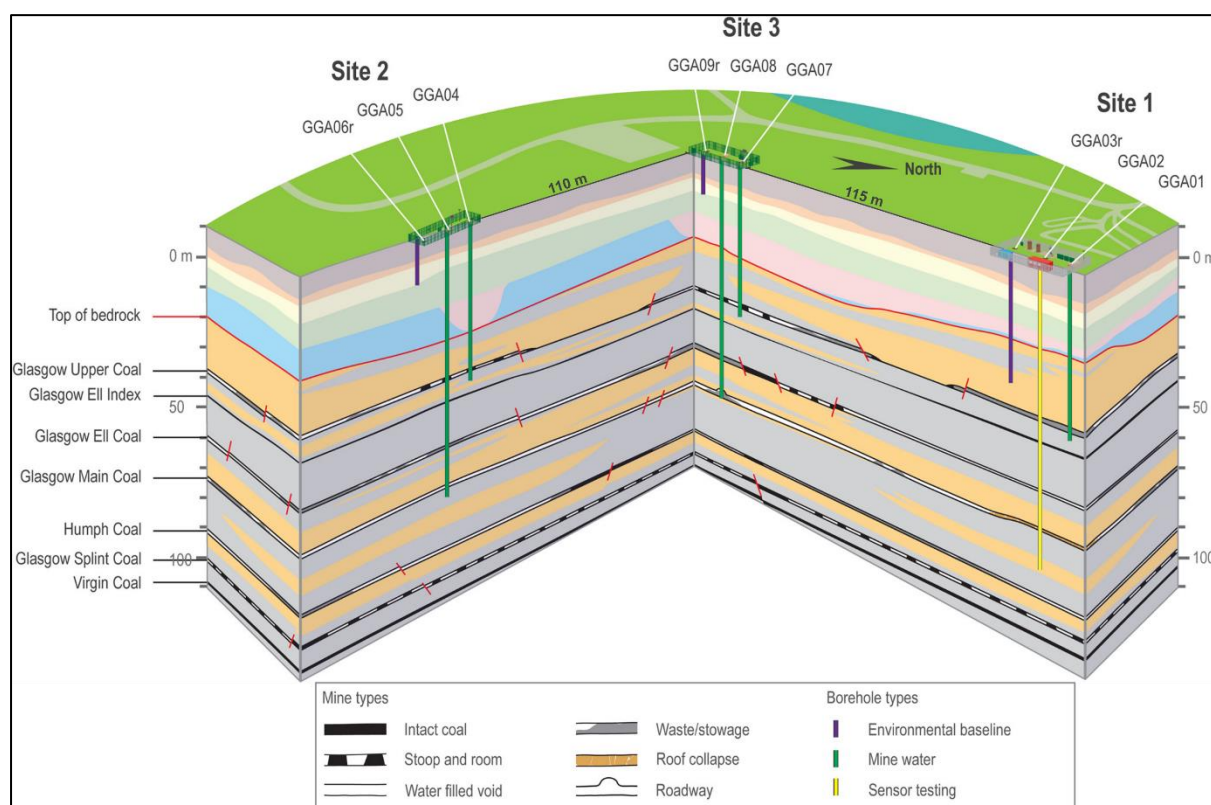


Figure 6.2 Block diagram showing the Cuningar Loop borehole array with coal seams labelled. No vertical exaggeration. Note depths are in metres relative to Ordnance Datum (m OD; sea level). Figure originally published by Monaghan *et al.* (2021c) ©BGS, UKRI 2021.

The boreholes at Cuningar Loop are clustered into three groups: Sites 1, 2 and 3, as described in Figure 6.2 and Table 6.1. Mine water boreholes at Cuningar Loop targeted the thickest seams in the area (between 1-1.5 m thick) (Hall *et al.*, 1998), where the abandonment plans showed a variety of mining types including pillar and stall, and areas of ‘total extraction’

(Monaghan *et al.*, 2021c). A comprehensive description of the mining history and borehole array can be found in Monaghan *et al.* (2021c). It should be noted, that whilst the Glasgow Upper Coal and the Glasgow Main Coal seams are the target horizons for borehole completion, the Glasgow Ell Coal seam was encountered with mining waste or voids in each of the 3 deepest boreholes (Figure 6.2 and 6.3) but were subsequently cased off during completion.

6.3 Methods

6.3.1 Drilling and test pumping

6.3.1.1 Dalmarnock

The cored, seismic monitoring borehole GGC01 was drilled in Dalmarnock (55.8411°N, 4.2227°W) between 19 November and 12 December 2018. Rotary coring was advanced using Glasgow's mains water as the direct flush drilling fluid (described in Section 6.3.1.2.1); specifically, a Geobore-S system was rotated downhole to drill a borehole of 151 mm outer diameter and recovered core of 102 mm diameter in 3 m lengths (Monaghan *et al.*, 2021a). The mains water drilling fluid had a geomicrobiological tracer added daily in an attempt to maintain a ratio of tracer to drilling fluid of 1:40,000; alongside this, a drilling additive called Insta-pac supplied by CETCO Europe was added to aid drilling (Monaghan *et al.*, 2021a). Following drilling, GGC01 was open hole wireline logged and reamed out to 156 mm diameter to install a 76.6 mm internal diameter uPVC Boode casing which houses a string of 5 seismometers. The annulus of the borehole was grouted with SP/F6 Portland cement-based from Tarmac (Monaghan *et al.*, 2021a, Tarmac, 2016).

6.3.1.2 Cuningar

The drilling, completion and pumping test methodologies for each of the eleven boreholes at Cuningar Loop are detailed in full in their respective British Geological Survey open reports (Barron *et al.*, 2020a, Barron *et al.*, 2020b, Elsome *et al.*, 2020, Monaghan *et al.*, 2020a, Monaghan *et al.*, 2020b, Shorter *et al.*, 2020b, 2020c, Starcher *et al.*, 2020a, Starcher *et al.*, 2020b, Walker-Verkuil *et al.*, 2020a, Walker-Verkuil *et al.*, 2020b)

6.3.1.2.1 *Drilling fluid and rock samples*

The Glasgow mains water which was used as the drilling fluid is ultimately derived (following treatment) from the freshwater Loch Katrine (56.25°N, 4.52°W), around 45 km NNW of Glasgow (Burnet, 1869; Engineering Timelines, 2020). The properties of the water

supplied to Cuningar from the Scottish Water plant in Milngavie and of BGS' mains water samples from Dalmarnock are shown in Table 6.2. During drilling, ingress of formation groundwater from responsive horizons will have contributed to the overall circulating drilling fluid. Sampled waters from the borehole and the return drilling fluid are most likely a mixture of the initial mains water and formation water. In some instances, bentonite mud was used as drilling fluid where superficial deposits were unstable. During drilling, water or bentonite drilling fluid returned rock chips to the surface; these were separated from the drilling fluid by use of a shaker. Following separation, the drilling fluid was directed into a series of settlement tanks to remove smaller suspended particles before recirculation as "clean" drilling fluid.

	Unit	Scottish Water Milngavie mean concentration (2021)	N	BGS Dalmarnock mean concentration (Dec 2018-Jan 2019)	N
pH	pH unit	7.93	36	8.79	2
Electrical conductivity	µS/cm	51	36	60	2
Sodium	mg/L	3.95	8	3.8	2
Calcium	mg/L	n.a.		5.4	2
Ammonium	mg/L as NH ₄ ⁺	0.05	36	n.a.	
Iron	mg/L	0.008	36	0.009	2
Manganese	mg/L	0.002	36	0.0004	2
Sulfate	mg/L as SO ₄ ²⁻	7.55	8	7.08	2
Nitrate	mg/L as NO ₃ ⁻	0.7	8	0.47	2
Chloride	mg/L as Cl ⁻	5.88	8	6.0	2
Alkalinity	meq/L	n.a.		0.15	2

Table 6.2 Mains water quality supplied by Scottish Water to the Cuningar area of Glasgow via Milngavie treatment works, average of 2021 (Scottish Water, 2021); and the average of the two mains water samples taken from the office at the Dalmarnock drilling location (Shorter et al., 2021b). n.a. – not analysed.

6.3.1.2.2 *Made ground and superficial deposits*

Each borehole was progressed through made ground with a BAM piling rig with an 880 mm auger. The made-ground in each was cased-off with permanent steel casing and the annulus was grouted with cement-based grout. The superficial deposits were drilled through to bedrock with tri-cone bits of 558.8 mm for GGA01, GGA02, GGA04, GGA05 and GGA08, and 374 mm for GGA03r and GGB05. GGA08 encountered mobile sands and gravels and hence required redrilling with direct flush duplex drilling method (457 mm outer diameter casing while drilling), GGA07 was drilled using this method to prevent against the same issue (Starcher *et al.*, 2020b). Mains water was used as the drilling fluid whilst progressing through the superficial deposits, except where stability of sand and gravel was an issue, in these instances bentonite mud was used as a drilling fluid, this is true of GGA04, GGA05, GGA08, GGB04 and BBG05. Upon reaching bedrock, the superficial deposits in each borehole were cased-off with permanent steel casing and the annulus was sealed with cement-based grout.

GGA06r, GGA09r and GGB04 were drilled at 191 mm into the superficial deposits and were terminated in the Quaternary Gourock Sand Member, above bedrock. GGA06r has a screened section of 113.8 mm outer diameter Boode BGP™ gravel coated PVC screen with 1 mm slot sizes from +0.31 m to -1.66 m OD, but remains hydraulically open with sand and portions of collapsed borehole in the annulus from +0.51 m to -3.77 m OD (Shorter *et al.*, 2020c). GGA09r has a screened section of 113.8 mm outer diameter Boode BGP™ gravel coated PVC screen with 1 mm slot sizes from -0.01 m to -1.89 m OD, but remains hydraulically open with sand and portions of collapsed borehole in the annulus from +0.02 m to -4.28 m OD (Walker-Verkuil *et al.*, 2020b). GGB04 has a screened section of 113.8 mm outer diameter Boode BGP™ gravel coated PVC screen with 1 mm slot sizes from +1.77 m to -0.13 m OD, but remains hydraulically open with sand and portions of collapsed borehole in the annulus from +1.90 m to -3.60 m OD (Elsome *et al.*, 2020).

6.3.1.2.3 *Bedrock*

The five mine water boreholes (GGA01, GGA04, GGA05, GGA07, and GGA08) and the sensor testing borehole (GGA02) were progressed into bedrock with a 406 mm tri-cone bit. The two environmental baseline monitoring boreholes were progressed into bedrock (GGA03r and GGB05) with a smaller 244 mm tri-cone bit. Mains water drilling fluid was used for each of the bedrock sections of the boreholes.

GGA03r and GGB05 were respectively terminated in bedrock c. 8 m and 5 m above the stratigraphically highest coal seam (Glasgow Upper Coal). GGA03r has a screened section of 165 mm outer diameter Boode BGP™ gravel coated PVC screen with 3 mm slot sizes from -26.96 m to -29.77 m OD, but it is hydraulically open with 4-10 mm filter gravel in the annulus from -25.96 m to -30.77 m OD (Shorter *et al.*, 2020b). GGB05 has a screened section of 191 mm outer diameter pipe with 3 mm slot sizes from -30.65 m to -32.45 m OD, but it is hydraulically open with 10 mm gravel in the annulus from -28.45 m to -33.65 m OD (Walker-Verkuil *et al.*, 2020a). Both GGA03r and GGB05 are screened across a sandstone horizon of the Scottish Middle Coal Measures Formation.

6.3.1.2.4 *Glasgow Upper Coal seam*

GGA01, GGA04, GGA07 were drilled as far as the stratigraphically highest coal seam (Glasgow Upper Coal). GGA01 encountered the Glasgow Upper Coal as waste from -36.72 m to -37.98 m OD. It has a screened section of 280 mm outer diameter Boode BGP™ gravel coated PVC screen with 4 mm slot sizes from -34.8 m to -38.4 m OD, but it is hydraulically

open from -34.1 m to -41.1 m OD without annulus fill below a rubber annular seal (Monaghan *et al.*, 2020a). GGA04 encountered the Glasgow Upper Coal as an intact or partially collapsed coal pillar and a possibly fractured sandstone roof. The coal was encountered from -37.05 m to -38.19 m OD. It has a screened section of 280 mm outer diameter Boode BGP™ gravel coated PVC screen with 4 mm slot sizes from -35.29 m to -38.89 m OD, but it is hydraulically open from -34.69 m to -41.22 m OD without annulus fill below a rubber annular seal (Starcher *et al.*, 2020a). GGA07 returned coal from the Glasgow Upper Coal seam with some staining and alteration, and thus was interpreted as a pillar in pillar and stall workings. However, the optical camera observed open (stall) portions of the workings indicating the borehole had penetrated the edge of a pillar. The coal was encountered from -40.57 m to -42.27 m OD. It has a screened section of 280 mm outer diameter Boode BGP™ gravel coated PVC screen with 4 mm slot sizes from -39.57 m to -42.27 m OD, but it is hydraulically open from -38.07 m to -45.27 m OD without annulus fill below a rubber annular seal (Starcher *et al.*, 2020b).

6.3.1.2.5 *Glasgow Ell and Glasgow Main Coal seams*

GGA02, GGA05 and GGA08 were drilled to the depth of the Glasgow Main Coal seam, penetrating worked or unworked portions of the Glasgow Upper Coal, and Glasgow Ell Coal seams. Mine water from the level of the Glasgow Upper Coal seam was purged and sampled in GGA02 to meet SEPA sampling requirements. The workings above the Glasgow Main in GGA02 were grouted with a cement-based grout to ensure no flow pathway was created between the different mine water aquifer horizons. This was only performed in GGA02 since GGA05 did not record evidence for worked coal seams above the Glasgow Main. Good and similar water qualities of the Glasgow Upper Coal and Glasgow Main Coal workings were proven prior to GGA08 drilling and hence SEPA were satisfied that drilling could progress without sealing the Glasgow Upper or Glasgow Ell Coal seams. It remained a requirement of the BGS and SEPA that permanent casing ensured a hydraulic seal between the mine workings upon borehole completion.

GGA02 encountered the Glasgow Upper Coal seam as packed waste from -36.89 m to -38.04 m OD, the Glasgow Ell Coal seam as a water filled void from -59.25 m to -59.85 m OD but the Glasgow Main Coal seam was not recognised during drilling and was later interpreted to reflect complete longwall collapse at around -72 m to -73 m OD. During completion cement-based grout entered the inside of the casing and cemented up the screened section of the borehole. GGA02 was repurposed as the sensor testing borehole and was not subject to pumping tests (Monaghan *et al.*, 2020b).

GGA05 encountered the Glasgow Upper Coal seam as intact coal (interpreted as a pillar) from -37.24 m to -38.78 m OD, the Glasgow Ell Coal seam was not identified during drilling and was later observed to be collapsed waste between -59.68 m and -60.38 m OD, and the Glasgow Main Coal seam was encountered as a void from -72.44 m to -73.14 m OD. GGA05 has a section of 280 mm outer diameter Boode plain PVCTM screen with 4 mm slot sizes from -71.48 m to -74.18 m OD, but it is hydraulically open from -70.88 m to -76.28 m OD without annulus fill below a rubber annular seal (Barron *et al.*, 2020a).

GGA08 encountered the Glasgow Upper Coal seam as possible mine workings from -40.68 m to -41.88 m OD, the Glasgow Ell Coal seam was observed as packed waste -62.88 m and -64.68 m OD, and the Glasgow Main Coal seam was encountered with a void, wood and mining waste from -75.88 m to -78.88 m OD. GGA08 has a section of 280 mm outer diameter Boode BGPTM gravel coated PVC screen with 4 mm slot sizes -73.71 m to -76.41 m OD, but it is hydraulically open from -72.48 m to -79.55 m OD without annulus fill below a rubber annular seal (Barron *et al.*, 2020a).

6.3.1.2.6 *Purging and test pumping*

Following completion and screen installation each borehole, except GGA02, was purged with the aim of removing any drilling-related material and fluid from inside the casing. In January and February 2020, after an interval of 1 to 4 months, each borehole was test pumped by a series of 5 step tests and a 5-hour constant rate test. Since GGB04 showed very low yield values during purging it was instead selected for a slug test between 17 and 19 February 2020, six months after purging (Elsome *et al.*, 2020).

6.3.2 Field collection

In this study, all fluid and rock samples from the GGERFS borehole suite were collected by BGS staff on behalf of the authors during construction and testing. Evaporite samples from the Ballagan Formation were collected by the authors.

6.3.2.1 Rock samples

The authors were granted access to 1 m of core sample from GGC01 at every 10 m interval. Visual inspection confirmed that one of the intervals contained pyrite-bearing coal from the Glasgow Main Coal seam at 132.6 m bgl. No pyrite was found during screening of the other sample intervals.

During reverse circulation rotary drilling of the boreholes at Cuningar Loop, returned drill cuttings were collected by the BGS from the cutting shaker at 1 m intervals to characterise the stratigraphy of the superficial deposits, intact bedrock and mined coal seams (Figure 6.3). Samples which were dominated by pyrite-rich or dark, organic-rich horizons were split into two duplicate subsamples whereby one was collected in plastic sample bags for the authors.

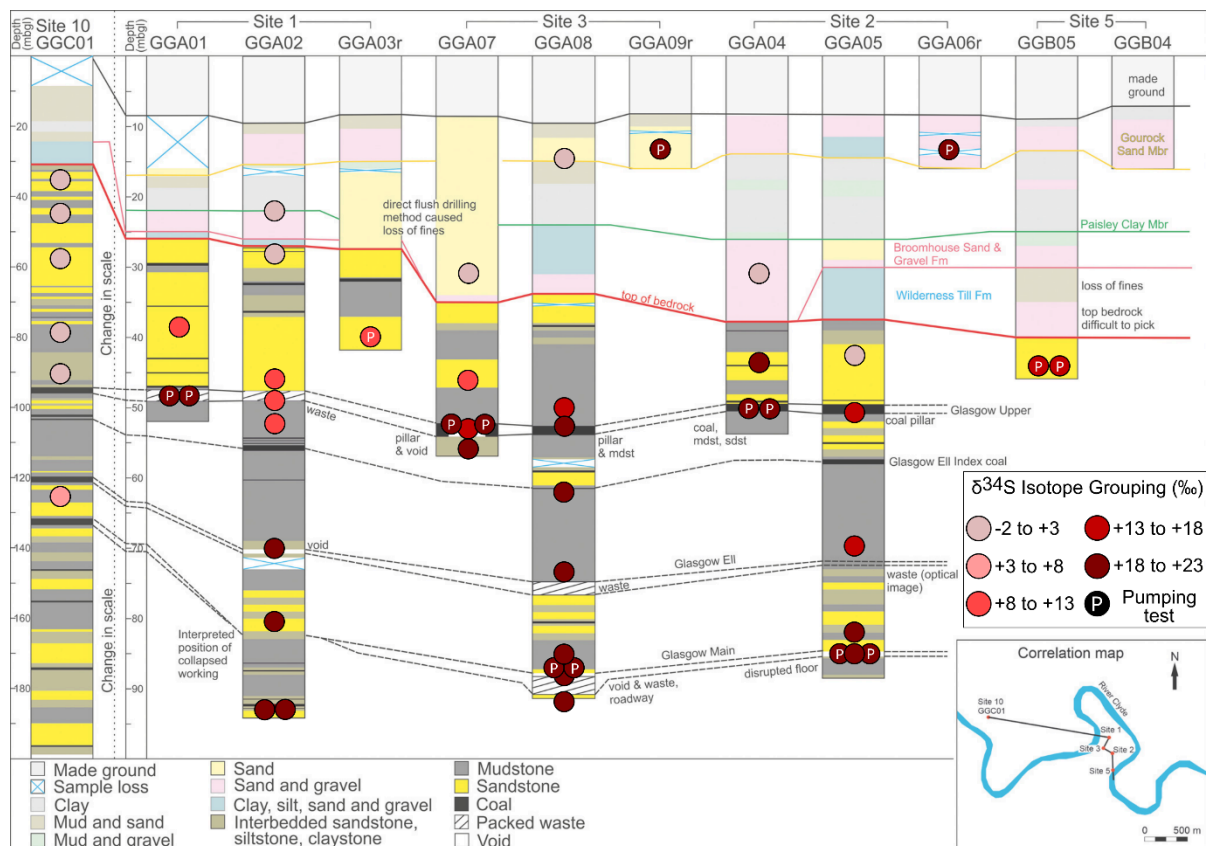


Figure 6.3 Lithostratigraphical correlation panel of the Glasgow Observatory boreholes modified from Monaghan *et al.* (2021c) (©BGS, UKRI 2021) by addition of coloured symbols representing groupings of sulfur isotopic values.

Tournaisian (Lower Carboniferous) field samples of gypsum were collected from the Ballagan Formation type locality in Ballagan Glen (55.99°N, 4.29°W, c. 15 km NNW of Cuningar Loop), either side of the Ballagan Glen Fault. These evaporites are the most regionally abundant evaporitic sulfate source within the Carboniferous sequence. Samples from 3 different facies of evaporite deposit were collected with the permission of the National Trust for Scotland. The Ballagan Formation is stratigraphically lower (Tournaisian) than target seams of the GGERFS in the Scottish Middle Coal Measures Formation (Westphalian) (British Geological Survey, 1992b, Monaghan *et al.*, 2017). The Ballagan Formation is expected to be 130 m to 245 m thick (Institute of Geological Sciences, 1978) at c. 1500 m depth below

Cuningar Loop. This depth estimate is calculated from the top of the Clyde Plateau Volcanic (CPV) Formation which directly overlies the Ballagan Formation. The CPV Formation is interpreted from gravity surveying and forward modelling to be at c. 1100 m depth (Watson, 2022) and of 300 – 500 m thickness (Hall *et al.*, 1998).

6.3.2.2 Water samples

During drilling of each borehole at the GGERFS locations (Cuningar Loop and Dalmarnock), water samples were collected in one litre Nalgene bottles by members of the BGS drilling supervision staff. They were filled with unfiltered, untreated waters and refrigerated until the authors collected the bottles, normally after 1-2 days, but up to one week later. Note that Dalmarnock only had sample types A and B collected, but these followed the same procedures as those from Cuningar Loop. The samples were sourced from the following:

Type A – “Borehole fluid”: taken from the static water in the borehole, prior to the start of any daily drilling activity (one per borehole per day on days when borehole was being drilled). Samples were obtained from just below rest water level by gently lowering a 1025 mL disposable plastic hand bailer into the borehole. Once submerged, the bailer was then slowly retrieved, ensuring that it was full of water (Shorter *et al.*, 2021a). There were instances when samples were taken following a long period (weeks or months) without drilling activity, allowing time for settlement or potential stratification of the water column. Samples were collected by the same means before and after the purging activities described above.

Type Bi – “Return fluid”: taken from the returning drilling fluid during drilling (one per borehole per day on days when borehole was actively drilled). The bottles were filled from the settling tank, just below the drilling fluid discharge pipe (Shorter *et al.*, 2021a). As described, the drilling fluid was derived from Glasgow’s mains tap water, and thus, return fluid samples are likely a mixture of groundwater or mine water with original mains water drilling fluid.

The following sample types were collected from Cuningar Loop only (i.e., all boreholes except GGC01)

Type Bii – “Return fluid – rock head”: taken as return fluid sample upon reaching rock head beneath the superficial deposits.

Type Biii – “Return fluid – mine water”: taken as a return fluid sample once mine workings encountered (as determined by drillers interpretation of subsurface conditions). The only exception for samples of this study was the sample taken from GGA02 in the Glasgow

Upper Coal working. Following connection with the mine working, approximately 20 m³ of water was purged from the borehole by airlifting. Afterwards, the sample was collected via a Hydrasleeve™ discrete bailer, lowered to the depth of the mine working (Shorter *et al.*, 2021a). Air lifting operations in GGA05 post-dated the samples provided to the authors; thus, these were collected by standard return fluid methods.

Type C – “Pumping test water”: taken from sample tap attached to the rising main of pump used for testing (Palumbo-Roe *et al.*, 2021a). Samples collected at midpoint and endpoint of five-hour constant rate pumping test each successfully completed borehole. These samples are the best representation of groundwater and mine water derived from the screened interval, since they have the smallest likelihood of influence by drilling fluids.

Sample types B and C are included in an “active samples” grouping, used in some figures. Sample type A (borehole fluid) is excluded since these were not sampled during active drilling or pumping and therefore the water column had the potential for stratification.

The depth associated with each of the water samples was taken as metres below ground level (m bgl) by the drilling contractor. The depth of the pumping test water samples is taken as the depth of the hydraulic response interval (open section or screen). These were converted to metres relative to Ordnance Datum (OD; sea level) using data from BGS elevation surveys (Barron *et al.*, 2020a, Barron *et al.*, 2020b, Monaghan *et al.*, 2020a, Monaghan *et al.*, 2021b, Monaghan *et al.*, 2020b, Shorter *et al.*, 2020b, 2020c, Starcher *et al.*, 2020a, Starcher *et al.*, 2020b, Walker-Verkuil *et al.*, 2020a, Walker-Verkuil *et al.*, 2020b).

6.3.3 Laboratory analysis

6.3.3.1 Rock samples

The single core sample from GGC01 of the Glasgow Main Coal seam was broken along cleat fractures to reveal fresh pyrite. Drill cutting samples were washed with deionised water to remove dust and small debris before being examined for visible pyrite under an incident light binocular microscope. Visible pyrite from both sample types was extracted by scalpel or mineral drill. Ballagan Glen Formation samples were prepared for isotopic analysis by drilling polished samples to obtain powdered gypsum.

6.3.3.2 Water samples

Upon receipt of one litre samples from refrigerated drill-site storage, each was transported to the University of Glasgow laboratories and decanted into following aliquots:

1. 0.45 μm filtered into 15 mL polypropylene screw-cap vial for major cation and anion analysis. Filtration was carried out at the laboratory using a 0.45 μm filter capsule mounted on a polypropylene syringe.
2. 100 mL (unfiltered) for determinations of pH, oxidation-reduction potential (ORP) and electrical conductivity (EC) using a handheld Myron P Ultrameter. Readings were automatically temperature corrected to a standard temperature of 25 °C.
3. A 100 mL (unfiltered) for alkalinity determination using a Hach Model 16900 digital titrator.
4. 0.45 μm filtered (as above) 15 mL polypropylene screw-cap vial, sealed with Parafilm to prevent sample evaporation, for $\delta^{18}\text{O}$ and $\delta^2\text{H}$ analysis.
5. Remaining volume (c. 770 mL) filtered using 0.45 μm qualitative filter paper and funnel before preparation for $\delta^{34}\text{S}$ analysis.

The results following analysis of aliquots 2 and 3 are not presented in this study and hence are not described in detail (but are included in Appendix 6A). Dissolved sulfate concentration was determined, alongside that of other major ions from aliquot 1, using ion chromatography on Dionex equipment in the labs of the School of Engineering at the University of Glasgow. For anions a 10 μL sample was passed through a Dionex IonPac AG14A guard column and AS14A-5u analytical column before analysis on an ICS-900, with the aid of displacement chemical regeneration suppression (ACRS 500). A mix of 8 mM sodium carbonate/1 mM bicarbonate eluent and 72 mN H_2SO_4 regenerant was pumped through the system at 0.5 mL/min. For cations a 10 μL sample was passed through a Dionex IonPac CG12A guard column and CS12A analytical column, set to 30 °C, before analysis on an ICS-1100. A 20 mM methanesulfonic acid eluent was pumped through the system at 0.25 mL/min and a CERS 500 was used as an electrolytic suppressor. For both anion and cation analyses a conductivity cell was used for peak detection complete with a 3-level calibration. The standard for anion measurement was a Thermo Scientific™ Dionex™ Combined Seven Anion Standard II and the cation standard was a Dionex™ Six Cation-II solution. Chromeleon 7 software was used for final data analysis and quantification.

Stable isotope analyses of water (aliquot 4), dissolved sulfate (aliquot 5) and sulfur-bearing rock samples were undertaken at the Scottish Universities Environmental Research Centre (SUERC) laboratories, East Kilbride. For $\delta^{34}\text{S}$ isotope analysis, gypsum samples were converted to BaSO_4 by dissolution in 2.5M hydrochloric acid, filtration, then precipitation

through addition of a 5% BaCl solution. Aliquot 5 was acidified to pH 3–4 using ultrapure concentrated hydrochloric acid and then dosed with excess 5% BaCl₂ solution to precipitate sulfate as BaSO₄ (Carmody *et al.*, 1998), which was allowed to settle. In both scenarios BaSO₄ precipitate was recovered from the sampling vessel, washed repeatedly in deionised water and dried. For analysis of the precipitate, SO₂ gas was liberated from each sample by combustion at 1125 °C with excess Cu₂O and silica, using the technique of Coleman and Moore (1978). For the sulfide mineral (pyrite), combustion at 1075 °C with excess Cu₂O followed the technique of Robinson and Kusakabe (1975). Raw ratios of SO₂ were measured on VG SIRA II mass spectrometer, and standard calculations applied to yield δ³⁴S ratios reported as per mille (‰) variations from the Vienna Canyon Diablo Troilite (V-CDT) standard.

For water δ¹⁸O analysis, each sample was over-gassed with a 1% CO₂-in-He mixture for 5 minutes and left to equilibrate for a further 24 hours. A sample volume of 2 mL was then analysed using standard techniques on a Thermo Scientific GasBench and Delta V mass spectrometer set at 25 °C. Final δ¹⁸O values were produced using the method established by Nelson (2000). For δ²H analysis, samples and standard waters were injected directly into a chromium furnace at 800 °C (Donnelly *et al.*, 2001), with the evolved H₂ gas analysed on-line via a VG Optima mass spectrometer. Final values for δ¹⁸O and δ²H are reported as per mille (‰) variations versus standard mean ocean water (V-SMOW) in standard delta notation.

6.3.4 Quality assurance

Each sample for IC analysis was run in duplicate with 5-point concentrations of anion and cation standard solutions. Laboratory blanks were created from ultrapure water and subjected to the same laboratory processes as the UKGEOS water samples to check for contamination. All laboratory blanks returned acceptable values which concluded there was no, or minimal interference from the processes of sample preparation and/or laboratory analyses. Duplicate analyses were checked for inconsistencies, if present the sample was run again in duplicate, if the values were consistent, the arithmetic mean was extracted.

Sulfur isotopic data were calibrated using both international (NBS-123 sphalerite: +17.4‰ and IAEA-S-3: -32.3‰) and internal standards (CP1 chalcopyrite: -4.5‰) and are reported with an error of reproducibility based on repeat analyses of the standards of $\pm 0.3\%$. For isotopic analysis of O and H, in-run repeat analyses of water standards (international standard V-SMOW and (Greenland Ice Sheet Precipitation) GISP, and internal standard Lt Std) gave a reproducibility typically better than $\pm 0.3\%$ for δ¹⁸O, $\pm 3\%$ for δ²H.

The Glasgow mains water is low in dissolved solute content (Table 6.2) and importantly for this study, has a sulfate concentration of 7 mg/L. The starting concentrations for major ions can be used to understand the solute contribution from the surrounding and interacting bedrock or superficial horizons. Most of the Cuningar water samples exhibited dissolved sulfate values far greater than that of the Glasgow mains water, where the 10th percentile was 97 mg/L, median 163 mg/L and 90th percentile 308 mg/L. The samples from Dalmarnock were closer to the mains water concentration of 7 mg/L, but still had dominant concentrations of sulfate contributed from groundwater. This confirms that the dominant signature of the $\delta^{34}\text{S}$ was from the formation water.

6.4 Results

6.4.1 Sulfide from rock samples

The $\delta^{34}\text{S}$ values of the seven pyrite samples from the Dalmarnock and Cuningar Loop boreholes (Table 6.3) range from -20.5‰ to +30.5‰, with a median of +9.4‰ and an arithmetic mean and standard deviation of $+5.0 \pm 15.5\%$ (n=7). Of the collected rock samples, only coal samples hosted pyrite. The other dark and organic-rich horizons did not. The wide range of values is similar to that which Bullock *et al.* (2018) observed in Carboniferous coal-bearing units of the Ayrshire coalfield, where $\delta^{34}\text{S}$ ranged from -26.3‰ to +18.4‰ with an overall mean of $+2.7 \pm 9.5\%$ (n=21). The mean values for both pyrite suites are plotted alongside dissolved sulfate $\delta^{34}\text{S}$ results in Figure 6.4.

Borehole	Depth (m bgl)	Stratigraphic horizon	$\delta^{34}\text{S}$ (‰)
GGA02	47-48	Glasgow Upper Coal	+11.8
GGA02	53-54	Ell Index Coal	+6.4
GGA05	49-50	Glasgow Upper Coal	-12.3
GGA07	38-39	Unnamed Coal	-20.5
GGA08	38-39	Unnamed Coal	+9.4
GGA08	52-53	Glasgow Upper Coal	+9.5
GGC01	132.6	Glasgow Main Coal	+30.5
Arithmetic mean and standard deviation (n=7)			+5.0 ±15.5

Table 6.3 Sulfide-sulfur isotope data from pyrite separated from coal horizons at the GGERFS ('GGA' Cuningar boreholes – drill cuttings) and stratigraphic and seismic monitoring Dalmarnock borehole (GGC01 – core sample). Their stratigraphic level is also presented in relation to the mined coal-bearing horizons from which they were collected (see. Figure 6.3)

6.4.2 Sulfate from GGC01 water samples

Table 6.4 shows sulfate $\delta^{34}\text{S}$ for the eight borehole and return fluid samples collected from GGC01 at Dalmarnock, which encountered no mined horizons at any depth. Values

display a tight range between -2.3‰ and +3.5‰, with a median of -0.1‰ and an arithmetic mean of $+0.3 \pm 2.1\%$ (n=8). The deepest three samples are slightly more enriched in ^{34}S (Figure 6.4) starting from 78.5 m bgl (-68.84 m OD), which loosely correlates with the first coal seam observed in GGC01 at c. 75m bgl (Monaghan *et al.*, 2021a). The mean value for these eight water samples lies comfortably within 1 standard deviation of mean pyrite $\delta^{34}\text{S}$ for regional Carboniferous coals from Bullock *et al.* (2018) ($+2.7 \pm 9.5\%$, n=21), and this study ($+5.0 \pm 15.5\%$, n=7).

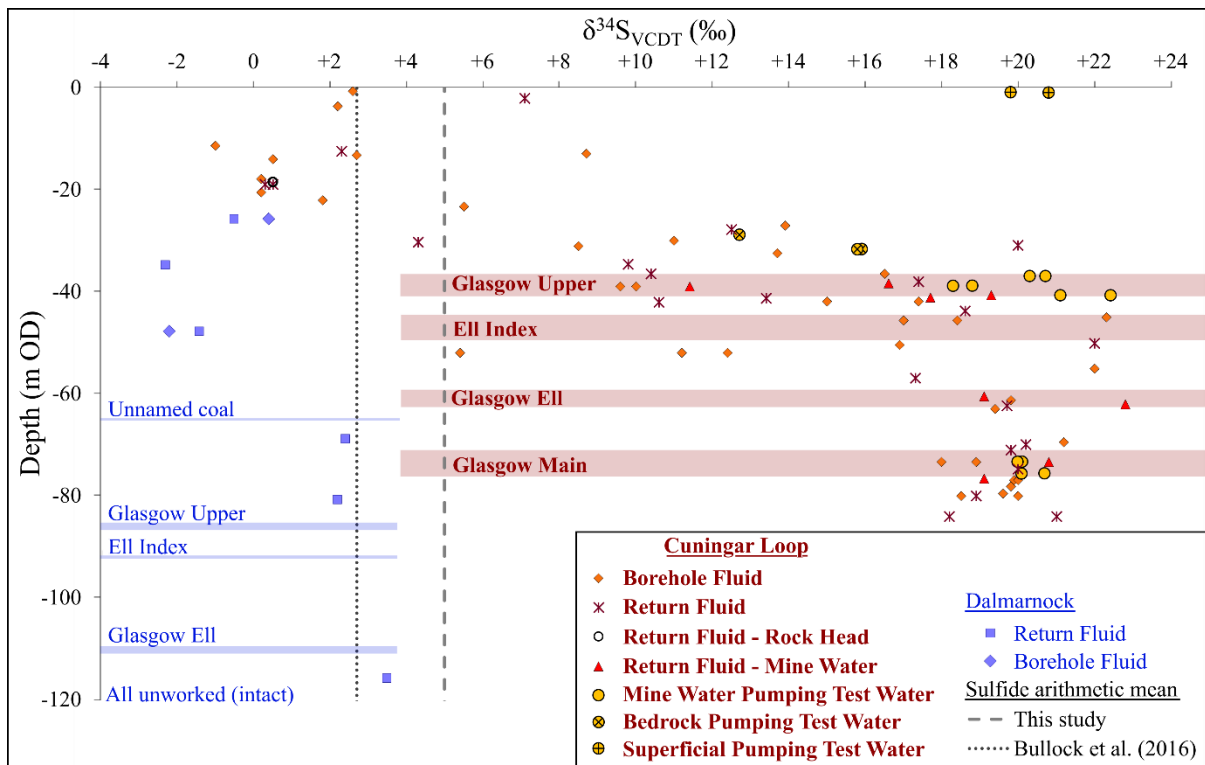


Figure 6.4 Plot of $\delta^{34}\text{S}$ isotope values versus depth for dissolved sulfate in water samples from both Dalmarnock and Cuningar Loop locations. Arithmetic means of the sulfide sulfur from this study and Bullock *et al.* (2018) are indicated by vertical dashed lines. Depths of coal seams are shown in blue bands (left) for the Dalmarnock location, and red bands (right) for Cuningar Loop. Note that the y-axis is in metres relative to Ordnance Datum (m OD), ground level is c. 10-12 m OD. Depth of the pumping test samples correlate with the depth of the screened section of the completed borehole.

6.4.3 Sulfate from Cuningar Loop water samples

Figure 6.4 plots $\delta^{34}\text{S}$ values from all 84 water samples from the boreholes at Cuningar Loop as well as the eight water samples from Dalmarnock (GGC01), against their respective depths. Note that despite being sampled from the surface, the borehole fluid samples are plotted relative to the total borehole depth at the time of sampling.

Sample Type	Date	Borehole depth (m bgl)	$\delta^{34}\text{S}$ (‰)
Borehole fluid	27/11/2018	35.5	+0.4
Borehole fluid	29/11/2018	57.5	-2.2
Return fluid	27/11/2018	35.5	-0.5
Return fluid	28/11/2018	44.5	-2.3
Return fluid	29/11/2018	57.5	-1.4
Return fluid	30/11/2018	78.5	+2.4
Return fluid	03/12/2018	90.5	+2.2
Return fluid	05/12/2018	125.5	+3.5
Arithmetic mean and standard deviation (n=8)			+0.3 ±2.1

Table 6.4 $\delta^{34}\text{S}$ isotope data from dissolved sulfate in fluids sampled during the drilling programme for the stratigraphic and seismic monitoring borehole (GGC01) at the Dalmarnock drilling location.

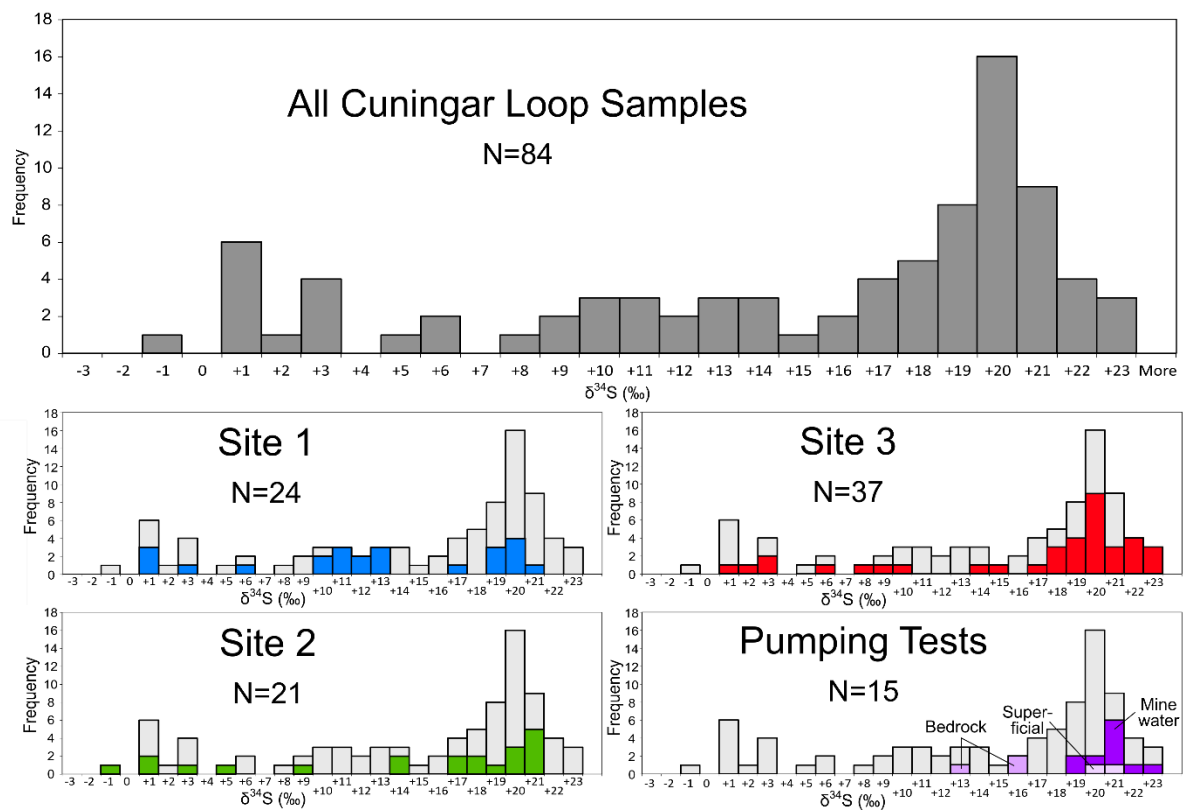


Figure 6.5 Histograms of $\delta^{34}\text{S}$ isotope values from the Cuningar Loop boreholes. (a) Active samples (Sample types B and C); all water samples except for borehole fluids as these were not sampled during active drilling or pumping (this histogram is repeated in all other plots as the background); (b) Site 1; (c) Site 2; (d) Site 3; (e) Pump test water samples only - all boreholes at Cuningar Loop combined.

6.4.3.1 Borehole Fluids and Return Fluids

The Cuningar Loop boreholes typically intersected coal workings at approximately -37 to -41 m OD (Glasgow Upper Coal seam), -59 to -63 m OD (Glasgow Ell Coal seam) and -71 to -76 m OD (Glasgow Main Coal seam) (Monaghan *et al.*, 2021c) (Figure 6.3). Overall, water samples from Cuningar Loop have $\delta^{34}\text{S}$ values which range between -1‰ and +23‰ with a

mode at +20‰ (Figure 6.5), however, further trends can be identified from Figure 6.4. $\delta^{34}\text{S}$ values of all Cuningar borehole fluid and return fluid samples taken between surface (c. +10 to +12 m OD) and -25 m OD fall within the range of -1‰ to +8.7‰. The mean for these depths (+2.3 \pm 2.7‰, n=15) is similar to that of the pyrite from rock samples, and that of the borehole fluid and return fluid samples of GGC01, where coal seams are intact. Below a depth of -25 m OD, the $\delta^{34}\text{S}$ values increase towards and cluster around values of +19‰ and +20‰ for the depth interval associated with the Glasgow Upper Coal seam (-37 to -41 m OD). In all Cuningar Loop boreholes, the samples from -65 m OD to the deepest sample locations at -84 m OD have a mean of +19.8 \pm 0.9‰ (n=21). The trend of $\delta^{34}\text{S}$ with depth in different boreholes can be visualised in Figure 6.3, where coloured symbols reflect the different groupings (buckets) of $\delta^{34}\text{S}$ values and represented by the histograms for each site in Figure 6.5. Sulfate isotopic values at Site 1 have a slightly different trend to the other two sites (2 and 3), Site 1 has an intermediate node, grouped around +10‰ to +13‰, described further in Section 6.4.3.3.

6.4.3.2 Cuningar Loop pumping test water

All water chemistry results of pumping test mine waters can be found in Palumbo-Roe *et al.* (2021b). Pumped groundwaters are bicarbonate (HCO_3^-) type with sodium (Na^+) as the dominant cation, except for boreholes GGA03r in bedrock and GGA09r in superficial deposits where calcium (Ca^{2+}) is the main cation (Palumbo-Roe *et al.*, 2021b). Pertinent chemical analyses from the pumping tests and other relevant samples, performed by the BGS, are summarised as arithmetic means presented in Table 6.5 alongside the major ion composition of typical modern seawater (Lenntech, 2022). Sulfate concentrations in the mains water supply to Dalmarnock are presented for 2021 as mean, minimum and maximum by Scottish Water (2021). They report a mean sulfate concentration of 7.55 mg/L (n=8) with a range between 7.20 and 8.40 mg/L. These values are low compared to the sulfate concentration in pumping test water samples from the boreholes completed into mine workings (n=10) which exhibit a mean of 171 mg/L and a range between 154 mg/L and 200 mg/L. We thus conclude that potential mixing of a component of drilling fluid in the samples is unlikely to significantly impact the dissolved sulfate $\delta^{34}\text{S}$ in the samples. The $\delta^{34}\text{S}$ values of dissolved sulfate in the pumping test water samples are shown as yellow circles in Figure 6.4 and are presented in Table 6.6. The boreholes which are completed into mine workings (-37 m OD and deeper) return a mean $\delta^{34}\text{S}$ value of +20.3 \pm 1.1‰ (n=10). The pumping test samples from bedrock above the coal seams return mean values of +15.9‰ (n=2) and +12.7‰ (n=1), from screened

		Units	Super-ficial (n=2)	Bedrock (n=3)	Glasgow Upper (n=6)	Glasgow Main (n=4)	Seawater from (Lenntech, 2022)
Field data	Temperature	°C	11.8	11.5	12.0	12.4	
	pH	pH units	7.1	7.0	7.1	7.2	
	Electrical Conductivity	µS/cm	1652	1812	1732	1684	
	Eh	mV	+211	+195	+166	+152	
	Alkalinity	meq/L	14.0	12.0	13.3	13.5	
Laboratory chemical data	F ⁻	mg/L	0.16	0.16	0.17	0.15	1
	Cl ⁻	mg/L	65.7	62.4	72.4	71.7	18,980
	SO ₄ ²⁻	mg/L	144	319	181	155	2649
	Br ⁻	mg/L	0.409	0.548	0.520	0.457	65
	Na	mg/L	139	152	181	174	10,556
	Ca	mg/L	143	131	108	107	400
	Mg	mg/L	49.3	62.5	53.5	54.9	1262
	K	mg/L	21.2	18.1	18.9	19.1	380
	Fe (dissolved)	µg/L	1895	13,030	3738	1910	
	Mn (dissolved)	µg/L	2522	500	409	331	
Chemical ratios	Cl ⁻ /Br ⁻ mass ratio		161	114	139	157	292
	SO ₄ ²⁻ /Cl ⁻ molar ratio		0.811	1.89	0.925	0.799	0.052
	Na/Cl ⁻ molar ratio		3.25	3.75	3.86	3.74	0.858
	(Ca+Mg)/SO ₄ ²⁻ meq ratio		3.72	1.75	2.59	3.05	2.24
	Ca/Mg molar ratio		1.76	1.27	1.23	1.18	0.192
	Ca/Alkalinity meq ratio		0.496	0.565	0.394	0.389	8.70
Iso-topes	δ ³⁴ S	‰	20.3	14.8	20.3	20.2	21.2

Table 6.5 Arithmetic means of the pump test water samples as grouped by the screen horizon. Field and laboratory chemical data from Palumbo-Roe et al. (2021b) compared with seawater from Lenntech (2022). Arithmetic mean sulfur isotopic values are added from this study, and Tostevin et al. (2014) for seawater.

sections at -34.3 m OD and -29 m OD respectively. The pumping test water samples from the boreholes completed into the superficial deposits, overlaid by significant thicknesses of made-ground (10-12m), in GGA06r (12.5 m bgl) and GGA09r (13 m bgl), returned δ³⁴S values of +19.8‰ and +20.8‰ respectively. The samples which were taken at the middle and end of each 5-hr pumping test proved to be consistent, the greatest difference (1.3‰) was between samples coming from GGA07.

Borehole	Screen depth (m bgl)	Screened Horizon	Test Stage	Sample Date	$\delta^{34}\text{S}$ (‰)
GGA06r	-0.9	Superficial deposits	End	31/01/2020	+19.8
GGA09r	-1.1	Superficial deposits	End	11/02/2020	+20.8
GGA03r	-29	Sandstone above workings	Middle	20/01/2020	+12.7
GGB05	-34.3	Sandstone above workings	Middle	14/02/2020	+15.9
GGB05	-34.3	Sandstone above workings	End	14/02/2020	+15.8
GGA04	-37	Glasgow Upper Coal	Middle	28/01/2020	+20.7
GGA04	-37	Glasgow Upper Coal	End	28/01/2020	+20.3
GGA01	-39.3	Glasgow Upper Coal	Middle	15/01/2020	+18.3
GGA01	-39.3	Glasgow Upper Coal	End	15/01/2020	+18.8
GGA07	-40.7	Glasgow Upper Coal	Middle	07/02/2020	+21.1
GGA07	-40.7	Glasgow Upper Coal	End	07/02/2020	+22.4
GGA05	-73.4	Glasgow Main Coal	Middle	23/01/2020	+20.1
GGA05	-73.4	Glasgow Main Coal	End	23/01/2020	+20
GGA08	-75.6	Glasgow Main Coal	Middle	04/02/2020	+20.1
GGA08	-75.6	Glasgow Main Coal	End	04/02/2020	+20.7

Table 6.6 $\delta^{34}\text{S}$ values from Cuningar pumping test water samples.

6.4.3.3 Concentration vs $\delta^{34}\text{S}$

The deepest borehole at each of the three Cuningar Loop sites (GGA02, GGA05 and GGA08) penetrated the worked Glasgow Main Coal seam (Figure 6.2). Comparisons of trends between dissolved sulfate concentration, sulfate $\delta^{34}\text{S}$ and depth of each water sample from GGA02, GGA05 and GGA08 are presented in Figure 6.6. They illustrate overall increasing $\delta^{34}\text{S}$ and sulfate concentration with depth. The sulfate concentration of all samples becomes more consistent with depth, plotting at c. 170 mg/L at depths associated with the Glasgow Main Coal. There is no obvious overall correlation between $\delta^{34}\text{S}$ and sulfur concentration. In each of these plots an anomaly is presented by GGA02 (Site 1), whereby the samples associated with the depth of the Glasgow Upper Coal workings (present at -39 m OD) have an elevated sulfate concentration (grouping around 250-400 mg/L) and show intermediate $\delta^{34}\text{S}$ values (+10.2 \pm 2‰, n=9). Note that some of these intermediate plots are deeper than the quoted horizon for the Glasgow Upper, but since the Glasgow Upper mine water likely dominates the drilling fluid until the next responsive horizon, the signature will likely remain. The Ell Index Coal seam was unworked in GGA02, and thus the next mine water signature was intersected at the Glasgow Ell Coal seam, at c. -60 m OD.

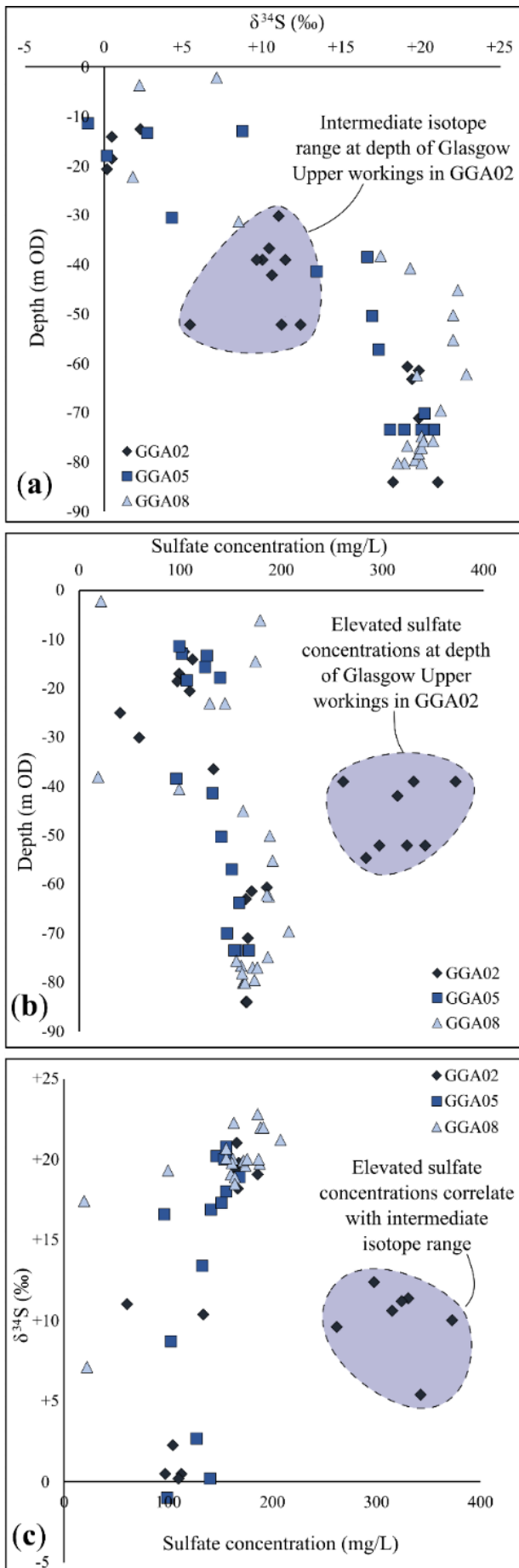


Figure 6.6 Plots from the deepest boreholes from each of Site 1, 2 and 3 within Cuningar Loop, showing **a)** $\delta^{34}\text{S}$ values with depth (m OD); **b)** sulfate concentration with depth; and **c)** $\delta^{34}\text{S}$ values plotted against sulfate concentration. Blue polygons highlight GGC02 anomalies with elevated sulfate concentrations and intermediate $\delta^{34}\text{S}$ values. Plot contains all sample types (A, B and C).

6.4.4 Sulfate S isotopes in Lower Carboniferous gypsum

The sulfur isotope data from the gypsum samples of the Ballagan Formation are shown in Table 6.7. $\delta^{34}\text{S}$ values range from +18.1‰ to +19.9‰, with a mean of $+18.9 \pm 0.5\text{‰}$ (n=17). Samples from west and east of the Glen Fault had means of $+18.7 \pm 0.4\text{‰}$, n=8 and $+19.0 \pm 0.5\text{‰}$, n=7, respectively. As the standard deviations cited on these means all overlap, there is little statistically significant difference between sample groups on either side of the fault. Similarly, there is little statistically significant difference between the three facies or the three distinct paragenetic presentations of the gypsum (yellow, orange and platy).

Sample	Facies	Fault side	$\delta^{34}\text{S}$ (‰)
BG1 clear	1	West	+18.1
BG1 orange	1	West	+18.7
BG1 orange (repeat)	1	West	+18.7
BG5 red plates	1	East	+19.3
BG5 red plates (repeat)	1	East	+18.4
BG5 red plates (repeat)	1	East	+19.0
BG5 red infill	1	East	+18.6
BG5 red infill	1	East	+19.3
BG5 yellow	1	East	+19.9
BG2 (upper)	2	West	+19.1
BG2 (upper) (repeat)	2	West	+19.2
BG3 (lower)	2	West	+18.1
BG3 (lower)	2	West	+18.3
BG6	2	East	+18.5
BG4	3	West	+19.1
BG4	3	West	+19.1
BLV 1	2	*	+19.5
Arithmetic mean and standard deviation (n=17)			+18.9 ±0.5

Table 6.7 $\delta^{34}\text{S}$ values of Ballagan Formation gypsum evaporite samples from Ballagan Glen. * - museum sample without record of fault side. Facies column indicates chrono-stratigraphical ordering of sample beds, where 1 is the oldest.

6.4.5 Oxygen and hydrogen isotopic data

O and H isotopic results of sampled waters are shown in Figure 6.7, plotted against the global meteoric water line (GMWL) (Craig, 1961) and a local meteoric water line (LMWL) derived from nearby Glasgow rainwater samples (Walls *et al.*, 2022). A single mains water sample from January 2019 returned values of -7.3‰ and -49‰ for $\delta^{18}\text{O}$ and $\delta^2\text{H}$ respectively, plotting on the GMWL and the LMWL. The mean values for the pumping test samples from the mine water boreholes are -7.6‰ and -49‰ for $\delta^{18}\text{O}$ and $\delta^2\text{H}$ respectively, falling close to the LMWL and GMWL.

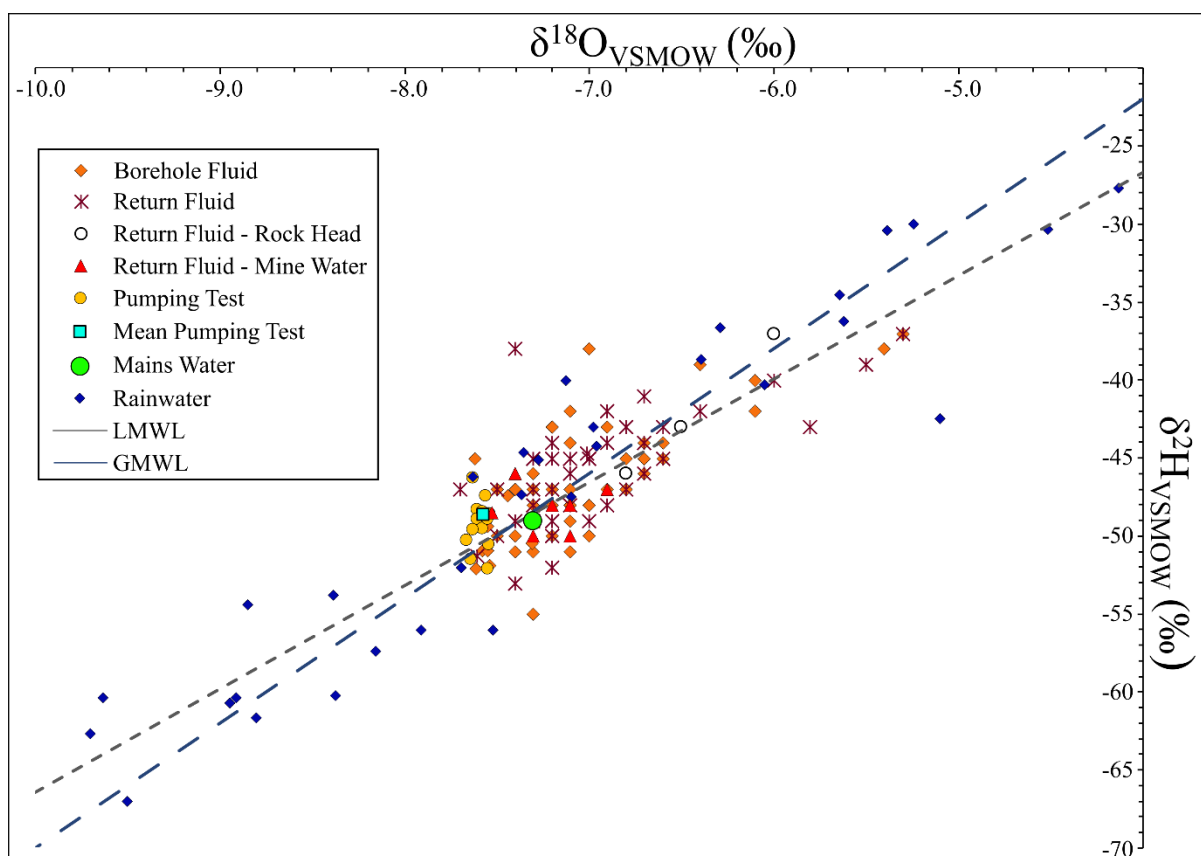


Figure 6.7 Standard $\delta^{18}\text{O}$ and $\delta^2\text{H}$ from all GGERFS water samples (including mains water), plotted against the global meteoric water line (Craig, 1961) and rainwater data collected at the University of Glasgow between December 2016 and February 2020 (Walls *et al.*, 2022), comprising the local meteoric water line.

6.5 Discussion

$\delta^{34}\text{S}$ analysis of pyrite in coal seams (worked and unworked) in and around the GGERFS show a large range, with a mean value of $+5.0 \pm 15.5\%$ ($n=7$). The range and mean value are consistent with regional pyrite values, which average $+2.7 \pm 9.5\%$ ($n=21$) (Bullock *et al.*, 2018). Borehole fluid and return water sulfate signatures from Dalmarnock (GGC01) show limited variation ($+0.3 \pm 2.1\%$, $n=8$), plotting within the value range and close to the mean of local pyrite, thus could be reasonably explained as a direct product of pyrite oxidation. A positive correlation between sulfate $\delta^{34}\text{S}$ values and depth in GGC01 may suggest subsurface processes driving minor enrichment of ^{34}S in unmined strata, however, return and borehole fluid samples each represent a bulk value of contributions from drilling fluid and all groundwater-bearing bedrock horizons encountered during drilling. Equally, the isotopically elevated values for the deepest three GGC01 samples may reflect a marginally high sulfide $\delta^{34}\text{S}$ signature related to the coal seams, indicated on Table 6.4.

Return fluid – mine water samples from the Cuningar Loop boreholes exhibit much higher values ($+18.4 \pm 3.4\%$, $n=8$) and mine water borehole pumping test water samples, which

most closely represent true mine water, have a mean $\delta^{34}\text{S}$ value of $+20.3 \pm 1.1\%$ (n=10). These elevated values cannot be simply explained by oxidation of host coal or sedimentary sequence pyrite alone and thus raise three questions:

- Since typical oxidation of sulfide minerals is widely accepted to proceed with negligible isotopic fractionation, what is the source of isotopically elevated sulfate in the mine water?
- Why does it only affect groundwater present in mined coal seams, and not groundwater from unmined strata?
- Why do the pumping test samples from the environmental baseline monitoring boreholes completed into superficial deposits show similarly elevated ^{34}S , and those into bedrock show somewhat elevated (intermediate) isotopic values?

Banks *et al.* (2020) found elevated sulfate $\delta^{34}\text{S}$ in deeper mine waters and found lower values, compatible with oxidised pyrite, in shallow mine waters across several European coalfields and a new study from North East England revealed the same phenomenon (Banks and Boyce, 2023). They concluded that elevated $\delta^{34}\text{S}$ in mine waters in Spain and Poland were compatible with evaporite dissolution, but noted that such a source was unlikely to explain elevated values at sites in England (Banks *et al.*, 2020).

The following sources of isotopic sulfate enriched in ^{34}S have been hypothesized (Banks *et al.*, 2020, Chen *et al.*, 2020, Younger *et al.*, 2015):

1. Concentrated brines which percolated into bedrock during formation of sabkhas or evaporites at surface; the evaporites may have since been eroded.
2. Infiltration of geologically recent marine water to the coal-bearing strata of Cuningar loop.
3. A residual (connate or derived from marine transgression in post Carboniferous geological time) saline water component in deep mine waters and Carboniferous strata.
4. Concentration of dissolved salts (including sulfate), upon deep freezing by permafrost conditions during Pleistocene glaciations.
5. Dissolution of evaporite minerals (gypsum or anhydrite) present in subjacent or superjacent strata (e.g., Carboniferous Ballagan Formation).
6. Bacterial reduction of sulfate to sulfide, preferentially removing ^{32}S and enriching the remaining sulfate with ^{34}S .

Banks *et al.* (2020) also propose that an equilibrium in groundwater/mine water may continually shift between $\delta^{34}\text{S}$ end members depending on the rates of input/removal of dissolved sulfate by weathering of sulfide and sulfate minerals, and/or bacterial/thermal sulfate reduction to sulfide minerals.

Exploring the potential sources of sulfate requires parallel analysis with other chemical properties, and correlation with local geologic setting/history. When including water chemistry analysis, it is important to understand the nature of the water samples and what they truly represent. Since mains water was used as the drilling fluid, each of the return fluid and borehole samples are a mix of ground water (mining-influenced or not) and mains water, thus elemental concentrations are diluted by the ion-poor mains water presented in Table 6.2 (Scottish Water, 2021, Shorter *et al.*, 2021b). It is important to note that diluted dissolved sulfate concentrations are unlikely to affect the $\delta^{34}\text{S}$ isotopic signature since the mean concentration in the tap water is only 7.08 mg/L (n=2) according to Shorter *et al.* (2021b) and around 7.5 mg/L according to Scottish Water (2021) (Table 6.2), but they will skew $\delta^{18}\text{O}$ and $\delta^2\text{H}$ isotopic ratios towards the mains water values. To avoid the issue of dilution, only pumping test water samples will be discussed, since they represent the truest samples from the target horizons. The following discussion uses the published hydrochemistry datasets for the UKGEOS water samples (Palumbo-Roe *et al.*, 2021b) which correlate with the pumping test water samples for $\delta^{34}\text{S}$ analysis in this study; the discussion also refers to baseline monitoring programmes for details on rainwater (O Dochartaigh *et al.*, 2011) and Lenntech's (2022) data for standard ocean water.

The following sections (6.5.1 – 6.5.5) address the six $\delta^{34}\text{S}$ enrichment process hypotheses outlined above and assess their potential influence on observed $\delta^{34}\text{S}$ values in the GGERFS system. Section 6.5.6 explores the mechanisms responsible for distributing elevated $\delta^{34}\text{S}$ sulfate through mine workings, whereas Section 6.5.7 addresses the sulfate concentration and isotopic anomaly observed at Site 1. Sections 6.5.8 and 6.5.9 postulate a source of high $\delta^{34}\text{S}$ in superficial and bedrock aquifer pumping test water samples respectively.

6.5.1 Hypothesis 1 - Concentrated brines

Walls *et al.* (2022) detail the geological setting of the Midland Valley of Scotland following the deposition of the Coal Measures strata. They suggest that evaporitic conditions from the Permian to Cretaceous could have led to percolating residual saline brines or dissolved paleo-evaporites, which in turn could contribute an isotopically elevated seawater/evaporite signature to the groundwater. Such brines are unlikely to be a major source of water molecules

to the groundwater since $\delta^{18}\text{O}$ and $\delta^2\text{H}$ isotopic ratios indicate that pumping test waters have not undergone significant fractionation from the GMWL and suggest a recent, Holocene meteoric origin (Darling *et al.*, 2003). Nonetheless, the sulfate from a small amount of concentrated brine could represent a significant component of the overall mine water sulfate concentration and influence its $\delta^{34}\text{S}$ signature. The dominance of modern meteoric water is typical for mine waters analysed for S isotopes across Europe (Banks *et al.*, 2020). Influence of a concentrated evaporitic brine which contributes sulfate enriched in ^{34}S in high enough concentrations to dominate the $\delta^{34}\text{S}$ isotopic signature without skewing the $\delta^{18}\text{O}$ and $\delta^2\text{H}$ signatures, cannot be ruled out.

6.5.2 Hypothesis 2 - Recent marine water

Recent marine water ingressions would impart a significant chloride content on mine waters. The chloride concentrations of the 10 pumping test waters from the Glasgow Upper and Main Coal seams range between 70.9 and 75.9 mg/L (Palumbo-Roe *et al.*, 2021b), which are elevated compared to the probable chloride concentration of infiltrating rainwater, c. 7 mg/L (O Dochartaigh *et al.*, 2011), even when evapotranspirative upconcentration is considered. Although it should be remembered that sulfate and chloride concentrations in rainfall would have been substantially greater in the period immediately following the industrial revolution (Fowler *et al.*, 1982), with values as high as 70 mg/L sulfate being reported in Glasgow rainfall by Smith (1872).

The observed chloride concentrations from UKGEOS also exceed the 75th percentile value for unmined Coal Measures groundwater (50 mg/L) (O Dochartaigh *et al.*, 2011), suggesting that there is an additional source of chloride in the mine waters, beyond that of infiltrating rainwater. They exceed the range for the River Clyde (16-40 mg/L) but plot within the range of the Tollcross Burn (41-138 mg/L, mean 65 mg/L) (Fordyce *et al.*, 2021), suggesting that chloride in the stream may be introduced by water influenced by urban activities e.g., salting roads. The Clyde adjacent to Cuningar Loop has a water level of c. +3 m OD and is non-tidal and fresh, the tidal limit being the tidal weir adjacent to Glasgow Green, built in 1901 at NS 59511 64374. It is interesting to speculate as to the degree tidal and marine (and hence saline) influence may have extended up the Clyde prior to its construction. Historically, the Clyde was tidal and navigable as far upstream as Rutherglen (Secret Scotland, 2023, Undiscovered Scotland, 2023). One should further note that the published geological

maps show raised marine and glaciomarine silts and clays as far inland as Cuningar, indicating marine inundation in Pleistocene times (British Geological Survey, 1992a).

The mine water samples all have sulfate/chloride molar ratios (mean = 0.87) much greater than modern seawater (0.05) (Lenntech, 2022), similarly, sodium/chloride molar ratios are greatly elevated (mean = 3.81) versus seawater (0.86) (Table 6.5). These ratios indicate that sulfate and sodium have been added to the system without chloride, i.e., from a source which is not of recent marine origin. The chloride/bromide mass ratios of the mine waters (mean = 147) are half that of seawater (292) (Lenntech, 2022), and within the range of typical shallow groundwater (100-200) (Davis *et al.*, 1998). Whilst the sulfur isotopic composition of modern seawater is similar to that found in the mine waters, the other aspects are distinct. This evidence is enough to eliminate recent marine ingress as a controlling factor on mine water $\delta^{34}\text{S}$ signature.

6.5.3 Hypothesis 3 - Residual saline water; and 4 - Cryoconcentration

The moderately low chloride content diminishes the possible role of percolating freeze-out concentrated groundwaters formed during Pleistocene permafrost formation. Moreover, although cryoconcentration could increase chloride and sulfate concentrations, it would not be expected to systematically elevate the $\delta^{34}\text{S}$. Similarly, the modest chloride concentrations argue against the influence of deeper chloride-rich saline waters, known to affect mine waters elsewhere in the UK, particularly the NE of England (Younger *et al.*, 2015).

6.5.4 Hypothesis 5 - Evaporite mineral dissolution

Ballagan Formation gypsum samples exhibit a narrow $\delta^{34}\text{S}$ range between +18.1‰ and +19.9‰ (mean +18.9 ± 0.5‰) (n=17), well within the range of $\delta^{34}\text{S}$ for Lower Carboniferous seawater sulfate (Claypool *et al.*, 1980), strongly suggesting that the sulfate source for Ballagan Formation gypsum deposits is contemporaneous marine sulfate. Dissolution of these evaporite deposits by groundwater would impart a distinct $\delta^{34}\text{S}$ isotopic signature on dissolved sulfate around 1.5‰ to 2‰ lower than the solid phase, thus around +16.9‰ to +17.4‰ (Driessche *et al.*, 2016). Dissolution of gypsum would contribute calcium to the waters whilst enriching the sulfate $\delta^{34}\text{S}$ isotopic signature; however, no clear correlation is observed between $\delta^{34}\text{S}$ and calcium concentration. Whilst these findings do not support evaporite dissolution, it should be noted that other processes including calcite saturation can suppress calcium concentrations, meaning that a correlation can be lost even with a shared generic origin.

The Ballagan Formation evaporite minerals are primarily gypsum, but there are anhydrite and halite present (Millward *et al.*, 2018). Dissolution of gypsum would contribute sulfate with the high $\delta^{34}\text{S}$ signature described above, whilst dissolution of halite would contribute chloride and importantly, impart a chloride/bromide ratio as high as 1000-10,000 (Davis *et al.*, 1998). As discussed for hypothesis 2, the mine water chloride/bromide ratios are below the values of seawater (292), and thus are well below these evaporite signatures. If halite comprises only a very minor portion of the evaporite solutes or are entirely absent, then the chloride/bromide ratio may not be affected, or may be buffered by elevated bromide in coals (Davis *et al.*, 1998). Furthermore, it cannot be ignored that the Ballagan Formation, despite being the most regionally abundant sulfate source within the Carboniferous sequence, has a significant c. 1500m stratigraphical separation from the Middle Coal Measures Formation and a mechanism for upwards evaporite brine migration from the Ballagan formation would need to be proposed for this to be a realistic hypothesis. Each of these points indicate that evaporite dissolution is an unlikely source for the enriched $\delta^{34}\text{S}$ isotopic signature, but it cannot be ruled out entirely.

6.5.5 Hypothesis 6 - Bacterial reduction

Detection of H_2S at the surface whilst penetrating mined coal seams during drilling (Barron *et al.*, 2020a, Monaghan *et al.*, 2020b) suggests that sulfate-reducing bacteria are present in the mine water at the site. It is accepted that bacterial fractionation can shift the bulk $\delta^{34}\text{S}$ of the dissolved sulfate phase towards its elevated end member, by preferential removal of ^{32}S . However, whether this process is significant enough to fractionate the hypothetical initial sulfate signature from oxidised pyrite ($+5.0 \pm 15.5\%$, $n=7$) to the higher values in measured mine water samples ($+20.3 \pm 1.1\%$, $n=10$) remains unclear. For this to be a viable hypothesis, the rate of bacterial sulfate reduction needs to be of a similar order of magnitude to that rate of sulfate introduction to groundwater (e.g., by pyrite oxidation). It is hypothesised that the rate of pyrite oxidation in completely flooded mine workings is likely to be relatively low (Younger, 1997). The data indicate that the $\delta^{34}\text{S}$ signature is relatively consistent at all levels of mine workings at the GGERFS, where all samples deeper than -65 m OD have a mean of $+19.8 \pm 0.9\%$ ($n=21$) and the pumping test water samples exhibit a mean of $+20.3 \pm 1.1\%$ ($n=10$) indicating that the mined system is well mixed.

$\delta^{34}\text{S}$ values and alkalinity for all samples exhibit an overall positive correlation, whereby the pumping test samples have the highest values of both. This trend can be an

indication of activity by sulfate-reducing bacteria in relatively stagnant, anoxic groundwater (Brown *et al.*, 2002). However, the trend may not be unique to sulfate reduction, since evaporite dissolution of the Ballagan Formation would require deep-seated, long residence time waters, evoking high alkalinity.

6.5.6 Movement of waters with elevated dissolved sulfate $\delta^{34}\text{S}$

Should elevated $\delta^{34}\text{S}$ observed in the mine water have originated from deeper ("sulfate-rich, chloride-poor") groundwaters, e.g., those affected by evaporite brines or dissolution (Hypotheses 1 and 5), then their upwards transport must be explored. A potential migration pathway to Scottish Coal Measures Formation strata is via discrete permeable features, such as the Shettleston Fault, 1-2 km to the north of Cuningar Loop (British Geological Survey, 1992b). Following vertical transfer, these fluids might flow slowly through Upper Carboniferous aquifers of relatively modest permeability. Alternatively, mined coal strata would provide preferential flow pathways for such fluids. This may explain why sulfate in the water samples of the unmined sequence (GGC01) do not return any elevated $\delta^{34}\text{S}$ values, while water in mined workings has been able to transmit the elevated $\delta^{34}\text{S}$ to the Cuningar area.

Furthermore, one could hypothesise that waters with elevated sulfate- $\delta^{34}\text{S}$ reflect longer residence times in deeper, reducing, oxygen poor mine waters where bacterial sulfate reduction may occur, removing sulphur as ^{32}S -enriched pyrite and leaving the residual dissolved sulphate enriched in ^{34}S . Waters with short residence times may be associated with pyrite oxidation dominated $\delta^{34}\text{S}$ since these waters will have been most recently in contact with the atmosphere, inducing oxidation. Networks of mined strata, connected by shafts and drifts, provide a potential throughflow and mixing environment with high lateral and vertical connectivity, allowing a component of longer residence high $\delta^{34}\text{S}$ sulfate-rich brines to manifest in the near surface environment.

6.5.7 Alternative contribution in Site 1

Water samples from borehole GGA02, within Site 1 at Cuningar Loop (see Figure 6.2), exhibit three distinct populations which increase in $\delta^{34}\text{S}$ with depth (Figure 6.6a). Shallow samples (to c. -20 m OD) reflect typical values of oxidised pyrite in the coal-bearing strata, similar to those seen through the entire sequence in the unmined strata of GGC01. Deep samples, from c. -60 m OD and below, likely influenced by the Glasgow Main Coal seam at -84 m OD, returned $\delta^{34}\text{S}$ values of sulfate between +19‰ and +20‰. The middle sequence of

samples (from c. -30 to -52 m OD), which are likely influenced by the Glasgow Upper Coal seam (-39 m OD), exhibit $\delta^{34}\text{S}$ values of intermediate range ($+10.2 \pm 2\%$, $n=9$).

Water samples taken during drilling through superficial deposits and bedrock above the first worked coal seam (Glasgow Upper Coal) contain sulfate concentrations with an arithmetic mean of 110 mg/L. Values from GGA05 and GGA08 show a gradual increase towards 170 mg/L in the basal Glasgow Main Coal samples. Glasgow Upper Coal related samples from GGA02 (arithmetic mean of 320 mg/L) stand apart from the rest of the data (Figure 6.6b). With their intermediate $\delta^{34}\text{S}$ values, these samples could be explained by either (a) a mixture of isotopically enriched ^{32}S -sulfate derived from intense pyrite oxidation with a component of deeper, ^{34}S -enriched groundwater, or (b) a lesser degree of bacterial sulfate reduction (BSR) relative to pyrite oxidation, resulting in a niche with higher sulfate concentrations and a correspondingly lower degree of BSR-related fractionation enrichment of ^{34}S in the dissolved sulfate.

Further relevant factors may be that GGA02 was the only borehole which used borehole purging to sample the Glasgow Upper Coal seam groundwater during drilling, potentially mixing stratified waters. It is noted that GGA05 was also purged but following collection of samples for this study. Otherwise, GGA02 was the only borehole subject to cement-based grouting in between drilling episodes, done to prevent connection of the Glasgow Upper and the other worked coal seams and mixing of the mine waters from different horizons as per SEPA requirement (Monaghan *et al.*, 2020b).

Portland cement often contains a small amount of sulfate (1-3% SO_3 as a percentage of total oxides), typically as a result of addition of gypsum during milling (Bogue, 1929, Builders Booklet, 2021, Kirby and Kanare, 1988, Zhang, 2011). Despite this, intermediate $\delta^{34}\text{S}$ values for three samples ($+10.4$ to $+11.4\%$), and elevated sulfate for the one return fluid - mine water sample (331 mg/L) pre-date the grouting episodes in GGA02, rules out grouting as a plausible explanation for the observations.

A potential explanation may be that the elevated sulfate and intermediate $\delta^{34}\text{S}$ results have arisen from greater rates of sulfide oxidation in the Glasgow Upper Coal seam and the surrounding strata, connected by extensive fracture networks. Site 1 is the only of the three to be mined via total extraction techniques, whereby older, elongated pillar and stalls were “robbed” (Monaghan *et al.*, 2020b), both Sites 2 and 3 were worked using the pillar and stall method (Barron *et al.*, 2020a, Barron *et al.*, 2020b). It may be that roof strata collapse and fracturing, not seen in Sites 2 and 3, allow a good hydraulic connection for meteoric waters to maintain oxidising conditions in the shallow Glasgow Upper Coal seam whilst simultaneously

granting access to the overlying fine grained sandstone which hosts occasional pyrite and traces of iron staining (Monaghan *et al.*, 2020b). It is also noted that subsequent groundwater sampling from the Glasgow Upper Coal seam by the BGS in an adjacent hole in Site 1, GGA01 (Figure 6.2) shows remarkably increased sulfate production from September 2020 to May 2021 rising from 1157 mg/L to a maximum of 1409 mg/L (Bearcock *et al.*, 2022). This correlates with an increase in iron concentration across the same timeline, further suggesting extensive pyrite oxidation.

6.5.8 Superficial groundwater dissolved sulfate $\delta^{34}\text{S}$

The groundwater from the superficial deposits have a high dissolved solute content, where pumping test water samples from GGA06r and GGA09r have arithmetic mean electrical conductivity values of 1675 $\mu\text{S}/\text{cm}$, interpreted as a result of anthropogenic inputs from the urban and industrial environment (Palumbo-Roe *et al.*, 2021a). High $\delta^{34}\text{S}$ values of the two pumping test water samples (+19.8‰ and +20.8‰) and where calcium is the dominant cation in GGA09r suggest influence of waters affected by dissolution of gypsum in building materials (plaster, cement). Gypsum for construction materials has been mined in the UK from primarily Permian and Triassic age deposits (Bell, 1994), and thus would host $\delta^{34}\text{S}$ between +10.9‰ and +25.8‰ (Kampschulte and Strauss, 2004). The superficial horizon accessed by these two environmental monitoring boreholes is the Gourock Sand Member. It exhibits moderate hydraulic conductivity values (median of 1.027 m day^{-1} (Williams *et al.*, 2017)) and lies directly beneath the anthropogenic made-ground, thus anthropogenically-altered groundwater can be expected to be sampled as part of the test pumping programme in GGA06r and GGA09r. Beneath the Gourock Sand Member, c. 11 m deposits of the Paisley Clay Member and c. 7 m of the Wilderness Till Formation with median hydraulic conductivities of 0.062 m day^{-1} and 0.032 m day^{-1} respectively (Williams *et al.*, 2017). It is likely that these are hydraulic barriers which prevent superficial groundwater flow from reaching bedrock in this locality. Furthermore, Shorter *et al.* (2020a) report resting groundwater head for superficial, bedrock and mine water aquifers which indicate the presence of an upwards hydraulic gradient. This source of elevated $\delta^{34}\text{S}$ should not be considered for the values exhibited by the samples from the mine workings.

6.5.9 Bedrock groundwater dissolved sulfate $\delta^{34}\text{S}$

The dissolved sulfate $\delta^{34}\text{S}$ of the test pumping samples from each of the two environmental baseline monitoring boreholes were +12.7‰ for GGA03r, and two samples of +15.9 and +15.8 for GGB05. These boreholes were terminated in bedrock c. 8 m (GGA03r) and 5 m (GGB05) above the stratigraphically highest coal seam (Glasgow Upper Coal). Upon test pumping, GGB05 gave a high transmissivity value of 580 m², rare for Carboniferous sandstones (Ó Dochartaigh *et al.*, 2015) and expected to be associated with extensive fracturing. It is suggested that the fracturing is induced by the mining beneath (Shorter *et al.*, 2020a), and it is likely that the fractures allow a portion of mine water to be abstracted during pumping. It is postulated that addition of a portion of mine water with elevated sulfate- $\delta^{34}\text{S}$ during pumping is responsible for increasing the $\delta^{34}\text{S}$ towards its ³⁴S enriched end member.

The bedrock test pumping samples exhibit the highest sulfate concentrations which suggests a considerable input from pyrite oxidation. The isotopic equilibrium between sulfate from oxidising pyrite and that from mine water influence is likely to be different for GGA03r. It has a calculated transmissivity value of 2.6 m², indicating that fractures are less dominant. GGA03r did, however, show responses to pumping each of the three boreholes completed in the Glasgow Upper Coal workings (Shorter *et al.*, 2020a) and hence is not hydraulically separate from the mine workings.

6.6 Conclusion

Mine waters from the UK Geoenergy Observatory's Glasgow Geothermal Energy Research Field Site have been sampled from multiple mined coal seams upon first entry via drilling at Cuningar Loop, and the $\delta^{34}\text{S}$ signature of their dissolved sulfate has been determined. Alongside samples of mine water, drilling fluids which had interacted with portions of mined and unmined strata of the same horizons were collected from the GGC01 borehole in Dalmarnock, as well as sulfide bearing minerals (pyrite) in the host bedrock and local evaporite (gypsum) deposits from the Ballagan Formation.

Samples of water which had interacted with the 199 m unmined sequence of Scottish Middle Coal Measures in GGC01 show dissolved sulfate- $\delta^{34}\text{S}$ values (+0.3 ±2.1‰, n=8) consistent with a sulfide oxidation origin (+5.0 ±15.5‰, n=7). A markedly different and higher dissolved sulfate $\delta^{34}\text{S}$ is observed in water from mined coal seams at the Cuningar Loop sites (+20.3 ±1.1‰, n=10). This is consistent with observations from previous European coal mine

systems and suggests that the origin of dissolved sulfate in coal mine waters cannot be fully explained by pyrite oxidation.

Across six boreholes at Cuningar Loop, drilled through three worked coal seams, the strongest influence of pyrite oxidation was observed in borehole GGA02 at the level of the Glasgow Upper Coal workings. This was indicated by intermediate $\delta^{34}\text{S}$ values and elevated sulfate concentrations and underlines the importance of spatial and temporal monitoring of flooded mine workings to identify the varied geochemical niches which may be present.

Potential explanations for the elevated dissolved sulfate $\delta^{34}\text{S}$ in most mine waters include incorporation of fluids derived from evaporite brines or dissolved (evaporite) minerals. The former involves contribution of elevated sulfate- $\delta^{34}\text{S}$ from ancient evaporitic brines, retained in Carboniferous bedrock following erosion of their (e.g., Mesozoic) parent sedimentary successions. A small component of brine could dominate the sulfur isotopic signature, without $\delta^{18}\text{O}$ and $\delta^2\text{H}$ diverging from the recent meteoric signals demonstrated by mine water samples. Any influence of evaporitic minerals likely requires $\delta^{34}\text{S}$ -enriched sulfate derived from the most regionally abundant sulfate source in the Carboniferous sequence - the Ballagan Formation. However, there remains a large vertical separation (c. 1500 m) between the Lower Carboniferous Ballagan Formation and the Upper Carboniferous Middle Coal Measures which hosts the GGERFS. Moreover, the $\delta^{34}\text{S}$ values of the UKGEOS mine waters ($+20.3 \pm 1.1\%$, $n=10$) are marginally higher than the Ballagan evaporites ($+18.9 \pm 0.5\%$, $n=17$). Both of these hypotheses remain theoretically feasible, but their influence as controlling sources is largely unlikely.

Finally, the extent of bacterial reduction and fractionation of sulfate is not clear but remains a potential influencing factor on sulfur isotopic signatures. Whether such fractionation can be significant enough to elevate typical pyrite oxidation derived sulfate- $\delta^{34}\text{S}$ values up to around $+20\%$ remains uncertain and will depend on the relative rates of pyrite oxidation and bacterial sulfate reduction. The presence of hydrogen sulfide gas in the UKGEOS mine waters provides evidence for the activity of sulfate reducing bacteria. Overall, sulfate- $\delta^{34}\text{S}$ signatures likely reflect residence time of the mine waters, where elevated signatures may indicate long residence times in reducing, oxygen-poor conditions promoting fractionation by bacterial sulfate reduction. Short residence times indicate more oxidising recently recharged waters, favouring sulfate- $\delta^{34}\text{S}$ values indicative of pyrite oxidation.

Declaration of interests

The authors declare that they have no known competing financial interests or personal relationships that could have appeared to influence the work reported in this paper.

Author contributions

DBW: conceptualisation (supporting), project administration (lead), methodology (supporting), investigation (lead), data curation (lead), formal analysis (lead), writing – original draft (lead), writing – review and editing (equal).

AJB: conceptualisation (equal), funding (supporting), methodology (lead), investigation (supporting), data curation (supporting), formal analysis (equal), writing – review and editing (equal), supervision (equal).

DB: writing – review and editing (equal), formal analysis (supporting), supervision (equal).

NMB: conceptualisation (equal), funding (lead), methodology (supporting), project administration (supporting), formal analysis (supporting), writing – review and editing (equal), supervision (equal).

Funding

This research was supported by NERC NEIF grant 2301.0920. N.M.B is funded by a University of Strathclyde Chancellor's Fellowship. A.J.B is funded by the NERC National Environmental Isotope Facility award at SUERC (NEIF-SUERC, NE/S011587/1).

Acknowledgements

The authors are grateful to the members of the BGS staff who collected samples from each of the two drilling locations and arranged their collection with us. Thanks goes to Alison MacDonald for her help with isotopic analyses at SUERC. Thanks also goes to Anne McGarrity for her help with UofG laboratory processing and analyses.

Chapter 7 Conclusions, Recommendations and Further Work

7.1 Conclusions

Using published literature, interviews, questionnaires, geographic information systems processing, field exploration work and laboratory analysis, each of the five research questions from Chapter 1 have been answered. The key findings for each of the research questions are detailed below:

RQ1: What are the principal challenges for successful delivery of MWG systems, and how can these be overcome?

Challenges to MWG heating/cooling systems were found to be present across a project's life cycle and could be categorised into four main groups: planning, construction, operational and economic. Challenges with planning stemmed from factors including inherent project risk, multiple permitting authorities, and matching a sustainable thermal resource with appropriate surface demand. The Mine Water Geothermal Resource Atlas for Scotland (MiRAS) has been able to partially address the latter in Scotland by facilitating early site feasibility appraisal. Challenges during construction were found to be largely governed by capital expenditure. A primary factor which can induce higher initial spend is unpredictable and excessive drilling costs, which can result from a number of scenarios, e.g., extra use of steel casing to seal off non-targeted voids or multiple re-drilling episodes where workings are not encountered as expected. Pilot exploratory boreholes are a useful tool to de-risk the subsurface and indicate where a project's best chances of encountering responsive mine water horizons are. These can also be completed as observation boreholes to monitor mine water conditions prior to, throughout development of, and during the lifetime of an operational MWG scheme.

Operational challenges were found to be largely due to chemical properties of mine water and hydraulic conditions. Challenging water chemistry sometimes required management of dissolved gases, iron ochre scaling and corrosion of infrastructure. There were "good-practices" highlighted by projects which had overcome some of these challenges, the risk of clogging, for example, can be reduced by: (a) careful management of dissolved gases and exclusion of oxygen from any pipe work or heat exchange apparatus; (b) prevention of

cascading in abstraction and reinjection wells; (c) monitoring of pressure differentials at key points in pipework systems and across heat exchangers; (d) visual or CCTV inspection; (e) a regular program of sampling of mine water chemistry (Walls *et al.*, 2021, Chapter 2).

Economic challenges can span the entire MWG project lifecycle, originating with high upfront costs for drilling, installation, and infrastructure. Similarly, high operational costs result from pumping where mine water head is deep below ground level. Maintenance costs can be induced from each of the operational challenges, especially if there is a lack of expert contractors. Clear communication of project CAPEX and OPEX costs, alongside predicted return-on-investment with sound estimates for future electricity prices and coefficients of performance can encourage project uptake. Construction in locations with suitable mine water head can minimise pumping expenditure, and developing a market for specialist mine water operations and maintenance contractors can help these costs be minimised.

RQ2: Where are the optimal locations for MWG application in the MVS?

As mentioned above, the CAPEX of MWG systems can be a deterrent to project progression, as a result, prospective schemes with significantly lower CAPEX and subsurface risk profiles are more favourable for development. Many of TCA's existing treatment schemes present promising MWG resources since they already bring mine water to the surface and do not have a requirement to drill new boreholes. The total calculated heat pump delivery for all TCA treatment schemes is 24 MW, the largest of which (Blindwells, Frances and Polkemmet) are proximal to surface thermal demands such as housing stock or industrial sites. Discharges which are not treated by TCA exist across the MVS and in turn present a combined heat pump delivery of 23.9 MW. It is recognised that some of these are distal from thermal demands and therefore, are not easily integrable thermal resources.

Where treatment schemes or suitable discharges are not available, the Mine Water Geothermal Resource Atlas for Scotland (MiRAS) can be used to indicate areas which are attractive for open loop MWG systems with the lowest expected CAPEX and OPEX. This tool has been created using archival mining data from abandonment plans and mine water levels across Scotland. It prioritises low drilling costs by ensuring that targets are less than 250 m below ground level and considers pumping cost OPEX since it highlights areas based on their expected depth to mine water head. The MiRAS identified the best placed MWG areas across each of the coalfields in the MVS, showing the greatest density in the Central Coalfield, particularly in North Lanarkshire. The two types of resources (surface and subsurface) have

been combined and presented as a series of mine water geothermal resource maps for each of the 19 affected Scottish local authorities in Appendix 4A.

RQ3: What are the chemical properties of mine water across the MVS, and what implications do these have for MWG systems?

Understanding water chemistry is imperative for smooth operation of MWG systems, so mine water discharges from coalfields across the MVS were sampled for chemical determination. The resultant dataset provides indicative information for potential MWG systems completed into associated or nearby workings. Parameters such as total vs dissolved iron concentration, oxidation-reduction potential and electrical conductivity can be early indicators of problematic conditions which could lead to clogging or corrosion. The total iron concentration from untreated discharges in Scotland ranges between 0.4 mg/L and 74.8 mg/L, where the median is 4.23 mg/L. The dataset produced from this research is primarily indicative of shallow mine waters and has not necessarily revealed the quality of mine water at depth where there may be significant chemical stratification.

Combining flow rate and iron concentration indicates overall “iron loading” pollution of sampled discharges in this study. Flow rate also has a positive correlation with heat availability, and hence some of the most polluting discharges to Scottish water courses host the greatest thermal resource. The most prominent of these is Junkies Adit/Old Fordell, which currently expels 202 kg/day of iron into the River South Esk; with a flow rate measured at 88 L/s (Walls et al., 2022, Chapter 3) it presents 2.5 MW of available heat in the centre of the town of Dalkeith. It is in these cases that mine water treatment and pollution remediation can be achieved in parallel with low-carbon heating. It is strongly recommended that treatment of this discharge is complemented by the installation of a heating or cooling system.

The importance of baseline and ongoing monitoring has been stressed many times throughout the thesis. Understanding the geochemical signature of mine water cannot be understated in when working to implement best practice. As an example, the values for pH and Eh of water samples collected as part of this thesis have been plotted on a Pourbaix diagram in Figure 7.1. It shows how Eh and pH control oxidation status of iron, where equilibrium lines separate areas of different iron states, assuming water temperatures of 25°C. The surface water course samples of Dollar Burn have been plotted alongside mine water samples of shallow borehole samples from Dollar, all mine water gravity discharges found across the MVS, and the record of the pumped sample from Polkemmet mine water treatment site.

The oxidation reduction potential (ORP) values presented in the other chapters were converted to true Eh for plotting by addition of 199 mV as explained in Chapter 3. The results show that the surface water course samples plot with higher pH values and Eh values than many of the borehole samples and the MVS discharges. The Dollar mine water discharges have a lower pH than the bulk of the surface water samples but show similar Eh values. Both of these groups plot well within the $\text{Fe}(\text{OH})_3$ shaded area, reflecting that iron in those environments would be precipitated as insoluble ferric iron in ochre if equilibrium has been reached. This is not unexpected, since the oxidising nature of surface water and exposure to oxygen is a driver of ochre precipitation.

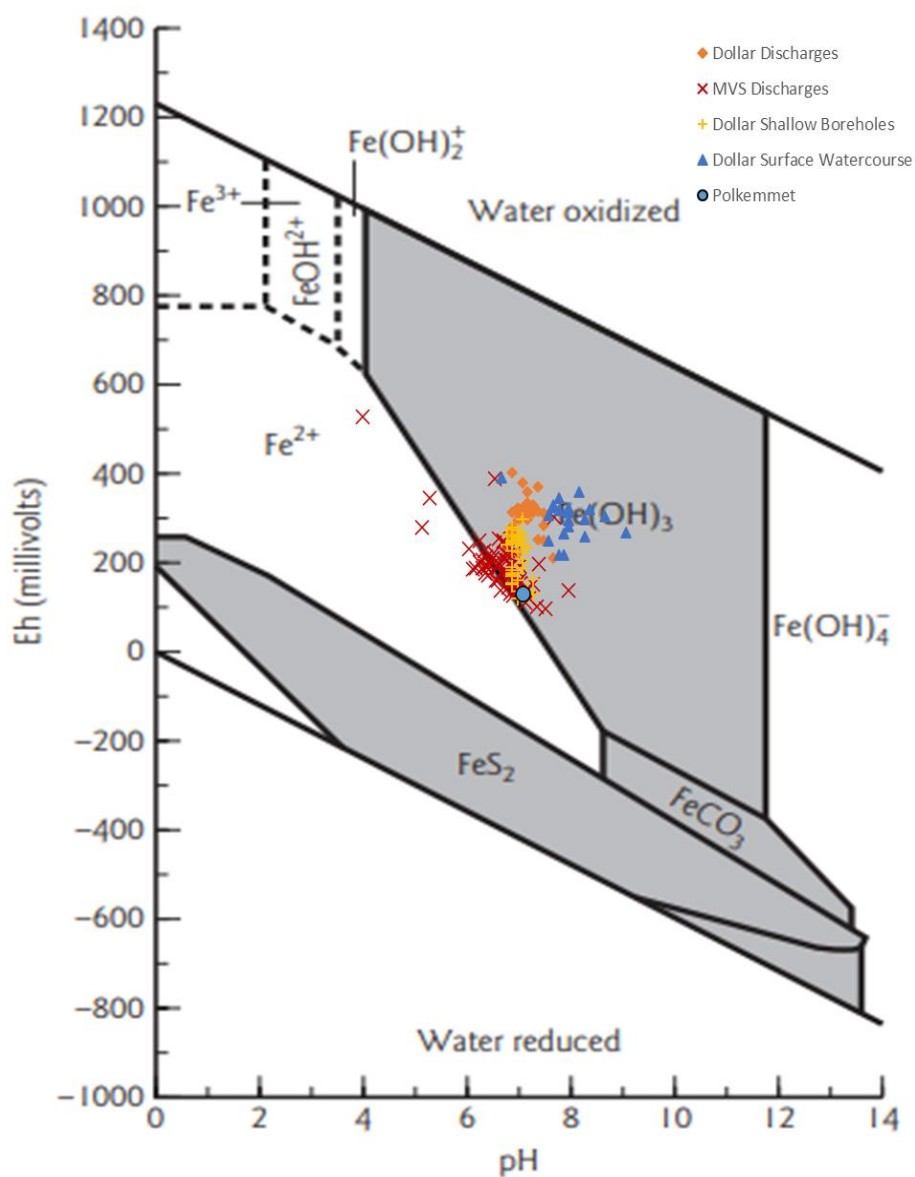


Figure 7.1 Pourbaix diagram for iron with samples plotted from Chapters 3 and 5 to indicate their iron status. Figure adapted from Younger (2007).

The values of the shallow (10-50 m BGL) mine water samples from the boreholes at the Dollar site show a constant pH around 7, but show a range of Eh values which deviate from the equilibrium line into the $\text{Fe}(\text{OH})_3$. This reflects the fact that despite being subsurface in origin, shallow mine workings can still have relatively fresh, oxidising waters which can host iron in both dissolved and non-dissolved states. Further analysis and longer pumping durations should be executed at Dollar before final conclusions are drawn about the long-term iron content as boreholes can create an access route for air. Hand pumping does not remove a significant volume of water despite pumping for over 5 minutes each time.

The discharges from across the MVS are sourced from a range of depths and derived from differing residence times, thus may host mine water representative of deeper mine workings, which has been characterised in Chapter 3 by higher solute content and more reducing conditions. The discharges are also circum-neutral, but typically show lower Eh values than the Dollar samples. The discharges are spread across the equilibrium line and thus, at the point of emergence, some discharges can be expected to host iron in its dissolved state (Fe^{2+}).

Similar analyses can be incorporated to the interpretation of baseline monitoring results to ensure project partners are well informed of what challenges may be present. Inclusion of expert hydrogeologists and geochemists will better inform mitigation strategies when dealing with problematic water chemistry.

RQ4: Can MWG investigation become more commonplace by inclusion of geothermal evaluations into routine ground stability investigations (GSI)?

Ground stability investigative drilling was employed at a research field site in Dollar, Clackmannanshire, where the landowner intends to construct a district heating network for up to 200 houses. The GSI operations were expanded to include MWG investigative boreholes which accessed mine workings marginally deeper than the original GSI scope, and mandated completion of GSI boreholes which intersected hydraulically responsive mine workings as observation boreholes. Combining GSI data with year-long monitoring and water sampling of the observation boreholes and discharges has demonstrated that the mine workings are hydraulically connected, and that a mine water geothermal system is feasible, provided that recommendations from the confidential ground stability report are adhered to.

The gravity discharge from the Dollar mine workings flows at rates between 5.6 L/s in summer and 9.1 L/s in winter, which could be harnessed to provide heating for new-build houses. The cost of GSI and exploratory drilling for MWG investigation are higher when done

separately. Thus, with some additional cost to the GSI budget, boreholes can be completed into shallow mines to assess geothermal potential. It is best practice for MWG systems that coal seams maintain hydraulic separation when drilling, so that short circuiting flow pathways are not created. Similarly, if trying to understand hydraulic conditions within the mines, exhaustive data collection on hydrogeologic features should be performed before initialising the drilling programme. Hydraulic regimes may change during drilling and a complete data set will assist understanding any changes that occur.

RQ5: How can stable isotope data contribute to understanding hydrogeology in MWG systems?

Stable isotopes of sulphur, oxygen and hydrogen were collected from MVS mine water discharges, as well as mine water held in excavated mine voids at depths of 10-90 m BGL, and water which had interacted with intact coal-bearing strata between 0 and 200 m BGL. Sulphur isotopic data was also collected from sulphide minerals (pyrite) in coal-bearing strata, and meteoric baseline values for oxygen and hydrogen isotopes were secured from monthly sampling of Glasgow rainfall. Comparison of oxygen and hydrogen signatures found that mine water from surface discharges and within excavated voids had a meteoric signature, suggesting a recent recharge water source.

Many of the gravity drainages showed dissolved sulphate $\delta^{34}\text{S}$ isotopic signatures in line with the mean from sulphide mineral samples suggesting a straightforward sulphide oxidation / dissolution explanation. However, there is a tendency for some mine water discharge sulphate to show heavier isotopic values than the sulphate in coal-bearing strata groundwater and the sulphide minerals. All mine water from the UKGEOS research site showed heavy values, whereas the samples from Dollar showed a range between that of the sulphide mean, and the heavy UKGEOS values. The processes contributing heavy sulphate ultimately remain unclear, however, a new process has been proposed in this thesis which may have an influence. Carbonate associated sulphur may be introduced to the mine water following dissolution of host rock carbonate minerals when buffering low pH mine waters. Existing source hypotheses were also explored, and it was found that sulphate from ancient evaporitic brines, dissolution of stratigraphically adjacent gypsum or anhydrite, or bacterial sulphate reduction could all have had a contribution to heavier sulphate-sulphur isotopic signatures.

Chapters 2 and 5 addressed the requirement for baseline and continued monitoring of hydrogeology and geochemistry to inform understanding of a geothermal system dynamics and origins (Ármansson, 2010; Younger et al., 2015). Whilst it is acknowledged that isotopic

signatures of oxygen, hydrogen and sulphur in mine water will likely have low influence on system installation, their monitoring is merited by their ability to detect changes in water origin. Inclusion alongside a comprehensive suite of elemental and physicochemical analyses will allow more detailed understanding of system dynamics and interpretation of pumping influence, enabling better mine water management during MWG scheme operations.

7.2 Recommendations

In a similar fashion to the recommendations which were outlined as a result of Chapter 5 on coupling ground investigative work with mine water geothermal investigation, this section compiles a series of recommendations which have been distilled as a result of the findings throughout the entire thesis.

7.2.1 Feasibility reporting

Chapter 2 found that thorough feasibility studies covering hydrogeological, geometric, engineering and thermal characteristics of mine systems and adjacent aquifers usually precede successful systems (Jardón *et al.*, 2013, Ordóñez *et al.*, 2012). Typically best practice during feasibility studies involves consulting archival and historic mining data from sources such as mining owners and regulators (The Coal Authority in the UK), local library archives and any independent historic collections held by local mining investigators (Harnmeijer *et al.*, 2017). These provide invaluable data on the type (longwall, pillar and room, total extraction), extent, dimensions, and connectivity of mined workings. The mine workings must be evaluated in the context of adjacent and regional aquifers.

7.2.2 Proximal thermal loads

Chapters 2 and 3 explained that in addition to evaluating the available resource from a mine water supply – surface discharge, treatment scheme or subsurface mine workings, other important factors must be considered, for example, proximity of a suitable and economically viable heat consumer (Bao *et al.*, 2018, Jardón *et al.*, 2013). A significant portion of the CAPEX of a DHN is the surface pipework, and lengthy connections can seriously impact a project's business case.

7.2.3 Mix of heating and cooling

Chapters 2 and 4 showed that since many systems perform optimally with balanced heating and cooling loads, one should ideally aim to identify a mix of heating and cooling customers when planning a mine water geothermal system. To use the mine water scheme in Heerlen as an example, the low temperature 5th Generation Heating and Cooling network uses mine water as one of a number of possible sources of heating and cooling and is also an important thermal store or buffer in the system (Boesten *et al.*, 2019).

7.2.4 Sound baseline monitoring

Chapters 2, 3, 5 and 6 explore the hydrochemistry of mine waters and highlight its importance when designing a heating and/or cooling system. Thorough hydrochemical and dissolved gas sampling of mine water prior to installation of heating infrastructure can assist in identifying risks of corrosion or clogging and inform selection of appropriate construction materials (Roijsen *et al.*, 2007, Walls *et al.*, 2020).

Sampling should be carried out prior to construction and during initial operation to identify chemical changes induced by pumping and reinjection. The sampling locations prior to drilling should ideally cover relevant mining related hydrogeological features including existing boreholes, discharges and adjacent watercourses. The relevant mine water data from this suite can be applied as a proxy for expected water chemistry, bearing in mind that often the mined systems exhibit stratification, and deeper pumped mine waters may show deviated chemical properties of the shallow sourced discharges.

Following drilling, further water chemistry analysis can be performed from the new access locations to the mine water aquifer and greater detail can be determined on the water's likely influence on the system components. In addition to water chemistry and temperature, sampling for stable isotopes (oxygen, hydrogen and sulphur isotopes) may aid understanding of mine water history and behaviours (Harnmeijer *et al.*, 2017).

7.2.5 Permitting process

Chapter 2 is the only place in this thesis which addresses the relevant permitting process, which in respect to development of mine water geothermal systems, is of utmost importance. In most national systems, the operation of a MWG system will require a system of permits, which may include:

- Overall planning permission

- An environmental permit to abstract mine water
- An environmental permit to discharge or reinject mine water
- A mining permit or heat extraction agreement from a mining authority
- Approval from a renewable energy or subsidising authority

Managing this permitting process can be a discouraging experience; it is not unknown for some permits to expire before others have been negotiated. The unpredictable hydrogeological behaviour of mine systems means that permitting authorities can have a poorly developed conceptual model, and valuable time can be expended agreeing appropriate testing and monitoring. Due to the high up-front risk and capital expenditure of many MWG systems, long delays in permitting imply negotiating an economic “chasm” between expenditure and realisation of revenue (Walls *et al.*, 2021).

7.2.6 Involvement of expertise

Chapters 2 and 4 explain how integration of mine water sourced heating and cooling into an efficient building thermal delivery system or district heating and cooling network involves a large, complementary expertise across the disciplines of engineering and geoscience, which should not be underestimated by scheme developers. A successful MWG system involves seamlessly integrating skills of hydrogeologists, mining engineers, chemists, HVAC and buildings services engineers, economists and planners.

The resource detailed in Chapter 4 by the MiRAS provides a valuable first-pass screening tool for interested individuals prior to, or at an early stage of project development. However, since the MiRAS provides no internal detail on mined areas it cannot inform borehole locations, probable underground flow pathways or resource size. It is strongly recommended that following initial identification of an optimal location for a MWG project, relevant professionals are engaged to execute planning and installation correctly.

7.2.7 Proving the resource

Chapters 2 and 5 support the use of small-diameter pilot boreholes, to prove a mine working target prior to drilling a full scale, wider diameter borehole. This practice provides a means to reduce the risk of loss of capital during drilling. Such pilot boreholes may allow measurement of water levels, water chemistry sampling and maybe even reconnaissance pumping tests before the hole is reamed out at full diameter and permanent casing installed.

7.2.8 Hydraulic understanding

Chapter 2 explains that conventional hydrogeological theory of aquifers cannot be readily applied to mine workings. The former uses assumptions of Darcy's Law (laminar flow through a permeable granular medium) and an ideal Theis scenario (radial flow towards a well in a homogeneous, isotropic aquifer of infinite extent) (Theis, 1935). None of these assumptions are valid in an interconnected network of mine voids: indeed, there are many aspects of mine water hydrogeology that are more similar to karst hydrogeology (Aldousa and Smartb, 1988, Elliot and Younger, 2014) than a conventional Darcian granular medium.

Factors such as collapses, inter-seam shafts and boreholes, water dams and fracturing can dramatically influence hydrogeological behaviour. It should come as no surprise that the hydraulic behaviour of mine workings is poorly predictable and that conventional numerical modelling approaches should be treated with great caution (approaches based on network modelling have shown some potential, however (Ferket *et al.*, 2011)).

7.2.9 Low hanging fruit

Chapters 3 and 4 between them have conveyed the most favourable locations for developing mine water geothermal energy in Scotland. The simplest means of expanding MWG heating/cooling application would be at locations considered the "lowest hanging fruit". These are locations where mine water is brought to the surface under gravity drainage or a Coal Authority pumping regime. Adaptation of these to include heating infrastructure would create projects with lower risk profiles than those accessing the subsurface for the first time. Lower project CAPEX in the absence of drilling could make a more economically advantageous system, and more so, if the pumping costs were covered by the party with the treatment responsibility. An advantage to the heating arrangement using these open-loop with discharge arrangements is that a greater temperature can be taken from the mine water. This, in turn, directly influences the total heat delivered by the heat pump and is acceptable since there is no risk of thermal feedback.

7.2.10 Combine treatment with heating or cooling

Further to the previous point, Chapter 3 states that there are many untreated discharges in Scotland which are enough of an environmental concern to merit treatment, and it is likely that there are similar situations in England and Wales too. Arranging a means to ensure the

discharges are adequately treated can be installed in-line with development of heating schemes. If done concurrently, it would prevent necessary adaptation of completed treatment arrangements, saving expenditure and time.

7.2.11 Moderate CAPEX by avoiding deepest workings

When using a mapping software to screen a large area for favourable mine water geothermal locations, a valuable limiting factor could be to remove the deepest workings. Whilst this would mean the project would not be able to access the highest temperatures available, it would see benefits in the form of:

1. Lower drilling CAPEX – a larger, more expensive drilling rig is more required to access deeper workings. Similarly, if pilot boreholes are unsuccessful and need redrilled, the costs per borehole are greater.
2. In Scotland, an influencing factor could be that SEPA General Binding Rules state that boreholes over 200 m require a more extensive permitting process.
3. The heat pump delivery equation explains how much heat can be supplied to a system. It has a positive correlation with the ΔT across the heating technology. A lower starting mine water temperature would not necessarily mean a smaller ΔT , thus the heat delivered can be the same. The efficiency of a heat pump system is impacted by the difference between source and demand temperatures, so a lower starting temperature will make a small difference, but minimising the demand temperatures of a system is the best way to ensure a high heat pump efficiency.

7.2.12 Avoid shallow workings (0-30 m)

Chapters 4 and 5 indicate that MWG schemes should avoid workings within 30 m of the surface to minimise subsidence risk and avoid targeting seams which have undergone stability grouting. This includes drilling through shallow workings in order to reach deeper seams since the processes of stabilisation or hydraulic sealing to continue drilling can be timely and expensive.

7.2.13 Consider combining MWGI with GSI

Chapter 5 addresses the challenges and opportunities of combining boreholes mandated for ground stability investigation with those that can be used for mine water geothermal

investigation. One of the principal challenges at the planning and investigation stages of mine water geothermal projects is sourcing capital funding for exploration. Hybridising GSI boreholes in areas where there are suspected shallow mine workings offers the opportunity for monitoring wells to be completed into the mine water geothermal reservoir. Chapter 5 shows that this allows for the measurement of water level, temperature and hydrochemical monitoring.

The overall budget is greater than that of GSI work alone, but less than separate campaigns of GSI and geothermal investigation. Indicative costs of combined GSI and MWGI have been included for a situation which completes three GSI boreholes as monitoring wells but are controlled by the scale of the additional MWGI work. A depth cut-off for when this technique becomes unattractive will likely depend on individual project economics.

7.2.14 Understand the target

Chapter 5 also explained that the extracted coal seam is not always the primary aquifer target. For collapsed longwall mining, and in some cases where collapse has occurred as a result of other mining methods, there exists a fracture network above the level of extraction. Whilst the range of flow rates obtainable from longwall goaf is unclear, the screened horizon of the borehole should extend across the worked seams and height of any overlying hydraulically responsive fracture zone. This can be identified by using core logging or proxies from open hole drilling: minor drops/faster penetration rates, H₂S odour from fracture pockets or loss of drilling fluid.

7.2.15 Avoid short circuits

Furthermore, Chapter 5 outlined that in locations of overlapping worked coal seams, care must be taken to avoid creating new hydraulic and thermal short circuits between them via borehole annulus pathways. To avoid time- and resource-consuming operations to isolate seams within boreholes, it is advised to drill to deeper target seams in places where shallower seams are unworked.

7.2.16 Managing clogging

Chapter 2, 3 and 5 address the prominent mine water risk of clogging, Chapter 2 indicated that many MWG systems have faced iron ochre clogging to date. It has been shown that risk of clogging can be reduced by:

- (a) careful management of dissolved gases and exclusion of oxygen for the pumping-heat exchange-discharge pipe work;
- (b) prevention of cascading in abstraction and reinjection wells;
- (c) monitoring of pressure differentials at key points in pipework systems and across heat exchangers;
- (d) visual or CCTV inspection;
- (e) a regular program of sampling of minewater chemistry.

7.2.17 Managing corrosion

Chapter 2 indicated that corrosion can be induced by factors including high salinity or H₂S concentration. In cases with high corrosion risk, titanium can be used as an alternative to stainless steel in wells, pipelines or heat exchangers or that high strength plastics for wells and pipes.

7.2.18 Thermal feedback

Chapters 2, 4 and 5 cover the issues and mitigating strategies around thermal feedback. Overall, they summarise that, at present, finding a reliable modelling approach to heat transfer in complex networks of subsurface mine voids is challenging. Good practice generally requires investigation into the mining history and hydrogeology of the desired site, and a clear conceptual model of heat, solute and water movement within the unstressed (i.e., pre-pumped) and hydraulically stressed (i.e. pump-perturbed) mine system.

The behaviour of many mine systems may be reliant on a few critical hydrogeological pathways (drifts, open shafts or roadways) and may be dramatically affected by unpredictable factors. The use of empirical techniques – appropriate pumping test techniques, solute and heat tracer tests, and diligent ongoing monitoring of abstracted and reinjected water temperature and chemistry – are to be encouraged (Walls *et al.*, 2021).

7.2.19 One Operations and Maintenance Contractor

Chapter 2 summarised the lifecycle of the Shettleston Housing Association MWG system, concluding that the reason for its cessation after 20 years of operation was a cumulative maintenance burden. The array of potential technical and regulatory challenges associated with MWG systems means that a project developer may opt to employ contractors who are willing to lead the operations and maintenance of the system. Thus, in the absence of a mature and

competitive maintenance market, complex MWG schemes may only be viable above a certain economic scale.

7.2.20 Continued monitoring

As outlined in Section 7.2.4, baseline monitoring is pertinent to understand the mine system dynamics. Continuation of monitoring throughout a project's lifetime is equally as critical as the baseline monitoring programme. Chapters 2, 3, 5 and 6 explain that regular monitoring of water chemistry and temperature can improve a system's longevity since they can be used to detect early indicators of hydraulic regime change, e.g., the abstraction of more corrosive waters or a temperature change induced by deeper or shallower sourced waters, or thermal feedback.

In line with this, it is important to understand that the water held in the mine may well show strong stratification where chemistry and temperature are constant throughout each horizon but show marked changes between them. This is caused by shallow-sourced waters with a lower solute content entering at the top of the water column and denser water with higher dissolved solute content remain at the water column's base (Nuttall and Younger, 2004). The dissolution of increasing amounts of pyrite oxidation salts and other minerals can accentuate the concentration and density difference. The response to pumping may be that the abstracted water quality deteriorates due to mixing of water chemistries and inclusion of the highly mineralised waters from a greater depth.

Since shallow mine water gravity drainages often reflect the uppermost mine water horizon, they may observe seasonal changes in water chemistry, temperature, and flow rate. The trend of which should have been captured by baseline monitoring and can be accounted for by a heat offtake arrangement.

7.2.21 Pumping Costs

Depth to mine water head is a crucial factor when considering the cost effectiveness of a MWG system since the energy expended for pumping is directly proportional to the pumping head depth. In their analysis Athresh *et al.* (2015) found that for 50 L/s, a dynamic pumping head of 10 m BGL gives annual pumping costs of £3700, compared to £37,000 for 100 m BGL. Areas with shallow resting head levels therefore present the most promising economic settings when considering pumping costs. It is feasible that a site with a resting head of 60 m BGL may

observe a dynamic head close to 100 m BGL if pumping higher flow rates, incurring costs close to £37,000 per annum as described.

If the resting head level is very close to surface, then there is the risk that reinjection of significant flowrates can induce upconing and breakout of mine water at the surface. Ensuring a good connection between the boreholes and mine workings can help mitigate this, but avoiding areas with extremely shallow head and ongoing monitoring of borehole water levels can prevent this.

7.3 Further Work

Expanding on systems documented as part of RQ1 would require interviews and questionnaires for each of the newly established schemes. There has been a marked increase in uptake of mine water geothermal heating and cooling in the last few years, with projects in the UK expanding to include those at Hebburn (South Tyneside Council, 2022), Holburn, Gateshead and Caerau (The Coal Authority, 2021b). A systematic approach to recording challenges and mitigations throughout the installation of these schemes would greatly benefit the wider mine water geothermal community.

Whilst TCA's treatment schemes are regularly monitored and sampled to record seasonal and long-term trends, most of the untreated discharges presented in Chapter 3 are not. Creation of a regular physicochemical and elemental data collection programme from each of the discharges, coupled with an improved means to monitor flow rate – creation of weirs, or portable flow-meter – would greatly de-risk the surface resources to confidently inform their thermal application. Continued water chemistry analysis would generate a bank of data, useful for developers and consultant geochemists to understand the ranges of parameters and the extent of chemical challenges (clogging, corrosion, etc.) as a result. A useful mapping exercise would be to pair each of the surface resources (pumped and gravity drainages) with the closest feasible thermal demand. This could convert the total heat available into a more realistic figure since some discharges are distal relative to a suitable thermal load.

Inclusion of the aforementioned “geo-factors” into the MiRAS would create a narrower selection of most optimal areas for MWG sites. Inclusion of iron concentrations or solute content data as spot values or, if feasible, as interpolated raster layers, may prove to be a beneficial addition for MWG resource management considerations. However, there is hesitancy to include such data since the current four criteria are largely unchanging properties, and other geo-factors may be more time or depth dependent. Of the four, only the mine water

head can change, whether that is by continued recovery of groundwater levels towards the pre-mining water table, or by inclusion of more datapoints across the coalfields to refine the interpolation outputs. The addition of surface heating and cooling profiles to the MiRAS would prove to be a valuable exercise to assess correlation of MWG resources with existing and future thermal energy demands. Perhaps such a layer on the MiRAS could be updated on an annual basis with areas denoted for development or seeking planning permission.

The established borehole array at Dollar, Clackmannanshire, as outlined in Chapter 5 would benefit greatly from pumping tests and further hydrogeological characterisation. Owing to the narrow diameter of the boreholes and an inability to find an electric submersible pump (ESP) with a significant flow rate at the correct size, these were not performed. As a result, the interpretations are constrained to natural groundwater fluctuation patterns. In order to replicate the work completed at Dollar, a second development site could be established by a similarly interested landowner. The technique whereby ground stability investigation boreholes have additional mine water geothermal investigation boreholes could be further refined and have the overall cost-savings calculated. Drawing from the limitations of the work in Chapter 5, drilling and completion of these wells at a larger diameter would bring value since it would facilitate easy access for a standard ESP. A parallel workflow could be performed to understand the overlap between standard closed loop boreholes and mine workings. If the boreholes, which may extend down to 200 m BGL, encounter workings unexpectedly then they could be completed to assess MWG potential.

A complimentary work package to the range of sulphur isotope work in this thesis would involve analysing the $\delta^{18}\text{O}$ isotopic ratios of the sulphate in mine waters. This could be completed by using the processes described in Chapters 3, 5 and 6, before including the methods detailed in (Hall *et al.*, 1991). Analysis of sulphate $\delta^{18}\text{O}$ would facilitate plotting on bi-axial plots with $\delta^{18}\text{O}$ on the x-axis and $\delta^{34}\text{S}$ on the y-axis. In doing so, one can more readily differentiate the coupled signatures of $\delta^{18}\text{O}$ and $\delta^{34}\text{S}$ from pyrite oxidation, evaporite dissolution and atmospheric precipitation (Chen *et al.*, 2020) and help determine if the sulphate is a primary or secondary oxidation product.

The most important work to follow on from this thesis will be promotional action and awareness raising. Community, governmental and stakeholder engagement are imperative to share the thesis findings and bring the low-carbon thermal resource and its locations to the forefront of the renewable energy movement in Scotland. The Mine Water Geothermal Resource Atlas for Scotland has been made publicly available; this means that influential bodies across Scotland can take the initiative to include mine water geothermal energy when

planning to decarbonise heating and cooling in residential, commercial, or public buildings. Deployment of mine water geothermal energy in Scotland will raise the nation's profile towards 'world-leader' in renewable heat, emulating successes in other renewable energy sectors. If this work was to be replicated for the extensive coalfields of England and Wales, then the whole of Great Britain could take significant steps towards tackling the challenge of decarbonising heating and cooling, and in doing so make impactful progress towards carbon neutrality.

References

- Abbate, Z., 2016, User Guide For the Coal Authority Shallow Workings Dataset, p. 12,
- Adams, C., Monaghan, A., and Gluyas, J., 2019, Mining for heat: *Geoscientist* 29 (4), p. 10 -15, <https://doi.org/10.1144/geosci2019-021>.
- Aldousa, P. J., and Smartb, P. L., 1988, Tracing Ground-Water Movement in Abandoned Coal Mined Aquifers Using Fluorescent Dyes: *Groundwater*, v. 26, no. 2, p. 172-178, <https://doi.org/10.1111/j.1745-6584.1988.tb00380.x>.
- Anderson, W., 1945, On the Chloride Waters of Great Britain: *Geological Magazine*, v. 82, no. 6, p. 267-273, 10.1017/S001675680008211X.
- Andrews, B. J., Cumberpatch, Z. A., Shipton, Z. K., and Lord, R., 2020, Collapse processes in abandoned pillar and stall coal mines: Implications for shallow mine geothermal energy: *Geothermics*, v. 88, p. 101904, <https://doi.org/10.1016/j.geothermics.2020.101904>.
- Armstrong, M., Bishop, A. C., Francis, E. H., and Read, W. A., 1974a, 39E, Alloa.: Institute of Geological Sciences, <https://webapps.bgs.ac.uk/data/maps/maps.cfc?method=viewRecord&mapId=10828>.
- Armstrong, M., Bishop, A. C., Francis, E. H., and Read, W. A., 1974b, Alloa; 1:50,000 Drift Edition; Sheet 39E: British Geological Survey,
- Athresh, A. P., 2017, Feasibility of using the water from the abandoned and flooded coal mines as an energy resource for space heating. PhD Thesis.: Nottingham Trent University, <http://irep.ntu.ac.uk/id/eprint/32936/1/Anup%20Athresh%202017%20Thesis.pdf>
- Athresh, A. P., Al-Habaibeh, A., and Parker, K., 2015, Innovative Approach for Heating of Buildings Using Water from a Flooded Coal Mine Through an Open Loop Based Single Shaft GSHP System: *Energy Procedia*, v. 75, p. 1221-1228, <https://doi.org/10.1016/j.egypro.2015.07.162>.
- Athresh, A. P., Al-Habaibeh, A., and Parker, K., 2016, The design and evaluation of an open loop ground source heat pump operating in an ochre-rich coal mine water environment: *International Journal of Coal Geology*, v. 164, p. 69-76, 10.1016/j.coal.2016.04.015.
- Athresh, A. P., Al-Habaibeh, A., and Parker, K., 2017, An Innovative and Integrated Approach for Using Energy from the Flooded Coal Mines for Pre-warming of a Gas Engine in Standby Mode Using GSHP: *Energy Procedia*, v. 105, p. 2531-2538, <https://doi.org/10.1016/j.egypro.2017.03.726>.
- Bailey, M. T., Gandy, C. J., Watson, I. A., Wyatt, L. M., and Jarvis, A. P., 2016, Heat recovery potential of mine water treatment systems in Great Britain: *International Journal of Coal Geology*, v. 164, p. 77-84, 10.1016/j.coal.2016.03.007.
- Bailey, M. T., Gandy, C. J., Jarvis, A. P., 2016, Reducing Life-Cycle Costs of Passive Mine Water Treatment by Recovery of Metals from Treatment Wastes, Annual Conference of the International Mine Water Association: Leipzig, Germany, Curran Associates Inc,
- Bailey, M. T., Moorhouse, A. M. L., and Watson, I. A., 2013, Heat extraction from hypersaline mine water at the Dawdon mine water treatment site, *in* Tibbett, M., Fourie, A. B., and Digby, C., eds., Eighth International Seminar on Mine Closure: Cornwall, Australian Centre for Geomechanics, p. 559-570, https://papers.acg.uwa.edu.au/p/1352_47_Bailey/
- Bald, R., 1838, Plan of the coalfield at Dollar. S4263 Sheet 1 of 2,
- Banks, D., 2008, An Introduction To Thermogeology: Ground Source Heating and Cooling, 9600 Garsington Road, Oxford OX4 2DQ, UK, Blackwell Publishing Ltd, 339 p, 978-1-4051-7061-1.
- Banks, D., Making the red one green - renewable heat from abandoned flooded mines. , *in* Proceedings 36th Annual Groundwater Conference, International Association of Hydrogeologists, Irish Group. "Sustaining Ireland's Water Future: The Role of Groundwater", Tullamore, Co. Offaly, Ireland., 12th-13th April 2016 2016, Volume Session VI, p. 1-9, <https://www.iah-ireland.org/conference-proceedings/2016.pdf>.
- Banks, D., 2017, Integration of Cooling into Mine Water Heat Pump Systems F1.1: School of Engineering, Glasgow University.

- Banks, D., Fessing up: risks and obstacles to mine water geothermal energy, *in* Proceedings Mine Water Heating and Cooling; A 21st Century Resource for Decarbonisation, Online conference organised by British Geological Survey, UK Department for Business Energy and Industrial Strategy and IEA Geothermal., 10th-11th March 2021, <https://iea-gia.org/workshop-presentations/2021-mine-water-geothermal-energy-symposium/>
- Banks, D., Athresh, A., Al-Habaibeh, A., and Burnside, N., 2019, Water from abandoned mines as a heat source: practical experiences of open- and closed-loop strategies, United Kingdom: Sustainable Water Resources Management, v. 5, no. 1, p. 29-50, 10.1007/s40899-017-0094-7.
- Banks, D., and Birks, D. C., 2020, Heat from the ground, *Geoscientist*, Volume 30, p. 12-17, <https://doi.org/10.1144/geosci2020-070>.
- Banks, D., and Boyce, A. J., 2023, Dissolved sulphate $\delta^{34}\text{S}$ and the origin of sulphate in coal mine waters; NE England: *Quarterly Journal of Engineering Geology and Hydrogeology*, 10.1144/qjegh2022-106.
- Banks, D., Boyce, A. J., Burnside, N. M., Janson, E., and Roqueñi Gutierrez, N., 2020, On the common occurrence of sulphate with elevated $\delta^{34}\text{S}$ in European mine waters: Sulphides, evaporites or seawater?: *International Journal of Coal Geology*, v. 232, p. 103619, <https://doi.org/10.1016/j.coal.2020.103619>.
- Banks, D., Fraga Pumar, A., and Watson, I., 2009, The operational performance of Scottish minewater-based ground source heat pump systems: *Quarterly Journal of Engineering Geology and Hydrogeology*, v. 42, no. 3, p. 347, 10.1144/1470-9236/08-081.
- Banks, D., Holden, W., Aguilar, E., Mendez, C., Koller, D., Andia, Z., Rodriguez, J., Saether, O. M., Torrico, A., Veneros, R., and Flores, J., 2002a, Contaminant source characterization of the San Jose Mine, Oruro, Bolivia: *Geological Society of London Special Publications*, v. 198, p. 215, 10.1144/gsl.Sp.2002.198.01.14.
- Banks, D., Parnachev, V. P., Frengstad, B., Holden, W., Vedernikov, A. A., and Karnachuk, O. V., 2002b, Alkaline mine drainage from metal sulphide and coal mines: Examples from Svalbard and Siberia, *Geological Society Special Publication*, Volume 198, p. 287-296, 10.1144/GSL.SP.2002.198.01.19.
- Banks, D., Skarphagen, H., Wiltshire, R., and Jessop, C., 2003, Mine water as a resource: Space heating and cooling via use of heat pumps: *Land Contamination & Reclamation*, v. 11, p. 191-198, 10.2462/09670513.814.
- Banks, D., Skarphagen, H., Wiltshire, R., and Jessop, C., 2004, Heat pumps as a tool for energy recovery from mining wastes, *Geological Society Special Publication*, Volume 236, p. 499-513, 10.1144/GSL.SP.2004.236.01.27.
- Banks, D., Steven, J., Black, A., and Naismith, J., 2022, Conceptual Modelling of Two Large-Scale Mine Water Geothermal Energy Schemes: Felling, Gateshead, UK: *International Journal of Environmental Research and Public Health*, v. 19, no. 3, p. 1643, <https://www.mdpi.com/1660-4601/19/3/1643>
- Banks, D., Steven, J. K., Berry, J., Burnside, N., and Boyce, A. J., 2017, A combined pumping test and heat extraction/recirculation trial in an abandoned haematite ore mine shaft, Egremont, Cumbria, UK: *Sustainable Water Resources Management*, v. 5, no. 1, p. 51-69, 10.1007/s40899-017-0165-9.
- Banks, D., Younger, P. L., Arnesen, R.-T., Iversen, E. R., and Banks, S. B., 1997, Mine-water chemistry: the good, the bad and the ugly: *Environmental Geology*, v. 32, no. 3, p. 157-174, 10.1007/s002540050204.
- Banks, D., Younger, P. L., and Dumbleton, S., 1996, The Historical Use Of Mine-Drainage And Pyrite-Oxidation Waters In Central And Eastern England, United Kingdom: *Hydrogeology Journal*, v. 4, no. 4, p. 55-68, 10.1007/s100400050091.
- Banks, S. B., 2003, The UK Coal Authority Minewater Treatment Scheme Programme: Performance of Operational Systems: *Water and Environment Journal*, v. 17, no. 2, p. 117-122, <https://doi.org/10.1111/j.1747-6593.2003.tb00444.x>.
- Banks, S. B., and Banks, D., 2001, Abandoned mines drainage: impact assessment and mitigation of discharges from coal mines in the UK: *Engineering Geology*, v. 60, no. 1, p. 31-37, [https://doi.org/10.1016/S0013-7952\(00\)00086-7](https://doi.org/10.1016/S0013-7952(00)00086-7).

- Bao, T., Liu, Z., Meldrum, J., and Green, C., 2018, Large-Scale Mine Water Geothermal Applications with Abandoned Mines, Proceedings of GeoShanghai 2018 International Conference: Tunnelling and Underground Construction, p. 685-695
- Bao, T., Meldrum, J., Green, C., Vitton, S., Liu, Z., and Bird, K., 2019, Geothermal energy recovery from deep flooded copper mines for heating: Energy Conversion and Management, v. 183, p. 604-616, <https://doi.org/10.1016/j.enconman.2019.01.007>.
- Barron, H. F., Starcher, V., Monaghan, A. A., Shorter, K. M., and Walker-Verkuil, K., 2020a, Mine water characterisation and monitoring borehole GGA05, UK Geoenergy Observatory, Glasgow. British Geological Survey Open Report, OR/20/025., 36 p,
- Barron, H. F., Starcher, V., Walker-Verkuil, K., Shorter, K. M., and Monaghan, A. A., 2020b, Mine water characterisation and monitoring borehole GGA08, UK Geoenergy Observatory, Glasgow. British Geological Survey Open Report, OR/20/028., 35 p,
- Barrowman, J., 1897, Slavery in the coal mines of Scotland.: Trans. Mining Institute of Scotland, p. 19, 117-126,
- Bateson, L., Cigna, F., Boon, D., and Sowter, A., 2015, The application of the Intermittent SBAS (ISBAS) InSAR method to the South Wales Coalfield, UK: International Journal of Applied Earth Observation and Geoinformation, v. 34, p. 249-257, <https://doi.org/10.1016/j.jag.2014.08.018>.
- Bearcock, J. M., Walker-Verkuil, K., Mulcahy, A., Palumbo-Roe, B., MacAllister, D. J., Goody, D., and Darling, W. G., 2022, UK Geoenergy Observatories: Glasgow baseline groundwater and surface water chemistry dataset release September 2020 - May 2021. British Geological Survey Open Report, OR/22/038., 151 p,
- Bell, F. G., 1986, Location of abandoned workings in coal seams: Bulletin of the International Association of Engineering Geology - Bulletin de l'Association Internationale de Géologie de l'Ingénieur, v. 33, no. 1, p. 123-132, 10.1007/BF02594714.
- Bell, F. G., 1994, A survey of the engineering properties of some anhydrite and gypsum from the north and midlands of England: Engineering Geology, v. 38, no. 1, p. 1-23, [https://doi.org/10.1016/0013-7952\(94\)90021-3](https://doi.org/10.1016/0013-7952(94)90021-3).
- Berg, B. I., 2021, Personal Communication,
- Bishop, I., Styles, P., and Allen, M., 1993, Mining-induced seismicity in the Nottinghamshire Coalfield: Quarterly Journal of Engineering Geology and Hydrogeology, v. 26, no. 4, p. 253-279, 10.1144/gsl.Qjagh.1993.026.004.03.
- Bjerkgaard, T., and Bjorlykke, A., 1996, Sulfide deposits in Folldal, southern Trondheim region Caledonides, Norway; source of metals and wall-rock alterations related to host rocks: Economic Geology, v. 91, no. 4, p. 676-696, 10.2113/gsecongeo.91.4.676.
- Bluck, B. J., 1984, Pre-Carboniferous history of the Midland Valley of Scotland: Transactions of the Royal Society of Edinburgh: Earth Sciences, v. 75, no. 2, p. 275-295, 10.1017/S0263593300013900.
- Boesten, S., Ivens, W., Dekker, S. C., and Eijndems, H., 2019, 5th generation district heating and cooling systems as a solution for renewable urban thermal energy supply: Adv. Geosci., v. 49, p. 129-136, 10.5194/adgeo-49-129-2019.
- Bogue, R. H., 1929, Calculation of the Compounds in Portland Cement: Industrial & Engineering Chemistry Analytical Edition, v. 1, no. 4, p. 192-197, 10.1021/ac50068a006.
- BoilerGuide, 2022, What size heat pump do I need?, www.boilerguide.co.uk/articles/size-heat-pump-need, Date Accessed: 03/03/2022.
- Brabham, P., Manju, M., Thomas, H., Farr, G., Francis, R., Sahid, R., and Sadasivam, S., 2020, The potential use of mine water for a district heating scheme at Caerau, Upper Llynfi valley, South Wales, UK: Quarterly Journal of Engineering Geology and Hydrogeology, v. 53, no. 1, p. 145, 10.1144/qjagh2018-213.
- Bracke, R., and Bussmann, G., Heat-storage in deep hard coal mining infrastructures., in Proceedings World Geothermal Congress, Melbourne, Australia, 2015,
- British Geological Survey, 1992a, Airdrie. Scotland Sheet 31W. Drift Geology. 1:50000, Keyworth, Nottingham: British Geological Survey,
- British Geological Survey, 1992b, Airdrie. Scotland Sheet 31W. Solid. 1:50 000 Geology Series,

- British Geological Survey, 2008, Ayr. Scotland Sheet 14W and part of 13. Bedrock. 1:50 000 Geology Series,
- British Geological Survey, 2020, UKGEOS Glasgow GGA02 borehole information pack, <https://dx.doi.org/10.5285/189dac62-b720-4fde-8260-f129fb9b0233>.
- British Standards Institution, 2009, BS EN ISO 10304-1: Water quality. Determination of dissolved anions by liquid chromatography of ions. Determination of bromide, chloride, fluoride, nitrate, nitrite, phosphate and sulphate, 978 0 580 65935 5.
- British Standards Institution, 2018, PD CEN/TS 17197:2018 Construction products: Assessment of release of dangerous substances - Analysis of inorganic substances in digests and eluates - Analysis by Inductively Coupled Plasma - Optical Emission Spectrometry (ICP-OES) method., 9780580850585.
- British Standards Institution, 2020, BS 5930:2015+A1:2020 Code of practice for ground investigations, BSI Standards Limited 2020, ISBN 978 0 539 05986 1.
- Brown, M. M. E., Jones, A. L., Leighfield, K. G., and Cox, S. J., 2002, Fingerprinting mine water in the eastern sector of the South Wales Coalfield: Mine Water Hydrogeology and Geochemistry, Geological Society, London Special Publications, v. 198, p. 275–286, <https://doi.org/10.1144/GSL.SP.2002.198.01.18>.
- Builders Booklet, 2021, Chemical composition of Portland Cement. , <https://www.buildersbooklet.com/concrete/chemical-composition-of-portland-cement/>, Date Accessed:
- Bullock, L. A., Parnell, J., Perez, M., Boyce, A., Feldmann, J., and Armstrong, J. G. T., 2018, Multi-stage pyrite genesis and epigenetic selenium enrichment of Greenburn coals (East Ayrshire): Scottish Journal of Geology, v. 54, no. 1, p. 37-49, 10.1144/sjg2017-010.
- Burnside, N. M., Banks, D., and Boyce, A. J., 2016a, Sustainability of thermal energy production at the flooded mine workings of the former Caphouse Colliery, Yorkshire, United Kingdom: International Journal of Coal Geology, v. 164, p. 85-91, 10.1016/j.coal.2016.03.006.
- Burnside, N. M., Banks, D., Boyce, A. J., and Athresh, A., 2016b, Hydrochemistry and stable isotopes as tools for understanding the sustainability of minewater geothermal energy production from a ‘standing column’ heat pump system: Markham Colliery, Bolsover, Derbyshire, UK: International Journal of Coal Geology, v. 165, p. 223-230, 10.1016/j.coal.2016.08.021.
- Cameron, I. B., and Stephenson, D., 1985, British Regional Geology: The Midland Valley of Scotland London, British Geological Survey, Geological Magazine, 172 p, ISBN 0 11 884365 6.
- Carmody, R. W., Plummer, N., Busenberg, E., and Coplen, T. B., 1998, Methods for collection of dissolved sulfate and sulfide and analysis of their sulfur isotopic composition, 97-234.
- Chałupnik, S., Wysocka, M., Chmielewska, I., and Samolej, K., 2020, Modern technologies for radium removal from water – Polish mining industry case study: Water Resources and Industry, v. 23, p. 100125, <https://doi.org/10.1016/j.wri.2020.100125>.
- Chen, X., Zheng, L., Dong, X., Jiang, C., and Wei, X., 2020, Sources and mixing of sulfate contamination in the water environment of a typical coal mining city, China: evidence from stable isotope characteristics: Environmental Geochemistry and Health, v. 42, no. 9, p. 2865-2879, 10.1007/s10653-020-00525-2.
- Cherni, A. B., 2011, Модернизация систем теплоснабжения шахтерских городов России [Modernisation of systems of heat supply to mining towns in Russia]. Энергосовет (Energy Advice), no. 4(17), p. 11-12, http://www.energsovet.ru/bul_stat.php?idd=191
- Clackmannanshire Council, 2022, Planning – Application Summary; 19/00018/PPP, <https://publicaccess.clacks.gov.uk/publicaccess/applicationDetails.do?activeTab=summary&keyVal=PM6XHJEYH6H00>, Date Accessed: 30/10/2022.
- Claypool, G. E., Holser, W. T., Kaplan, I. R., Sakai, H., and Zak, I., 1980, The age curves of sulfur and oxygen isotopes in marine sulfate and their mutual interpretation: Chemical Geology, v. 28, p. 199-260, [https://doi.org/10.1016/0009-2541\(80\)90047-9](https://doi.org/10.1016/0009-2541(80)90047-9).
- Clough, C. T., Hinxman, L.W., Wright, W.B., Anderson, E.M., and Carruthers, R G., 1926, The economic geology of the Central Coalfield of Scotland, description of area V, Glasgow East, Coatbridge and Airdrie. Memoir of the Geological Survey of Scotland.,
- Coleman, M. L., and Moore, M. P., 1978, Direct reduction of sulphates to sulphur dioxide for isotopic analysis: Anal. Chem., v. 28, p. 199-260,

- Committee on Climate Change, 2019, UK housing: Fit for the future?, p. 135, <https://www.theccc.org.uk/wp-content/uploads/2019/02/UK-housing-Fit-for-the-future-CCC-2019.pdf>.
- Craig, H., 1961, Isotopic Variations in Meteoric Waters: *Science*, v. 133, no. 3465, p. 1702-1703, doi:10.1126/science.133.3465.1702.
- Crooks, J., Clean energy from the coalfields, *in* Proceedings Mining the Future: Innovation in heating and cooling, The Hague, The Netherlands, 3rd October 2018,
- Darling, W. G., Bath, A. H., and Talbot, J. C., 2003, The O and H stable isotope composition of freshwaters in the British Isles. 2. Surface waters and groundwater: *Hydrology and Earth System Sciences Discussions*, v. 7, no. 2, p. 183-195, <https://hal.archives-ouvertes.fr/hal-00304768>
- Davis, S. N., Whittemore, D. O., and Fabryka-Martin, J., 1998, Uses of Chloride/Bromide Ratios in Studies of Potable Water: *Groundwater*, v. 36, no. 2, p. 338-350, <https://doi.org/10.1111/j.1745-6584.1998.tb01099.x>.
- de Romero, M., The Mechanism of SRB Action in MIC, Based on Sulfide Corrosion and Iron Sulfide Corrosion Products, *in* Proceedings CORROSION 2005,
- Dean, G., Craig, J., Gerali, F., MacAulay, F., and Sorkhabi, R., 2018, The Scottish oil-shale industry from the viewpoint of the modern-day shale-gas industry, Geological Society of London, History of the European Oil and Gas Industry, 9781786203632.
- Diamond, J., 2022, Personal Communication - Drilling Cost Estimates, TownRock Energy,
- Dmitrienko, V., Merenkova, N., Zanina, I., and Dmitrienko, N., 2019, Use of low potential wastewater heat: E3S Web Conf., v. 104, <https://doi.org/10.1051/e3sconf/201910401007>
- Dollar Museum, 2014, Cuttings from 1744 onward and maps and articles about Dollar Mines and Sheardale, Blairingone, Harvieston, Bessie Glen; and runaway serfs and an early miners' strike., Dollar Museum,
- Donnelly, L., 2020, Coal mining subsidence in the UK: Geological Society, London, Engineering Geology Special Publications, v. 29, no. 1, p. 291-309, 10.1144/egsp29.11.
- Donnelly, T., Waldron, S., Tait, A., Dougans, J., and Bearhop, S., 2001, Hydrogen isotope analysis of natural abundance and deuterium-enriched waters by reduction over chromium on-line to a dynamic dual inlet isotope-ratio mass spectrometer: *Rapid Communications in Mass Spectrometry*, v. 15, no. 15, p. 1297-1303, 10.1002/rcm.361.
- Driessche, A. E. S. V., Canals, A., Ossorio, M., Reyes, R. C., and García-Ruiz, J. M., 2016, Unraveling the Sulfate Sources of (Giant) Gypsum Crystals Using Gypsum Isotope Fractionation Factors: *The Journal of Geology*, v. 124, no. 2, p. 235-245, 10.1086/684832.
- Elliot, T., and Younger, P. L., 2014, Detection of Mixing Dynamics During Pumping of a Flooded Coal Mine: *Groundwater*, v. 52, no. 2, p. 251-263, <https://doi.org/10.1111/gwat.12057>.
- Elsome, J., Walker-Verkuil, K., Starcher, V., Barron, H. F., Shorter, K. M., and Monaghan, A. A., 2020, Environmental baseline characterisation and monitoring borehole GGB04, UK Geoenery Observatory, Glasgow. British Geological Survey Open Report, OR/20/030., 22 p,
- Energy Saving Trust, 2021, Renewable Heat in Scotland 2020 report, p. 38, <https://energysavingtrust.org.uk/wp-content/uploads/2021/10/Renewable-heat-in-Scotland-2020-report-version-2.pdf>.
- Environmental Agency, 2021, Mine waters: challenges for the water environment, p. 22, <https://www.gov.uk/government/publications/mine-waters-challenges-for-the-water-environment>.
- Ericsson, B., and Hallmans, B., 1996, Treatment of saline wastewater for zero discharge at the Debiensko coal mines in Poland: *Desalination*, v. 105, no. 1, p. 115-123, [https://doi.org/10.1016/0011-9164\(96\)00065-3](https://doi.org/10.1016/0011-9164(96)00065-3).
- Farr, G., and Busby, J., 2020, The Thermal Resource of Mine Waters in Abandoned Coalfields; Opportunities and Challenges for the United Kingdom, World Geothermal Conference: Reykjavik, Iceland, <https://pangea.stanford.edu/ERE/db/WGC/papers/WGC/2020/41021.pdf>.
- Farr, G., Busby, J., Wyatt, L., Crooks, J., Schofield, D. I., and Holden, A., 2021, The temperature of Britain's coalfields: *Quarterly Journal of Engineering Geology and Hydrogeology*, v. 54, no. 3, p. qjgeh2020-2109, 10.1144/qjgeh2020-109.

- Farr, G., Sadasivam, S., Manju, Watson, I. A., Thomas, H. R., and Tucker, D., 2016, Low enthalpy heat recovery potential from coal mine discharges in the South Wales Coalfield: *International Journal of Coal Geology*, v. 164, p. 92-103, [10.1016/j.coal.2016.05.008](https://doi.org/10.1016/j.coal.2016.05.008).
- Feng, R., Beck, J. R., Hall, D. M., Buyuksagis, A., Ziomek-Moroz, M., and Lvov, S. N., 2017, Effects of CO₂ and H₂S on Corrosion of Martensitic Steels in Brines at Low Temperature: *Corrosion*, v. 74, no. 3, p. 276-287, [10.5006/2406](https://doi.org/10.5006/2406).
- Ferket, H. L. W., Laenen, B. J. M., and Van Tongeren, P. C. H., 2011, Transforming flooded coal mines to large-scale geothermal and heat storage reservoirs: what can we expect?, *in* Rüde RT, F. A. W. C., ed., *IMWA Congress 2011: Aachen, Germany*, p. 171-175,
- Fernandez, A. P., 2017, Eficiencia energética y ambiental con la digestión anaerobia secuencial. [Energy and environmental efficiency with sequential anaerobic digestion.] Presentation at LoCAL Project Coordination Meeting, Oviedo, Spain. 7-8 March
- Fichtner, V., Strauss, H., Immenhauser, A., Buhl, D., Neuser, R. D., and Niedermayr, A., 2017, Diagenesis of carbonate associated sulfate: *Chemical Geology*, v. 463, p. 61-75, <https://doi.org/10.1016/j.chemgeo.2017.05.008>.
- Findlay, C., McDonald, B. and Cunningham, J., 2020, *A History of Coal Mining in Rutherglen and Cambuslang*. Rutherglen Heritage Society,
- Finkelman, R. B., Orem, W., Castranova, V., Tatu, C. A., Belkin, H. E., Zheng, B., Lerch, H. E., Maharaj, S. V., and Bates, A. L., 2002, Health impacts of coal and coal use: Possible solutions: *International Journal of Coal Geology*, v. 50, no. 1-4, p. 425-443, [10.1016/S0166-5162\(02\)00125-8](https://doi.org/10.1016/S0166-5162(02)00125-8).
- Finsås Wika, S., 2012, Pitting and crevice corrosion of stainless steel under offshore conditions, Masters Thesis.: Trondheim, Norway,
- Florčinská, P., 2014, Možnosti využití důlních vod čerpaných na povrch a vypouštěných do povrchového toku v rámci vodní jámy Jeremenko [Possibilities of use of mine water pumped to surface and discharged to a surface watercourse in the framework of Jeremenko Pumping Shaft], <https://core.ac.uk/download/pdf/94758257.pdf>
- Fordyce, F. M., Shorter, K. M., Walker-Verkuil, K., Barlow, T., Sloane, H. J., Arrowsmith, C., Hamilton, E. M., Everett, P. A., and M., B. J., 2021, UK Geoenery Observatories, Glasgow Environmental Baseline Surface Water Chemistry Dataset 1. Open Report OR/20/061,
- Fowler, D., Cape, J. N., Leith, I. D., Paterson, I. S., Kinnaird, J. W., and Nicholson, I. A., 1982, Rainfall acidity in northern Britain: *Nature*, v. 297, no. 5865, p. 383-385, [10.1038/297383a0](https://doi.org/10.1038/297383a0).
- Fraser-Harris, A. P., McDermott, C. I., Receveur, M., Mouli-Castillo, J., Todd, F., Cartwright-Taylor, A., Gunning, A. P., and Parsons, M., 2022, The Geobattery Concept: A Geothermal Circular Heat Network for the Sustainable Development of Near Surface Low Enthalpy Geothermal Energy to Decarbonise Heating: *Earth Science, Systems and Society*, <https://doi.org/10.3389/esss.2022.10047>.
- Fursova, I. N., Dyuzhakov, D.V., 2012, Оценка эффективности использования теплоты шахтных вод для нужд централизованного теплоснабжения. (An evaluation of the efficiency of the use of mine water heat for district heating). *Инженерный Вестник Дона (Engineering Journal of the Don)*, v. 4(1), <http://www.ivdon.ru/magazine/archive/n4p1y2012/1166>
- Gasho, E. G., Kozlov, S.A., Puzakov, V.S., Razoryonov, R.N., Sveshnikov, N.I. Stepanova, M.V., 2017, Тепловые насосы в современной промышленности и коммунальной инфраструктуре. Информационно – методическое издание. [Heat pumps in modern industry and municipal infrastructure. Informational - methodical edition], Pero, Moscow, 978-5-906927-01-9.
- Ge, H.-H., Zhou, G.-D., and Wu, W.-Q., 2003, Passivation model of 316 stainless steel in simulated cooling water and the effect of sulfide on the passive film: *Applied Surface Science*, v. 211, no. 1, p. 321-334, [https://doi.org/10.1016/S0169-4332\(03\)00355-6](https://doi.org/10.1016/S0169-4332(03)00355-6).
- Ghoreishi Madiseh, S. A., Ghomshei, M. M., Hassani, F. P., and Abbasy, F., 2012, Sustainable heat extraction from abandoned mine tunnels: A numerical model: *Journal of Renewable and Sustainable Energy*, v. 4, no. 3, [10.1063/1.4712055](https://doi.org/10.1063/1.4712055).
- Gillespie, M., Crane, E., and Barron, H., 2013, Study into the Potential for Deep Geothermal Energy in Scotland, [10.13140/2.1.1186.4322](https://doi.org/10.13140/2.1.1186.4322).

- Glyn, A., and Machin, S., 1997, Colliery Closures and the Decline of the UK Coal Industry: *British Journal of Industrial Relations*, v. 35, no. 2, p. 197-214, <https://doi.org/10.1111/1467-8543.00048>.
- GOV.UK, 2021, Mine water heat recovery access agreements, <https://www.gov.uk/government/publications/minewater-heat-recovery-access-agreements>, Date Accessed: 13.05.2021.
- Gunning, A., Henman, T., Kelly, T., Anderson, B., and McGuire, C., 2019, Research project to investigate prevalence of CO₂ from disused mineral mines and the implications for residential buildings, <https://www.gov.scot/publications/research-project-investigate-prevalence-co2-disused-mineral-mines-implications-residential-buildings/>
- Gzyl, G., and Banks, D., 2007, Verification of the “first flush” phenomenon in mine water from coal mines in the Upper Silesian Coal Basin, Poland: *Journal of Contaminant Hydrology*, v. 92, no. 1, p. 66-86, <https://doi.org/10.1016/j.jconhyd.2006.12.001>.
- Hall, A., Scott, J. A., and Shang, H., 2011, Geothermal energy recovery from underground mines: *Renewable and Sustainable Energy Reviews*, v. 15, no. 2, p. 916-924, 10.1016/j.rser.2010.11.007.
- Hall, A. J., Boyce, A. J., Fallick, A. E., and Hamilton, P. J., 1991, Isotopic evidence of the depositional environment of Late Proterozoic stratiform barite mineralisation, Aberfeldy, Scotland: *Chemical Geology: Isotope Geoscience section*, v. 87, no. 2, p. 99-114, [https://doi.org/10.1016/0168-9622\(91\)90044-W](https://doi.org/10.1016/0168-9622(91)90044-W).
- Hall, I. H. S., Browne, M. A. E., and Forsyth, I. H., 1998, Geology of the Glasgow district. Sheet 30E (Scotland). *Memoir of the British Geological Survey*. British Geological Survey, Keyworth., 117 p,
- Hall, J., Glendinning, S., and Younger, P., 2005, Is mine water a source of hazardous gas?: *Proceedings of the 9th International Mine Water Association Congress 2005*, Oviedo,
- Hammarstrom, J. M., Seal, R. R., Meier, A. L., and Kornfeld, J. M., 2005, Secondary sulfate minerals associated with acid drainage in the eastern US: recycling of metals and acidity in surficial environments: *Chemical Geology*, v. 215, no. 1, p. 407-431, <https://doi.org/10.1016/j.chemgeo.2004.06.053>.
- Harker, S. D., and Trewin, N. H., 2002, Cretaceous, *The Geology of Scotland*, Geological Society of London, p. 0
- Harnmeijer, J., Schlicke, A., Barron, H. F., Banks, D., Townsend, D., Steen, P., Nikolakopoulou, V., Lu, H., and Zhengao, C., 2017, The Fortissat Minewater Geothermal District Heating Project: A Case Study, 10.1049/etr.2016.0087.
- Haunch, S., 2020, Discharges associated with historic mining - Personal communication,
- Haunch, S., MacDonald, A., and McDermott, C., 2021, Variability in mine waste mineralogy and water environment risks: a case study on the River Almond catchment, Scotland., *in* Stanley, P., Wolkersdorfer, C., and Wolkersdorfer, K., eds., *IMWA 2021 - Mine Water Management for Future Generations*, Volume 181-187, International Mine Water Association, https://www.imwa.info/docs/imwa_2021/IMWA2021_Haunch_181.pdf
- Headworth, H. G., Puri, S., and Rampling, B. H., 1980, Contamination of a Chalk aquifer by mine drainage at Tilmanstone, East Kent, U.K: *Quarterly Journal of Engineering Geology and Hydrogeology*, v. 13, no. 2, p. 105-117, 10.1144/gsl.Qjeg.1980.013.02.05.
- Healy, P. R., and Head, J. M., 1984, *Construction over abandoned mine workings*, London, 086017 218 X.
- Hill, S. R., 2004, The physical and geochemical characterization of oxygen-depleted breathing wells in Central Alberta. *Masters Thesis: University of Alberta*, Edmonton, Alberta, Canada,
- Hollis, D., and Perry, M., 2004, A new set of long-term averages for the UK, *in* Met Office, ed., Volume 2.0: Devon, United Kingdom, p. 21, https://www.metoffice.gov.uk/binaries/content/assets/metofficegovuk/pdf/weather/learn-about/uk-past-events/papers/lta_uk.pdf
- Hopkins, P., 2021, Personal Communication,
- Houben, G. J., 2003, Iron oxide incrustations in wells. Part 1: Genesis, mineralogy and geochemistry: *Applied Geochemistry*, v. 18, no. 6, p. 927-939, 10.1016/S0883-2927(02)00242-1.

- Hyria, A., Czysta energia – drugie życie kopalni (LoCAL): Zrównoważone wykorzystanie zatopionych wyrobisk po eksploatacji węgla kamiennego jako źródła energii cieplnej Przykłady wdrożeń: Polska – doświadczenia i perspektywy (Clean energy - the second life of a mine (LoCAL): Sustainable use of flooded coal mine workings as a source of thermal energy. Examples of implementations: Poland - experiences and prospects – in Polish), *in* Proceedings Final LoCAL Conference, Katowice, Poland, 1st June 2017 2017, Institute of Geological Sciences, 1978, IGS Boreholes 1977. Report of the Institute of Geological Sciences. No.78/21
- James Hutton Institute, 2016, Feasibility Report of Fortissat Community Minewater Geothermal Energy District Heating Network, Edinburgh, The Scottish Government, 104 p, 978-1-78652-131-6
- Janson, E., 2021, Personal Communication,
- Janson, E., Boyce, A. J., Burnside, N., and Gzyl, G., 2016, Preliminary investigation on temperature, chemistry and isotopes of mine water pumped in Bytom geological basin (USCB Poland) as a potential geothermal energy source: *International Journal of Coal Geology*, v. 164, p. 104-114, [10.1016/j.coal.2016.06.007](https://doi.org/10.1016/j.coal.2016.06.007).
- Janson, E., Gzyl, G., and Banks, D., 2009, The Occurrence and Quality of Mine Water in the Upper Silesian Coal Basin, Poland: *Mine Water and the Environment*, v. 28, no. 3, p. 232, [10.1007/s10230-009-0079-3](https://doi.org/10.1007/s10230-009-0079-3).
- Janson, E., Gzyl, G., Głodniok, M., and Markowska, M., 2017, Use of Geothermal Heat of Mine Waters in Upper Silesian Coal Basin, Southern Poland – Possibilities and Impediments, *in* C.Wolkersdorfer, L. S., M. Sillanpää i A. Häkkinen, ed., IMWA conference materials, Volume Mine Water & Circular Economy, vol I: Lappeenranta, Finland, p. 415-422,
- Jardón, S., Ordóñez, M. A., Alvarez, R., Cienfuegos, P., and Loredó, J., 2013, Mine Water for Energy and Water Supply in the Central Coal Basin of Asturias (Spain): *Mine Water Environ*, v. 32, p. 139-151, [10.1007/s10230-013-0224-x](https://doi.org/10.1007/s10230-013-0224-x).
- Jensen, E. B., 1983, Mine Water Used to Heat Ventilation Air at Henderson Molybdenum Mine: *Mining Engineering*, v. 35, no. 1, p. 17-20, <https://www.onemine.org/document/abstract.cfm?docid=4886>
- Jessop, A. M., 1995, Geothermal energy from old mines at Springhill, Nova Scotia, Canada., *in* Barbier, E., ed., *World Geothermal Congress: Firenze, Italy.*, p. 463-468, <https://www.geothermal-energy.org/pdf/IGAstandard/WGC/1995/1-jessop2.pdf>
- Jessop, A. M., MacDonald, J. K., and Spence, H., 1995, Clean energy from abandoned mines at Springhill, Nova Scotia: *Energy Sources*, v. 17, no. 1, p. 93-106, [10.1080/00908319508946072](https://doi.org/10.1080/00908319508946072).
- Jirakova, H., Stibitz, M., Frydrych, V., and Durajova, M., 2015, Geothermal Country Update for the Czech Republic, *World Geothermal Congress 2015: Melbourne, Australia*, p. 7, <https://docplayer.net/21262315-Geothermal-country-update-for-the-czech-republic.html>
- Johnsrud, T., 2021, Personal Communication,
- Johnston, D., Potter, H., Jones, C., Rolley, S., Watson, I., and Pritchard, J., 2008, Abandoned mines and the water environment, *in* The Environment Agency, ed.: Bristol, UK, p. 40, ISBN: 978-1-84432-894-9.
- Jones, N. S., 2007, The West Lothian Oil-shale Formation: Results of a sedimentological study., *British Geological Survey*, p. 63, Internal Report IR/05/046.
- Jones, N. S., Holloway, S., Creedy, D. P., Garner, K., Smith, N. J. P., Browne, M. A. E., and Durucan, S., 2004, UK Coal Resource for New Exploitation Technologies. Final Report. *British Geological Survey CR/04/015N*,
- Kaczmarczyk, M., Tomaszewska, B., and Operacz, A., 2020, Sustainable Utilization of Low Enthalpy Geothermal Resources to Electricity Generation through a Cascade System: *Energies*, v. 13, no. 10, p. 2495, <https://doi.org/10.3390/en13102495>.
- Kampschulte, A., Bruckschen, P., and Strauss, H., 2001, The sulphur isotopic composition of trace sulphates in Carboniferous brachiopods: implications for coeval seawater, correlation with other geochemical cycles and isotope stratigraphy: *Chemical Geology*, v. 175, no. 1, p. 149-173, [https://doi.org/10.1016/S0009-2541\(00\)00367-3](https://doi.org/10.1016/S0009-2541(00)00367-3).

- Kampschulte, A., and Strauss, H., 2004, The sulfur isotopic evolution of Phanerozoic seawater based on the analysis of structurally substituted sulfate in carbonates: *Chemical Geology*, v. 204, no. 3, p. 255-286, <https://doi.org/10.1016/j.chemgeo.2003.11.013>.
- Karpiński, M., and Sowizdzał, A., 2018, Kopalnie węgla kamiennego źródłem ciepła dla pomp ciepła [Hard coal mines as a source of heat for heat pumps], *Rynek instalacyjny: Poland*, p. 35, <http://www.rynekinstalacyjny.pl/artukul/id4458,kopalnie-węgla-kamiennego-zrodlem-ciepła-dla-pomp-ciepła>
- Kaya, T., and Hoshan, P., Corrosion and material selection for geothermal systems, *in Proceedings World Geothermal Congress, Antalya, Turkey, 24-29 April 2005*,
- Kearsey, T., Gillespie, M., Entwisle, D., Damaschke, M., Wylde, S., Fellgett, M., Kingdon, A., Burkin, J., Starcher, V., Shorter, K., Barron, H., Elsome, J., Barnett, M., and Monaghan, A., 2019, UK Geoenery Observatories Glasgow: GGC01 Cored, seismic monitoring borehole – intermediate data release. British Geological Survey Open Report, OR/19/049.,
- Kirby, R. K., and Kanare, H. M., 1988, Portland cement chemical composition standards (blending, packaging and testing). US National Bureau of Standards special publication, v. 260-110, <https://nvlpubs.nist.gov/nistpubs/Legacy/SP/nbsspecialpublication260-110.pdf>.
- Korb, M., 2021, Personal Communication,
- Korb, M. C., 2012, Mine Pool Geothermal In Pennsylvania: Pennsylvania Department of Environmental Protection.
- Koteeswaran, M., 2010, CO2 and H2S corrosion in oil pipelines. Masters Thesis.: University of Stavanger, Norway,
- Kotková, J., Kullerud, K., Šrein, V., Drábek, M., and Škoda, R., 2018, The Kongsberg silver deposits, Norway: Ag-Hg-Sb mineralization and constraints for the formation of the deposits: *Mineralium Deposita*, v. 53, no. 4, p. 531-545, 10.1007/s00126-017-0757-1.
- Lara, L. M., Colinas, I. G., Mallada, M. T., Hernández-Battez, A. E., and Viesca, J. L., 2017, Geothermal use of mine water: *European Geologist*, v. 43, p. 40-45, <https://eurogeologists.eu/european-geologist-journal-43-viesca-geothermal-use-of-mine-water/>.
- Larsen, K. R., 2020, Diagnosing microbiologically influenced corrosion in a pipeline, <http://www.materialsperformance.com/articles/material-selection-design/2014/12/diagnosing-microbiologically-influenced-corrosion-in-a-pipeline>, Date Accessed: 13.05.21.
- Laurence, D., 2006, Optimisation of the mine closure process: *Journal of Cleaner Production*, v. 14, no. 3-4, p. 285-298, 10.1016/j.jclepro.2004.04.011.
- Lenntech, 2022, Composition of seawater, <https://www.lenntech.com/composition-seawater.htm>, Date Accessed: 03/03/2022.
- Li, S., Zeng, Z., Harris, M. A., Sánchez, L. J., and Cong, H., 2019, CO2 Corrosion of Low Carbon Steel Under the Joint Effects of Time-Temperature-Salt Concentration: *Frontiers in Materials*, v. 6, no. 10, 10.3389/fmats.2019.00010.
- Limberger, J., Boxem, T., Pluymaekers, M., Bruhn, D., Manzella, A., Calcagno, P., Beekman, F., Cloetingh, S., and van Wees, J.-D., 2018, Geothermal energy in deep aquifers: A global assessment of the resource base for direct heat utilization: *Renewable and Sustainable Energy Reviews*, v. 82, p. 961-975, <https://doi.org/10.1016/j.rser.2017.09.084>.
- Liu, Q., Lin, B., Zhou, Y., and Li, Y., 2021, Permeability and inertial resistance coefficient correction model of broken rocks in coal mine goaf: *Powder Technology*, v. 384, p. 247-257, <https://doi.org/10.1016/j.powtec.2021.02.017>.
- Loredo, C., Banks, D., and Roqueñí, N., 2017a, Evaluation of analytical models for heat transfer in mine tunnels: *Geothermics*, v. 69, p. 153-164, 10.1016/j.geothermics.2017.06.001.
- Loredo, C., Banks, D., and Roqueñí, N., 2018, Corrigendum to “Evaluation of analytical models for heat transfer in mine tunnels” [*Geothermics* 69C (2017) 153–164]: *Geothermics*, v. 71, p. 69, <https://doi.org/10.1016/j.geothermics.2017.08.009>.
- Loredo, C., Ordonez, A., Garcia-Ordiales, E., Alvarez, R., Roqueni, N., Cienfuegos, P., Pena, A., and Burnside, N. M., 2017b, Hydrochemical characterization of a mine water geothermal energy resource in NW Spain: *Sci Total Environ*, v. 576, p. 59-69, 10.1016/j.scitotenv.2016.10.084.

- Loredo, C., Roqueñí, N., and Ordóñez, A., 2016, Modelling flow and heat transfer in flooded mines for geothermal energy use: A review: *International Journal of Coal Geology*, v. 164, p. 115-122, [10.1016/j.coal.2016.04.013](https://doi.org/10.1016/j.coal.2016.04.013).
- Lund, J. W., and Boyd, T. L., 2016, Direct utilization of geothermal energy 2015 worldwide review: *Geothermics*, v. 60, p. 66-93, [10.1016/j.geothermics.2015.11.004](https://doi.org/10.1016/j.geothermics.2015.11.004).
- MacAskill, D., Power, C., and Mkandawire, M., 2015, Researching the Geothermal Potential of the Former Springhill Mine: Report to the Cumberland Energy Authority,
- Manju, M., 2020, Personal Communication,
- Mayes, W. M., Perks, M. T., Large, A. R. G., Davis, J. E., Gandy, C. J., Orme, P. A. H., and Jarvis, A. P., 2021, Effect of an extreme flood event on solute transport and resilience of a mine water treatment system in a mineralised catchment: *Science of The Total Environment*, v. 750, p. 141693, <https://doi.org/10.1016/j.scitotenv.2020.141693>.
- McLaughlan, R. G., 2014, Corrosion of Water Wells, American Society of Civil Engineers, *Hydraulics of Wells : Design, Construction, Testing, and Maintenance of Water Well Systems*,
- Menendez, J., and Loredo, J., 2020, Mine water in the closure of a coal basin: From waste to potential resources., *Advances in Science, Technology & Innovation (IEREK Interdisciplinary Series for Sustainable Development)*, Springer, Cham, *Frontiers in Water-Energy-Nexus—Nature-Based Solutions, Advanced Technologies and Best Practices for Environmental Sustainability*, https://doi.org/10.1007/978-3-030-13068-8_75.
- Met Office, 2022, UK climate averages; Kinross (Perth and Kinross). <https://www.metoffice.gov.uk/research/climate/maps-and-data/uk-climate-averages/gcvxf0h8c>, Date Accessed: 17/05/2022.
- Michel, A. F., Utilization of Abandoned Mine Workings for Thermal Energy Storage in Canada, *in Proceedings The 11th International Conference on Energy Storage (Effstock 2009)* Stockholm, Sweden, Jul 14-17, 2009 2009, http://intraweb.stockton.edu/eyos/energy_studies/content/docs/effstock09/Session_11_1_Case%20studies_Overviews/105.pdf
- Millward, D., Davies, S. J., Williamson, F., Curtis, R., Kearsey, T. I., Bennett, C. E., Marshall, J. E. A., and Browne, M. A. E., 2018, Early Mississippian evaporites of coastal tropical wetlands: *Sedimentology*, v. 65, no. 7, p. 2278-2311, <https://doi.org/10.1111/sed.12465>.
- Minewater-Project, Minewater as a renewable energy resource: An information guide based on the Minewater Project and the experiences at pilot locations in Midlothian and Heerlen., *in Proceedings The Minewater Project (INTERREG).2008*, http://skrconline.net/content/images/stories/documents/mine_water_renewable_energy_guide.pdf
- Monaghan, A., 2021, Personal Communication,
- Monaghan, A., Damaschke, M., Starcher, V., Fellgett, M. W., Kingdon, A., Kearsey, T., Hannis, S., Gillespie, M., Shorter, K., Elsome, J., and Barnett, M., 2021a, UK Geoenergy Observatories Glasgow: GGC01 cored, seismic monitoring borehole – final data release. British Geological Survey Open Report, OR/21/031., 64 p,
- Monaghan, A. A., 2014, The Carboniferous shales of the Midland Valley of Scotland: geology and resource estimation.: British Geological Survey for Department of Energy and Climate Change, London, UK.,
- Monaghan, A. A., Barron, H. F., Starcher, V., Shorter, K. M., and Walker-Verkuil, K., 2020a, Mine water borehole GGA01, UK Geoenergy Observatory, Glasgow. British Geological Survey Open Report, OR/20/021., 28 p,
- Monaghan, A. A., Bateson, L., Boyce, A. J., Burnside, N. M., Chambers, R., de Rezende, J. R., Dunnet, E., Everett, P. A., Gilfillan, S. M. V., Jibrin, M. S., Johnson, G., Luckett, R., MacAllister, D. J., MacDonald, A. M., Moreau, J. W., Newsome, L., Novellino, A., Palumbo-Roe, B., Pereira, R., Smith, D., Spence, M. J., Starcher, V., Taylor-Curran, H., Vane, C. H., Wagner, T., and Walls, D. B., 2022, Time Zero for Net Zero: A Coal Mine Baseline for Decarbonising Heat: *Earth Science, Systems and Society*, v. 2, [10.3389/esss.2022.10054](https://doi.org/10.3389/esss.2022.10054).
- Monaghan, A. A., Damaschke, M., Starcher, V., Fellgett, M. W., Kingdon, A., Kearsey, T., Hannis, S., Gillespie, M., Shorter, K., Elsome, J., and Barnett, M., 2021b, UKGEOS Glasgow GGC01

- Final Borehole Information Pack: NERC EDS National Geoscience Data Centre.,
<https://doi.org/10.5285/e38c58a6-48ec-4ad1-a996-6c6144968d7d>.
- Monaghan, A. A., O Dochartaigh, B., Fordyce, F., Loveless, S., Entwisle, D., Quinn, M., Smith, K., Ellen, R., Arkley, S., Kearsley, T., Campbell, S. D. G., Fellgett, M., and Mosca, I., 2017, UKGEOS - Glasgow Geothermal Energy Research Field Site (GGERFS): Initial summary of the geological platform., *in* British Geological Survey, ed.: Nottingham, UK., p. 205,
- Monaghan, A. A., Starcher, V., Barron, H. F., Shorter, K., Walker-Verkuil, K., Elsome, J., Kearsley, T., Arkley, S., Hannis, S., and Callaghan, E., 2021c, Drilling into mines for heat: geological synthesis of the UK Geoenergy Observatory in Glasgow and implications for mine water heat resources: Quarterly Journal of Engineering Geology and Hydrogeology, p. qjehg2021-2033, 10.1144/qjehg2021-033.
- Monaghan, A. A., Starcher, V., Barron, H. F., Shorter, K. M., and Walker-Verkuil, K., 2020b, Borehole GGA02, UK Geoenergy Observatory, Glasgow. British Geological Survey Open Report, OR/20/022., 31 p,
- Monaghan, A. A., Starcher, V., Ó Dochartaigh, B., Shorter, K., and Burkin, J., 2019, UK Geoenergy Observatories: Glasgow Geothermal Energy Research Field Site; Science Infrastructure Version 2, *in* British Geological Survey, ed.: Keyworth, Nottingham., British Geological Survey, p. 49, UKGEOS Report G0100, BGS Open Report OR/19/032.
- National Coal Board, 1954, Abandonment plan of Wallsend coal workings from Dollar Mine. S147 Sheet 3 of 4.,
- National Coal Board, 1955, Abandonment plan of Coalsnaughton Main coal workings from Dollar Mine. S147 Sheet 4 of 4: The Coal Authority.,
- NELEP, 2021, The Case for Mine Energy – unlocking deployment at scale in the UK. A mine energy white paper, p. 35, <https://www.northeastlep.co.uk/wp-content/uploads/2021/05/Mine-Energy-White-Paper-FINAL.pdf>
- Nelson, S. T., 2000, A simple, practical methodology for routine VSMOW/SLAP normalization of water samples analyzed by continuous flow methods: Rapid Communications in Mass Spectrometry, v. 14, no. 12, p. 1044-1046, 10.1002/1097-0231(20000630)14:12<1044::Aid-rcm987>3.0.Co;2-3.
- Nordell, B., Scorpo, A. L., Andersson, O., Rydell, L., and Carlsson, B., 2016, Long Term Evaluation of Operation and Design of the Emmaboda BTES. : Operation and Experiences 2010-2015: Luleå tekniska universitet, 978-91-7583-530-3 (ISBN) 14021528 (ISSN).
- Novák, P., Kasíková, J., Vaněček, M., Brož, M., Uhlík, J., Šindelář, M., and Záruba, J., 2011, Atlas of the mine water geothermal potential in the Czech Republic., ISA Tech Ltd. , http://www.isatech.cz/uploads/tx_jgfirmdocuments/Atlas_of_the_Mine_Water_Geothermal_Potential_in_the_Czech_Republic.pdf
- Nuttall, C. A., and Younger, P. L., 2004, Hydrochemical stratification in flooded underground mines: An overlooked pitfall: Journal of Contaminant Hydrology, v. 69, no. 1-2, p. 101-114, 10.1016/S0169-7722(03)00152-9.
- Ó Dochartaigh, B. É., MacDonald, A. M., Fitzsimons, V., and Ward, R., 2015, Scotland's aquifers and groundwater bodies. British Geological Survey Open Report, OR/15/028., p. 76,
- O Dochartaigh, B. E., Smedley, P. L., MacDonald, A. M., Darling, W. G., and Homoncik, S., 2011, Baseline Scotland : groundwater chemistry of the Carboniferous sedimentary aquifers of the Midland Valley. British Geological Survey Open Report, OR/11/021., p. 105, <http://nora.nerc.ac.uk/id/eprint/14314/>
- Oblast', R., 2014, Концепция развития угольной промышленности Ростовской области на период до 2030 года (Development concept of the coal potential of Rostov oblast' in the period to 2030). Governments of the Rostov region,
- Oglethorpe, M. K., 2006, Scottish Collieries: an inventory of the Scottish coal industry in the nationalized era., Royal Commission on the Ancient and Historical Monuments of Scotland, Edinburgh., 978-1-902419-47-3.
- Oppelt, L., Grab, T., Pose, S., Storch, T., and Fieback, T., 2021, Mine water geothermal energy as a regenerative energy source - status quo and results from five years of monitoring, Oil Gas EUROPEAN MAGAZINE, Volume 47th Edition, p. 15-19, 10.19225 / 2103054.

- Optimised Environments Ltd., 2020, *ClimatEvolution: A vision for a place-based transition to climate resilience in East Lothian*, p. 80, https://eastlothianconsultations.co.uk/housing-environment/climateevolution/supporting_documents/191381_Strategy%20and%20Action%20Plan%20Report%20v4_200514.pdf
- Ordnance Survey, 2017, *OS TERRAIN 5*, User guide and technical specification, p. 31, <https://www.ordnancesurvey.co.uk/documents/os-terrain-5-user-guide.pdf>
- Ordóñez, A., Jardón, S., Álvarez, R., Andrés, C., and Pendás, F., 2012, Hydrogeological definition and applicability of abandoned coal mines as water reservoirs: *Journal of Environmental Monitoring*, v. 14, no. 8, p. 2127-2136, 10.1039/c2em11036a.
- Paces, T., and Čermák, V., 1975, Subsurface temperatures in the Bohemian massif: geophysical measurements and geochemical estimates, 2nd U.N. Symp. Development Use Geothermal Resources, San Francisco, p. 803-807, <https://pascal-francis.inist.fr/vibad/index.php?action=getRecordDetail&idt=PASCALGEODEBRGM7720385326>
- Palumbo-Roe, B., Shorter, K. M., Fordyce, F. M., Walker-Verkuil, K., Ó Dochartaigh, B., Goody, D., and Darling, W. G., 2021a, UK Geology Observatories: Glasgow Borehole Test Pumping - Groundwater Chemistry. British Geological Survey Open Report, OR/21/030., 73 p.
- Palumbo-Roe, B., Shorter, K. M., Fordyce, F. M., Walker-Verkuil, K., Ó Dochartaigh, B., Goody, D., and Darling, W. G., 2021b, UKGEOS Glasgow Test Pumping Groundwater Chemistry Data Release, <https://doi.org/10.5285/53ded3f2-a4e9-4f49-8084-2c8b3b485268>
- Peiffer, S., and Wan, M., 2016, Reductive Dissolution and Reactivity of Ferric (Hydr)oxides: New Insights and Implications for Environmental Redox Processes, *Iron Oxides*, p. 31-52 <https://doi.org/10.1002/9783527691395.ch9783527691393>
- Pluta, I., 2001, Barium and radium discharged from coal mines in the Upper Silesia, Poland: *Environmental Geology*, v. 40, no. 3, p. 345-348, 10.1007/s002540000175.
- Popoola, L. T., Grema, A. S., Latinwo, G. K., Gutti, B., and Balogun, A. S., 2013, Corrosion problems during oil and gas production and its mitigation: *International Journal of Industrial Chemistry*, v. 4, no. 1, p. 35, 10.1186/2228-5547-4-35.
- Preene, M., and Younger, P. L., 2014, Can you take the heat? – Geothermal energy in mining: *Mining Technology*, v. 123, no. 2, p. 107-118, 10.1179/1743286314y.0000000058.
- Present, T. M., Adkins, J. F., and Fischer, W. W., 2020, Variability in Sulfur Isotope Records of Phanerozoic Seawater Sulfate: *Geophysical Research Letters*, v. 47, no. 18, <https://doi.org/10.1029/2020GL088766>.
- Prestwich, J., 1887, On underground temperature; with observations on the conductivity of rocks; on the thermal effects of saturation and imbibition; and on a special source of heat in mountain ranges: *Proceedings of the Royal Society of London*, v. 41, no. 246-250, p. 1-116, 10.1098/rspl.1886.0082.
- Ramos, E. P., Breede, K., and Falcone, G., 2015, Geothermal heat recovery from abandoned mines: a systematic review of projects implemented worldwide and a methodology for screening new projects: *Environmental Earth Sciences*, v. 73, no. 11, p. 6783-6795, 10.1007/s12665-015-4285-y.
- Rawson, P. F., 2006, Cretaceous: sea levels peak as the North Atlantic opens, *in* Brenchley, P. J., and Rawson, P. F., eds., *The Geology of England and Wales*, Geological Society of London. 9781862392007
- Reimann, C., Filzmoser, P., Garrett, R., and Dutter, R., 2008, *Statistical Data Analysis Explained*, Chichester, England, John Wiley and Sons Ltd., 359 p, 978-0-470-98581-6.
- Reinecker, J., Gutmanis, J., Foxford, A., Cotton, L., Dalby, C., and Law, R., 2021, Geothermal exploration and reservoir modelling of the united downs deep geothermal project, Cornwall (UK): *Geothermics*, v. 97, 10.1016/j.geothermics.2021.102226.
- Rinder, T., Dietzel, M., Stammeier, J. A., Leis, A., Bedoya-González, D., and Hilberg, S., 2020, Geochemistry of coal mine drainage, groundwater, and brines from the Ibbenbüren mine, Germany: A coupled elemental-isotopic approach: *Applied Geochemistry*, v. 121, p. 104693, <https://doi.org/10.1016/j.apgeochem.2020.104693>.

- Rippon, J., Read, W. A., and Park, R. G., 1996, The Ochil Fault and the Kincardine basin: key structures in the tectonic evolution of the Midland Valley of Scotland: *Journal of the Geological Society*, v. 153, no. 4, p. 573-587, [10.1144/gsjgs.153.4.0573](https://doi.org/10.1144/gsjgs.153.4.0573).
- Robins, N. S., 1990, *Hydrogeology of Scotland*, HMSO, London., 0118844687.
- Robinson, B. W., and Kusakabe, M., 1975, Quantitative preparation of sulfur dioxide, for sulfur-34/sulfur-32 analyses, from sulfides by combustion with cuprous oxide: *Analytical Chemistry*, v. 47, no. 7, p. 1179-1181, [10.1021/ac60357a026](https://doi.org/10.1021/ac60357a026).
- Robinson, S., 2022, Personal Communication: Myron L® Company,
- Roijen, E., Op 't Veld, P., and Demollin-Schneiders, E., 2007, The Minewaterproject Heerlen - low exergy heating and cooling in practice., 2nd PALENC Conference and 28th AIVC Conference on Building Low Energy Cooling and Advanced Ventilation Technologies in the 21st Century: Crete, Greece, p. 839-844,
- Ross, R., and Kavanaugh, C., 1993, Development and application of geothermal minewater energy from the abandoned coal mines in the Springhill Coal Fields, Springhill, Nova Scotia.: *Proceedings of the 106th Annual Meeting of The Mining Society of Nova Scotia*, June 23-25,
- Rowley, A., 2013, Questions raised over mining operations in Fife, <http://www.alexrowley.org/questions-raised-over-mining-operations-in-fife/>, Date Accessed: 14.05.2021.
- Scottish Environment Protection Agency, 2022, Daily Rainfall Totals; Tillicoultry, <https://www2.sepa.org.uk/rainfall//data/index/15158>
- Scottish Government, 2019, Improving energy efficiency in owner occupied homes: consultation, *in* Housing and Social Justice Directorate, ed., ISBN: 9781839603990.
- Scottish Government, 2020a, Securing a green recovery on a path to net zero: climate change plan 2018–2032 - update, ISBN 9781800044302.
- Scottish Government, 2020b, Update to the Climate Change Plan 2018 – 2032: Securing a Green Recovery on a Path to Net Zero., p. 255, ISBN 9781800044302.
- Scottish Government, 2020c, Annual Compendium of Scottish Energy Statistics 2020, p. 83, <https://www.gov.scot/binaries/content/documents/govscot/publications/statistics/2019/05/annual-compendium-of-scottish-energy-statistics/documents/annual-compendium-december-2020/annual-compendium-december-2020/govscot%3Adocument/ACSES%2B2020%2B-%2BDecember.pdf>
- Scottish Government, 2022, New Build Heat Standard Consultation: Part II., p. 35, ISBN 9781804356463.
- Scottish Water, 2021, Water Register; Date range of sample: 01/01/2021 to 31/12/2021; Regulation Zone = Milngavie C2, <https://www.scottishwater.co.uk/-/media/ScottishWater/Water-Quality/Data/73/202209/Water-202101-Milngavie-C2-Calendar-Year.pdf>.
- Secret Scotland, 2023, Clyde Tidal Weir, <https://www.secretscotland.org.uk/index.php/Secrets/ClydeTidalWeir>, Date Accessed: 28/01/2023.
- SEPA, 2016, Supporting Guidance (WAT-SG-85): Application of Standards to Thermal Discharges, p. 12, https://www.sepa.org.uk/media/149827/wat_sg_85.pdf
- SEPA, 2022, SEPA's Requirements for Activities Related to Geothermal Energy v1.3, p. 11, <https://www.sepa.org.uk/media/594535/geothermal-october-2022.pdf>
- Shorter, K. M., MacDonald, A. M., O Dochartaigh, B. E., Elsome, J., and Burke, S., 2020a, Data release and initial interpretation of test pumping of boreholes at the Glasgow UK Geoenergy Observatory. *British Geological Survey. Open Report, OR/21/016*. 104pp., 104 p,
- Shorter, K. M., Palumbo-Roe, B., Ó Dochartaigh, B. E., Fordyce, F., and Walker-Verkuil, K., 2021a, UK Geoenergy Observatories Glasgow: Groundwater chemistry data collected during the borehole construction phase, *British Geological Survey Open Report, OR/21/015*., 45 p,
- Shorter, K. M., Palumbo-Roe, B., Ó Dochartaigh, B. E., Fordyce, F., and Walker-Verkuil, K., 2021b, UKGEOS Glasgow Construction Phase Groundwater Chemistry Data Release. NERC EDS National Geoscience Data Centre. (Dataset). <https://doi.org/10.5285/295984e5-5f2a-43aa-aa3d-6995a80ac8ed>,

- Shorter, K. M., Starcher, V., Barron, H. F., Walker-Verkuil, K., and Monaghan, A. A., 2020b, Environmental baseline characterisation and monitoring borehole GGA03r, UK Geoenergy Observatory, Glasgow. British Geological Survey Open Report, OR/20/023. , 23 p,
- Shorter, K. M., Starcher, V., Barron, H. F., Walker-Verkuil, K., and Monaghan, A. A., 2020c, Environmental baseline characterisation and monitoring borehole GGA06r, UK Geoenergy Observatory, Glasgow. British Geological Survey Open Report, OR/20/026. , 23 p,
- Smith, J., and Colls, J. J., 1996, Groundwater Rebound in the Leicestershire Coalfield: Water and Environment Journal, v. 10, no. 4, p. 280-289, <https://doi.org/10.1111/j.1747-6593.1996.tb00046.x>.
- Smith, R. A., 1872, Air and rain: the beginnings of a chemical climatology, Longmans, Green, and Company,
- South Tyneside Council, 2022, Hebburn Minewater Project, <https://www.southtyneside.gov.uk/article/70283/Hebburn-Minewater-Project>, Date Accessed: 14/07/2022.
- Sowter, A., Bateson, L., Strange, P., Ambrose, K., and Syafiudin, M. F., 2013, DInSAR estimation of land motion using intermittent coherence with application to the South Derbyshire and Leicestershire coalfields: Remote Sensing Letters, v. 4, no. 10, p. 979-987, 10.1080/2150704X.2013.823673.
- Sparling, C., 2013, Fordell Day Level is so important to future quality of land, Central Fife Times, <https://www.centrafifetimes.com/opinion/13548609.fordell-day-level-is-so-important-to-future-quality-of-land/>
- Spears, D. A., and Amin, M. A., 1981, Geochemistry and mineralogy of marine and non-marine Namurian black shales from the Tansley Borehole, Derbyshire: Sedimentology, v. 28, no. 3, p. 407-417, <https://doi.org/10.1111/j.1365-3091.1981.tb01689.x>.
- Starcher, V., Barron, H. F., Monaghan, A. A., Shorter, K. M., and Walker-Verkuil, K., 2020a, Mine water characterisation and monitoring borehole GGA04, UK Geoenergy Observatory, Glasgow. British Geological Survey Open Report, OR/20/024., 28 p,
- Starcher, V., Walker-Verkuil, K., Shorter, K. M., Monaghan, A. A., and Barron, H. F., 2020b, Mine water characterisation and monitoring borehole GGA07, UK Geoenergy Observatory, Glasgow. British Geological Survey Open Report, OR/20/027., 29 p,
- Steven, J., From Venture Pit to Walker Shore, coal and heat and fathoms of core': Mine water Heat Exploitation in Newcastle/Gateshead, in Proceedings 2021 Mine Water Geothermal Energy Symposium, "Mine Water Heating and Cooling – A 21st Century Resource for Decarbonisation", Webinar, 10th-11th March 2021 2021a, <https://iea-gia.org/workshop-presentations/2021-mine-water-geothermal-energy-symposium/>
- Steven, J., 2021b, Personal Communication,
- Stumm, W., and Sulzberger, B., 1992, The cycling of iron in natural environments: Considerations based on laboratory studies of heterogeneous redox processes: Geochimica et Cosmochimica Acta, v. 56, no. 8, p. 3233-3257, [https://doi.org/10.1016/0016-7037\(92\)90301-X](https://doi.org/10.1016/0016-7037(92)90301-X).
- SUST, 2006, Glenalmond Street Housing, Glasgow, Case Study.: SUST–Scottish Executive. World Wide Web Address: https://www.ads.org.uk/wp-content/uploads/7615_glenalmond-pdf.pdf,
- Tarmac, 2016, Technical Data Sheet Flow Modified Grout Range, <https://www.pozament.co.uk/wp-content/uploads/2013/02/Flow-Modified-Grout-Range-Technical-Datasheet-July-2016.pdf>.
- Taylor, K., Banks, D., and Watson, I., 2016a, Characterisation of hydraulic and hydrogeochemical processes in a reducing and alkalinity-producing system (RAPS) treating mine drainage, South Wales, UK: International Journal of Coal Geology, v. 164, p. 35-47, <https://doi.org/10.1016/j.coal.2016.05.007>.
- Taylor, K., Banks, D., and Watson, I., 2016b, Heat as a natural, low-cost tracer in mine water systems: The attenuation and retardation of thermal signals in a Reducing and Alkalinity Producing Treatment System (RAPS): International Journal of Coal Geology, v. 164, p. 48-57, <https://doi.org/10.1016/j.coal.2016.03.013>.
- The Coal Authority, 2017, Guidance for developers; Risk based approach to development management, Volume Version 4, p. 22, https://assets.publishing.service.gov.uk/government/uploads/system/uploads/attachment_data/

file/588157/Resources_for_Developers_Risk-Based_Approach_to_Development_Management_Version_4.pdf

- The Coal Authority, 2018, Case study: Dawdon mine water treatment scheme, <https://www.gov.uk/government/case-studies/dawdon-mine-water-treatment-scheme>, Date Accessed: 04/03/2021.
- The Coal Authority, 2020, Seaham Garden Village mine energy district heating scheme, https://www2.groundstability.com/wp-content/uploads/2020/01/CA_Seaham_Brochure.290120.pdf,
- The Coal Authority, 2021a, Annual report and accounts 2020-21, 115 p, ISBN 978-1-5286-2770-2.
- The Coal Authority, 2021b, Mine water heat, <https://www.gov.uk/government/collections/mine-water-heat>, Date Accessed: 14/07/2022.
- The Coal Authority, 2022, Interactive Map, <https://mapapps2.bgs.ac.uk/coalauthority/home.html>, Date Accessed: 25/11/2021.
- The Coal Authority, Health and Safety Executive, The British Drilling Association, The Federation of Piling specialists, and The Association of Geotechnical and Geoenvironmental Specialists, 2019, Guidance on managing the risk of hazardous gases when drilling or piling near coal - version 2, https://assets.publishing.service.gov.uk/government/uploads/system/uploads/attachment_data/file/810431/Guidance_on_managing_the_risk_of_hazardous_gases_when_drilling_or_piling_near_coal.pdf
- Theis, C. V., 1935, The relation between the lowering of the Piezometric surface and the rate and duration of discharge of a well using ground-water storage: Eos, Transactions American Geophysical Union, v. 16, no. 2, p. 519-524, <https://doi.org/10.1029/TR016i002p00519>.
- Thomson, M. E., 1978, IGS Studies of the geology of the Firth of Forth and its Approaches, London, HMSO, 70 p, ISBN 0118840657.
- Thomson, W., Lyell, C., Maxwell, J. C., Phillips., Symons, G. J., Balfour, S., Ramsay., Geikie, A., Glaisher, J., Graham., Binney, E. W., Maw, G., Pengelly, W., Mackie, S. J., and Everett, J. D., 1871, Third report of the committee for the purpose of investigating the rate of increase of underground temperature downwards in various localities of dry land and under water.: Report of the 40th Meeting of the British Association for the Advancement of Science., p. 29-41, <https://archive.org/details/reportofbritisha71brit/page/n127>
- Tipper, L. J., 2015a, User Guide For the Coal Authority In Seam Levels Dataset, *in* The Coal Authority, ed., p. 11,
- Tipper, L. J., 2015b, User Guide for the Coal Authority Underground Working Dataset, *in* The Coal Authority, ed., p. 12,
- Todd, F., McDermott, C., Harris, A. F., Bond, A., and Gilfillan, S., 2019, Coupled hydraulic and mechanical model of surface uplift due to mine water rebound: implications for mine water heating and cooling schemes: Scottish Journal of Geology, v. 55, no. 2, p. 124-133, 10.1144/sjg2018-028.
- Tokarz, M., and Mucha, W., 2013, Wykorzystanie energii geotermalnej pochodzącej z odwadniania zakładów górniczych, na przykładzie rozwiązań zastosowanych w SRK S.A. Zakładzie CZOK w Czeladzi: Technika Poszukiwań Geologicznych, v. 52, p. 103-114,
- Tostevin, R., Turchyn, A. V., Farquhar, J., Johnston, D. T., Eldridge, D. L., Bishop, J. K. B., and McIlvin, M., 2014, Multiple sulfur isotope constraints on the modern sulfur cycle: Earth and Planetary Science Letters, v. 396, p. 14-21, <https://doi.org/10.1016/j.epsl.2014.03.057>.
- TownRock Energy, 2018, Dollar Minewater Geothermal Pre-Feasibility; Confidential report for Harviestoun Home Farm,
- Townsend, D., Naismith, J., Townsend, P., Milner, M., and Fraser, U., 2020, “On The Rocks” – Exploring Business Models for Geothermal Heat in the Land of Scotch, World Geothermal Congress: Reykjavik, Iceland, <https://pangea.stanford.edu/ERE/db/WGC/papers/WGC/2020/08025.pdf>
- Trueman, A., 1954, The Coalfields of Great Britain., London, Edward Arnold Ltd., 396 p, 0016-7568.
- Tukey, J. W., 1977, Exploratory Data Analysis., Reading, Mass. — Menlo Park, Cal., London, Amsterdam, Don Mills, Ontario, Sydney Addison-Wesley Publishing Company, Biometrical Journal, v. 4, 0323-3847.

- Twigg, R. J., 1984, Corrosion of steels in sour gas environment (Research Report No. INFO-0118), *in* Atomic Energy Control Board, ed.: Ottawa, Canada.,
- UK Government, 2021a, Heat and buildings strategy., p. 244, ISBN 978-1-5286-2459-6.
- UK Government, 2021b, Net Zero Strategy: Build Back Greener., p. 368, ISBN 978-1-5286-2938-6.
- Underhill, J. R., Monaghan, A. A., and Browne, M. A. E., 2008, Controls on structural styles, basin development and petroleum prospectivity in the Midland Valley of Scotland: Marine and Petroleum Geology, v. 25, no. 10, p. 1000-1022, <https://doi.org/10.1016/j.marpetgeo.2007.12.002>.
- Undiscovered Scotland, 2023, Rutherglen, <https://www.undiscoveredscotland.co.uk/glasgow/rutherglen/index.html>, Date Accessed: 28/01/2023.
- UNECE, I., 2022, Supplementary Specifications for the application of the United Nations Framework Classification for Resources (Update 2019) to Geothermal Energy Resources, *in* United Nations Economic Commission for Europe, I. G. A., ed.: Geneva, https://unece.org/sites/default/files/2022-12/UNFC_Geothermal_Specs_25October2022.pdf
- United Nations, 2019, Report of the Secretary-General on the 2019 climate action summit and the way forward in 2020., *in* Proceedings Climate Action Summit, New York City, 11th December 2019, p. 38, www.un.org/sites/un2.un.org/files/cas_report_11_dec_0.pdf
- van Hunen, J., MacKenzie, M., Mouli-Castillo, J., Graham, S., and Adams, C., Modelling mine water flow and heat exchange in open-loop mine systems, *in* Proceedings 2022 Mine water geothermal energy symposium, <https://iea-gia.org/workshop-presentations/2022-mine-water-geothermal-energy-symposium/>, 2022,
- Verhoeven, R., Eijdens, H., Wenmeckers, M., and Harcouët-Menou, V., 2016, Update (Geo-) Thermal Smart Grid Mijwater Heerlen, European Geothermal Congress: Strasbourg, France, EGEC,
- Verhoeven, R., Willems, E., Harcouët-Menou, V., De Boever, E., Hiddes, L., Veld, P. O., and Demollin, E., 2014, Minewater 2.0 Project in Heerlen the Netherlands: Transformation of a Geothermal Mine Water Pilot Project into a Full Scale Hybrid Sustainable Energy Infrastructure for Heating and Cooling: Energy Procedia, v. 46, p. 58-67, 10.1016/j.egypro.2014.01.158.
- Videla, H. A., Herrera, L.K., 2005, Microbiologically influenced corrosion: looking to the future: *Int Microbiol*, v. 8, p. 169–180,
- Walker-Verkuil, K., Starcher, V., Barron, H. F., Shorter, K. M., Elsome, J., and Monaghan, A. A., 2020a, Environmental baseline characterisation and monitoring borehole GGB05, UK Geoenery Observatory, Glasgow. British Geological Survey Open Report, OR/20/031., 23 p,
- Walker-Verkuil, K., Starcher, V., Barron, H. F., Shorter, K. M., and Monaghan, A. A., 2020b, Environmental baseline characterisation and monitoring borehole GGA09r, UK Geoenery Observatory, Glasgow. British Geological Survey Open Report, OR/20/029. ,
- Wallis, G., 2017, Restoring the Elsecar Newcomen Engine—High Ideals, Deep Mysteries: *The International Journal for the History of Engineering & Technology*, v. 87, no. 2, p. 154-164, 10.1080/17581206.2018.1462629.
- Walls, D., Burnside, N. M., and Boyce, A. J., 2020, ‘Old versus new’: Comparing mine water geothermal systems in Glasgow, World Geothermal Congress: Reykjavik, Iceland., https://pure.strath.ac.uk/ws/portalfiles/portal/139102484/Walls_etal_WGC_2021_Old_versus_new_comparing_mine_water_geothermal_systems_in_Glasgow.pdf.
- Walls, D. B., Banks, D., Boyce, A. J., and Burnside, N. M., 2021, A Review of the Performance of Minewater Heating and Cooling Systems: *Energies*, v. 14, no. 19, p. 6215, <https://doi.org/10.3390/en14196215>.
- Walls, D. B., Banks, D., Peshkur, T., Boyce, A. J., and Burnside, N. M., 2022, Heat Recovery Potential and Hydrochemistry of Mine Water Discharges From Scotland’s Coalfields: *Earth Science, Systems and Society*, v. 2, 10.3389/esss.2022.10056.
- Wang, Z., Zhang, L., Tang, X., Cui, Z.-y., Xue, J.-p., and Lu, M.-x., 2017, Investigation of the deterioration of passive films in H₂S-containing solutions: *International Journal of Minerals, Metallurgy, and Materials*, v. 24, no. 8, p. 943-953, 10.1007/s12613-017-1482-6.

- Waterra, 2022, Waterra Groundwater Sampling Pump for Monitoring Wells and Piezometers, <https://waterra.com/waterra-groundwater-sampling-pump/>, Date Accessed: 07/11/2022.
- Waters, C. N., Browne, M. A. E., Dean, M. T., and Powell, J. H., 2007, Lithostratigraphical framework for Carboniferous successions of Great Britain (onshore). British Geological Survey Research Report, RR/10/07., p. 174,
- Watson, I. A., 2007, Managing minewater in abandoned coalfields using engineered gravity discharges, *in* Cidu, R., and Frau, F., eds., IMWA Symposium 2007: Water in Mining Environments: Cagliari, Italy, https://www.imwa.info/docs/imwa_2007/IMWA2007_Watson.pdf
- Watson, S. M., 2022, An investigation of the geothermal potential of the Upper Devonian sandstones beneath eastern Glasgow. PhD Thesis, University of Glasgow. 10.5525/gla.thesis.82687,
- Watzlaf, G. R., and Ackman, T. E., 2006, Underground Mine Water for Heating and Cooling using Geothermal Heat Pump Systems: Mine Water and the Environment, v. 25, no. 1, p. 1-14, 10.1007/s10230-006-0103-9.
- Whitworth, K., England, A., and Parry, D., 2012, Overview of Mine Water in the UK Coalfields. WYG Report for Coal Authority, Annesley, UK, 390 p,
- Wieber, G., and Pohl, S., 2008, Mine Water: A Source of Geothermal Energy - Examples from the Rhenish Massif: Mine Water and the Environment, Proceedings, http://imwa.de/docs/imwa_2008/IMWA2008_051_Wieber.pdf
- Williams, J. D. O., Dobbs, M. R., Kingdon, A., Lark, R. M., Williamson, J. P., MacDonald, A. M., and Ó Dochartaigh, B. É., 2017, Stochastic modelling of hydraulic conductivity derived from geotechnical data; an example applied to central Glasgow: Earth and Environmental Science Transactions of The Royal Society of Edinburgh, v. 108, no. 2-3, p. 141-154, 10.1017/S1755691018000312.
- Wood, S. C., Younger, P. L., and Robins, N. S., 1999, Long-term changes in the quality of polluted minewater discharges from abandoned underground coal workings in Scotland: Quarterly Journal of Engineering Geology and Hydrogeology, v. 32, no. 1, p. 69-79, 10.1144/gsl.Qjeg.1999.032.P1.05.
- Wu, N., Farquhar, J., and Strauss, H., 2014, $\delta^{34}\text{S}$ and $\Delta^{33}\text{S}$ records of Paleozoic seawater sulfate based on the analysis of carbonate associated sulfate: Earth and Planetary Science Letters, v. 399, p. 44-51, <https://doi.org/10.1016/j.epsl.2014.05.004>.
- Yang, W., Zhou, J., Xu, W., and Zhang, G., 2010, Current status of ground-source heat pumps in China: Energy Policy, v. 38, no. 1, p. 323-332, <https://doi.org/10.1016/j.enpol.2009.09.021>.
- Yang, X., Sasaki, K., Zhang, X., and Sugai, Y., 2018, Permeability estimate of underground long-wall goaf from P-wave velocity and attenuation by lab-scale experiment on crushed rock samples: Journal of Applied Geophysics, v. 159, p. 785-794, <https://doi.org/10.1016/j.jappgeo.2018.09.009>.
- Younger, P., 1995a, Minewater pollution in Britain: past, present and future: Mineral planning, v. 65, p. 38-41,
- Younger, P., and Robins, N., 2002, Challenges in the characterization and prediction of the hydrogeology and geochemistry of mined ground: Geological Society, London, Special Publications, v. 198, p. 1-16, 10.1144/GSL.SP.2002.198.01.01.
- Younger, P. L., 1995b, Hydrogeochemistry of minewaters flowing from abandoned coal workings in County Durham: Quarterly Journal of Engineering Geology, v. 28, no. supplement_2, p. S101-S113, doi:10.1144/GSL.QJEGH.1995.028.S2.02.
- Younger, P. L., 1997, The longevity of minewater pollution: A basis for decision-making: Science of the Total Environment, v. 194-195, p. 457-466, 10.1016/S0048-9697(96)05383-1.
- Younger, P. L., 2000a, Iron, *in* Darcy, B. J. D., Ellis, J.B., Ferrier, R.C., Jenkins, A., Dils, R., ed., Diffuse Pollution Impacts, Terence Dalton Publishers, Lavenham, for Chartered Institution of Water and Environmental Management, p. 95-104
- Younger, P. L., 2000b, Predicting temporal changes in total iron concentrations in groundwaters flowing from abandoned deep mines: a first approximation: Journal of Contaminant Hydrology, v. 44, no. 1, p. 47-69, [https://doi.org/10.1016/S0169-7722\(00\)00090-5](https://doi.org/10.1016/S0169-7722(00)00090-5).

- Younger, P. L., 2001, Mine water pollution in Scotland: nature, extent and preventative strategies: *Science of The Total Environment*, v. 265, no. 1, p. 309-326, [https://doi.org/10.1016/S0048-9697\(00\)00673-2](https://doi.org/10.1016/S0048-9697(00)00673-2).
- Younger, P. L., 2004, 'Making water': the hydrogeological adventures of Britain's early mining engineers: Geological Society, London, Special Publications, v. 225, no. 1, p. 121-157, 10.1144/gsl.Sp.2004.225.01.09.
- Younger, P. L., 2007, *Groundwater in the Environment: An Introduction.*, Oxford, UK & Malden, Massachusetts., 318 p, 1-4051-2143-2.
- Younger, P. L., 2016, Abandoned coal mines: From environmental liabilities to low-carbon energy assets: *International Journal of Coal Geology*, v. 164, p. 1-2, 10.1016/j.coal.2016.08.006.
- Younger, P. L., and Adams, R., 1999, Predicting Mine Water Rebound R&D Technical Report W179 Environment Agency, 1857050509.
- Younger, P. L., Boyce, A. J., and Waring, A. J., 2015, Chloride waters of Great Britain revisited: from subsea formation waters to onshore geothermal fluids: *Proceedings of the Geologists' Association*, v. 126, no. 4-5, p. 453-465, 10.1016/j.pgeola.2015.04.001.
- Younger, P. L., and LaPierre, A. B., 2000, 'Uisge Mèinne': mine water hydrogeology in the Celtic lands, from *Kernow* (Cornwall, UK) to *Ceap Breattain* (Cape Breton, Canada): Geological Society, London, Special Publications, v. 182, no. 1, p. 35, 10.1144/GSL.SP.2000.182.01.04.
- Zakirov, D. G., Petin, Y.M., Zakirov, D.D., 2013, Теплонасосные технологии в горнорудной, угольной промышленности и в сфере ЖКХ (Heat pump technology in the ore and coal industries and in the area of housing and communal services). *Энергосбережение (Energy Saving)*, Volume 7, p. 80-96, https://www.abok.ru/for_spec/articles.php?nid=5666
- Zgórska, A., Trzaski, L., and Wiesner, M., 2016, Environmental risk caused by high salinity mine water discharges from active and closed mines located in the Upper Silesian Coal Basin (Poland), in Drebenstedt, C., and Paul, M., eds., *Mining Meets Water - Conflicts and Solutions - International Mine Water Association Conference 2016*: Freiberg, Germany, p. 85-92,
- Zhang, C., Tu, S., Zhang, L., Bai, Q., Yuan, Y., and Wang, F., 2016, A methodology for determining the evolution law of gob permeability and its distributions in longwall coal mines: *Journal of Geophysics and Engineering*, v. 13, no. 2, p. 181-193, 10.1088/1742-2132/13/2/181.
- Zhang, H., 2011, 4 - Cement, Woodhead Publishing, *Building Materials in Civil Engineering*, 46-423 p, 978-1-84569-955-0.